Propene Oligomerization Over Steam Dealuminated and Boron and Phosphorus Modified ZSM-5

By

Bo Andersen (BSc. Chem. Eng.)

Submitted to the University of Cape Town

in fulfilment of the requirements for the degree of

DOCTOR OF PHILOSOPHY

Department of Chemical Engineering
University of Cape Town
Rondebosch
Cape Town
South Africa

June 1991

ACKNOWLEDGEMENTS

I would like to thank my supervisor, Professor Cyril O'Connor, for his help and guidance during the project and for all the support he so readily provided during difficult times. A special thank you also to my co-supervisors Dr. Masami Kojima and Dr. Jack Fletcher for all the advice and assistance.

To Rad and Miles, thanks for the company and the advice, freely given and to Stefan and Alison for a prod in the right direction. A big thank you also to Alex for being there when it counted.

To the rest of the research group, especially the girls, Connie, Leslie and Pam, thanks for everything.

The following people and institutions are also gratefully acknowledged:

The technical staff, especially Mr. Rob Senekal and Mr. Tony Barker, who made much of the equipment and who cheerfully revamped it when required.

SASOL, the CSIR and the FRD for financial assistance at UCT. Noel at the NMR in the Chemistry Department at UCT.

Finally, I would also like to thank my parents, Ulvard and Josephine, for their patience and understanding, Roz for the typing and Jo-Ann for being my friend.

SYNOPSIS

ZSM-5 was modified with boron and phosphorus compounds in an attempt to improve the selectivity of the catalyst with respect to the linearity of the liquid product of propene oligomerization.

Boron was incorporated into the zeolite framework by inclusion in the synthesis gel. Boralite catalysts made in this way and containing very low Al contents had only weak acidity as was evident from only one, low temperature NH_3 desorption peak at ca. 190 °C. These catalysts showed poor propene oligomerization activity as a result of the weak acidity arising from the weak B(OH)Si site and reduced catalyst free volume. The latter was ascribed to occluded B_2O_3 species. Activity of these catalysts was proportional to Al, rather than B content. No appreciable selectivity changes were observed for any of these catalysts. In an attempt to enhance the acidity and hence the activity of the boralite catalysts, mild fluorination treatments were carried out. A boralite catalyst containing 550 ppm Al and 1.2 wt% boron was treated with mild HF at room temperature. The activity of the catalyst was significantly reduced. The activity of the catalyst was essentially restored to its former level upon subsequent NH_4F treatment. The catalyst then contained 120 ppm Al and 0.8 wt% boron. Although some activity enhancement was achieved through mild fluorination, the catalyst utilization values (CUV) remained an order of magnitude lower than the CUV of unmodified ZSM-5. Catalytic activity remained proportional to trace Al content.

Attempts to alter the selectivity of ZSM-5 with boric acid, phosphoric acid and trimethylphosphite also proved unsuccessful. Although significant improvements in p-xylene selectivity for o-xylene isomerization occurred with a boric acid impregnated ZSM-5, no corresponding increase was observed in the amount of linear products formed during propene oligomerization. The activities of the impregnated catalysts compared to unmodified ZSM-5 were reduced as a result of the reduced amount of strong acidity and reduced catalyst pore volume. Adsorption data, indicated that different methods of boric acid impregnation could result in the location of boron at different positions in the catalyst pores. The carbon number distributions of liquid products of the impregnated catalysts were more dependent on reaction temperature than on B and P content. The cetane numbers, as measured by the Gautier correlation were essentially the same as that of unmodified ZSM-5, namely 41, irrespective of manner or degree of modification.

Incorporation of phosphoric acid in the synthesis gel produced catalysts containing phosphates occluded in the pores. No evidence was found for the presence of framework

phosphorus and the activity of these catalysts was comparable to ZSM-5 catalysts modified by phosphoric acid and trimethylphosphite impregnation.

In an attempt to elucidate the role played by the presence of water in the pretreatment procedure, the activity and lifetime of various steam dealuminated ZSM-5 catalysts were examined for high pressure hexene oligomerization. Steam dealumination was achieved by saturating a dry nitrogen stream with water vapour using a double-stage saturator. Steaming temperature, water concentration, steaming time and wet stream (steaming) flowrate were found to have a significant effect on catalytic behaviour. It was found that by carefully optimizing steaming parameters, catalytic activity could be enhanced relative to unmodified ZSM-5. Optimum steaming conditions determined for maximum activity enhancement were: steaming temperature = 300 °C, water concentration = 78 mm Hg, steaming time = 2 hours and steaming flowrate = 60 ml/min.

At these conditions activity enhancement was also observed for propene oligomerization at 250 °C and 5 MPa with the CUV increasing from 120 g/g to 199 g/g upon steaming. The effect of flowrate as a steaming parameter, not previously reported, was ascribed to the existence of substantial film diffusion resistances during steam dealumination. Consequently it was recommended that the effect of flowrate on dealumination rates should not be overlooked when steam dealuminating catalysts. Although a maximum in catalytic activity for hexene oligomerization was observed at 78 mm Hg water concentration, it was also noted that above a water concentration of ca. 150 mm Hg equilibrium of the dealumination reaction was reached. It was suggested that the same site, viz. a specific Lewis site, is responsible for the activity enhancement observed in this study for olefin oligomerization as that observed by other researchers for hexane cracking. It is further proposed that the activity enhancement observed by other researchers for hexane cracking could be further optimized by steaming at ca. 300 °C rather than at higher temperatures (540 °C). The effect of steam dealumination on a catalyst with a silicon-rich outer layer was also examined. Prior to steaming, the activity of this catalyst for hexene oligomerization was comparable to that of unmodified ZSM-5. The response of the silicalite coated catalyst to steam dealumination, however, was different. Variations in steaming flowrate, for example, were no longer significant. This was ascribed to the hydrophobic nature of the catalyst, next to which film diffusion effects were negligible.

Attempts to elucidate the nature of the acid site responsible for enhanced activity using NH_3 TPD and pyridine desorption infrared studies were largely unsuccessful. The stability of the ZSM-5 structure to steaming was evident from both X-ray diffraction and IR optical density ratios. It was concluded that steaming at the conditions used in this study does not

significantly affect the physical characteristics of ZSM-5. Moreover, while altered acidity was felt to be responsible for enhanced activity, these changes could not be readily detected by either ammonia TPD or pyridine desorption IR studies.

TABLE OF CONTENTS

APPENDICES

LIST OF FIGURES

Page

LIST OF TABLES

Chapter 1
Introduction

INTRODUCTION

1.1 Production Routes to Synthetic Fuels

The roots of synthetic fuels production in South Africa lie in the formation of the South African Coal, Oil and Gas Corporation (SASOL) in 1950. SASOL produces liquid fuels via the Fischer-Tropsch (FT) process, first reported in 1923 by Franz Fischer and Hans Tropsch, and involves the conversion of CO and H_2 to hydrocarbons using an alkylized iron catalyst (Dry, 1981).

The first commercial FT plant in South Africa, SASOL 1, was commissioned at Sasolburg in 1955. Following the OPEC oil crisis in 1973 two much larger plants were built at Secunda, namely SASOL 2 and SASOL 3, which were to concentrate mainly on gasoline and distillate fuels production. A general layout of the SASOL plants at Secunda is shown in Figure 1.1. More recently, with the discovery of natural gas deposits at Mossel Bay, another FT plant (MOSGAS) is presently under construction to convert natural gas to liquid fuels.

The major primary products are ethane, gasoline and diesel (Dry, 1982a). At present, the propene as well as the C_4 and C_5 olefins are oligomerized to gasoline and diesel, although a plant is being constructed to convert some of the propene to higher value polypropylene (Dry, 1990). Tables 1.1 and 1.2 show the composition of the products from the SASOL fixed bed and Synthol reactors. For the Synthol reactors less than 50% of the products fall in the gasoline and diesel range. Substantial amounts of C_3 and C_4 alkenes are also produced.

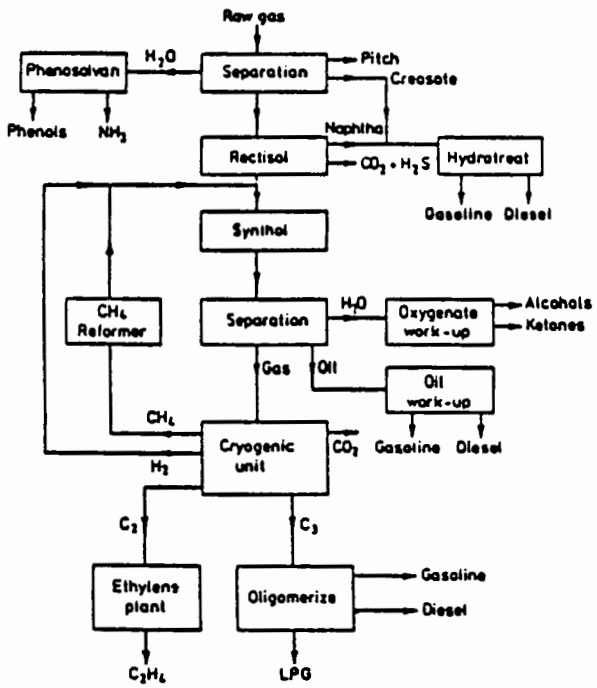

Figure 1.1 Flow diagram of the Secunda SASOL Plant

Table 1.1 Products from SASOL Fixed Bed and Synthol Reactors

Product	Composition / % carbon atom	
	Fixed bed at 493 K	Synthol at 598 K
CH_4	2.0	10
C_2H_4	0.1	4
C_2H_6	1.8	4
C_3H_6	2.7	12
C_3H_8	1.7	2
C_4H_8	3.1	9
C_4H_{10}	1.9	2
C_5 to C_{11} (gasoline)	18	40
C_{12} to C_{18} (diesel)	14	7
C_{19} to C_{23}	7	
C_{24} to C_{35} (Medium Wax)	20	4
$>C_{35}$ (Hard Wax)	25	
Water soluble non-acid chemicals	3.0	5
Water soluble acids	0.2	1

Table 1.2 Properties of Products from SASOL Reactors

Product Cut	Property	Fixed Bed[a]	Synthol[a]
Gasoline C_5-C_{11}	Olefins	32%	65%
	Paraffins	60%	14%
	Aromatics	0%	7%
	Alcohols	7%	6%
	Ketones	0.6%	6%
	Acids	0.4%	2%
	n-Paraffins	95%	55%[b]
	RON (Pb free)	~35	88
Diesel C_{12}-C_{18}	Olefins	25%	73%
	Paraffins	65%	10%
	Aromatics	0%	10%
	Alcohols	6%	4%
	Ketones	<1%	2%
	Acids	0.05%	1%
	%n-Paraffins	93%[b]	60%[b]
	Cetane No	75	55
Medium Wax C_{24}-C_{35}	Olefins	10%	-

a wt.% of cut except for RON and cetane No

b % of the paraffins which are straight chained

There are, however, a number of problems associated with fuels production via the FT process. At low reaction temperatures, the main primary products are linear 1-alkenes, alkanes, alcohols and aldehydes. While the linearity of these products provides the waxes with a unique combination of high melting point and low viscosity and while it provides the diesel fuel cut with a high cetane number (75) and zero aromatics content, it produces a gasoline that requires extensive upgrading (Dry, 1990). This is done by isomerizing the C_5 and C_6 alkenes and by platforming the C_7-C_{11} fraction. The gasoline can also be blended with oligomerized products to obtain a leaded fuel with RON = 93 (Brink and Swart, 1982). The diesel product of oligomerization, however, is too branched. The hydrogenated product yields a cetane number of 33-35. Blending this with the Synthol diesel results in a

fuel with a cetane number of 46 (Brink and Swart, 1982). Although this conforms to South African standards, SASOL have been concerned about the poor quality of diesel. At higher reaction temperatures secondary reactions (e.g. aromatization) occur, increasing the gasoline octane number, but further decreasing the cetane number of the blended diesel fraction.

Another associated problem with the SASOL FT process is connected to the South African market forces. The South African fuel market demands a gasoline to diesel ratio of approximately 1:1 (Dry, 1990). The Synthol reactors typically produce a ratio of about 3:1 (Dry, 1990). This ratio cannot be increased easily since the FT process is limited to a maximum of about 25% diesel fraction by the Schulz-Flory distribution (Jager *et al.,* 1982). To increase the final diesel yields, SASOL employs two secondary processes, namely olefin oligomerization and wax cracking. By varying the process conditions for these reactions, the varying market demands can be met (Dry, 1990).

The SASOL process, therefore, is not optimal. Firstly, the demands of the market place cannot be easily met. Secondly, the gasoline produced is of poor quality, while blended diesel fuels have lower than desired cetane numbers. There is a great demand for alternative routes to fuels, especially in the distillate range. Some of these routes are discussed briefly below.

1.1.1 Fixed Bed FT Process

From Tables 1.1 and 1.2 it can be seen that the Arge fixed bed reactors produce far better diesel fuels than the Synthol reactors. Moreover, it is possible to obtain diesel to gasoline ratios of between 3:1 and 6:1 with cetane numbers of about 65 (Dry, 1982b).

1.1.2 Methanol Conversion

Since it was first discovered in the early 1970's by researchers at Mobil (Argauer and Landolt, 1972), it has become apparent that ZSM-5 is an extremely efficient catalyst for the conversion of methanol to olefins, gasoline and diesel. The methanol-to-gasoline, methanol-to-olefins and the Mobil olefin to gasoline/distillate processes are discussed below.

1.1.2.1 Methanol to gasoline (MTG)

The reaction path for converting methanol to hydrocarbons is shown in Figure 1.2. The first step is the conversion of methanol to dimethylether (DME) and water. These are then transformed to olefins which react to form heavier olefins and aromatics.

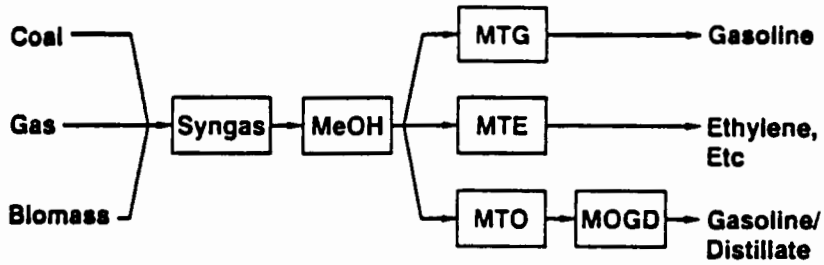

Figure 1.2 Production of fuels and chemicals from methanol

This process has been used commercially in New Zealand (Maiden, 1988). Crude methanol containing ca. 17% water is converted to hydrocarbons and water. The conversion reaction is highly exothermic and a product gas recycle stream is used to limit the temperature rise. The recycle also ensures that the gasoline product is both highly aromatic and highly alkylated, resulting in gasoline of high octane number (Meisel, 1976). The major products are gasoline (85%) and LPG (13-14%) and unlike the Fischer-Tropsch process only contain ca. 1-2% undesired methane (Dry, 1981) An unusual byproduct of the process is durene (1,2,4,5 -tetramethylbenzene). This necessitates that the raw gasoline be distilled and the heavy fraction treated to reduce the durene content to a satisfactory level.

1.1.2.2 Methanol to olefins (MTO)

In this process, methanol is converted at high temperatures (470-515 °C) which results in the heavy hydrocarbons formed at these conditions being cracked to lighter products, mainly propene and butene. The ethane content in the product is low. The process operates at almost complete conversion and hence no recycle stream is needed. The process produces ca. 56% light olefins ($C_2^=$ to $C_4^=$) and about 36% gasoline (C_5 to C_{11}). Table 1.3 shows a comparison of MTO and FT product yields (Dry, 1981).

Table 1.3 A Comparison between MTO and FT Yields

	MTO* Product	F-T Product
C_1	1.4	10.0
C_2	0.3	4.0
C_3	2.3	2.0
C_4	3.9	2.0
$C_2^=$	5.0	4.0
$C_3^=$	31.8	12.0
$C_4^=$	19.6	9.0
Gasoline C_5-C_{11}	35.7	40.0
Diesel C_{12}-C_{18}	-	7.0
Heavy Product C_8^+	-	4.0
Water Soluble Oxygenate	0.3	6.0
	100.0	100.0
Total Light Saturates (C_1-C_3)	4.0	16.0
Total Light Olefins ($C_2^=$-$C_4^=$)	56.3	25.0

*482°C 102 kPa methanol partial pressure

Table 1.4 MOGD Process Yields

	Distillate Mode	Gasoline Mode
C_1-C_3	1	4
C_4	2	5
C_5-165 °C Gasoline	15	-
165 °C$^+$ Distillate	82	-
C_5-200 °C Gasoline	-	84
200 °C$^+$ Distillate	-	7

1.1.2.3 Mobil olefin to gasoline/diesel (MOGD)

In the MOGD process light olefins are reacted to produce gasoline and diesel products (Owen *et al.,* 1984). The ZSM-5 catalyst used has a Si/Al ratio of ~35 and is extruded with 35 wt% alumina as binder for industrial application. Typical operating conditions are fixed bed reactor at 190-310 °C, 4-10 MPa and a WHSV feed rate of 0.5-1 for distillate mode operation. In this mode 80 wt% of the product may be diesel with a cetane number of > 55 after hydrogenation. Operating at higher temperatures and lower pressures (285-375°C, 0.4-3 MPa) produces a gasoline with RON of 92. The paraffinic MOGD diesel fuel has low density, but its low pour point and extremely low sulphur content make it an exceptionally good blending stock (Tabak and Yurchak, 1990). The MOGD process also makes excellent jet fuels due to its isoparaffinic structure and low aromatics content. If necessary a single MOGD plant has the flexibility to produce both gasoline and diesel to satisfy changes in demand for liquid product. Table 1.4 shows the gasoline and diesel yields from both type of operation while Table 1.5 shows some of the product characteristics.

Tabak (1981) has shown that ZSM-12 with Si/Al ratios > 40 oligomerizes alkenes when contacted with liquid feed at 40-150 °C, 2.8-5.3 MPa, WHSV = 0.5-1. At a WHSV = 0.6, 40- 50 °C and 4.1 MPa the major products formed were trimers and tetramers. Under these conditions ZSM-12 was more active than ZSM-5.

Chu and Valyocsik (1987) reported similar product distributions (to those obtained using ZSM-5) when oligomerizing light alkenes to hydrocarbons using ZSM-48. Conditions used were 200-260 °C, 5-7 MPa, WHSV = 0.3-0.4.

Generally it appears that ZSM-type catalysts are superior oligomerization catalysts for diesel fuels production.

Table 1.5 MOGD Product Characteristics

	Distillate	
	Raw	Hydrogenated
Specific gravity 15°/15°	0.79	0.78
Bromine no.	79	4.0
Aromatic, vol. %	-	3.0
Pour point, °C	<-50	<-50
Viscosity, cs @ 40 °C	-	2.5
Cetane no. (Engine)	33	56
Sulfur, wt. %	<0.002	<0.002
90% B.P., °C	333	343
	Gasoline	
Specific gravity 15°/15°	0.73	
Octane no.	92	
Research Octane no.	92	
Motor Octane no.	79	

1.1.3 Alkene Oligomerization

In South Africa olefin oligomerization has been used to satisfy the shortfall in the supply of diesel that arises as a result of the FT product spectrum (discussed earlier). At SASOL the CATPOLY process (using a phosphoric acid/kieselguhr catalyst) has been employed to overcome this. The CATPOLY catalyst readily produces about 75% diesel. The diesel obtained, however, has a low molecular weight with a low viscosity (1.8 cSt at 40 °C (Dry, 1990)) and is highly branched. While the process produces fairly good quality gasoline, the cetane number of the diesel produced is low (mentioned earlier). Zeolite ZSM-5, with its intermediate pore size and channel structure, has been shown to be an excellent oligomerization catalyst when used in the MOGD process. (see Section 1.1.2.3). The low propensity for coking combined with the higher temperatures at which ZSM-5 can operate make it extremely attractive for this process. Alkene oligomerization will be discussed more fully in the following section.

1.2 Alkene Oligomerization

Oligomerization generally refers to the synthesis of molecules consisting of a small number of monomer units as opposed to polymerization which implies production of high molecular weight products. Although alkene oligomerization is an important industrial route for the production of motor fuels, additives, resins, dyes, medicines, detergents and plasticisers, in the South African context it is the possibility of fuel production that is of significant importance. Moreover, with environmental pressures being exerted to ensure the removal of aromatics from fuels, the possibility of aromatic free fuels production via alkene oligomerization makes this process internationally interesting. There are a number of sources of alkenes for such a process. One source is the offgas from Fischer-Tropsch Synthesis. Another is the MTO process (see Section 1.1.2.2). It is also thought that the heavy liquid fraction from crude oil cracking may become an important feedstock for alkene production.

Alkene oligomerization may be carried out via both heterogeneous and homogeneous catalysis. While the heterogeneous acid catalysts, such as zeolites, have been used to oligomerize light olefins to distillate fuels, homogeneous catalysts have largely been used as dimerizing catalysts. Some of the different catalytic routes and their advantages and disadvantages for alkene oligomerization are discussed below.

1.2.1 Oligomerization via Heterogeneous Catalysis

1.2.1.1 Zeolites

Since it was discovered in the seventies (Argauer and Landolt, 1972) the zeolite ZSM-5 has shown itself to be an excellent oligomerization catalyst. It has been shown to produce excellent quality diesel and gasoline in the MOGD process (see Section 1.1.2.3). The low rate of coke deposition and the ease of regeneration make the ZSM catalysts ideally suited for this process. Zeolites will be discussed more fully in Section 1.3.

1.2.1.2 Non-zeolites

1.2.1.2.1 Phosphoric acid

Supported on kieselguhr, this catalyst has been shown to convert alkenes primarily into gasoline (Ipatieff, 1935; McClean, 1988). Used in the CATPOLY process, reaction typically takes place at about 200 °C and 3 MPa. The major products can be shifted from trimer to tetramer by increasing acid concentration from 92% to 109% (Bethea and Karchmer, 1956). The CATPOLY process, however, produces poor quality diesels (low molecular weight, highly branched) while the catalyst itself is highly corrosive.

1.2.1.2.2 Silica-alumina

Amorphous silica-alumina is superior to phosphoric acid on kieselguhr in that a heavier liquid product is produced. The diesel is still highly branched, however, resulting in a distillate fuel with a lower than desired cetane number. The incorporation of nickel results in a more active catalyst, but the product spectrum is shifted from 48 wt% tetramer (at 200 °C and 4 MPa) to 12 wt% (Harms *et al.,* 1989). Nickel-silica-alumina is therefore more suited to gasoline production, yielding a RON of 90.4 (Hogan *et al.,* 1955).

1.2.1.2.3 Synthetic mica montmorillonite (SMM) and Ni SMM

Fletcher *et al.* (1986) studied propene oligomerization at 6 MPa over SMM. High conversion and long lifetimes were obtained in the presence of Lewis sites. The presence of moisture was thought to rehydrate Lewis sites to more active Bronsted sites, resulting in catalysts with high activity and consequently prone to temperature runaways and rapid deactivation. Ni SMM had a higher initial activity, but a similar lifetime to SMM and showed little deactivation at a WHSV of 0.6 after 70 hours. Both catalysts produced liquid product with almost 65 wt% of the product in the diesel range (O'Connor *et al.,* 1988).

1.2.1.2.4 Cation exchange resins

Haag (1967) oligomerized 89% of isobutene at 16 °C, 1 MPa and LHSV = 180 using a sulphonated styrene divinylbenzene copolymer. The product contained about 30% dimer, almost 60% trimer and 10% tetramer. These catalysts, however, exhibit poor thermal

stability above 130 °C. This problem may be overcome by sulfonating trimethoxybenzylsilane bonded to previously activated silica. Loss of sulphonic groups and deactivation of others by esterification, however, result in a 50% decrease in activity over 120 hours at 130 °C (Sans and Schmidl, 1985). O'Connor *et al.* (1985) oligomerized butene over amberlyst 15 with some success. At least 50% of the product was dimer, however, the RON of the gasoline cut was 99 while the diesel fraction cetane number was 35. This catalyst could therefore be considered as being more effective for gasoline production.

1.2.2 Oligomerization via Homogeneous Catalysis

The Shell Higher Olefin Process (SHOP) uses a homogeneous nickel catalyst to oligomerize ethene, producing in excess of one million tons of linear olefins per annum. The reaction takes place in a polar solvent immiscible with the alkene products of the reaction, at temperatures ranging from 80-120 °C and pressures of 7-14 MPa. A mixture of mainly C_4-C_{20} α-olefins are formed with a Schulz-Flory distribution. The catalyst used is a non-Ziegler nickel ligand based catalyst (Bauer *et al.*, 1972). The main drawback of homogeneous routes such as SHOP is the difficulty of product separation of solvent and catalyst. Chemical and thermal stability can also be a problem.

1.2.3 The Mechanism of Alkene Oligomerization

The origin of zeolite activity for alkene oligomerization is found in the ability of the Bronsted acid sites to attack the double bond of the various alkenes as shown below:

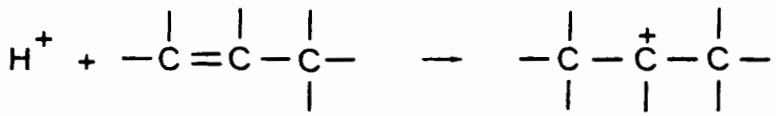

The carbenium ion thus formed may then attack another propene molecule which may be further oligomerized to heavier molecules or be isomerized to hexene. It has been said (Evans and Polanyi, 1947) that oligomerization proceeds via Markownikoff addition and is consequently dependent on the stability of the carbenium ion which decreases in the following order:

Tertiary > Secondary > Primary

Apart from oligomerization and site regeneration other reactions may also take place. These may include hydrocarbon cracking, isomerization, cyclization and saturation of alkenes with H_2 formed during cyclization (McMahon *et al.*, 1963). Oligomerization, therefore, is not a straightforward reaction and can be taken in most cases to be a combination of all of the above reactions.

Tabak (1985) proposed that alkene oligomerization be represented by the schematic model shown below:

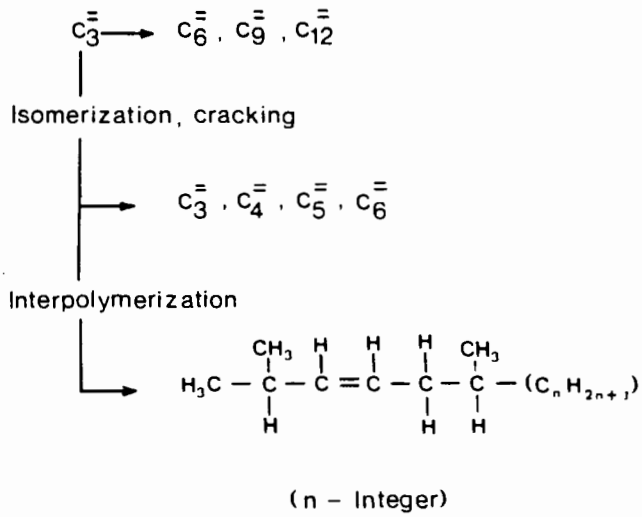

Products formed will, of course, depend on the stability of the carbenium ion as well as on the zeolite channel configuration. Quann *et al.* (1988), for example, showed that at 232 °C and 5.5 MPa the trimer was the preferred product. The increased trimer content relative to the dimer was ascribed to the greater stability of the tertiary carbenium ion of the dimer than that of the secondary carbenium ion of the monomer. The dimer consequently stands a greater chance of oligomerizing with another monomer, favouring trimerization rather than dimerization. Quann *et al.* (1988) also showed that oligomerization products were far less branched for ZSM-5 than for non-shape selective catalysts. Moreover, the ZSM-5 product contained ca. one methyl group per 4-5 carbon atoms. In the hexene isomer product formed at 227 °C and 4.2 MPa less 2,3-dimethylbutane was formed than was expected from equilibrium. These phenomena were ascribed to the pore sizes of ZSM-5.

1.2.4 Thermodynamics of Oligomerization

Investigations of the thermodynamics of oligomerization have been complicated by the number of alkene isomers that can be involved in an oligomerization reaction. There are,

for example, an estimated 12.7 x 10^9 isomers of C_{25} alkenes (O'Connor and Kojima, 1990). Alberty (1987a) proceeded by treating oligomerization as an equilibrium reaction of exothermic reactions, which yield progressively fewer molecules. Although it was correctly predicted that oligomerization was favoured at high pressures and low temperatures, calculations were complicated by the large number of isomers at higher molecular weights. It is hardly surprising therefore that many models have relied on the grouping of thermodynamic properties (Smith, 1959; Tabak *et al.*, 1986) The model reaction data used by Tabak (1985) has been shown in the previous section. Using this model Alberty (1987b) proposed a 30-step mechanism providing for all possible reactions of oligomer groups.

1.3 Zeolites

The word "zeolite" has Greek origins and means "boiling stones", a reference to the noticeable loss of water that occurs when zeolites are heated. Zeolites can be defined as 3-dimensional crystalline aluminosilicates whose structures are composed of corner linked $(AlO_4)^{5-}$ and $(SiO_4)^{4-}$ tetrahedra in which the ratio of oxygen to silicon and aluminium is 2 or, where (O/(Al + Si)) = 2 (Barrer, 1982).

The corner linked tetrahedra have small atoms situated at the centre with oxygen at the corners. In natural zeolites the tetrahedral atoms are Al and Si, although B, Ga, Ge, and P can be incorporated in synthetic zeolites. Typically the unit cell formula is given by

$$M_pD_q(Al_{p+2q}Si_rO_{2p+4q+2r}).sH_2O \quad \text{(Smith, 1979)}$$

where M and D represent monovalent and divalent cations respectively.

The zeolite frameworks are porous and contain channels and cavities which may contain not only cations needed to neutralize the charge on the framework, but also water and salt molecules. Figure 1.3 shows a schematic representation of silica and alumina tetrahedra, while Figure 1.4 shows a representation of the sodalite unit found in many zeolite frameworks.

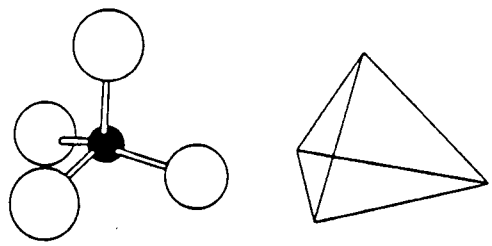

Figure 1.3 **Representations of $[SiO_4]^{4-}$ and $[AlO_4]^{5-}$ tetrahedra**

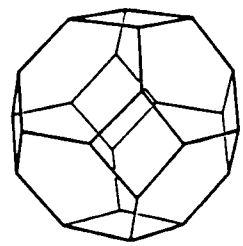

Figure 1.4 **The truncated octahedron or sodalite unit in zeolite frameworks**

The very open frameworks of zeolites provide an environment in which cations and water molecules have a high degree of mobility, resulting in good ion-exchange properties and the capacity for reversible hydration.

1.4 The Structure of Zeolites

Due to the way in which the silica and alumina tetrahedra are connected, zeolites typically have crystalline frameworks which result in regular pore structures. The sizes of these pores, as well as their nature are characteristic of the zeolite concerned. It has therefore been possible to classify zeolites in 3 major groups according to their pore systems.

1.4.1 Small Pore Zeolites

This group of zeolites have pore openings whose diameters are generally less than 5 Å. Their pore structures consist of interconnecting 8-membered oxygen ring systems. These

zeolites also contain cages ("supercages") whose dimensions are considerably larger than the pore openings. This group of zeolites, examples of which are erionite and chabazite, may only sorb straight chain molecules such as n-paraffins due to their narrow pore openings.

1.4.2 Medium Pore Zeolites

all of the medium pore zeolites of commercial catalytic interest are synthetic in origin. This group is often called "pentasils" because their frameworks also contain 5-membered oxygen rings and, in general, are more siliceous than other zeolites. With the exception of ZSM-5 and ZSM-11, which have 2-dimensional interconnecting networks, the channel systems of this group are unidirectional and non-intersecting.

1.4.3 Dual Pore and Large Pore Zeolites

These zeolites have interconnecting channels of either 12- and 8- or 10- and 8-membered oxygen ring openings. Examples of zeolites with dual pore systems are mordenite, offretite and clinoptilolite. While the smaller channels are accessible only to small molecules, the large pores may sorb both small and large molecules, resulting in some quite distinct catalytic properties. Due to stacking faults the dual pore catalysts may behave as small pore zeolites for some reactions.

Faujasite and mazzite are examples of large pore zeolites, with pore opening diameters of greater than 7 Å. The large pore openings are due to the presence of 12-membered oxygen rings. Table 1.6 lists some zeolites according to their pore systems and pore sizes.

Table 1.6 Pore Structure of Zeolites (Chen and Garwood, 1986)

Name	Pore System	Pore Dimensions (Å)
Bikitaite	8	3.2 x 4.9
Brewsterite	8	3.2 x 5.0
Chabazite	8	3.6 x 3.7
Dachiardite	10; 8	3.7 x 6.7 ; 3.6 x 4.8
TMA-E(AB)	8	3.7 x 4.8
Edingtonite	8	3.5 x 3.9
Epistilbite	10; 8	3.2 x 5.3 ; 3.7 x 4.4
Erionite	8	3.6 x 5.2
Faujasite (X,Y)	12	7.4
Ferrierite	10; 8	4.3 x 5.5 ; 3.4 x 4.8
Gmelinite	12; 8	7.0 ; 3.6 x 3.9
Heulandite	10; 8	4.0 x 5.5 ; 4.4 x 7.2
ZK-5	8	3.9
Linde Type A	8	4.1
Linde Type L	12	7.1
Mazzite	12	7.4
ZSM-11	10	5.1 x 5.5
ZSM-5	10	5.4 x 5.6 ; 5.1 x 5.5
Mordenite	12; 8	6.7 x 7.0 ; 2.9 x 5.7
Offretite	12; 8	6.4 ; 3.6 x 5.2
Paulingite	8	3.9
Rho	8	3.9 x 5.1
Stilbite	10; 8	4.1 x 6.2 ; 2.7 x 5.7

1.4.4 Secondary Building Units

Due to the diversity of zeolites and their properties, and the subsequent difficulties one may have in classifying their topologies, Meier (1968) proposed that it may be more useful to describe and classify zeolites by referring to small groupings of linked tetrahedra or secondary building units. On the basis of the 25 zeolite structures then known, Meier suggested eight secondary building units required to describe zeolite frameworks. With the

discovery of other topologically distinct zeolite networks the list of subunits proposed by Meier has grown to the 16 SBUs shown in Figure 1.5 (Meier and Olson, 1978).

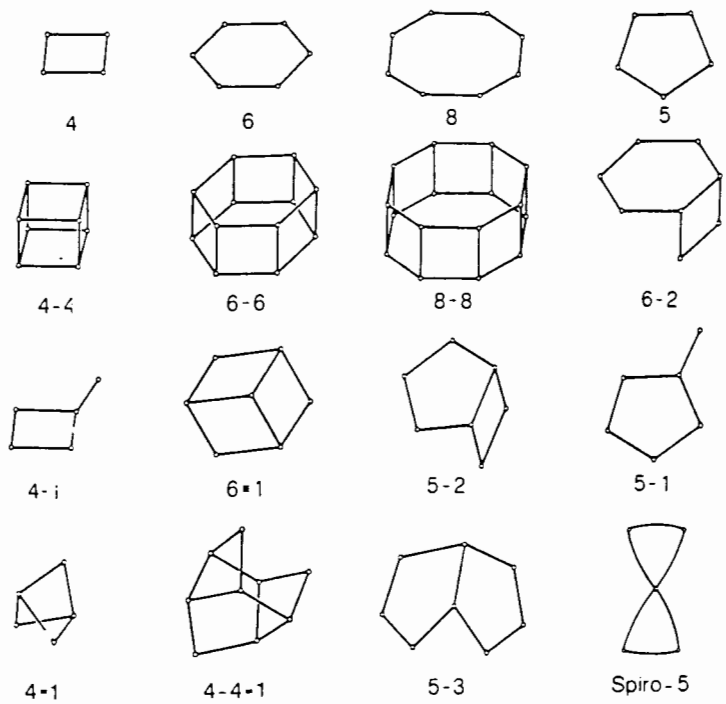

Figure 1.5 Secondary building units for zeolite identification

In Figure 1.5 the T atoms are represented by each corner or termination. Oxygen atoms are not shown, but lie near the midpoints of lines joining pairs of T atoms. Although most zeolite frameworks can be formulated using the secondary building units shown in Figure 1.5, these SBU's could also polymerize to form larger building blocks.

It should be emphasized at this point that the concept of secondary building units should only be used as a means of classifying different zeolite structure types. Although high-field ^{29}Si n.m.r. spectroscopy combined with ^{29}Si isotopic enrichment has provided conclusive evidence for the existence of at least 18 silicate species in alkaline solution (Harris and Knight, 1983), there is no evidence to suggest that the SBUs shown in Figure 1.5 bear anything other than a cursory resemblance to these species.

The topologies of some of the more well-known zeolites are presented in Figure 1.6 (Meier, 1971).

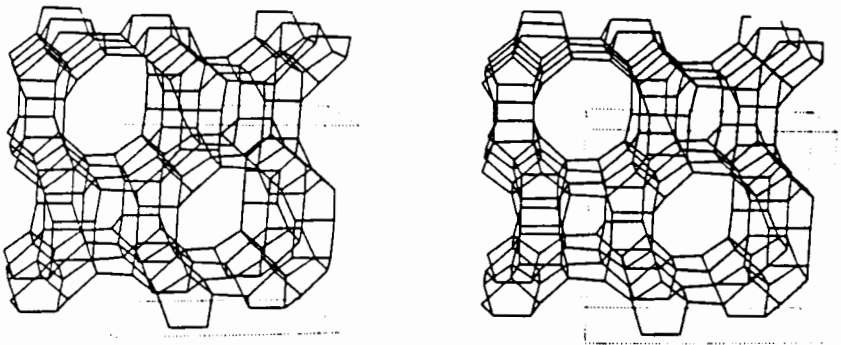

Stereodiagram of framework topology of mordenite

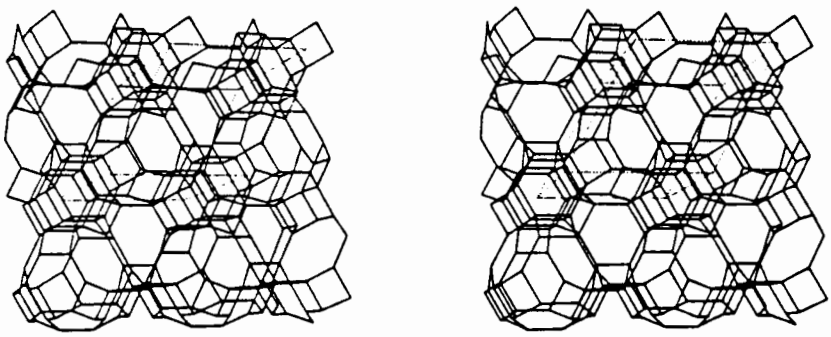

Stereodiagram of framework topology of erionite

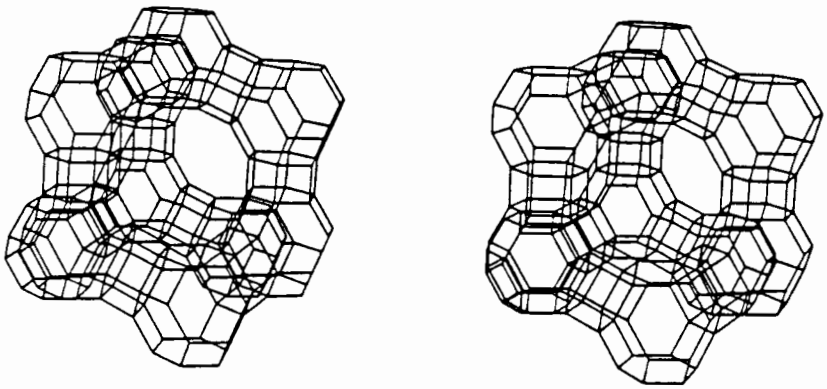

Stereodiagram of framework topology of faujasite

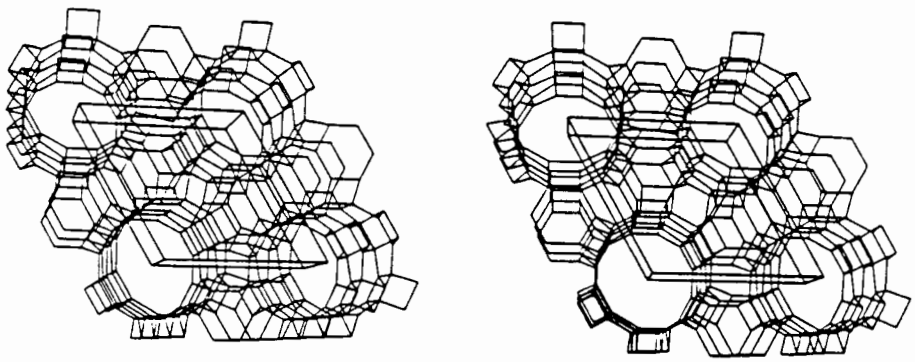

Stereodiagram of framework topology of mazzite

Figure 1.6 Topologies of mordenite, erionite, faujasite and mazzite

1.5 The Nature and Origin of Zeolite Acidity and Activity

As discussed earlier (see Section 1.3), zeolites are composed of tetrahedrally bound silicon and aluminium atoms joined by bridging oxygen atoms. The tetrahedral coordination of aluminium results in a net negative charge to the framework for each aluminium atom present. The charge on the framework is balanced by the presence of exchangeable cations in the zeolite channels. It is this charge balancing effect that is responsible for the catalytic acidity and activity of zeolites.

Zeolites are commonly synthesized in the sodium form. The open nature of the zeolite frameworks, however, enables ammonium ions to be readily ion-exchanged for the sodium ions. Upon heat treatment ammonia is evolved to yield the active protonic form of the catalyst proposed by Uytterhoeven *et al.* (1965) and shown in Figure 1.7 below:

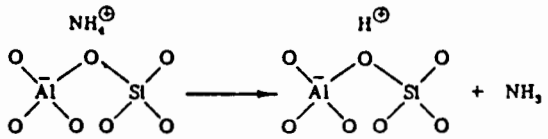

Figure 1.7 The generation of the proton form of zeolites

The acid sites of the zeolite are then generated by the reversible reaction shown in Figure 1.8 below:

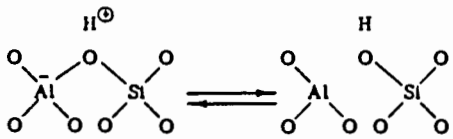

Figure 1.8 Zeolitic acid sites (Barrer, 1982)

The silanol OH group in the neighbourhood of the trigonal aluminium behaves as a powerful proton donor resulting in an acid site stronger than those present in amorphous silica-alumina cracking catalysts.

Ward (1967), in agreement with work done by other researchers (Uytterhoeven *et al.*, (1965), Hughes and White (1967)), observed that 3 hydroxyl group stretching bands were present in the infrared spectra of zeolite Y following high temperature deammoniation. These bands were at 3742 cm^{-1}, 3643 cm^{-1} and 3540 cm^{-1}. The band at 3742 cm^{-1} was ascribed to either SiOH hydroxyl groups terminating the lattice or to amorphous siliceous impurities. The 3540 cm^{-1} and 3643 cm^{-1} bands were ascribed to hydroxyl groups at different crystallographic locations. This was in agreement with the proposals of Eberly (1965) who concluded from adsorption experiments that the ca. 3550 cm^{-1} band was due to hydroxyl groups located in hexagonal prisms in the zeolite Y framework. The hydroxyl adsorption band at ca. 3640 cm^{-1} was ascribed to hydroxyls in supercages.

Ward (1967) noted that the hydroxyl group concentration of zeolite Y reached a maximum for calcination temperatures of 350 °C, whereafter it stayed constant until 500 °C. Above 500 °C the hydroxyl group concentration decreased with increasing temperature (see Figure 1.9). Ward concluded that the hydroxyl groups which functioned as Bronsted acids were largely responsible for catalytic activity.

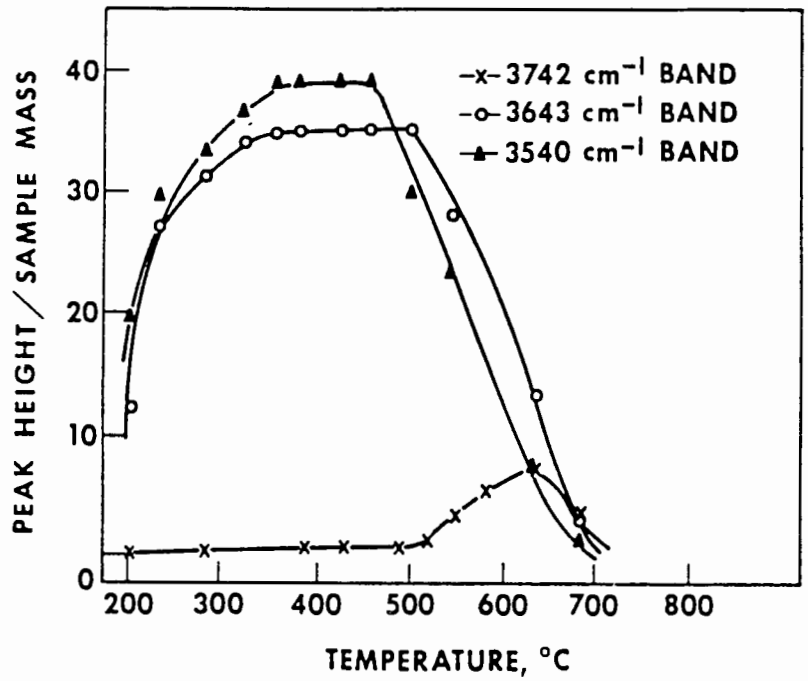

Figure 1.9 **Intensity of hydroxyl bands on H-zeolite Y as a function of calcination temperature**

While Bronsted acidity decreased rapidly above a calcination temperature of 500 °C, the concentration of Lewis sites was small below 475 °C but increased rapidly at higher temperatures (see Figure 1.10).

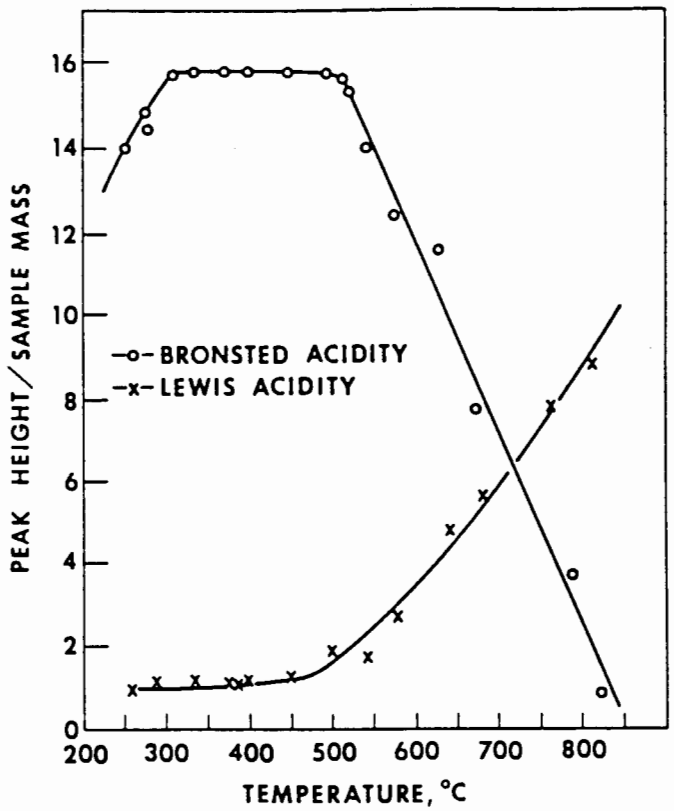

Figure 1.10 Acid site populations on zeolite Y as a function of calcination temperature

It was proposed that increasing calcination temperatures resulted in the dehydroxylation of Bronsted sites to give tricoordinated aluminium atoms responsible for Lewis acidity, according to the schematic depicted in Figure 1.11

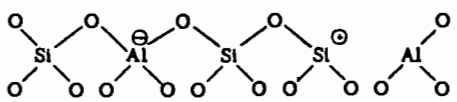

Figure 1.11 Tricoordinated aluminium as a Lewis site

Although Ward felt that Bronsted acidity was largely responsible for catalytic activity he did subsequently concede (Ward *et al.*, 1969) that other factors must be involved.

Indeed, Lunsford (1968) pointed out that catalytic data alluded to by Ward (1967) showed that while Bronsted acidity was decreasing in the range 500 °C to 600 °C, catalytic activity was clearly increasing. Lunsford proposed that partial dehydration of the catalyst at elevated temperatures could lead to the formation of defect sites of the type shown in Figure 1.12. Lunsford suggested that these sites could act inductively on local hydroxyls to form strong acids. An optimal concentration of these sites could explain the catalytic behaviour discussed by Ward (1967).

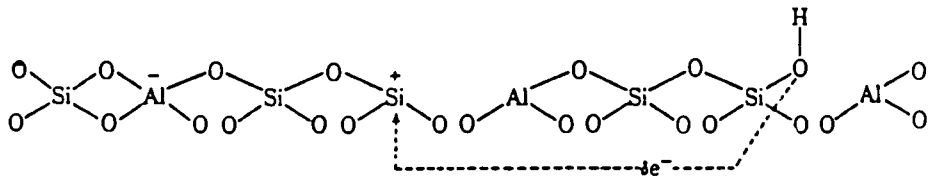

Figure 1.12 Acid site enhancement via the inductive effect

The tricoordinated Al atoms shown in Figures 1.11 and 1.12 corresponding to Lewis acidity have been the subject of much debate. Kühl, for example, using X-ray fluorescence, was unable to detect the presence of trigonal aluminium in dehydroxylated zeolite Y. Instead he found evidence for the presence of 28-44% of the aluminium in the catalyst being hexacoordinated (Kühl, 1976).

Subsequent work by Jacobs and Beyer (1979) on copper-Y-zeolite supported this and it was concluded that Lewis sites are not trigonal aluminium atoms but hexacoordinated (AlO^+) species leached from the framework during calcination.

1.6 Shape Selectivity

Shape selectivity is the ability of a catalyst to discriminate, often to a significant degree, between different sizes and shapes of molecules involved in a reaction, thereby influencing the outcome of a process. Zeolites possess well-defined pore openings which can enable a catalyst to selectively sorb some molecules into their pores while rejecting others on the basis of larger molecular size. This feature, combined with good catalytic activity, means that zeolites are ideal catalytic vehicles for shape selective catalysis.

Csicsery (1984) stated that if most acid sites are inside the catalyst pore structure, and if pore dimensions are small, then the fate of reactant molecules and product formation is governed by molecular dimensions and configurations. Indeed, Weisz (1973) had earlier

suggested that where the structural dimensions of a catalyst approach those of sorbing or reacting molecules then even subtle changes in the dimensions of a molecule can result in large changes in diffusivity. This was termed configurational diffusion and was used to explain the much faster rate of hydrogenation of trans-2-butene than cis-2-butene over Pt/zeolite A despite the small size difference of 0.2 Å (Chen and Weisz, 1967).

It is apparent, therefore, that a number of factors can play a role in determining the influence of shape selectivity. The sizes and diffusivities of reactant and product molecules as well as the nature and sizes of zeolite channels can be critical to shape selectivity. Furthermore shape selectivity may be controlled by at least three distinct mechanisms, viz: reactant, product and transition state shape selectivity.

Reactant selectivity occurs when only some of the reactant molecules are small enough to enter the catalytic pores. An example of reactant selectivity is shown in Figure 1.13.

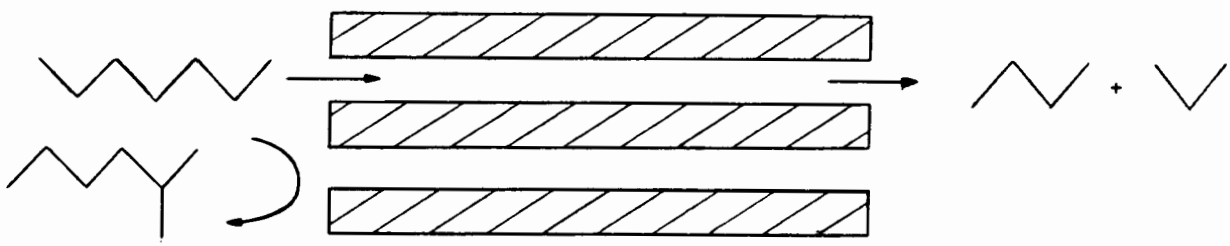

Figure 1.13 Reactant selectivity

Product selectivity occurs when product molecules, formed in a reaction, are unable to diffuse out of the catalyst due to their size or shape. Such a product molecule may then be cracked to smaller molecules which diffuse out of the catalyst pores or it may lead to catalyst deactivation (see Figure 1.14).

Restricted transition state selectivity occurs when both reactant and product are small enough to diffuse in and out of the catalyst, but where reaction intermediates are large and are prevented from forming due to insufficient space in the cavities and channels. This type of selectivity was first observed by Csicsery (1969) for the disproportionation of dialkylbenzene over mordenite.

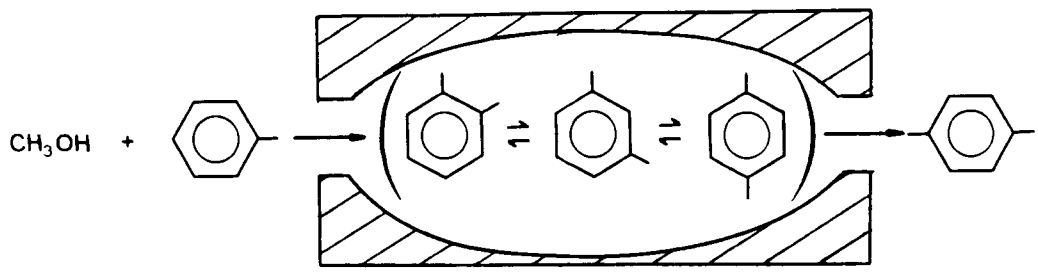

Figure 1.14 Product selectivity

Molecular traffic control was a concept used by Dérouane and Gabelica (1980) to explain the apparent lack of counterdiffusion effects in the ZSM-5 catalyzed conversion of methanol. These researchers proposed that, where catalysts have more than one type of intersecting channels, reactant molecules may diffuse in via one type of channel while products diffuse out of the other. The subsequent lack of counterdiffusion can result in increased reaction rates and altered selectivities. Comparison of ZSM-11, however, having only one type of interconnecting channel, with ZSM-5 showed no substantial differences in activity or product distribution for reactions such as methanol conversion and toluene methylation, thereby largely negating the importance of this effect. (Dérouane *et al.,* 1982).

Sequential adsorption experiments carried out by Pope (1981) also failed to support the molecular traffic control hypothesis although Dérouane disputed whether kinetic phenomena of the type suggested by this theory could be either proven or disproven by adsorption experiments.

Another type of shape selectivity was proposed by Fraenkel *et al.* (1984). More recently termed the "nest effect" by Dérouane (1986), this model proposed that acid sites in the half-cavities on the crystal surface could influence selectivity through the optimization of van der Waals interactions of adsorbed molecules with the catalyst framework. Dérouane (1986) indicated that this model could suggest that molecular shape selective effects may not necessarily be restricted to the intracrystalline volume of zeolites.

When investigating shape selectivity one needs to consider, however, not only the sizes of molecules involved, but also the dynamics of the molecular structures. A cage or window effect has been observed over erionite and zeolite T (Chen *et al.,* 1969; Gorring, 1973).

This window effect manifested itself in 3 ways:

- diffusion coefficient versus chain length shows a maximum at C_{12} and a minimum at C_8
- hydrocracking rates of n-hexane, n-decane and n-undecane are much higher than for n-octane
- n-C_7, n-C_8, and n-C_9 are not present in the cracked products of longer n-paraffins

This behaviour was ascribed to the fact that n-octane with a length of 12.82 Å fits almost exactly into the 13 Å cavity of erionite (Chen *et al.,* 1969). The result is that n-C_8 has a very low mobility. It stays up to 100 times longer in the cavity than any other molecule and consequently has more time to be cracked to smaller molecules. Dodecane, on the other hand, being longer, diffuses out of the cage quickly and is left almost intact.

In another example of the importance of molecular dynamics, Weisz *et al.* (1979) showed that a molecule as large as $C_{57}H_{104}O_6$ can easily attain, through molecular dynamics, a dimension small enough to enter the pores of ZSM-5.

Shape selectivity, therefore, in a number of ways, can play a critical role in determining the outcome of a reaction. The use of a shape selective catalyst, and modifications made to such a catalyst can even result in a catalyst which yields product distributions which deviate from thermodynamic equilibrium concentrations. A number of researchers have shown, for example, that modified shape selectivity can result in catalysts producing p-xylene yields in excess of equilibrium levels for toluene methylation (Kaeding *et al.,* 1981a and 1981b; Chen *et al.,* 1979; Ratnasamy *et al.,* 1986a).

1.7 Catalyst Characterization using Model Reactions

Maxwell (1986) in a review paper, discussed some of the more important industrial applications of shape selective catalysis. These included catalytic dewaxing, reforming, aromatic synthesis and the production of gasoline from methanol. In order to decide whether or not a catalyst is suited for a particular application, information on the following catalytic features must be known (Jacobs and Martens, 1986):

- the nature and strength of acid sites
- the intracrystalline void space and/or pore size
- catalytic stability

In the light of the discussion on shape selectivity, it is hardly surprising therefore, that a number of model reactions have been proposed for determining the intracrystalline void space of zeolites. Some of these model reactions are discussed below.

The constraint index test is useful for distinguishing medium pore zeolites from small and large pore zeolites. The constraint index is defined as:

$$\text{constraint index} = \text{c.i.} = \frac{\log (\text{fraction n-}c_6 \text{ remaining})}{\log (\text{fraction 3-methylpentane remaining})}$$

and depends on the selectivity of cracking n-hexane and 3 methylpentane simultaneously (Frilette, 1981). The constraint index is also approximately equal to the ratio of the first order cracking rate constants of n-C_6 and 3 methylpentane. For medium pore zeolites $1 \leq \text{c.i.} \leq 12$, with small pore and large pore zeolites lying to the right and left of this range, respectively.

While the constraint index has been used to identify the presence of medium pore zeolites from those with smaller and larger pores, it is not able to discriminate accurately between different medium pore zeolites. The meta-xylene conversion reaction, however, is far more suited to this task. This reaction has been used to probe medium pore zeolites with some success by Kokotailo *et al.* (1978a). More recently, Martens and Jacobs (1986) reviewed the potential of the n-decane hydroconversion reaction for characterization of zeolite pore structures. It has also been proposed by Weitkamp *et al.* (1988) that the molar ratio of isobutane and n-butane obtained by hydrocracking C_{10}-napthene is a function of increasing catalyst void space. These researchers called this ratio the Spaciousness Index and provided a list of indices for a variety of zeolites.

1.8 ZSM-5

1.8.1 Structure and Characteristics

ZSM-5 was first synthesized by researchers at Mobil (Argauer and Landolt, 1972) and is a medium pore zeolite which can be regarded as an end member of the pentasil family. The unit cell formula for the sodium form of ZSM-5 is shown below, with n typically having a value of 3 or less.

$$Na_nAl_nSi_{96-n}O_{192} \sim 16H_2O$$

The ZSM-5 framework is comprised of a configuration of linked tetrahedra joining to form a unit of eight five-membered rings (Figure 1.15a). These units can then be joined together to form chains (Figure 1.15b) which can be linked to form sheets which result in the 3-dimensional framework structure of ZSM-5 (Kokotailo *et al.*, 1978b).

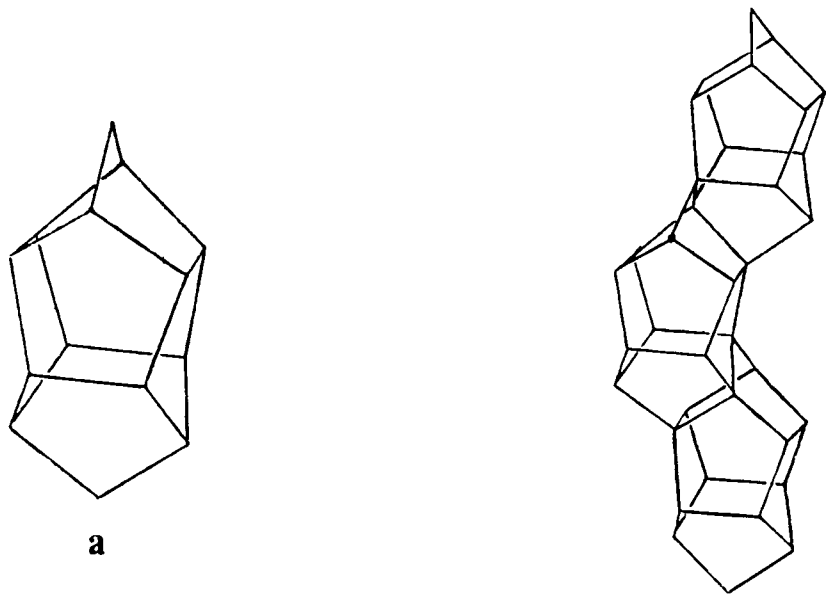

Figure 1.15 Characteristic building unit of ZSM-5 (a) and the linkeage to form chains (b)

The ZSM-5 framework contains two interconnecting channel systems : zigzag channels of near circular diameter running parallel to [001] and elliptical straight channels running parallel to [010] (Olson *et al.*, 1981). The straight channels of ZSM-5 have been shown to have pore diameters of ca. 5.2 x 5.8 Å, while the zigzag channels have pore diameters of ca. 5.4 x 5.6 Å (Meier and Olson, 1978). The different channel structures of ZSM-5 are shown in Figure 1.16.

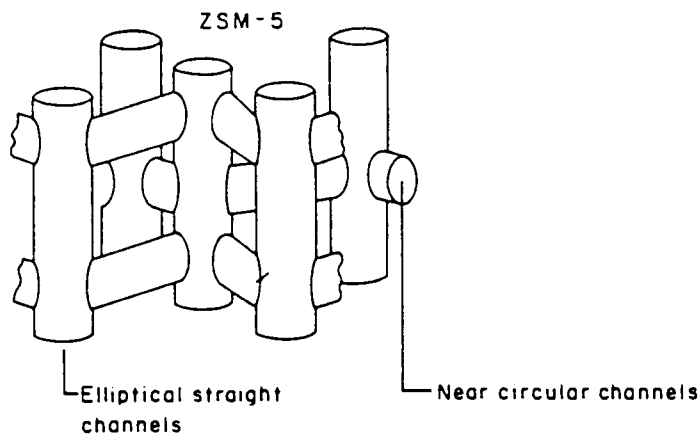

Figure 1.16 The channel structures of ZSM-5

It has been shown from X-ray diffraction studies that as-synthesized ZSM-5 crystallizes with orthorhombic symmetry and has lattice constants a = 20.07, b = 19.92 and c = 13.42 Å (Olson *et al.,* 1981). Monoclinic symmetry, however, has also been observed (Wu *et al.,* 1979). A computer simulated X-ray diffraction pattern for H-ZSM-5 is shown in Figure 1.17.

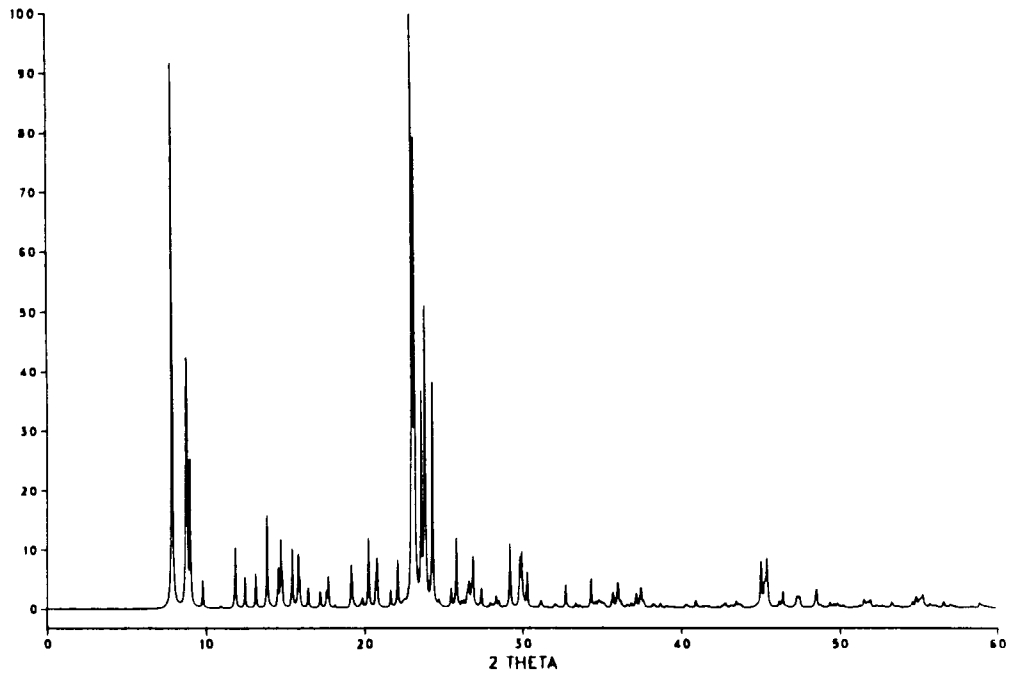

Figure 1.17 X-ray diffraction pattern of H-ZSM-5 (von Ballmoos, 1984)

It has been shown that the X-ray diffraction pattern, ZSM-5 pore size and volume, as well as framework density and refractive index are structural features and are essentially composition independent (Olson *et al.,* 1981). On the other hand, ion-exchange capacity,

catalytic activity and water sorption vary linearly with aluminium content and can be extrapolated to the end member of the ZSM-5 substitutional series, a pure silica ZSM-5. It was shown, for example, that the activity of a series of H-ZSM-5 catalysts for n-hexane cracking is a linear function of aluminium content (Olson *et al.*, 1980). Over a 400-fold change in Al content, the activity per aluminium of ZSM-5 for n-hexane cracking was constant.

In contrast to zeolite Y which was found to have 3 infrared hydroxyl group absorption bands, ZSM-5 has been shown to have two types of hydroxyl groups. These are characterized by absorption bands at 3720 cm^{-1} and 3605 cm^{-1}, with a small shoulder present at 3665 cm^{-1} (Védrine *et al.*, 1979). The 3720 cm^{-1} band was ascribed to terminal SiOH groups. Subsequent work by Auroux *et al.* (1983) confirmed this assignment. It was noted that the 3720 cm^{-1} band intensity increased with decreasing zeolite particle size due to increasing surface to bulk ratios. Jacobs and von Ballmoos (1982) found that for a pure ZSM-5 no 3720 cm^{-1} OH band was present. For a less pure sample the 3720 cm^{-1} OH band was found, the presence of which was ascribed to siliceous impurities. The absence of the 3720 cm^{-1} band in the pure sample was ascribed to highly crystalline catalyst with negligible terminal silanol groups due to the large crystal size. The ca. 3600 cm^{-1} OH band corresponded well with the Al content of the catalyst. When pyridine was adsorbed on the impure ZSM-5 a small band indicating Lewis coordinated pyridine was seen at ca. 1450 cm^{-1}. It was proposed that, for this catalyst, part of the Al was occluded in the siliceous impurities and does not give rise to strong Bronsted acidity.

Work carried out by Védrine *et al.* (1979) monitoring the 3605 cm^{-1} OH band as a function of calcination temperature suggested that dehydroxylation of the Bronsted sites on ZSM-5 only occurs at a calcination temperature of 400 °C or higher. This did not agree entirely with their results from infrared pyridine adsorption work in which the pyridinium ion band at 1550 cm^{-1}, which corresponds to pyridine adsorbed on a Bronsted acid, started decreasing only above a calcination temperature of ca. 500 °C. It was noted, however, that unlike earlier findings with zeolite Y (Ward, 1967), dehydroxylation of Bronsted sites to Lewis sites was not entirely reversible by rehydration. Moreover, dehydration was accompanied by a small amount of dealumination. This would tend to support the hypothesis discussed earlier in Section 1.5, namely that Lewis sites are not due to the presence of trigonal aluminium atoms, but to extraframework Al species.

1.8.2 ZSM-5 Synthesis

With the possible exception of "silicalite", the end member of the ZSM-5 series, zeolites are synthesized in an oxide system containing H_2O-SiO_2-Al_2O_3 - (alkali, alkaline earth, organic cations) at temperatures below 200 °C and at autogenous pressure (Sand, 1980). The synthesis of ZSM-5 was patented in the early seventies (Argauer and Landolt, 1972) and essentially followed the gel method of synthesis proposed in the 1940's by Barrer. The main variables of the gel method for zeolite synthesis are:

- Temperature
- pH
- the nature of the Si source
- the aluminium content
- the alkali metal cation
- the organic cation or template

Some of these variables and their influence on catalyst characteristics are discussed in the following section.

Si n.m.r. studies (Boxhoorn *et al.*, 1983) have provided evidence for the presence of the double five ring silicate shown in Figure 1.18. With a relatively small number of breaking and formation of Si-O bonds, the building block for ZSM-5 can be obtained (Kokotailo *et al.*, 1978b).

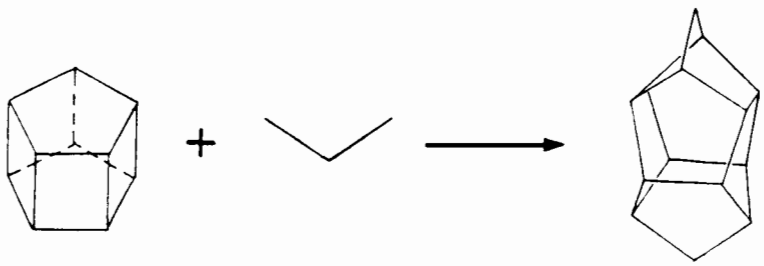

Figure 1.18 Formation of the ZSM-5 building block from a double 5-ring silicate

Provided the pH conditions are high enough (> 10.5 for the presence of $Al(OH)_4^-$) it has been proposed that an intermediate aluminosilicate species may be formed via a condensation reaction (Roozeboom *et al.*, 1983). These species could give rise to aluminium analogues of the siliceous ZSM-5 building blocks shown in Figure 1.18.

1.8.2.1 The role of the template during synthesis

Dérouane *et al.* (1981) found that tetrapropylammonium (TPA) ions which are used as a template during ZSM-5 synthesis (Argauer and Landolt, 1972) form complexes with aluminosilicate and silicate species, subsequently replicating the framework via stereospecific interaction. They called this the templating effect.

Rollmann (1983) showed that TPA^+/SiO_2 ratios greater than 0.05 are required for complete zeolite pore filling and correspondingly good synthesis yields. This corresponds to about 3-4 TPA molecules per ZSM-5 unit cell and agrees well with work done by Nagy *et al.* (1983) who found that 3.3-3.8 TPA cations are normally present in ZSM-5 and that these are located at channel intersections. It was suggested that if there are theoretically 4 channel intersections/unit cell then on average there is approximately 1 TPA molecule per channel intersection.

Rollman (1983) proposed that the synthesis reaction rate would no longer be influenced by the TPA content of the synthesis gel after complete pore filling of ZSM-5 has occurred. This essentially agreed with work carried out earlier by Calvert and Rollmann (1981) which suggested that at low TPA contents the template was important for zeolite nucleation and not really for subsequent crystal growth. It was proposed (Rollmann, 1983) that at complete pore filling the reaction mechanism changes from one of solution phase to one of surface nucleation.

Hou *et al.* (1986) found that, for TPA/SiO_2 ratios below 0.09, crystallization was strongly dependent on TPA content. This was fairly similar to the figure obtained by Howden (1982) who suggested that at a value of 0.08 pore filling was complete. These values are higher than that obtained by Rollmann (1983). They do not, however, necessarily contradict the explanation of pore filling proposed by him since syntheses of Hou *et al.* (1986) and Howden (1982) were carried out at higher temperatures and basicity. It is possible, therefore, that under these conditions Hoffmann elimination may occur according to:

$$(C_3H_7)_4N^+OH \rightarrow (C_3H_7)_3N + H_2O + C_3H_6$$

The importance of TPA to ZSM-5 synthesis was also underlined by the work of Rollmann and Valyocsik (1981). They found that at high TPA concentrations, surface nucleation is faster than the arrangement of aluminosilicate units around TPA ions. This resulted in a change in catalyst morphology under these conditions. Support for the influence of TPA on

catalyst morphology was provided by Gabelica *et al.* (1984a) who confirmed that size and structure forming/breaking properties of organic cations can substantially affect crystal morphology, size, composition and homogeneity. These researchers further suggested that crystal formation and growth is dependent on competitive TPA alkali-cation interactions. It was proposed that where different organic cations are used, the nature of phases formed are determined more by pore filling ability than by the location of the template at channel intersections. The clathrating or templating role played by the TPA ions, however, was emphasized. The chemical nature of the template was also felt to be an essential factor in determining the structure that is formed.

Subsequent work by Araya *et al.* (1986) largely agreed with the conclusions reached by Gabelica *et al.* (1984a). These researchers concluded that TPA acts as a true structure directing template while organic compounds such as piperazine, hexane and 6-diol act as hydrophobic pore fillers. 1,6-hexanediamine was thought to play an intermediate role.

Van der Gaag *et al.* (1985) found that 1,6-hexanediamine worked almost as well as TPABr at low Si/Al ratios for ZSM-5 synthesis. When looking at a number of amines and alcohols it was found that the range of starting Si/Al ratio giving pure ZSM-5 increased in the following order:

alcohols < amines < TPABr

The better performances of amines relative to alcohols was attributed to their ability to interact more efficiently with complex silicate anions via H complexes with terminal SiOH groups of the anion.

It has recently been shown that it is possible to synthesize ZSM-5 in the absence of any organic compound, but in a narrow set of well defined conditions (Jacobs and Martens, 1987; Bellussi *et al.,* 1988). Bellussi *et al.* (1988) for example showed that ZSM-5 could be synthesized without any templating or pore filling organic compound and in the absence of seeding (i.e. residual nuclei for crystallization) for both sodic and potassic systems. For these systems the OH^-/SiO_2 ratio was seen to control the silica solubility and consequently the amount of Al incorporation in the framework. The use of colloidal silica (Ludox) containing high molecular weight silicate species was seen to favour the formation of pure ZSM-5, as opposed to ZSM-5/mordenite mixtures. Tissler *et al.* (1989) have subsequently claimed that organic free synthesis produces crystals of homogeneous aluminium distribution resulting in enhanced selectivities for the disproportionation of ethylbenzene. They are also known, however, to produce large crystallites which are often catalytically undesirable.

1.8.2.2 The influence of pH

Rollmann (1983) stressed the importance of the OH^-/SiO_2 ratio claiming it as the dominant factor influencing nucleation and crystallization rates as well as crystal size and morphology. High basicity, it was stated, will give rise to small, dispersed crystals while low OH^-/SiO_2 ratios (< 0.01) will result in well defined large crystals. Gabelica *et al.* (1984a) went further and stated that low pH results in long crystallization times and incomplete gel transformations. High pH, on the other hand, produces ZSM-5 at much shorter synthesis times with smaller and more homogeneous crystals. It was suggested that at high OH^-/SiO_2 crystal growth and dissolution are competing phenomena. The result if an equilibrium is reached, is smaller crystals (Rollmann and Volyocsik, 1981). Generally then, the OH^- concentration should be high enough to maintain sufficient dissolved hydroxysilicate, but not so high as to prevent nucleation and crystal growth (Gabelica *et al.* 1984a). Moreover, increasing the OH^- concentration increases supersaturation leading to increased crystallization rates and decreases in crystallite size (Gabelica *et al.,* 1984a; Hou *et al.,* 1986).

Guth *et al.* (1986) have shown that ZSM-5 can be crystallized at much lower pH levels (pH = 3-10) than previous methods had allowed. This was achieved by preparing synthesis gels containing F^- anions and tetra-, tri- and di-propylammonium cations as templates. Not surprisingly the lower pH range resulting from the presence of the F^- anions can result in the production of large crystals without any undesired phases (Guth *et al.,* 1986; Patarin *et al.,* 1989).

1.8.2.3 The effect of aluminium content

It has been shown (Rollman and Valyocsik, 1981; Romannikov *et al.*, 1983; Chao *et al.,* 1981) that the crystallization rate and hence crystallite size increases when the Al content is lower. The more aluminium that there is present the more difficult it becomes for Al to be incorporated into the structure. Since Al incorporation is disruptive it seems logical that the presence of Al should encourage the growth of small crystals when compared to silicalite. Other workers in the field (Van der Gaag *et al.,* 1985) also observed the formation of larger crystals with lower Al content.

Another factor which may result in smaller crystals is the influence of agitation. This may have the effect of increasing the homogeneity of the synthesis mixture and hence of the aluminium contained in the synthesis gel and, consequently, may result in smaller crystals.

Another explanation for smaller crystallite sizes was proposed by Pohlisch *et al.* (1989) who found that for a potassium-nitrate-water system there was a decrease in particle size distribution with agitation. This was ascribed to attrition. Mechanical attrition, due to collisions of crystals with each other, was felt to limit the maximum particle size and reduce size distributions.

1.8.2.4 The effect of Si source

Gabelica *et al.* (1984a) observed that where polymeric silica was used as a silica source with Al rich ingredients, a small number of nuclei crystallize via liquid phase ion transportation producing large single crystals. At lower Si/Al and with monomeric sodium silicate as the silica source, crystallization proceeded via a solid hydrogel reconstruction producing numerous small microcrystallites. It was proposed that the two mechanisms were essentially dependent on the silica source and the relative concentrations of the reactants.

1.8.2.5 The effect of alkali metal cation

Gabelica *et al.* (1984a) suggested that depending on size, alkali metal cations have either a structure forming (templating) effect (Li, Na) or a structure breaking effect (K, Rb, Cs, NH_4). The electrostatic potential (proportional to r^{-1}) was thought to determine how efficiently the alkali metal cations compete with each other and with TPA for charge compensation of the aluminosilicate anions. It was found, for example, that for Na/(Na + TPA) < 0.3, ZSM-5 crystallized immediately. At higher Na/(Na + TPA) ratios crystallization of ZSM-5 becomes more difficult with other phases such as analcime and mordenite often being present.

Fegan and Lowe (1986) found that at a Na/TPABr value of 6.7 the synthesis yield was zero. This was reported to be in good agreement with work done by Flanigan and Grose (1977) who found it necessary to have less than 6.5 moles of alkali metal oxide (e.g. Na_2O) per mole of TPA_2O. Fegan and Lowe (1986) further noted that increased sodium content (and hence alkalinity) decreased crystallite sizes. Larger crystals formed at lower alkalinities and had the highest aspect (length/width) ratios. The crystallization rate was estimated to be a maximum at Na/TPABr = 3.

Jablonski *et al.* (1986) found that crystal morphology changed with different alkali metal cations (Na vs. K), and not with temperature. The presence of both Na and K resulted in

twinned spheroidal and tablet shaped crystallites. Na and K sources were oxides. Both ZSM-5 and ZSM-11 were present as products of crystallization. It was concluded that the organic cation acts not as a template, but affects the chemical thermodynamics and kinetics to promote the growth of one species over another; ZSM-11 intergrowths being favoured at high K/(K + Na) and lower temperatures (130 °C).

Mostowicz and Sand (1983) grew ZSM-5 agglomerates of up to 80 μm in diameter using sodium salt rather than sodium hydroxide as their alkali metal cation. Large crystal sizes, however, were felt to be due to low water content, resulting in increased reactant concentrations. Gharmani *et al.* (1983), however, suggested that using alkali metal salts rather than hydroxides as the cation source results in a considerable reduction in the pH of the gel. This should lead to decreased reaction rates and larger crystallites. Indeed, Mueller and Unger (1988) synthesized crystals up to 350 μm in length in an alkaline free mixture, although they attributed crystal size and yield to a dependence on water content and aluminium source.

1.9 Modified ZSM-5

Medium pore zeolites, with channels made of ten membered oxygen rings are, as mentioned earlier, ideally suited to shape selective catalysis. ZSM-5, in particular, has some unique shape selective properties due to its novel channel configuration. Not only can ZSM-5 discriminate and exclude molecules due to size constraints, but it can also discriminate between simple aromatics. It has been shown, for example, that p-xylene diffuses ca. 1000 times faster than the other two xylene isomers (Chen and Garwood, 1978).

Allied to the shape selective properties of ZSM-5 is the fact that the catalyst can be produced with activities and diffusion characteristics varying over a wide range by changing aluminium content and crystallite sizes. With the discovery that ZSM-5 can selectively convert methanol to hydrocarbons in the gasoline range (Meisel *et al.,* 1976) it is hardly surprising that much work has been carried out in an attempt to tailor the selectivity and activity of ZSM-5 for other reaction systems. Although ZSM-5 has been modified with a variety of elements ranging from gallium and zinc (Thomas and Liu, 1986; Ono *et al.,* 1988) to iron (Iton *et al.,* 1983; Szostak and Thomas, 1986; Szostak *et al.,* 1987) to platinum (Inui and Okazumi, 1984) the following sections will look more closely at modifications of ZSM-5 by boron, phosphorus and steam dealumination.

1.9.1 Boron Modified ZSM-5

Barrer (1982) suggested that substitution of aluminium in a zeolite framework by an element such as boron should be possible. Indeed, it has been shown by Ione *et al.* (1984) that boron can occupy a tetrahedral position in the ZSM-5 lattice. These researchers hypothesized that the acid strength of such a catalyst should depend, to a rough approximation on the value of $^{e}/_{r}$. Consequently, they concluded that such a boralite catalyst should be more acidic than the Al form. Boron incorporation in the ZSM-5 framework has also been confirmed by X-ray diffraction (Meyers *et al.,* 1985; Taramasso *et al.,* 1980, Coudurier *et al.,* 1987) as well as by ^{11}B MAS n.m.r (Coudurier and Védrine, 1986; Wendlandt *et al.,* 1988; Kessler *et al.,* 1987). Moreover, these studies have shown that boron incorporation results in shrinkage of the ZSM-5 unit cell.

Weitkamp *et al.* (1986) suggested that it should be possible to control the shape selective properties of pentasil-type zeolites by controlled isomorphous substitution of boron. Galya *et al.* (1985) found that for a sepiolite bound boralite (750 ppm Al), oligomerized propene products were less branched than for unmodified ZSM-5 of SiO_2/Al_2O_3 = 77.5. Conversion levels were good : 96.5 wt% at 315 °C compared to 64.4 wt% for unmodified ZSM-5 at the same temperature and feed rate (WHSV = 1.0).

Further evidence of enhanced shape selectivity was provided by Wendlandt *et al.* (1988) who determined constraint indices using a pulse micro-reactor. The c.i. increased when there were more than 2 boron atoms per unit cell, leading these researchers to conclude that altered shape selectivity as a result of boron inclusion is possible. No evidence was found, however, for correlations between activity and boron content. Instead catalyst acidity and activity were found to be strongly dependent on the Al concentration, a conclusion reached by other researchers. Sayed *et al.* (1989) for example, found that although boron incorporation did enhance selectivity to p-xylene for toluene disproportionation, this was at the expense of both catalytic acidity and activity. Chu *et al.* (1985) provided convincing evidence that the catalytic activity of boralite for a number of reactions was due mainly, if not entirely to trace amounts of Al in the ZSM-5 framework. It was concluded that the acidity of the B(OH)Si site proposed by Scholle *et al.* (1984) is dependent on the position of the following equilibrium:

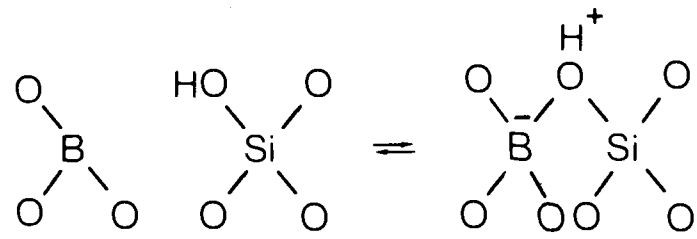

and that this equilibrium lies almost completely to the left

Ratnasamy *et al.* (1986b) found only the low temperature peak for ammonia temperature programmed desorption. The enhanced concentrations of propene and butene for methanol conversion and reduced aromatics were ascribed to the presence of weak Si-OH-B acid sites : strong enough to form light olefins by dehydration and alkylation, but not strong enough to further oligomerize these to C_5^+ products. Cornaro and Wozchiechowski (1989) found boron in the lattice resulted in sites capable of double bond shift, but not skeletal isomerization, the next most demanding hydrogen conversion reaction. Increased coke formation and enhanced deactivation rates were observed. Similar observations were made by Chang *et al.* (1985) who noted instability of framework boron and its ready substitution by aluminium.

Evidence of the mobility of boron in the ZSM-5 framework has been observed by a number of researchers (Datka and Piwowarska, 1989; Kessler *et al.*, 1987). Coudurier *et al.* (1987) using n.m.r. and Fourier transform infrared spectroscopy provided evidence for the presence of 4-coordinated boron in the hydrated state and 3-coordinated boron in the dehydrated state. The reversible transformation of 4-to 3-coordinated boron, while unusual in zeolites was ascribed to the thermal instability of B in the lattice. Further evidence of this instability was provided by Bodart *et al.* (1986) who demonstrated the preference of the MFI framework for Al compared to B, and by Sayed (1987) who on the basis of infrared work clearly demonstrated the presence of water as a mobility determining factor.

On the basis of infrared work which showed B-ZSM-5 to have two hydroxyl group bands at 3740 cm^{-1} (in common with ZSM-5) and one at ca. 3725 cm^{-1}, it was concluded that the B(OH)Si site was more acidic than SiOH but less than Al(OH)Si. A further band at 3460 cm^{-1} was ascribed by Datka and Piwowarska (1989) to a strong hydrogen bond between two adjacent OH groups, probably corresponding to the kind of hydrogen bonding that occurs when boron is bonded to silicon according to the site proposed by Sayed (1987) and shown below.

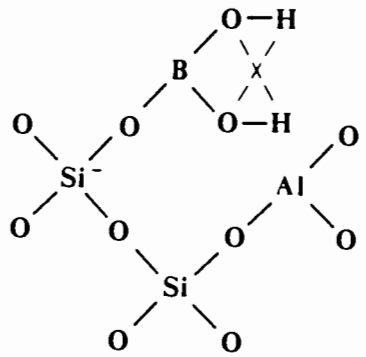

Hölderich *et al.* (1984) showed, for methanol conversion, that although boralites had lower activities than unmodified ZSM-5, they also had reduced tendency to form aromatics, resulting in catalysts with longer time-on-stream before the onset of deactivation. Modification of a boralite catalyst (10 ppm Al) with HCl and HF resulted in a catalyst with significantly increased activity and lifetime. This was accompanied by an increase in C_2-C_4 olefin selectivity. Transfer of Al into the zeolite, after mixing boralite with alumina followed by hydrothermal treatment, has also been shown to considerably enhance the cracking activity of the catalyst as measured by the α - test (Chang *et al.,* 1985).

While there appears to be agreement amongst many researchers about the effect of boron in the framework on acidity and activity, controversy still exists about its effect on shape selectivity. Coudurier and Védrine (1987) saw no appreciable shape selectivity changes due to the presence of lattice boron. Impregnation with boron, however, led to a decrease in acidity and hence activity but sharply enhanced shape selectivity as evidenced by increased para-xylene in the products of toluene methylation and disproportionation. It was shown that impregnation with H_3BO_3 followed by calcination could result in boron partly isomorphously substituting for Si and/or Al. Excess of boron created additional diffusional constraints and further enhanced shape selectivity.

Similar conclusions were reached by other researchers (Sayed, 1987; Sayed and Védrine, 1986; Sayed *et al.,* 1986, Kaeding *et al.,* 1981a). Sayed (1987) suggested that for non-calcined samples boron exists as H_3BO_3, but that pretreatment at 0.1 mPa/673 K effects the condensation of H_3BO_3 with Bronsted acid sites into the $=Si\text{-}O\text{-}B(OH)_2$ species shown previously. It has also been shown that impregnation with boric acid can induce pore plugging (Sayed *et al.,* 1987, Kaeding *et al.,* 1981a) and that this is accompanied by remarkably enhanced shape selectivity (Kaeding *et al.,* 1981a).

1.9.2 Phosphorus Modified ZSM-5

A number of researchers have proposed that modifying the pore geometry and surface acidity of ZSM-5 by impregnation with various phosphorus compounds enhances shape selectivity effects and reduces deactivation (Nunan *et al.*, 1984; Kaeding *et al.*, 1980, & 1981a, 1981b; Chandawar *et al.*, 1982).

Kaeding *et al.* (1980, 1981a & 1981b) showed that toluene would be selectively alkylated with methanol to produce over 90% of the para isomer of xylene and proposed that this was due to a reduction in effective pore openings as well as to poisoning of non shape selective surface sites. In a correlated study, Chen *et al.* (1979) found that crystal size could play a significant role in determining the shape selectivity of ZSM-5 catalysts for the m-xylene isomerization reaction. Increasing crystal size from 0.5 to 3 μm resulted in para-xylene yields in excess of the thermodynamic equilibrium.

Nunan *et al.* (1984), in a toluene methylation study found that high para-xylene selectivities were observed when ZSM-5 was poisoned with quinoline and trimethylphosphite while infrared work showed that trimethylphosphite could poison both external and internal sites. These researchers, on the basis of reaction work, ascribed selectivity changes to poisoning of surface hydroxyls. Jinxiang *et al.* (1988) and Jentys *et al.*, (1989) noted reduced activity levels for methanol conversion and benzene ethylation, respectively, when impregnating ZSM-5 with phosphoric acid. Reduced activity levels and enhanced selectivities were in both cases ascribed to the elimination of strong Bronsted acidity which was monitored by temperature programmed desorption of ethylamine and ammonia.

Jentys *et al.* (1989), in pyridine infrared experiments, found that increasing the amounts of impregnated phosphoric acid and trimethylphosphite on ZSM-5 led to a decrease in both catalytic activity as well as the amount of strong acidity. Phosphorus modification converted strong Bronsted sites into weak sites and it was suggested that OH^- ion substitution by H_3PO_4 takes place during impregnation. They further suggested that a significant amount of dealumination also occurs, leading to a decrease in overall acidity. Vinek *et al.* (1989) noted that phosphoric acid and trimethylphosphite impregnation reduced the amount of strong Bronsted acidity of ZSM-5, as measured by pyridine desorption. They proposed that phosphorus modifies the Bronsted acid sites according to the model shown below:

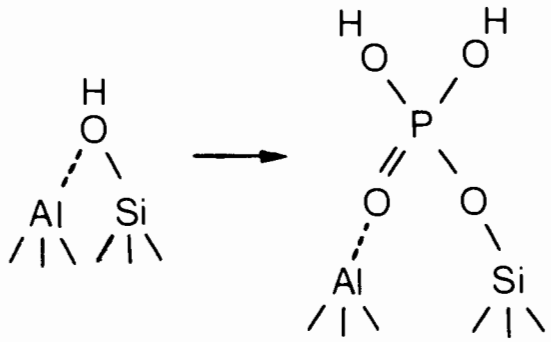

Substitution of the Bronsted hydroxyl group by $H_2PO_4^-$ has three implications, namely,

i) strong Bronsted sites are converted into weak Bronsted sites
ii) the number of acid sites increases
iii) because the OH^- and $H_2PO_4^-$ groups have almost the same electronegativity, the acid strength of the remaining unmodified OH^- groups is unaffected

Corresponding to reduced strong acidity, Vinek *et al.* (1989) observed a decrease in activity for toluene alkylation and hexane cracking.

In another phosphorus impregnation study, Védrine *et al.* (1982) found that trimethylphosphite impregnation resulted in reduced acidity. The strongest sites were, however, unaffected, resulting in a catalyst which showed enhanced selectivity to C_2 and C_4 olefins and reduced amounts of C_9^+ aromatics in methanol conversion. No decrease in catalytic activity was observed.

Recently it has been shown for the SAPO class of catalysts, that the inclusion of phosphorus in the aluminosilicate framework results in a more weakly acidic catalyst than ZSM-5 (Inui *et al.*, 1990). The result is a catalyst that has a lower activity than ZSM-5, but which is highly selective to light olefins for methanol conversion. This is in keeping with the suggestion that olefins produced from methanol react to give a paraffinic/aromatic mixture and that olefin formation could be decoupled from aromatization by a combination of high temperature and low acidity (Chang *et al.*, 1984). Dejaifve *et al.* (1984) have also showed that for methanol conversion it is the strong sites that are responsible for the dehydrocyclization of C_6^+ olefins into aromatics.

1.9.3 Hydrothermally Dealuminated ZSM-5

Dealumination has traditionally been of significant interest in heterogeneous acid catalysis due to the practical problems it may pose to industrial catalysts. It is hardly surprising, therefore, that substantial work has been carried out on the effect of water vapour and hydrothermal treatments on both the acidity (Lago *et al.*, 1986) and selectivity (Namba *et al.*, 1986) of H-ZSM-5. Dealumination of the zeolite catalyst has been performed both chemically (Dwyer *et al.*, 1981) and hydrothermally (Nayak *et al.*, 1984).

1.9.3.1 Characterization of dealuminated ZSM-5

1.9.3.1.1 Infrared studies

Infrared (IR) investigations carried out by Loeffler *et al.* (1988) showed that for unmodified ZSM-5 there is a linear relationship between framework Al content and the frequency of the asymmetric lattice stretching vibrations. When catalysts were dealuminated by steaming (500 °C steam for between 1.5 and 24 hours) it was found that the IR band of the asymmetric T-O-T stretching vibration shifted from 1090 cm^{-1} to 1104 cm^{-1}. This shift corresponded linearly to the degree of dealumination. Examination of the ratio of the 550 cm^{-1} to 450 cm^{-1} intensities showed that no destruction of the zeolite framework had taken place. Yakhaev *et al.* (1986), in similar experiments, found no evidence to suggest lattice breakdown. This supported earlier findings which showed ZSM-5 to have a far higher steam stability than many other zeolite catalysts (Wang *et al.*, 1979).

Loeffler *et al.* (1988) further showed that short steaming times increased the intensity of the 3665 cm^{-1} band, and proposed that this was due to increasing amounts of non-framework aluminium. They proposed that further increases in steaming times could lead to dehydroxylation of non-framework Al species, with the result that the 3665 cm^{-1} band intensity is not directly proportional to the amounts of extra-framework Al in dealuminated catalysts. This finding was supported by ^{1}H MAS n.m.r. studies carried out by Engelhardt *et al.* (1987) on the same catalysts. Loeffler and his co-workers (1988) saw no increase in the number of terminal OH groups (3745 cm^{-1} band) that were expected to appear due to the presence of lattice defects arising as a result of dealumination. They therefore proposed an interaction between non-framework Al and terminal OH groups.

In another infrared study Dessau *et al.* (1987) provided evidence, however, for both the

presence of internal silanol groups as well as for the annealing of these sites upon steam treatment. Steam treatment was carried out for 1 hour at 25 Torr water vapour pressure and 538 °C.

A possible mechanism for the annealing of terminal hydroxyls, by high temperature steaming has been proposed by Chen (1981) and later by Hunger *et al.* (1987).

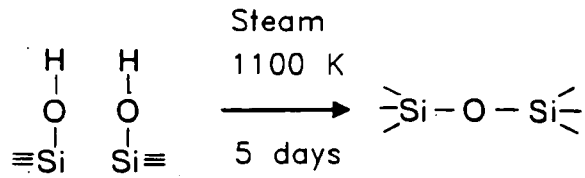

In a response to the work carried out by Dessau *et al.* (1987), Kraushaar *et al.* (1988) suggested that silanol groups exist in clusters where T atoms are missing from the lattice. Although they conceded that the evidence for annealing of lattice defects appears to be substantial, they proposed that during steaming the vacancies at lattice defects may in fact be migrating to the external surfaces of the zeolite, possibly via a T- jump mechanism.

Infrared studies of pyridine adsorbed on ZSM-5 at various temperatures carried out by Topsøe *et al.* (1986) showed that higher steaming temperatures lead to a decrease in the number of pyridinium ions corresponding to a loss of framework Al.

1.9.3.1.2 N.M.R. studies

In ^{29}Si and ^{27}Al MAS n.m.r. investigations it was found that for steam and $SiCl_4$ dealuminated zeolite Y, extra-framework Al can exist as octahedrally coordinated Al or as aluminium in what is either a pentacoordinated state or a distorted tetrahedral environment (Sanz *et al.*, 1988).

Samoson *et al.* (1987) came to similar conclusions about ZSM-5 steamed for various times at 500 °C. In ^{27}Al n.m.r. spectra they assigned peaks at ca. 60 ppm, 30 ppm and 0 ppm to tetrahedral framework Al, extra-framework Al in a distorted tetrahedral environment and octahedrally coordinated extra-framework Al, respectively. A fourth signal at 74 ppm has recently been ascribed to distorted tetrahedral framework aluminium (Hamdan *et al.*, 1989).

In an ^1H MAS n.m.r. study of some of the same catalysts used by Samoson *et al.* (1987), Engelhardt *et al.,* (1987) found that steamed ZSM-5 gave spectra with three characteristic lines having chemical shifts of 2.5 ppm, 4 ppm, and 7 ppm. These peaks were attributed to hydroxyl groups of non-framework hydroxyaluminium species (AlOH), acidic bridging hydroxyl groups (SiOHAl) and to terminal silanol groups (SiOH), respectively. The origins of a shoulder at ca. 4 ppm and a second weak peak at ca. 1 ppm were, however, unexplained. It was found that increasing the severity of the steam treatments led to increasing dealumination. This was seen as a decrease in the intensity of the peak at 4 ppm and an increase in the peak at 2.5 ppm. The AlOH peak intensity did not, however, correlate directly to the amount of extra-framework aluminium in the catalysts. This was ascribed to dehydroxylation reactions of non-framework hydroxyaluminium species.

The intensity of the SiOH peak decreased with increasing steam treatment suggesting that some annealing of lattice defects was taking place. These researchers felt that this may occur via Si migration. Leaching was found to increase the intensity of the SiOH peak, however. This was attributed to either the creation of additional lattice defects or partial amorphization of the ZSM-5 structure. Dessau *et al.* (1987) found that steaming catalysts enhanced the resolution of Si n.m.r. signals which they ascribed not to the loss of framework Al, but rather to the annealing of internal silanol groups.

In an unrelated n.m.r. study of dealuminated ZSM-5, Sano *et al.* (1987) found that the rate of dealumination is second order with respect to framework Al concentration. The same researchers also provided evidence that the introduction of alkali metal cations by ion-exchange inhibits the dealumination of ZSM-5 by steaming (Suzuki *et al.,* 1987).

1.9.3.1.3 Temperature programmed desorption studies

Temperature programmed desorption of pyridine was carried out by Nayak *et al.* (1984) on ZSM-5 catalysts steamed at various temperatures and water vapour partial pressures. It was found that both the total number of acid sites as well as the number of strong sites were reduced by increasing the steam pressure, period and temperature during hydrothermal treatment. XPS data also showed a significant increase in the Al concentration on the zeolite surface.

Ammonia t.p.d. experiments carried out by Lago *et al.* (1986) also showed that increasing steam pressure reduced the total acidity of ZSM-5. Similar results were obtained by Yashima *et al.* (1981) who saw a substantial drop in both strong (Bronsted) acidity as well as a decrease in weak acidity (often ascribed to the presence of silanol groups).

1.9.3.2 The effect of steaming on catalytic activity and selectivity

Yakhaev *et al.* (1986) after steaming ZSM-5 at 750 °C for 6 hours found that the activity for hexane cracking was significantly reduced. This drop in activity was accompanied by an increase in selectivity to aromatics.

When Topsøe *et al.* (1986) steamed ZSM-5 at 1 atmosphere water vapour pressure for 5 hours at different temperatures, activities for n-hexane cracking as a function of temperature did not show simple straight line relationships. Instead a maximum activity was found for a catalyst steamed at 623 K. The slope of the pyridine desorption curve for this catalyst was the flattest, indicating that the acid sites on this catalyst were stronger than those of catalysts calcined at higher and lower temperatures.

Lago *et al.* (1986) also found that severe steaming resulted in catalysts of substantially reduced activity, where the loss in activity was proportional to the amount of framework aluminium removed from the lattice. Mild steaming (540 °C, 2.5 hours, < 200 Torr steam) resulted in catalysts with up to four-fold activity increases for hexane cracking relative to unmodified ZSM-5, (see Figure 1.19).

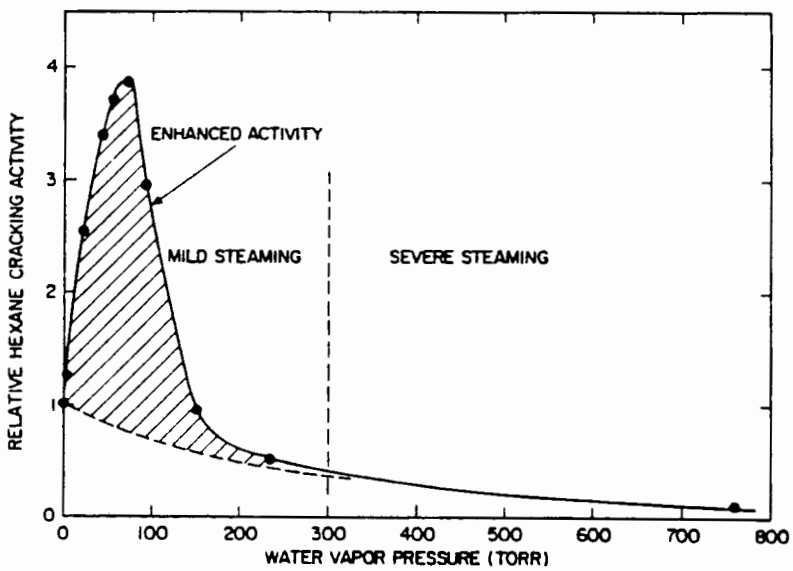

Figure 1.19 The effect of steaming pressure on the hexane cracking activity of H-ZSM-5 of Si/Al = 35 (Lago *et al.*, 1986).

The degree of activity enhancement was found to be a strong function of the tetrahedral Al content of the starting zeolite. These researchers proposed that mild steaming results in sites of enhanced activity which are only formed in the presence of paired Al centres. Very little or no activity enhancement was found for catalysts with silica/alumina ratios higher than about 200. For a ZSM-5 catalyst with an Si/Al ratio of 35, maximum activity occurred when 20-25% of the tetrahedral aluminium was removed. This corresponded to a concentration of enhanced sites to tetrahedral aluminium of about 6%. From data obtained over cesium exchanged catalysts these researchers concluded that steam enhanced acid sites may be as much as 45 times as active as unmodified sites for hexane cracking at 538 °C.

Nayak *et al.* (1983, 1984) found that steaming ZSM-5 at a variety of conditions produced catalysts with reduced activity for xylene isomerization, cumene cracking, methanol and ethanol conversion reactions. In the case of the alcohol conversion reactions aromatization decreased. Concentrations of benzenes and toluenes in the aromatics also decreased. Concentrations of xylenes, ethylbenzenes and C_9^+ aromatics increased while p-/m-xylene and p-/o-xylene ratios increased. Although increased aromatization is usually the result of increased acid strength, Nayak and his co-workers attributed this to a dependence of aromatization and the distribution of aromatics on secondary reactions (such as isomerization and dealkylation). The increase in p-xylene selectivity was ascribed to modifications of the pore channels as a result of extra-framework aluminium species. Kürshner *et al.* (1987) ascribed such selectivity changes after hydrothermal treatment to diffusion barriers caused by the presence of non-framework Al.

In an effort to modify the selectivity of ZSM-5, Namba *et al.* (1986) dealuminated the external catalyst surfaces by treating ZSM-5 with $SiCl_4$ vapour at temperatures between 723 K and 923 K. They proposed that since the external surface acid sites of ZSM-5 reduce catalyst selectivity, selective removal of the Al on the catalyst surface should provide a ZSM-5 catalyst with enhanced shape selectivity without a significant reduction in activity. These researchers found that it was possible to selectively dealuminate ZSM-5 in this way. They further found that dealumination was more surface selective the higher the temperature. ZSM-5 thus treated exhibited higher shape selectivity for the alkylation of 1,2,4-trimethylbenzene with methanol than unmodified ZSM-5. Moreover, modified catalysts showed reduced deactivation rates for the cracking of cumene.

Yashima *et al.* (1981) had earlier used a similar approach when steaming ZSM-5 at 950 °C. They found that p-xylene selectivity could be considerably enhanced by almost completely removing catalyst activity. They concluded that to favourably enhance selectivity to p-

xylene for xylene isomerization reactions, the active sites on the catalyst external surface should be removed in order to force the reaction to take place in the pores. The catalysts modified in this way, however, had greatly reduced activities; no doubt due to the high degree of dealumination that had taken place, not only on the external surface. This was born out by ammonia t.p.d. studies which showed the catalysts to have almost no strong Bronsted acidity and only small amounts of weak acidity.

1.10 Objectives of Research

The objective of this research was to investigate the effect of boron, phosphorus and hydrothermal dealumination on the activity and selectivity of ZSM-5 for propene oligomerization. Boron and phosphorus modifications, in particular, were carried out with a view to favourably enhancing the selectivity of ZSM-5 to linear oligomer products. When studying the effect of boron and phosphorus modification on ZSM-5, the following questions were addressed.

(i) What effect does boron inclusion in the zeolite framework have on catalytic activity and selectivity? Are changes in activity the result of trace aluminium only?

(ii) Can the activity of boralite catalysts be enhanced by fluorination?

(iii) Can the selectivity of ZSM-5 be altered by impregnation with boron and phosphorus compounds?

(iv) What effect does phosphorus inclusion in the synthesis gel have on catalyst activity and selectivity?

The steam dealumination work was carried out in an attempt to elucidate the role played by steaming on the activity and lifetime of zeolite catalysts. A number of parameters were examined in an attempt to achieve the activity enhancement claimed by some researchers.

The steaming parameters investigated were:

1. steaming temperature
2. steam partial pressure
3. steaming time
4. wet stream (steam) flowrate

While propene oligomerization is the main probe reaction investigated, hexene oligomerization was used as a probe reaction for much of the dealumination study. Ortho-xylene isomerization was also used to examine selectivity changes due to modifications.

Chapter 2

Experimental

EXPERIMENTAL

2.1 Catalyst Synthesis

2.1.1 Synthesis Mixture

The basic synthesis mixture used for the synthesis of ZSM-5 of Si/Al = 40 is based on the patent by Argauer and Landolt (1972). The molar composition for this mixture is listed in Table 2.1. Also listed are the chemical masses required by an autoclave with a volume of 250 ml.

Table 2.1 Composition of the ZSM-5 Synthesis Mixture

Component	Molar Composition	Chemical Source and Purity	Mass (g)
Na^+, OH^-	8.2	NaOH (Merck, pure)	2.16
Si	40.0	Ludox HS-40 (Dupont. tech. grade)	39.70
TPABr	17.6	TPABr (Fluka, >98%)	31.13
H_2O	992	distilled water	118.1
Al	1.0	$Al(OH)_3$ (BDH, pure)	0.5154

(Ludox ~ 40 wt % colloidal silica)

$Al(OH)_3$ and NaOH were dissolved in a minimum of water at boiling point. This solution was then placed in a teflon beaker in a stainless steel autoclave. A teflon stirrer bar was added and the $Al(OH)_3$ - NaOH mixture was stirred using a magnetic stirrer (see Section 2.1.2). To this solution was added a solution of the template, TPABr, while stirring. The Ludox was then added dropwise while agitating.

To synthesize catalysts with different Si/Al reactant ratios the amount of $Al(OH)_3$ used was changed accordingly. To synthesize a catalyst of Si/Al reactant ratio of 20, for example, 1.031 g of $Al(OH)_3$ was dissolved in the synthesis gel. No aluminium source was used in the synthesis of boralite and silicalite catalysts, the trace aluminium being provided by impurities in the silica sources. In order to synthesize boralites of extremely low Al content

Aerosil, rather than Ludox was used as the silica source. Boric oxide (B_2O_3) was used to provide the boron source for these catalysts and was added to the synthesis gel according to the procedures outlined above.

2.1.2 Synthesis Autoclave

The reactant mixtures prepared in the previous section were added to 250 ml teflon beakers. These had previously been washed with concentrated NaOH to remove all traces of zeolite from previous syntheses. The teflon beakers were then placed in stainless steel autoclaves cleaned in a similar fashion. A diagram of the autoclaves is shown below in Figure 2.1. Agitation was provided by a magnetic stirrer placed below the autoclave with a clean teflon stirrer bar placed inside the teflon beaker.

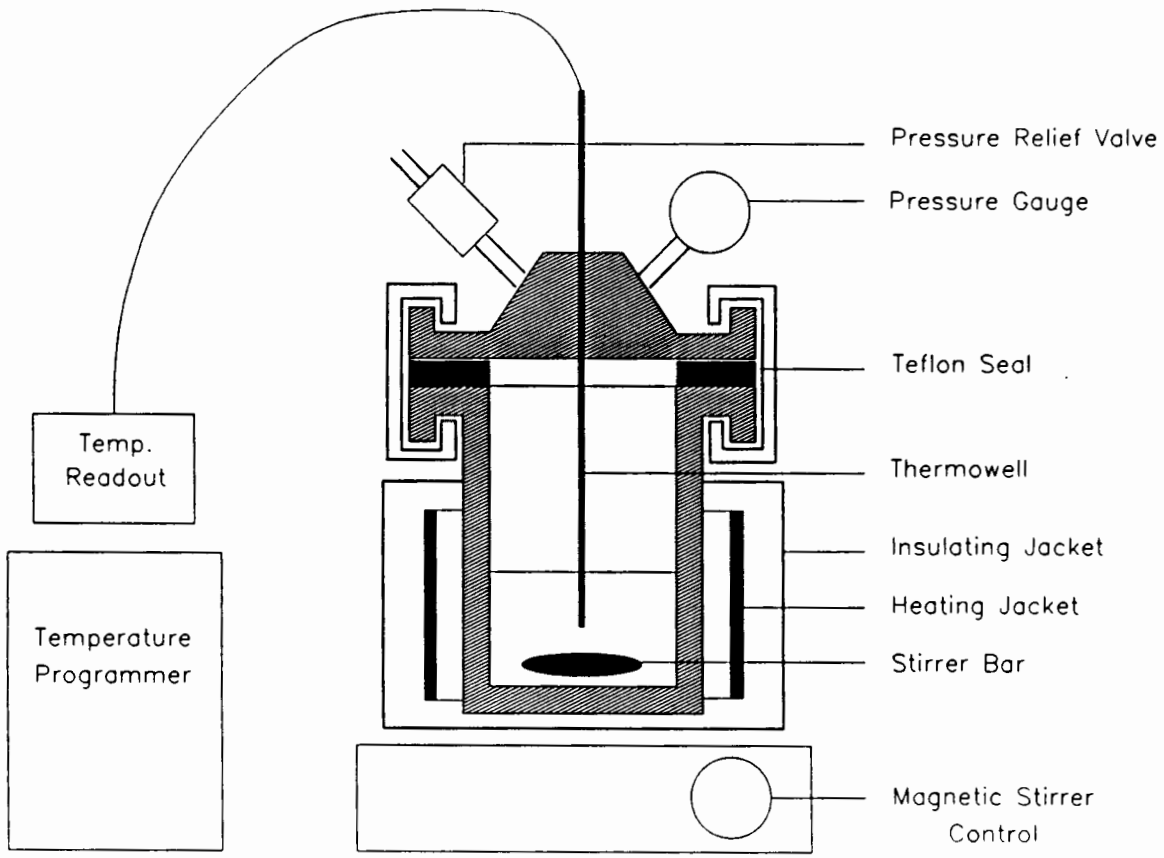

Figure 2.1 The magnetically stirred autoclave

The internal diameter of the autoclave was 7 cm while the depth was 9 cm. Once the gel was being thoroughly agitated by the stirrer bar, the autoclave was sealed and the temperature was ramped at 1 °C/min. to the synthesis temperature (156-159 °C). The temperature of the reactant mixture was measured by a thermocouple inserted into a thermowell situated axially in the autoclave. It was possible to maintain the final reactant temperature for any specified time, although typically a synthesis time of 3 days was used. At the end of this period, the autoclave was allowed to cool down before opening and before switching off the magnetic stirrers.

2.2 Catalyst Characterization

Catalysts were characterized using the following techniques:

- X-ray diffraction (XRD)
- scanning electron microscopy (SEM)
- energy dispersive X-ray spectroscopy (EDX)
- X-ray fluorescence (XRF)
- atomic absorption (AA)
- temperature programmed desorption (TPD)
- Fourier transform infrared spectroscopy (FTIR)
- thermogravimetric and differential thermal analysis (TG/DTA)
- magic angle spinning nuclear magnetic resonance (MAS n.m.r.)

2.2.1 X-ray Diffraction (XRD)

All catalysts were characterized using a Philips X-ray diffractometer with Cu-Kα radiation. Crystallinity was determined by comparing the sum of the peak heights of the five most intense peaks in the range, $5° < 2\theta < 25°$, to that of a chosen crystalline standard ZSM-5, (Si/Al reactant = 40, 3 day synthesis time). The range $44° < 2\theta < 48°$ was also scanned in an attempt to monitor changes in the unit cell dimensions due to changing amounts of boron and aluminium in the zeolite framework (Meyers *et al.*, 1985; Bibby *et al.*, 1981). The parameters used for the Philips diffractometer are given below in Table 2.2.

Table 2.2 XRD Parameters

voltage	40 kV		
current	30 mA	slits	
range	4×10^3	divergent	½ °
time constant	1	receiving	½ °
scanning speed	2 (2θ °/min)	anti-scattering	1 °

In order to standardize catalyst water content as much as possible, catalysts were equilibrated at 25% relative humidity for 24 hours prior to XRD analysis.

2.2.2 Atomic Absorption (AA)

Sodium, boron and trace aluminium content were analyzed using a Varian Spectra AA-30 spectrometer attached to a DS 15 data station. Sodium analyses were performed to confirm that the ammonium ion-exchange procedure (outlined in Section 2.4.3) had been complete. Analyses for boron and aluminium content were also carried out. The sample preparation procedure for these analyses was essentially the same. Care, however, had to be exercised in ensuring that sufficient catalyst was dissolved to enable the sodium (1-4 ppm), boron (400-1600 ppm), and aluminium (40-200 ppm) contents to fall within the measurable concentration ranges of the AA. Samples were prepared by dissolving approximately 0.2-0.5 g of NH_4^+ exchanged catalysts in a mixture of 5 ml 40% HF and 5 ml concentrated HNO_3. This was done in teflon and polypropylene beakers to prevent contamination by dissolved glass. Where the aluminium content was very low more catalyst had to be used. This was then made up to a 50 ml dilute solution by adding distilled water. Detailed calculations of sodium, boron and aluminium contents for NH_4^+- exchanged catalysts are given in Appendix 1.

2.2.3 Scanning Electron Microscopy (SEM)

Micrographs of catalysts as well as average crystallite sizes were obtained using a Cambridge S180 scanning electron microscope. Samples were mounted on aluminium stubs covered with a water-based glue and colloidal carbon mixture. Catalysts were sprinkled onto this background and coated with a thin Au/Pd film. The SEM parameters used are presented in Table 2.3.

Table 2.3 SEM Parameters

		Low resolution	High resolution
Accelerating voltage	(kV)	22	12.5
Beam current	(μA)	250	250
Lens currents: C_1	(A)	0.9	1.0
C_2	(A)	0.4	0.8
Final Lens C_3	(V)	4.6	4.6

2.2.4 Energy Dispersive X-ray Analysis (EDX)

Si/Al ratios of ZSM-5 were obtained using the Si(Li) detector of the Kevex model 7000 energy dispersive X-ray spectrometer mounted in the sample chamber of the SEM. This was only done for samples with Si/Al reactant ratios of ca. 20 and ca. 40. For catalysts with lower Al contents, the aluminium content was determined by AA (see Section 2.2.2). Samples were mounted on aluminium stubs according to the procedure detailed in Section 2.2.3 and coated with a thin carbon film. Zeolite Y with Si/Al = 2.37 (determined from its chemical formula) and ZSM-5 of Si/Al = 19 and 174 were used to calibrate the system. The system parameters chosen also ensured that electron penetration was such that bulk analyses of Si/Al could be obtained without there being any penetration to the aluminium stub. The EDX parameters used are listed in Table 2.4

2.2.5 Thermogravimetric/Differential Thermal Analysis (TG/DTA)

TG/DTA analyses were carried out using a Stanton-Redcroft STA-780 Thermogravimetric Balance. Detemplations were carried out on as-synthesized ZSM-5. 10 mg of catalyst were heated at 10 °C/min in a stream of flowing nitrogen (30 ml/min) to 500 °C. The temperature was subsequently held at 500 °C for one hour under flowing nitrogen after which air (30 ml/min) was introduced for a further two hours.

Table 2.4 EDX Parameters

Si peak centroid	1.74 keV
Si window width	0.29 keV
Al peak centroid	1.47 keV
Al window width	0.19 keV
horizontal distance from sample to detector	25 mm
working distance between final lens and sample	23.5 mm
accelerating voltage	9.5 kV
beam current	250 μA
acquisition time	125 s
tilt angle of stub	20 °
angle of incidence	70 °
lens currents : C_1	0.5 A
C_2	~0.3 A
C_3 (final lens)	3.072 V

Trimethylbenzene, n-hexane and cyclohexane adsorption experiments were also carried out using TG/DTA. 10 mg of the ammonium forms of the catalysts were calcined in N_2 (30 ml/min) by heating the samples from room temperature to 500 °C at 10 °C/min and holding the temperature at 500 °C for 1 hour. Thereafter the sample was cooled to 30 °C under flowing nitrogen, at which stage the N_2 stream was passed through a double stage saturator containing the relevant hydrocarbon. Saturation temperature in the second stage was maintained at 20 °C (condensation). Nitrogen saturated with hydrocarbon at 20 °C would then pass through the furnace where the sample was held at a constant temperature of 30 °C. The line from the saturator to the furnace was heated to 120 °C to ensure that all the hydrocarbon remained in the vapour phase. The weight gains that occurred were recorded on a dry catalyst basis.

Decoking of deactivated catalysts was also performed. In these experiments about 10 mg of coked catalyst was heated to 500 °C at 10 °C/min under 30 ml/min of flowing N_2. After one hour at 500 °C, air at 30 ml/min was passed over the catalyst for a further 3 hours. The mass loss that occurred under N_2 was considered to be due to the desorption of high molecular weight hydrocarbon while that lost under flowing air was termed "graphitic" coke. These terms in no way reflect the nature of the coke and are merely used for the sake of convenience.

2.2.6 Fourier Transform Infrared Spectroscopy (FTIR)

Infrared spectra of the NH_4^+- forms of the zeolites were obtained with a Nicolet FTIR model 5ZDX spectrometer using KBr discs that contained approximately 0.25 wt% zeolite. The scanning range was 4000 - 400 cm^{-1}.

Spectra were also recorded of catalysts after the adsorption and desorption of pyridine. Pyridine adsorption and desorption were carried out in situ using the spectrometer mentioned above. Self supporting zeolite wafers of ca. 10 mg with a surface area of 1.327 cm^2 were calcined in a quartz cell at appropriate calcination temperatures while under vacuum (2×10^{-6} mm Hg) for a minimum of 6 hours. The sample was then cooled to room temperature. Pyridine (at a vapour pressure corresponding to room temperature) was then adsorbed on the wafer for 30 min. The quartz reactor was then evacuated (2×10^{-6} mm Hg) while the sample was heated to the desired desorption temperature. After a minimum of 12 hours desorption (overnight) the sample was then cooled to room temperature and scanned (4000-400 cm^{-1}). The behaviour of the pyridine absorption bands at 1540 cm^{-1} corresponding to pyridine bonded to Bronsted sites (pyridinium ion) and at 1450 cm^{-1} (pyridine bounded to Lewis sites) were used to monitor changes in Bronsted and Lewis Acidity. A diagram of the quartz cell and the sample holder is shown in Figure 2.2.

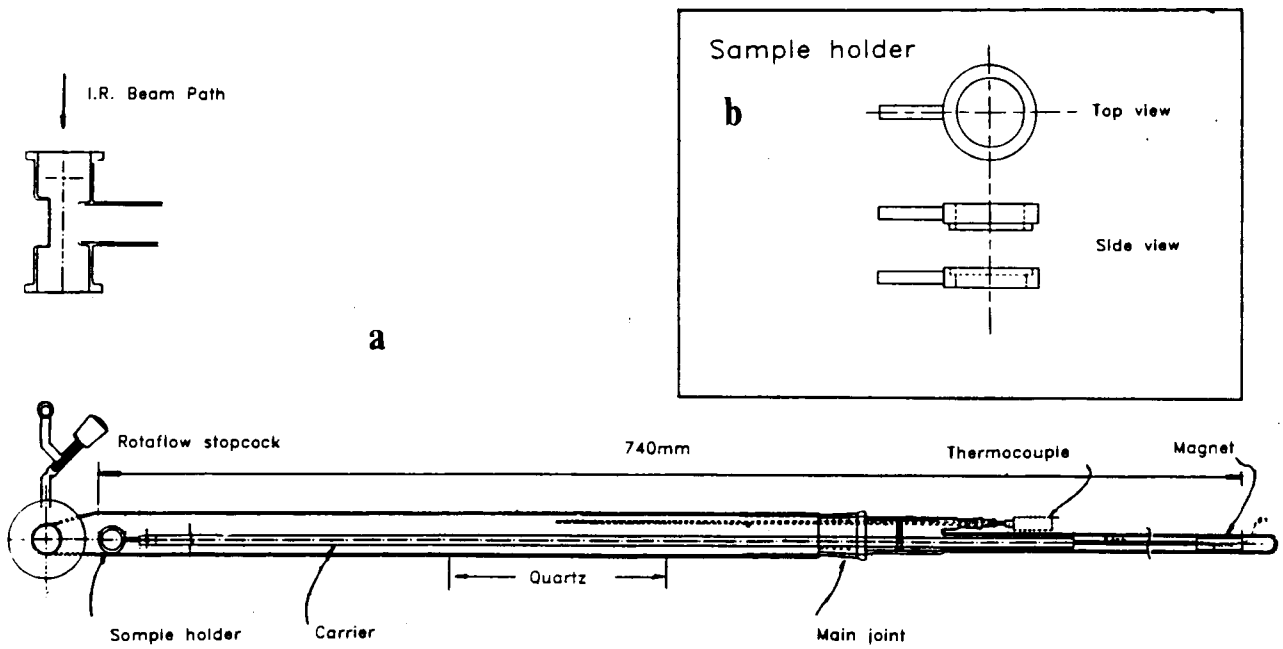

Figure 2.2 (a) Quartz cell configuration used for in-situ pyridine adsorption/desorption FTIR studies (b) Wafer sample holder

2.2.7 Ammonia Temperature Programme Desorption (TPD)

NH_3-TPD experiments were carried out at a heating rate of 10 °C/min between 100 and 600 °C using a quartz sample cell which held 0.5 g of the powdered catalyst. Before desorption commenced the sample was first calcined at 500 °C in air. Ammonia (4% in helium) at 60 ml/min was then adsorbed at 100 °C for 45 minutes whereafter desorption in helium took place (60 ml/min) for a further 45 minutes. Temperature programmed desorption was then started with ammonia being detected by a thermal conductivity detector (TCD).

2.2.8 Aluminium Magic Angle Spinning n.m.r (^{27}Al MAS n.m.r.)

The MAS n.m.r. spectra of some of the hydrothermally dealuminated catalysts as well as those of some of the phosphorus catalysts were recorded using a Bruker AM 300 spectrometer with a spinning speed of 5000 Hz.

2.3 Reaction Systems

2.3.1 Alkene Oligomerization

The apparatus used for high pressure propene oligomerization work is shown in Figure 2.3. The same apparatus was used for the oligomerization of 1-hexene. While liquified propene was fed to the system from a pressurized gas cylinder, 1-hexene was fed from a sealed polypropylene measuring cylinder. The feed was dried over 3 Å molecular sieves and then passed through a 0.5 μm physical filter. A Lewa FLM1 high pressure pump was used to pump the feed to reaction pressure (5 MPa) against a back pressure regulator which was set at pressure (5 MPa). The backpressure regulator was heated by a heating tape (set at 40 °C) to compensate for heat removal due to the vaporization of unreacted feed. The reactor is a stainless steel tube 200 mm long with an internal diameter of 18 mm. The reactor was heated by a brass block containing 4 cylindrical heating elements connected to a PI temperature controller. Temperatures in the reactor were measured by means of a thermocouple which could be moved up and down a thermowell situated axially in the reactor. Various flare lines as well as a bursting disc and pressure relief valve were included as safety features.

Liquid products were condensed in a catchpot cooled by a water jacket maintained at 25 °C while gas samples could be taken using a gas sampling loop. Measurement of off-gas rates was provided by a wetgas flowmeter.

2.3.2 Xylene Isomerization

A schematic diagram of the xylene isomerization rig is shown in Figure 2.4. Nitrogen was saturated with ortho-xylene by passing it through a double stage saturator, the first stage of which was maintained at 40 °C by water pumped from a heated waterbath. Condensation at ambient water temperature (ca. 23 °C) in the second stage ensured that N_2 was saturated with o-xylene at about 23 °C. Condensation of o-xylene in the lines was prevented by heating them to 120 °C. The saturated N_2 was then passed into a stainless steel reactor identical to the one described in the previous section (Section 2.3.1). The products of xylene isomerization were analyzed online using a sample loop attached to a Varian 3700 G.C. with a 2 m $^1/_{8^{th}}$ inch o.d. column packed with Bentone 34 and DIDP supported on chromosorb WAW 50 and coupled to a Varian 4270 integrator. The effluent gas flowrates were measured with a soap bubblemeter.

2.4 Catalyst Preparation and Activation

2.4.1 Washing

After completion of a catalyst synthesis, the contents of the synthesis autoclave were filtered using a Buchner funnel, washed with 1 litre of distilled water and dried in an oven at 80 °C for four hours.

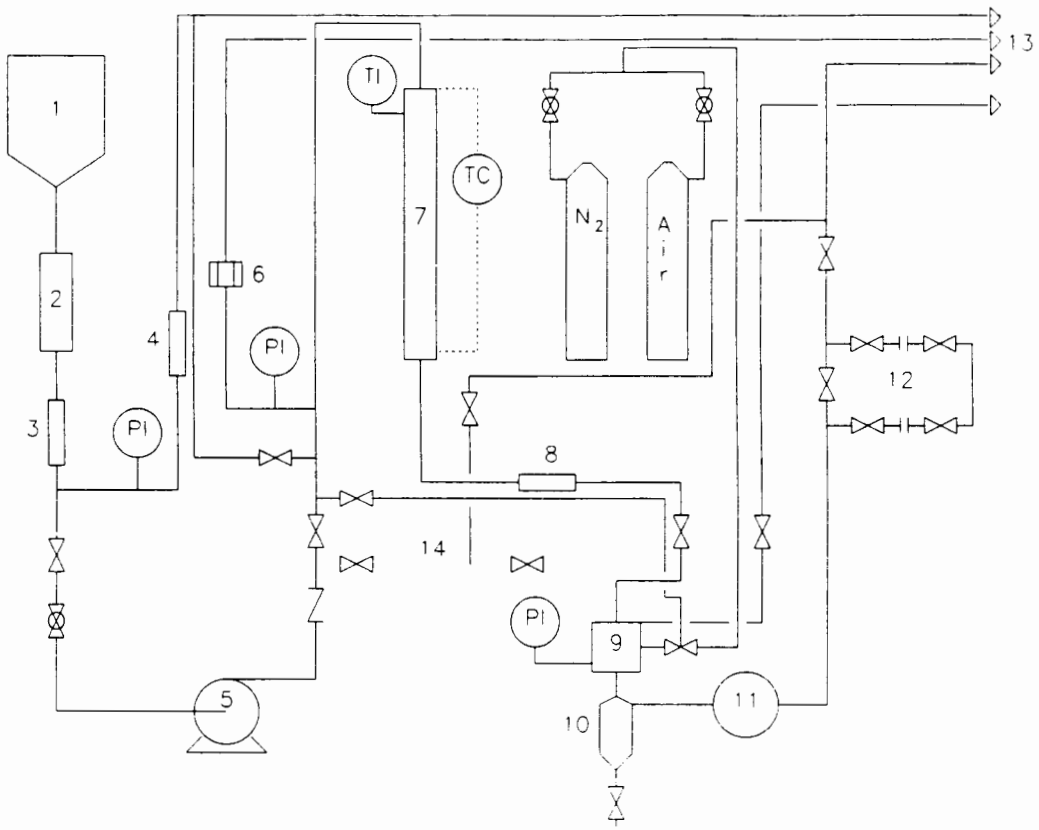

1. Feed cylinder
2. Molecular sieves (3 Å)
3. 0.5 μm filter
4. Pressure relief valve
5. High pressure diaphragm pump
6. Bursting disk
7. Reactor
8. 0.5 μm filter
9. Back pressure regulator
10. Liquid catchpot
11. Wet gas flowmeter
12. Gas sampling loop
13. Flare lines
14. Bypass line

PI Pressure gauge
TI Temp. readout
TC Temp. controller

Figure 2.3 High pressure propene oligomerization rig

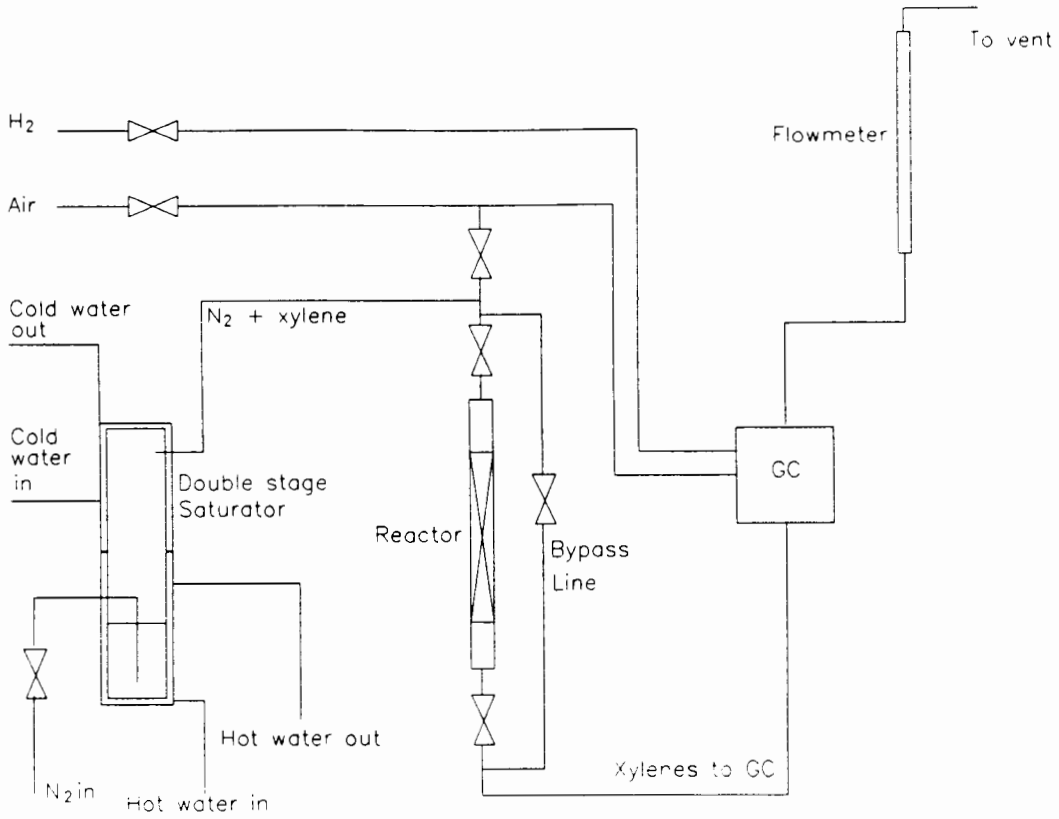

Figure 2.4 Xylene isomerization rig

2.4.2 Detemplation

Detemplation of the tetrapropylammonium bromide cation used in the synthesis of ZSM-5 was carried out on as-synthesized catalyst in the oligomerization reactors described in Section 2.3.1. Detemplation essentially followed the procedure outlined in Section 2.2.5. The as-synthesized catalyst was loaded in the reactor (see Section 2.4.4) and calcined at 500 °C first in N_2 (60 ml/min) for 6 hours and then in air (60 ml/min) for 6 hours. The air flowrate, however, was slowly increased to its final flowrate of 60ml/min to minimize the exothermic heat of reaction resulting from the oxidation of remnants of the template. At most, due to the size of the reactors used, a maximum of about 10 to 15 g of catalyst could be detemplated at one time. Detemplation removes the organic cation from the catalyst framework leaving behind the sodium form of the catalyst, i.e., Na-ZSM-5.

2.4.3 Ion Exchange

After detemplation the catalyst was added slowly to 1 litre of 2 molar solution of ammonium nitrate. Care was taken when adding the hydrophobic zeolite ZSM-5 to water

to prevent fine particles being lost to the atmosphere. The solution of ammonium nitrate and catalyst in a glass autoclave was stirred by means of a stirrer bar in conjunction with a magnetic stirrer-hotplate. The mixture was heated under reflux at 90 °C for between 20 and 24 hours. Thereafter the mixture was cooled, washed and dried as outlined previously. After this time the ion exchange reaction as shown below was essentially complete.

$$Na^+\text{-ZSM-5} + NH_4NO_4 \rightarrow NH_4^+\text{-ZSM-5} + NaNO_3$$

2.4.4 Calcination

To activate the catalyst prior to reaction, the ammonium form of the catalyst is calcined to yield the more active protonic form of the catalyst. This takes place according to the reaction scheme shown below:

$$NH_4^+\text{-ZSM-5} \xrightarrow[\text{heat}]{\text{air}} NH_3(g) + H^+\text{-ZSM-5}$$

Calcination was carried out in the reactors described previously (Section 2.3.1). Figure 2.5 shows how the catalyst was loaded in the reactor for calcination. When calcining a small amount of catalyst (ca. 0.5 g) care needs to be taken to ensure that the catalyst bed is of uniform thickness. If this is not done, channeling may occur during reaction leading to poor catalyst performance and reproducibility.

For propene oligomerization, approximately 1 g of catalyst was packed according to the scheme shown in Figure 2.5. For xylene isomerization and 1-hexene oligomerization over steam dealuminated ZSM-5 approximately 0.5 g of catalyst was loaded in the reactor. Where binder was used in conjunction with boralite catalysts, the % binder was accounted for so that the same mass of zeolite catalyst was still packed. Calcination was carried out at 500 °C under flowing air (60 ml/min) for a minimum of 4 hours, although 6 hours calcination time was more typical.

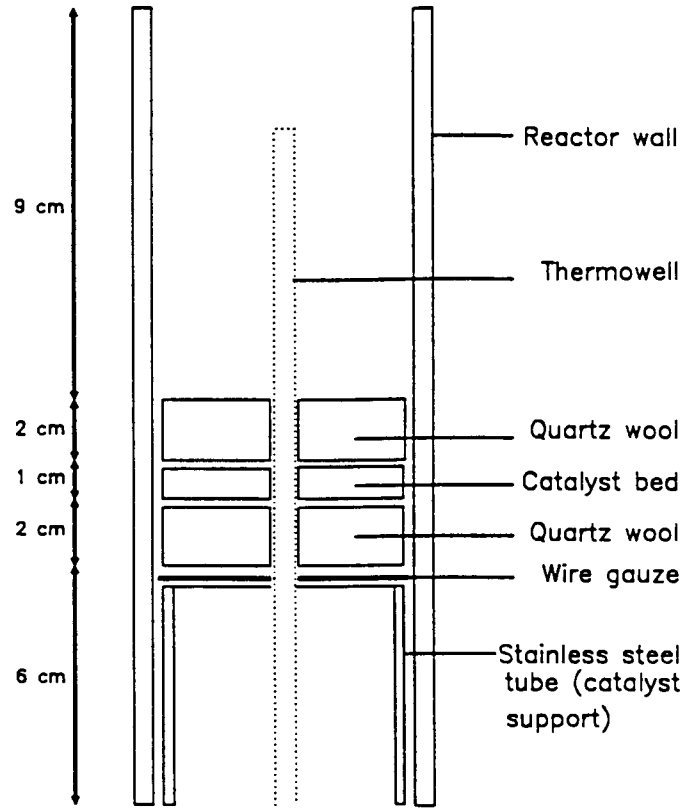

Figure 2.5 Schematic representation of packed catalyst bed in reactor

2.4.5 Catalyst Modification

2.4.5.1 Catalyst impregnation

ZSM-5 catalysts synthesized according to the method of Argauer and Landolt (1972) were impregnated with boric acid, phosphoric acid and trimethylphosphite (TMP).

Some ZSM-5 was impregnated with boric acid using the incipient wetness technique. This was done by dissolving 1.364 g of H_3BO_3 in a minimum of water and mixing with 11.91 g of ZSM-5 (Si/Al = 41). The weight % of boron per mass of catalyst loaded in this way was 2.001 wt %. The catalyst contained 1.5 wt % B as measured by AA. A portion of this catalyst was washed with 500 ml distilled water, filtered and dried (4 hours at 80 °C) to yield a catalyst containing 0.38 wt % B. Some catalyst was also impregnated with H_3BO_3 by dissolving the desired amount of boric acid (2.001 wt % B per mass of catalyst) in 100 ml of distilled water. This was then added to the unmodified catalyst and the resulting mixture was heated under reflux at 90 °C for 3 hours while stirring. Unmodified ZSM-5 catalysts were impregnated by H_3PO_4 in the same manner.

ZSM-5 was also impregnated with TMP according to the method outlined by Vinek *et al.* (1989). In this method ca. 10 g of catalyst was dried in flowing N_2 for 1 hour. The catalyst was then suspended in 50 ml of n-octane. A small volume of TMP was added and the resulting solution was refluxed for 14 hours. The suspension was filtered and the remainder washed with methylene chloride and n-pentane. The resulting catalyst was dried at 125 °C for 1 hour and at 225 °C for 2 hours in flowing N_2. The catalyst was finally calcined at 500 °C or 17 hours in air.

2.4.5.2 Modification with HF and NH_4F

Some boralite catalysts were slurried in dilute HF and NH_4F solutions at room temperature. 4.2 g of one boralite catalyst containing 1.2 wt % boron and 550 ppm aluminium was stirred at room temperature (in a teflon beaker with a teflon stirrer bar) in 100 ml of 0.02 molar HF for 20 hours. 3 g of the resulting catalyst (labelled boralite-HF) was then treated in a similar fashion with 100 ml of 0.014 molar NH_4F for 2 hours. This catalyst was labelled boralite-HF-NH_4F. 6.08 g of another boralite catalyst was also agitated for 2 hours with a 0.028 molar in solution of NH_4F. The resulting catalyst, labelled boralite-NH_4F, contained 1.38 wt % boron and 100 ppm Al.

2.4.5.3 Steam dealumination

Catalysts were steam dealuminated using the apparatus shown in Figure 2.6.

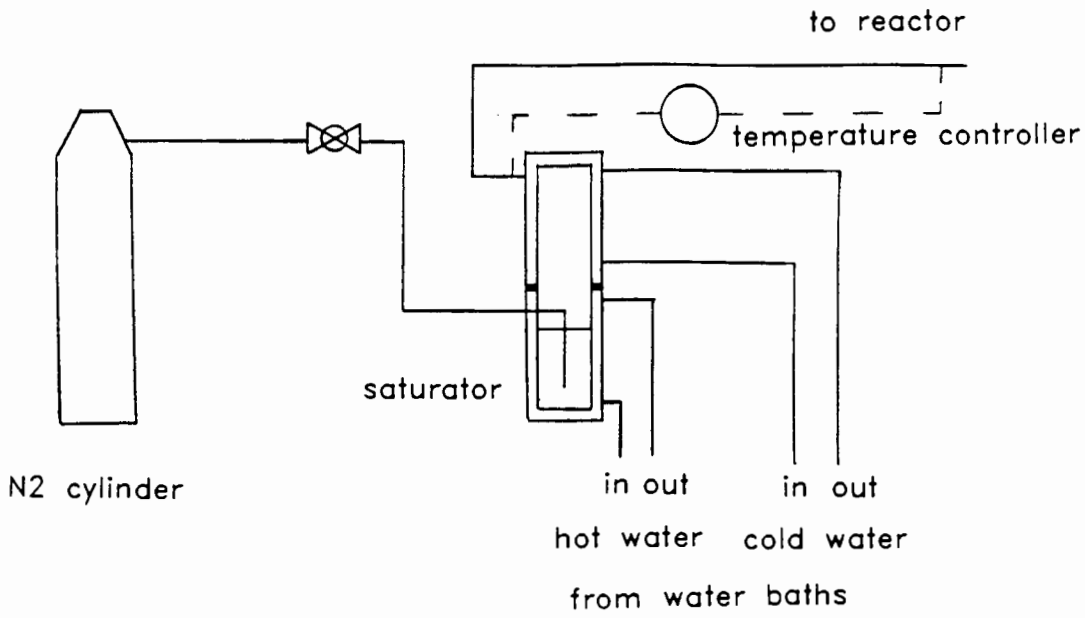

Figure 2.6 Steam dealumination apparatus

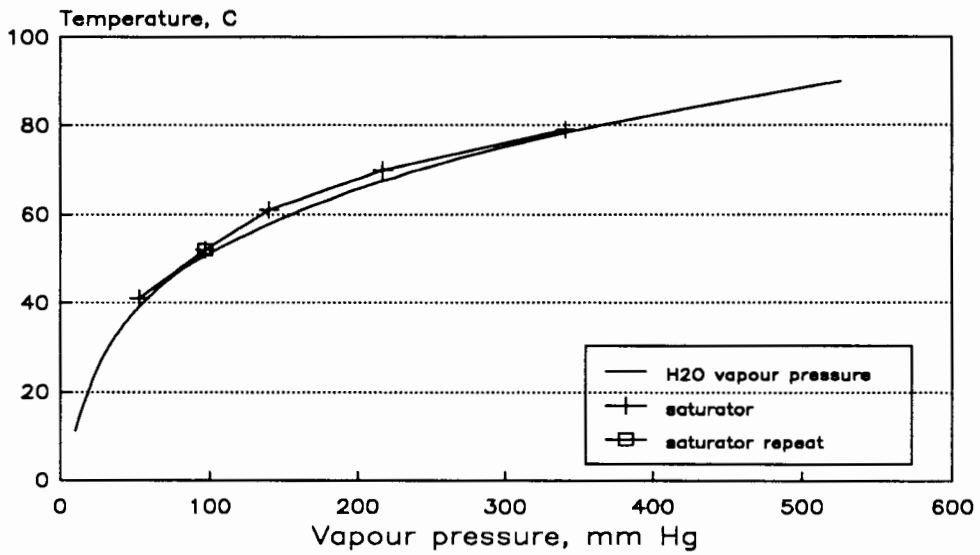

Figure 2.7 Saturator calibration chart

Nitrogen was saturated with water at a given temperature by passing it through a double stage saturator. The temperature of the first stage was held at a temperature 10 °C higher than that of the second stage which was set to the desired saturation temperature. Flow of nitrogen through the system was regulated using a needle valve, while the wet nitrogen flow was measured using a bubblemeter which could be attached to the end of the steaming line. Water was prevented from condensing out in the line after the saturator by heating the line to 30 °C above the desired steaming saturation temperature. The system was calibrated by connecting it to an acetone/dry-ice trap and a wet gas flowmeter. It was then possible to determine the concentration of water in the gas phase. A detailed calculation for the calibration procedure is presented in Appendix 2. The calibration chart for the system thus derived is shown in Figure 2.7. Also shown for comparison purposes is a curve showing the vapour pressure data for nitrogen saturated with water as a function of temperature. The good agreement between the two sets of data indicates that the saturator is performing correctly.

Catalysts were steamed by loading 0.5 g into one of the reactors described in Section 2.3.1 followed by air calcination at 500 °C and 60 ml/min air for 4 hours. Before calcination was complete the water baths circulating water through the saturator were set to the required temperature and turned on. The heating tape was also set to the desired temperature (30 °C above that of the second stage). The outlet of the apparatus was then connected to a bubblemeter and the N_2 flowrate was set.

Once the calcination was completed, the reactor was cooled to the desired reactor steaming temperature. When this was reached, the steaming apparatus was connected to the reactor inlet and the catalyst steamed for the desired time. Upon completion of the steaming process, the flowrate of saturated N_2 was checked to ensure that no change in flowrate had occurred. The reactor was then reconnected to the oligomerization line and cooled to 120 °C at which stage hexene oligomerization runs were started according to the procedure laid out in Section 2.5.1.1.

2.5 Run Procedure

2.5.1 Alkene Oligomerization

2.5.1.1 Start-up

Upon completion of the calcination procedure the reactor was allowed to cool down. While the reactor and furnace were cooling down, the glycol pump and glycol fridge were switched on. The glycol pump was used to pump cold glycol (maintained at -20 °C in the glycol fridge) through the head of the high pressure Lewa pump to prevent feed from flashing in the pump head. The pressure on the backpressure regulator was then set to 5 MPa while the heating tape to the regulator was set to 40 °C. The cooling water to the liquid catchpot (controlled at 25 °C) was also turned on.

For propene oligomerization the reactor was cooled to 30 °C while for 1-hexene oligomerization it was cooled to 120 °C. At this stage the reactor was pressurized to 5 MPa using high pressure N_2 and sealed off with shut-off valves. The reactor was then checked for leaks using "snoop" leak detector, a soapy solution which bubbles when N_2 escapes from the isolated reactor system. At this stage the rest of the oligomerization rig was pressurized by pumping feed through the bypass line. This was done for 10 minutes after which the bypass line was shut and feed was pumped through the reactor. Heating to reaction temperature was then started.

For 1-hexene oligomerization the temperature was ramped from 120 °C to the reaction temperature of 220 °C over a period of 40 minutes (2.5 °C/min) at which stage the run log was started. For propene oligomerization the reactor was heated from 30 °C to 180 °C at 3 °C/min and thereafter at never more than 2 °C/min as temperature runaways occurred easily. This is hardly surprising when one considers the highly exothermic nature of the propene oligomerization reaction. Attempts were made to inhibit temperature runaways by diluting catalyst beds with glass beds, but this was unsuccessful. Further evidence of the exothermic nature of propene oligomerization was provided by the existence of large temperature gradients through the catalyst bed, which were recorded by measuring temperatures at the top, middle and bottom of the bed. In order to avoid confusion, however, the reaction temperatures presented in this study are the temperatures recorded at the reaction front in the catalyst bed. Once at reaction temperature, the run log was started when the first drop of liquid product was collected, as conversion of propene to liquid product was taken as a measure of activity.

Two different run types were used in this study:

1. Ramping temperature runs: For these runs reaction temperature was held constant until the onset of deactivation whereafter the temperature was ramped to the next level. The temperature range used for these studies was 220-290 °C. Unless a catalyst was inactive below 300 °C, the temperature was never taken above 300 °C to limit undesirable cracking and aromatization reactions. Temperature levels of 220, 250, 270 and 290 °C were used depending on catalytic activity. In the case of weakly active catalysts requiring high reaction temperatures, i.e. temperatures exceeding 300 °C, a blank run was carried out in an empty reactor at 300 °C to confirm that reactor wall effects could be ignored.

2. Constant temperature runs: Reaction temperatures were held constant. For propene oligomerization a temperature of 250 °C was used, but for 1-hexene oligomerization over steam dealuminated ZSM-5 reaction temperatures were held at 220 °C.

2.5.1.2 Run data and calculation procedures

Calculation of conversion levels with time on stream for 1-hexene oligomerization is a fairly simple procedure since at 220 °C in the absence of cracking, all of the product is liquid. The hexene used as feed was 98.6 wt % 1-hexene with 1.4 wt % 1-hexene isomers. At the end of a time interval (t) the liquid product would be taken from the catchpot and analyzed with the Varian 3600 GC megabore. The conversion of hexene was taken as being the amount of hexene converted to oligomer product. The isomerization of 1-hexene to hexene isomers was not considered as being part of the oligomerization activity and conversion for hexene oligomerization was therefore taken as being:

$$\text{Conversion of hexene} = (100 - \%\ \text{hexene isomers in liquid sample})$$

Conversion for propene oligomerization was considered as being conversion of propene to liquid product. Since both gas and liquid form part of the product the calculational procedure is more complex than for hexene oligomerization.

The following data were collected during a propene run:

1. Liquid samples were collected and weighed at the end of a time interval (t)

2. Wet gas flowmeter readings were taken at the beginning (WGFM1) and end (WGFM2) of the same time interval
3. Wet gas flowmeter temperature (T)
4. Gas samples were taken and analyzed at the midpoint of the time interval
5. Reactor temperature setpoint
6. Actual reactor temperatures at the top and bottom of the catalyst bed
7. Reactor pressure
8. Pumpstroke setting of the Lewa pump
9. The mass of catalyst in the catalyst bed
10. The mass of the feed container at the beginning and the end of the run

Gas samples were used to calculate the average molecular mass of the exit gases by converting mass fractions of the components in the stream to mole fractions. A detailed calculation is presented in Appendix 3.

The volumetric flowrate of the exit gas was calculated by multiplying the difference in flowmeter readings for the interval by a correction factor as shown in the equation below:

$$V = C_f \times (WGFM2 - WGFM1)/t$$

where V = flowrate (l/hr)

C_f = a correction factor for the WGFM (see Appendix 4)

WGFM1, WGFM2 = flowmeter readings in litres

t = time interval (hrs)

A compressibility factor, Z, was calculated for the exit gas mixture using compressibility charts (Himmelblau, 1982). This is shown in Appendix 5. The mass rate of the exit gas could then be calculated from the following equation:

$$PV = ZnRT, \text{ T in Kelvin}$$

If the molecular mass of the gas (MW) is known then this equation can be rearranged to yield:

$$M = P \times V \times MW/(Z \times n \times R \times (T+273))$$

where M = gas flowrate (g/hr)

R = gas constant (8.314 J/gmol/K)

P = atmospheric pressure (101.3 kPa)

T = WGFM temperature (°C)

This reduces to:

$$M = 12.187 \times V \times MW/(Z \times (T + 273))$$

The mass of liquid formed (L) is obtained by weighing the liquid product, although the mass of the dissolved gases must be subtracted from it to obtain the true liquid mass, L_t.

The activity of the catalyst (A) can be calculated from:

$$A = L_t/(t + c)$$

where A = catalyst activity (g. liq./hr/g. catalyst)
c = catalyst mass (g)

The feed rate (WHSV) is calculated using the following equation:

$$WHSV = (L/t + m)/c$$

Care should be taken, however, since this equation assumes that there is no error in the mass balance, in other words, feed to the system is assumed to leave as either gas or liquid product. If the error in the mass balance was < 5% this assumption was taken as being valid. The mass balance was calculated from initial and final masses of the propene feed cylinder or from initial and final volumes of liquid hexene feed. The mass leaving the system was determined by summing the gaseous and liquid products over all time intervals as shown below.

$$\text{Mass out} = \Sigma (L + m \times t) \text{ for all time intervals}$$
$$\text{Mass in} = \text{Cylinder Mass}_{\text{before}} - \text{Cylinder Mass}_{\text{after}}$$

If the differences between these two values was < 5% then the assumptions made in determining the WHSV are satisfactory. Conversion (Co), based on total feed, is then given by the expression:

$$Co = 100 \times A/WHSV$$

Because the WHSV as calculated above is based on total feed which contains both alkanes and alkenes, (see Table 2.8), the conversion based on reactive alkene feed (Co') is given by:

$$Co' = Co/(\%\ \text{alkenes in feed}) \times 100$$

A detailed calculation is shown in Appendix 6.

2.5.2 Xylene Isomerization

2.5.2.1 Start-up

While the reactor was cooling from the calcination temperature to reactor temperature, the waterbaths and heating tapes were switched on. Once at reaction temperature, the desired N_2 flowrate was set using the bypass line. The flow of saturated N_2, once set, was then switched through the reactor. After 5 minutes the exit gas from the reactor was analyzed using the online G.C. The flowrate was then changed again, altering the conversion level, which was once again determined using the online G.C. The procedure was repeated until sufficient points had been taken to plot the relevant conversion curves.

2.5.2.2 Run data and calculation procedure

The following data was collected:

1. Mass of zeolite packed (c)
2. Flowrate of saturated N_2 (V)
3. Cooling water temperature in the second stage of the saturator (T_w)
4. Ambient temperature (T_a), i.e. T at which V is measured
5. Reaction temperature

Since the reaction was carried out at low pressures, Raoult's law could be applied:

$$P_o = X_o \times P_o^{sat}$$

where P_o = partial pressure of o-xylene in the gas phase
P_o^{sat} = vapour pressure of o-xylene at a given temperature
X_o = mole fraction of o-xylene in the liquid phase

Since $X_o = 1$, $P_o^{sat} = P_o$ and so, assuming ideal behaviour (implicit in using Raoult's law):

$$P_oV = N_oRT_a$$

and rearranging gives: $N_o = P_oV/(RT_a)$
where N_o = molar flowrate of o-xylene

The vapour pressure of ortho-xylene as a function of temperature can be calculated using the expression determined by Stuckey and Saylor (1940), shown below, although other researchers have determined similar expression (Kassel, 1936):

$$P_o = 10^{(-2908.07/T - 5 \log T + 27.95279)}$$

where P_o = vapour pressure of o-xylene in mm Hg
T = Temperature (K) = T_w

Since P_o can therefore be calculated, V and T_a are measured and R is a constant, the mass rate of o-xylene can be determined using:

$$M_o = 106.17 \times N_o$$

where M_o = mass rate of o-xylene

The WHSV is simply given by WHSV = M_o/c. A more detailed calculation is presented in Appendix 7. At varying WHSV, the conversion of o-xylene changes and since selectivity is given by the expression:

$$\text{selectivity} = (\text{mass p-xylene in product})/(\text{mass o-xylene converted})$$

It is therefore possible to examine the effect of changing selectivity for various catalysts by plotting a graph of % p-xylene in the product against the mass of o-xylene converted. An example is given in Appendix 7.

2.6 Product Analysis

2.6.1 Liquid Analysis

2.6.1.1 Gas Chromatography

The products of propene and 1-hexene oligomerization were analyzed using a Varian 3600 gas chromatograph with a 0.351 mm ID, 30 m long fused silica megabore column coated with a 1.5 μm film of DB-1 (100% methylpolysiloxane). GC settings and flowrates are shown below.

Table 2.5 Varian 3600 GC Parameters

Flow rates :	N_2 (column)	5 ml/min
	N_2 (detector)	25 ml/min
	Air	300 ml/min
	H_2	30 ml/min
Injector temperature		150 °C
Detector temperature		250 °C
Column temperature		40 °C (1 min)
program		10 °C/min to 230 °C
		230 °C (5 min)
Detector		Flame ionization
Sample injection		0.4 μl

The products of oligomerization were grouped into oligomer fractions as follows:

Table 2.6 Oligomer Groupings

	Propene feed	1-Hexene feed
Dimer	C_6 - C_8	C_{12} - C_{17}
Trimer	C_9 - C_{11}	C_{18} - C_{23}
Tetramer	C_{12} - C_{14}	C_{24}^+
Pentamer	C_{15} - C_{17}	
Hexamer$^+$	C_{18}^+	

2.6.1.2 ^{1}H- n.m.r.

^{1}H- n.m.r. spectra of propene oligomerization products were carried out on a Brüker 90 MHz spectrometer. Tetramethylsilane was used as a reference. The sweep width was 0-10 ppm. Aromatic products were identified by peaks in the regions 6.5-7.3 and 2.1-3.0 ppm.

2.6.1.3 Cetane number determination

The Gautier correlation (Gautier, 1988), shown below, was used to obtain cetane numbers of some of the liquid products of oligomerization. The correlation is valid only for samples essentially free of olefins. This required that products be hydrogenated before cetane numbers could be determined. The autoclave used for hydrogenation was essentially the same as those used for catalyst synthesis. Hydrogenation was carried out at 150 °C and 3 MPa over a palladium on activated carbon catalyst (Aldrich 5% Pd, 50% H_2O). Approximately 1 g of catalyst was used for every 25 ml of product hydrogenated. A minimum sample volume of about 20-25 ml was hydrogenated per batch. Agitation of the catalyst-liquid mixture was by means of a teflon coated stirrer bar inside the autoclave which was placed on top of a magnetic stirrer. When the autoclave was sealed H_2 was fed to the autoclave via stainless steel tubing which ended just below the level of the liquid product. This enabled H_2 to bubble through the liquid ensuring good contact with the liquid and catalyst. Hydrogenation was maintained at the required temperature for about 12 hours. When hydrogenation was complete, the liquid product was cooled and filtered. The autoclave was thoroughly cleaned with ethanol and acetone before re-use. Cetane numbers, determined by the Gautier correlation, were then obtained from ^{1}H- n.m.r. spectra of the hydrogenated products. The Gautier correlation is:

$$\text{Cetane number (CN)} = -0.571H_3 + 0.935H_2 - 0.454H - 0.718H_a + 0.102H_d$$

where H, H_2, H_3, H_a, and H_d are protons attached to various carbon groups as determined by ^{1}H- n.m.r. and shown below. The total number of protons must be normalized to 100%.

H_3 = relative amount of H in CH_3 groups; range = 0.5-1.06 ppm
H_2 = relative amount of H in CH_2 groups; range = 1.06-1.8 ppm
H = relative amount of H in CH groups; range = 1.8-4.0 ppm
H_a = relative amount of H in aromatic rings; range = 6.5-7.05 ppm
H_d = relative amount of H is attached to aromatic ring-junction carbon; range = 7.05-9.0 ppm

The relative amounts of protons were obtained from integrated peak areas of the relevant chemical shift ranges shown above. A detailed calculation of a cetane number is given in Appendix 8.

2.6.2 Gas Analysis

Analysis of the propene feed as well as that of the effluent gases was performed with a GOWMAC 750 p GC using a 6.35 mm OD, 3 m long stainless steel column packed with n-octane/poracil C. The settings used for the GC are shown in Table 2.7. Table 2.8 shows a typical propene feed composition as determined by the GOWMAC 750 p GC.

Table 2.7 GOWMAC 750 p GC settings

Flowrates:	N_2	40 ml/min
	H_2	31 ml/min
	Air	300 ml/min
Temperatures:	Injector	150 °C
	Detector	250 °C
	Column	50 °C isothermal for 28 mins
Sample volume		10 μl
Detector		Flame ionization

Table 2.8 Typical Propene Feed Composition

Component	Mass %
ethane	0.201
propane	13.103
propene	86.696

Chapter 3
Results

RESULTS

3.1 Boron Modified ZSM-5

3.1.1 Boralite Catalysts

3.1.1.1 Catalyst nomenclature

All boralite catalysts were named according to the following code:

B - m (-O)

where B - indicates that the catalyst is a boralite i.e. has the ZSM-5 structure but contains boron, not Al, in the framework

m - a number identifying the catalyst batch

O - an option indicating the relevant fluorination treatment where

O may be		
	HF	signifying hydrofluoric acid wash
	NH_4F	signifying ammonium fluoride exchange
	$HF\text{-}NH_4F$	signifying acid wash followed by NH_4F exchange

A ready reference guide for catalyst coding has been included as a fold-out in Appendix 11.

3.1.1.2 Characterization

3.1.1.2.1. Relative crystallinity

XRD

Relative crystallinities of the boralite catalysts as determined by XRD are shown below in Table 3.1. Included in the Table are a silicalite catalyst and, for comparative purposes, an unmodified ZSM catalyst of Si/Al = 41.

Table 3.1 Crystallinities of Boralite Catalysts (normalized w.r.t. Boralite B-3)

Catalyst	% Crystallinity
B-1	92
B-2	92
B-2-HF-NH_4F	89
B-3	100
B-3-NH_4F	100
B-4	67
B-5	84
B-6	67
Silicalite	76
ZSM-5	95

It can be seen that the mild H and NH_4 treatments did not reduce the crystallinity of the catalysts to any significant extent, if at all. The crystallinities of the boralites were generally high (> 80%), the exceptions being boralites B-4 and B-6 with only 67% crystallinity. The crystallinity of the silicalite catalyst was also low. The crystallinities of the catalysts were all determined by measuring the cumulative peak heights of the 5 major peaks shown in Figure 3.1 and comparing these to the value obtained by catalyst B-3 which had the highest value. Meyers *et al.,* (1985) showed that changes in the cumulative d-values of the four peaks between 2θ = 45 °C and 48 °could be used to determine unit cell contractions due to boron incorporation in the lattice. In this work, however, although changes in the d-value of these peaks could be seen, no clear trend emerged.

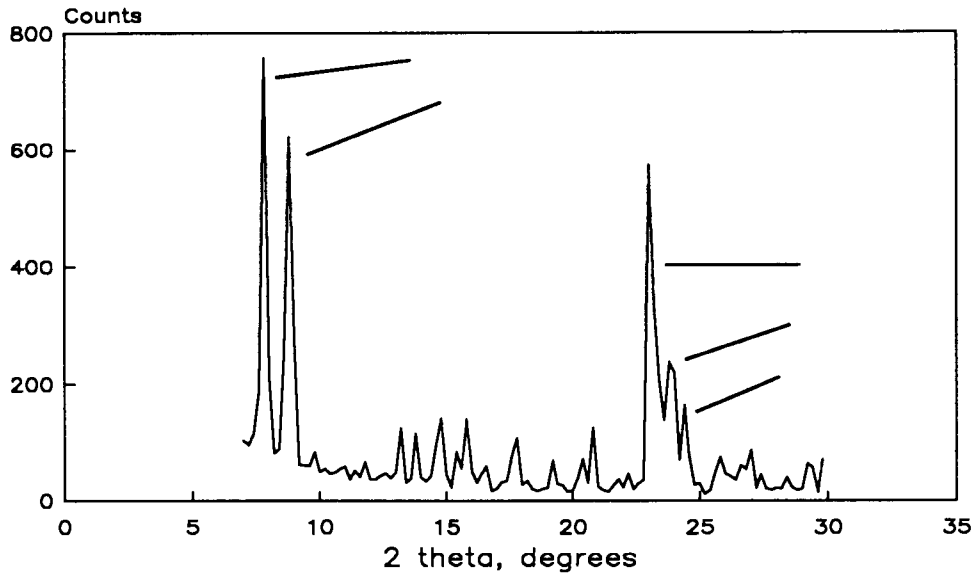

Figure 3.1 XRD spectrum of Boralite B-5

FTIR

An estimate of the optical density ratio, R, of the absorbances of the 550 cm^{-1} to 450 cm^{-1} bands, was also used to estimate the crystallinity of the catalysts. The band at ca. 450 cm^{-1} has been assigned to internal vibrations of the Si- and Al- tetrahedra (T-O-T band), while the band at ca. 550 cm^{-1} has been ascribed to the external linkeages of double rings (Flanigan, 1979). The R values for the boralite catalysts are shown in Table 3.2. Coudurier and Védrine (1987) suggested a value of 0.62 for calcined ZSM-5 type catalysts is indicative of highly crystalline catalysts. Coudurier *et al* (1982) considered the optical density ratio a good test for the crystallinity of ZSM-5, although they noted that quantitatively the method is not very precise.

Table 3.2 Optical Density Ratios of Boralites

Catalyst	Optical Density Ratio, R
B-1	0.60
B-2	0.68
B-3	0.67
B-3-NH_4F	0.66
B-4	0.62
B-5	0.65
B-6	0.63
Silicalite	0.65

The values shown in the Table are all in the region 0.6-0.68 confirming the crystalline nature of the catalysts.

3.1.1.2.2 Crystallite size and morphology

Crystallite sizes were determined from electron micrographs. Number average crystallite sizes of the catalysts are shown in Table 3.3 below, while micrographs of boralites B-4, B-5 and B-6 as well as a silicalite are presented in Figures 3.2 (a-e). Boralite catalysts, with the exception of B-1, all had twinned crystallite morphologies with very uniform, narrow size distributions. Boralite B-1 had spherical crystallites with an average size of 4 μm while silicalite had a binodal size distribution with very small crystallites of 1-2 μm and bigger crystallites of about 10 microns.

3.1.1.2.3 Thermogravimetric analysis

Detemplation

Figure 3.3 shows a detemplation curve for B-1. The catalyst was detemplated first in dry N_2 (30/ml/min) for one hour and then in air, also for one hour at 30 ml/min. The mass loss upon detemplation (11.6 wt%) is a little lower than for unmodified ZSM-5 which typically loses ca. 13-14 wt%. It can be seen that there was only a small further mass loss upon the introduction of air.

Table 3.3 Average Crystallite Sizes and Morphologies

Catalyst	Average Crystallite Size (μm)	Morphology
B-1	4.0	spherical
B-2	1.0	twinned
B-3	1-2	twinned
B-4	3-3.5	twinned
B-5	3-3.5	twinned
B-6	1.5	twinned
Silicalite	1-2; 10 (binodal)	spherical

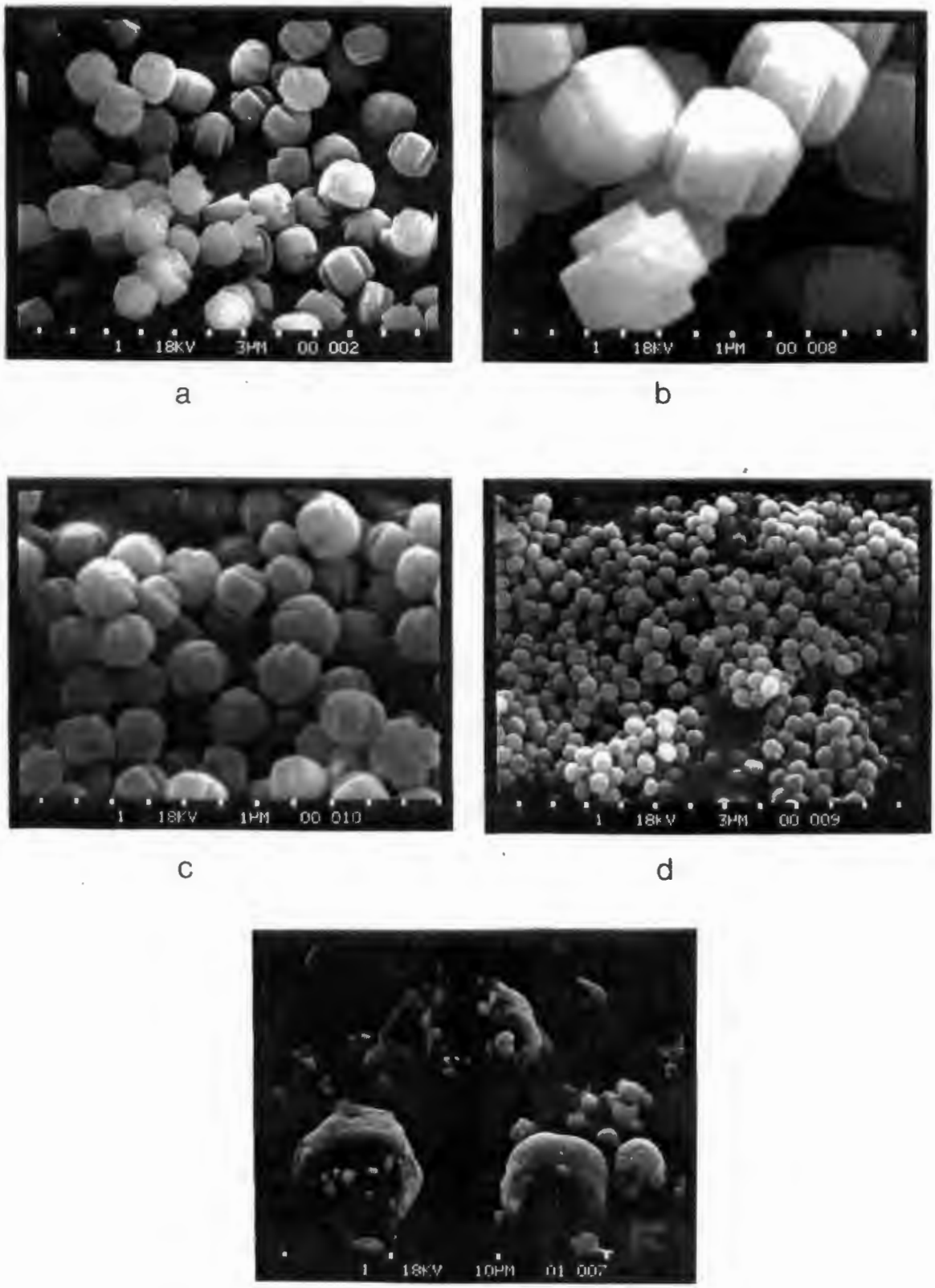

Figure 3.2 **Micrographs of a) B-4 b) B-5 c) B-6 d) B-6 e) silicalite**

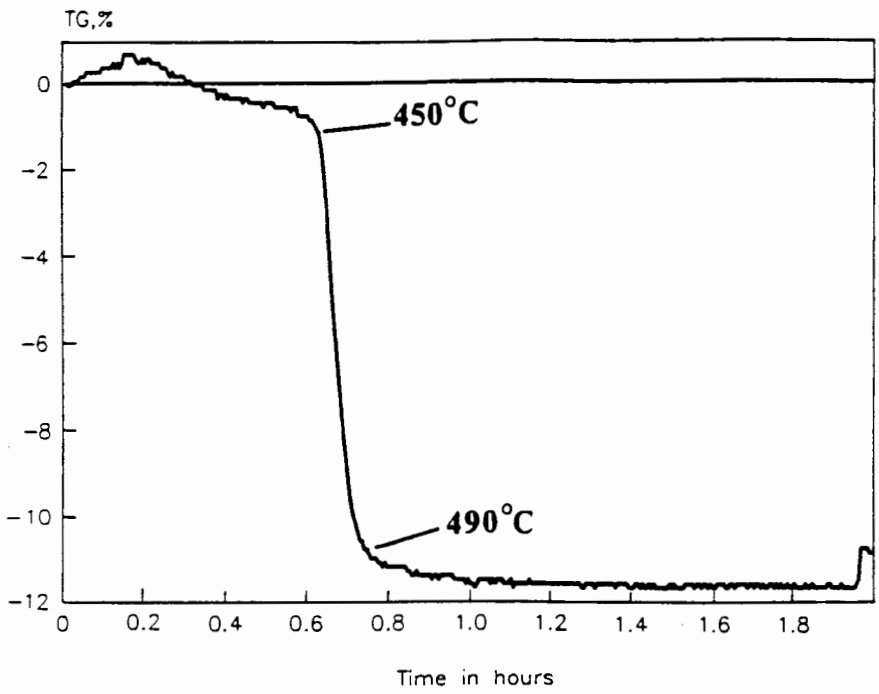

Figure 3.3 Mass loss upon boralite detemplation in N_2 and air

Cyclohexane Adsorption

A curve showing the adsorption of cyclohexane at 30 °C for boralite B-1 compared to various boron modified catalysts is presented elsewhere (see Figure 3.14 in Section 3.1.2.1.5). The adsorption rate for this catalyst was slower than that of the other catalysts. If one includes the weight gain observed when cooling from calcination temperature to adsorption temperature, then this catalyst (B-1) adsorbed 6.9 wt% cyclohexane, substantially less than for unmodified ZSM-5 (ca. 11 wt%). Other researchers (Gabelica *et al.,* 1984b) also noted a weight change when cooling to adsorption temperature and attributed this to the physisorption of nitrogen and/or water which is displaced by adsorbing hydrocarbon.

3.1.1.2.4 Boron and aluminium content

Boron and aluminium contents of the catalysts, determined by atomic absorption, are shown in Table 3.4. It should be noted that the Al content of all of these catalysts arises as a result of impurities in the synthesis reagents, notably the silica source. The Al contents of

the two silica sources used, namely Aerosil and Ludox, have been included in the Table. It can be seen that in general the use of Aerosil, containing less Al impurities than Ludox resulted in catalysts with lower trace Al contents. The purpose of this study was to determine the activity of framework boron in ZSM-5 catalysts for propene oligomerization. With the exception of boralite B-1 which has a B/Al ratio of 7 the catalysts had much lower Al contents with B/Al ratios ranging from 22 for B-2 to 244 for B-5. The Al contents of these catalysts could be further reduced by using tetraethoxysilane as a silica source. As will be seen in the discussion, however, the Al contents of the catalysts presented in Table 3.4 are sufficiently low to enable valid interpretations to be made regarding the activity of boron in the ZSM-5 framework. Sodium contents of the ammonium forms of these catalysts were all below 0.05 wt% Na indicating a good degree of ammonium exchange.

Table 3.4 Boron and Aluminium Contents of Boralites

Catalyst	Si Source	Al Content (ppm)	Boron (wt%) Content
B-1	Ludox	760	0.51
B-2	Aerosil	550	1.20
B-2-HF-NH_4F	Aerosil	120	0.98
B-3	Aerosil	200	0.85
B-3-NH_4F	Aerosil	100	0.81
B-4	Ludox	330	0.59
B-5	Aerosil	25	0.61
B-6	Aerosil	77	0.86
Silicalite	Ludox	350	-
	Ludox	37.5	-
	Aerosil	16	-

3.1.1.2.5 Al coordination

^{27}Al MAS n.m.r. was carried out on B-4. A single peak at ca. 60 ppm shift, indicative of Al in a tetrahedral co-ordination (Samoson *et al.*, 1987), suggests that the trace Al in the catalyst was present in the framework.

3.1.1.2.6 Catalyst acidity

Catalyst acidity was measured using ammonia temperature programmed desorption. Unlike the unmodified ZSM-5 catalyst which showed two ammonia desorption peaks above 100 °C (see Figure 3.17 in Section 3.1.2.2.7) the boralites only exhibited one weak desorption peak with a maximum at ca. 180 °C. This was in agreement with work done by Coudurier and Védrine (1987) and Ratnasamy *et al.* (1986b) who noted the presence of a site at ca. 180-200 °C, but found no desorption peak corresponding to stronger acid sites. Only B-4 and silicalite exhibited any signs of stronger sites. The amount of strong acidity was extremely small, however, when compared to unmodified ZSM-5 of Si/Al = 40 (see Section 3.1.2.2.7). The greatest amount of weak acidity was shown by B-1 which desorbed 0.15 mmol NH_3/g. cat. Table 3.5 presents the desorption data for the catalysts, while a desorption profile of B-4 is shown in Figure 3.4. A desorption curve of B-5 compared to unmodified ZSM-5 is shown later in Figure 3.17.

Table 3.5 Boralite Acidities Measured by NH_3 TPD

Catalyst	Weak Sites* (mmol/g.cat.)	Strong Sites** (mmol/g/cat.)
B-1	0.15	-
B-2	0.06	-
B-2-HF	0.05	-
B-2-HF-NH_4F	0.06	-
B-3	0.07	-
B-4	0.08	0.02
B-5	0.07	-
B-6	0.10	-
Silicalite	0.04	0.02

* Desorption peak temp : 180-190 °C

** Desorption peak temp : 380-400 °C

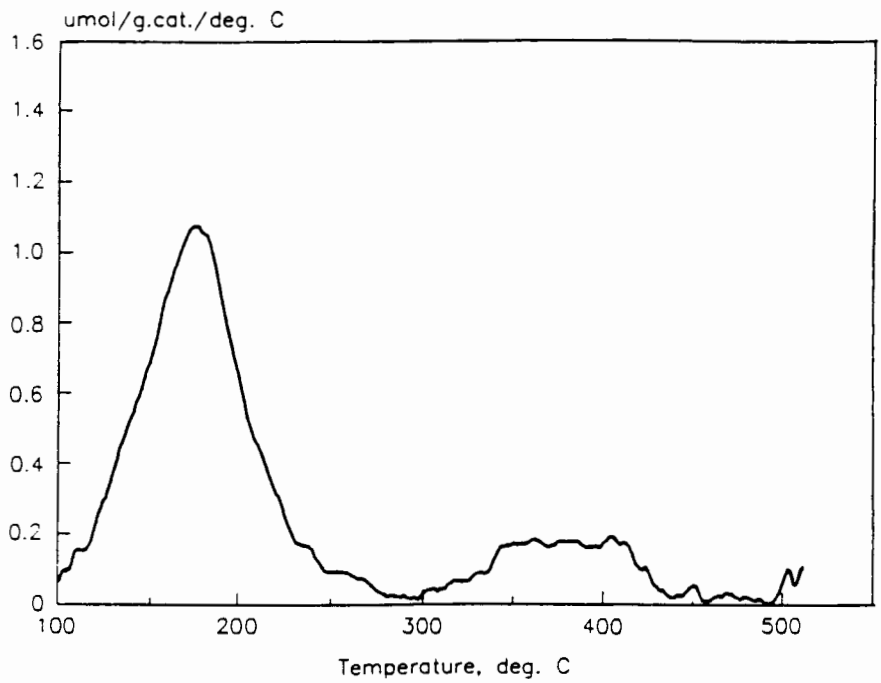

Figure 3.4 NH_3 Desorption profile for boralite (B-4)

3.1.1.3 Xylene isomerization

The xylene isomerization selectivity of B-1 is shown in Figure 3.5. The reaction temperature was 350 °C. It is evident that the incorporation of boron in the synthesis gel to produce a boralite catalyst has no effect on the selectivity of ZSM-5 to para-xylene.

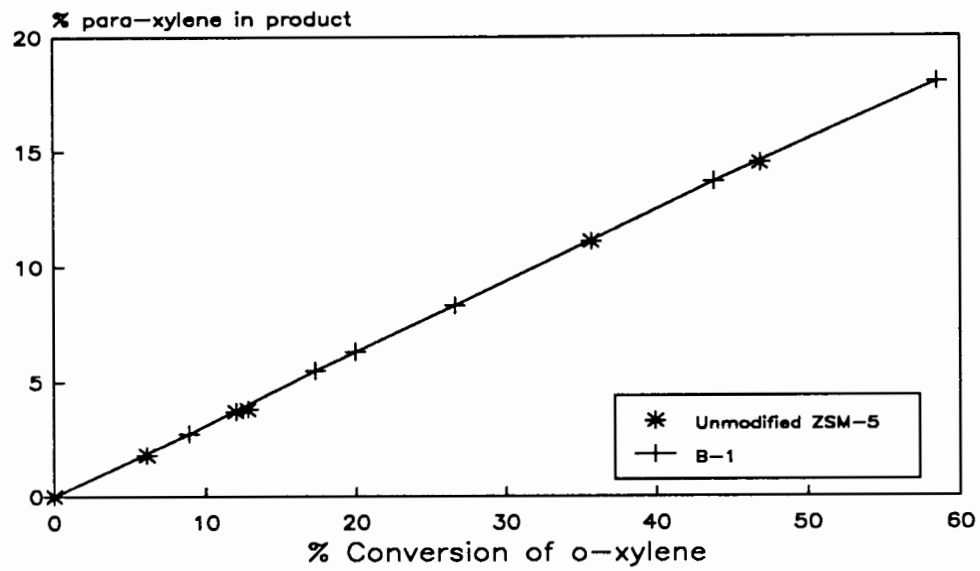

Figure 3.5 Para-xylene selectivity of boralite (B-1)

3.1.1.4 Propene oligomerization

Propene oligomerization was carried out at 5 MPa and WHSV of 12-16. The conversion versus time-on-stream data for boralites B-1, B-2, B-4 and B-6 are shown in Figure 3.6. The performance of silicalite relative to that of B-4, with similar Al content, is shown in Figure 3.7; while B-2 is compared to its fluorine modified forms (B-2-HF and B-2-HF-NH_4F) in Figure 3.8.

When comparing different catalysts for a particular reaction (e.g. propene oligomerization) a useful indicator of catalyst performance (i.e. activity and lifetime) is the catalyst utilization value, CUV. This is defined as the mass of liquid product formed per gram of catalyst. For the purposes of this thesis activity is defined as percentage conversion.

All of these catalysts were essentially inactive below 300 °C, although liquid product was formed over B-1, containing 760 ppm Al, at 258 °C. The activity below 300 °C, however, was low and only upon raising the temperature to 330 °C did the conversion rise to 90%. The catalyst utilization value (CUV) was 37 g/g. B-2 (550 ppm Al, 1.2 wt% B) was not active below 300 °C. At 300 °C, however, there was a sudden temperature rise to 360 °C. The reaction was subsequently carried out between 340 and 350 °C giving a CUV of 39 g/g.

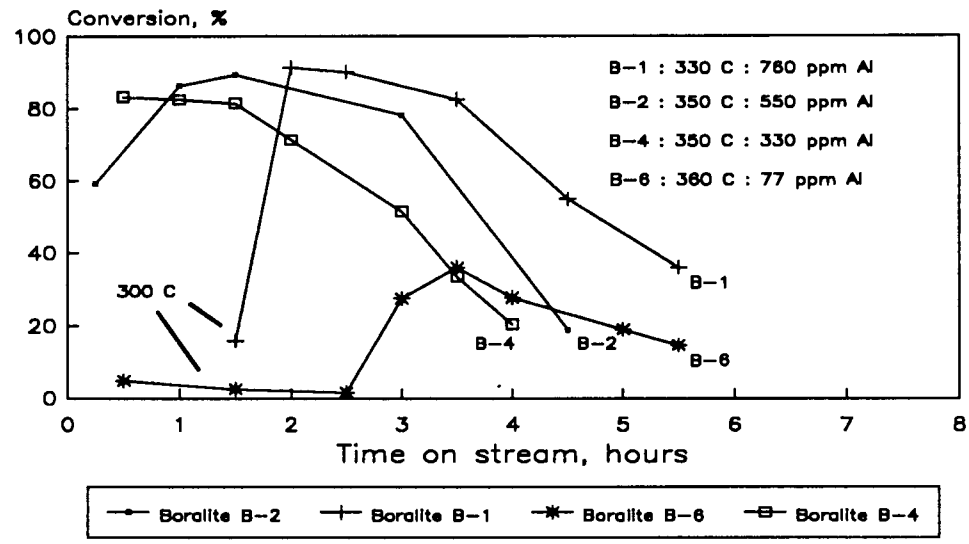

Figure 3.6 Propene oligomerization activity of boralite catalysts

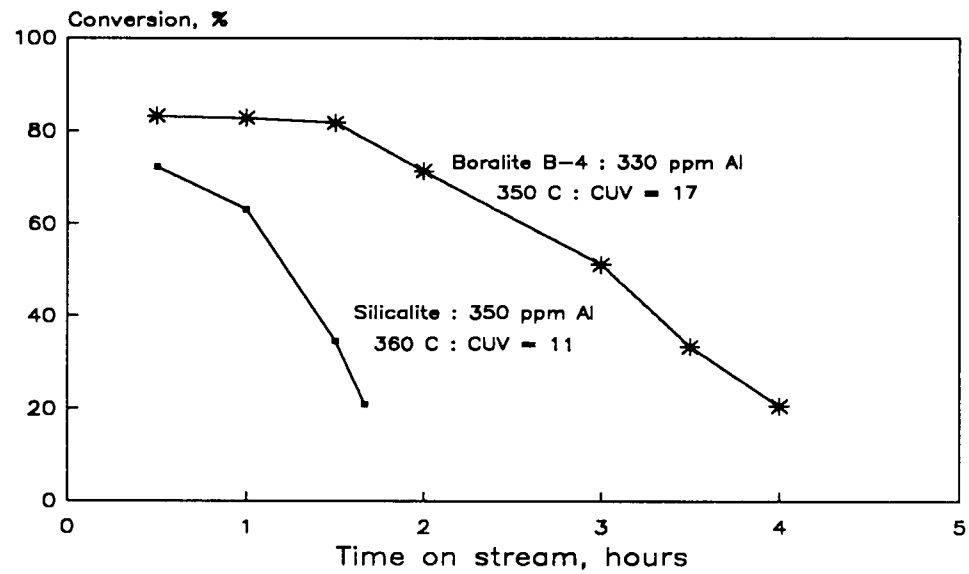

Figure 3.7 Activity of silicalite for propene oligomerization

B-4, containing 330 ppm Al and 0.59 wt% B, produced only 17 g/g at 350 °C. B-6, with even less Al, showed a small degree of activity (<5% conversion) at 300 °C, and reached a maximum conversion of ca. 36% at 360 °C.

Although B-4 and the silicalite catalyst have similar Al contents the boralite catalysts shows greater activity and longer time-on-stream. It would be tempting to attribute the greater activity of B-4 to the presence of boron. It should be noted, however, that silicalite had a different (binodal) crystallite size distribution with crystallites as large as 10 μm. The differences in crystallite sizes rather than the presence of boron could be responsible for the differences in activity.

B-2, with a CUV of 39 g/g, performed poorly once treated with HF (B-2-HF) with a CUV of only 7 g/g at 345-350 °C. When some of this catalyst was then treated with NH_4F, the resulting catalyst was not active until 315 °C at which stage there was a slow temperature rise to 350 °C. Most of the reaction was carried out at 360 °C with a CUV of 30 g/g.

Boralite B-3-NH_4F experienced a sharp temperature runaway during startup, the temperature rising from 320 °C to 395 °C within half a minute. This was followed by a rapid drop in bed temperature, indicating catalyst deactivation. Subsequent activity was low with a CUV of 6 g/g at 355 °C. When B-3 was treated with ten times less NH_4F than for B-3-NH_4F the resulting catalyst produced no liquid at 350 °C or less.

It is hardly surprising that a temperature runaway was observed when one considers the high reaction temperatures required for boralite activity. Attempts to prevent temperature runaway over B-3-NH_4F by diluting the bed with glass beads were unsuccessful.

3.1.1.4.1 Liquid product

Liquid product distributions as well as some cetane numbers for some of the catalysts are shown in Table 3.6. Data for unmodified ZSM-5 has been included for comparison.

Table 3.6 Liquid Product

Catalyst	T(°C)	WHSV	% Conv	Dim.	Tri.	Tetr.	Pent.	Hex^+	Cet. No.
ZSM-5	299	12	100	19	23	28	16	14	41.7
B-1	331	15	90	33	28	21	10	8	40.1
B-2	346	16	86	36	34	24	6	0	39
B-2-HF-NH_4F	366	15	86	38	35	21	5	1	n.d.
B-3-NH_4F	355	14	63	31	38	24	6	1	n.d.
B-6	360	12	36	36	33	24	6	1	43.6
Silicalite	360	14	72	39	28	20	8	5	n.d.

n.d. = not determined

Meaningful comparisons between the liquid product distributions of various catalysts should only be made if the analyses are carried out at similar reaction temperatures, WHSV and conversion levels (less than 100%). This is clearly difficult to achieve, considering the high reaction temperatures required for boralite activity and the propensity for temperature runaways any attempts to achieve similar conversion levels at a given temperature are likely to be singularly unsuccessful. If one considers oligomerization as the sum of a series of consecutive reactions one could reasonably expect total conversion to affect (dimer + trimer) / (tetramer + higher oligomer) ratios to a significant extent. Extensive work on propene oligomerization, however, carried out in this laboratory over a wide range of catalysts has not shown this to be the case. Studies over ZSM-5, for example, showed that (dimer + trimer) / (tetramer + higher oligomer) ratios were only slightly dependent on conversion level, but strongly dependent on reaction temperature (Schwarz, 1991). One should bear this in mind when making comparisons.

From the data presented in Table 3.6 one can see, however, that the boralite and silicalite catalysts have reduced C_{12}^+ fractions and substantially lower C_{18}^+ fractions compared to ZSM-5 (at 299 °C). The dimer and trimer fractions of these catalysts, however, are higher. The G.C. trace for B-2's product (at 346 °C and 86% conversion) is shown in Figure 3.9a. Compared to that of unmodified ZSM-5 at 250 °C and 80% conversion one can see the noticeable lack of oligomer groupings in the product of the boralite catalyst. The presence of aromatics in the liquid products of the boralite catalysts was confirmed using ^{1}H-n.m.r. A ^{1}H-n.m.r. spectrum for B-6 at 300 °C is shown in Figure 3.10. The peaks identifying the presence of aromatics are clearly evident.

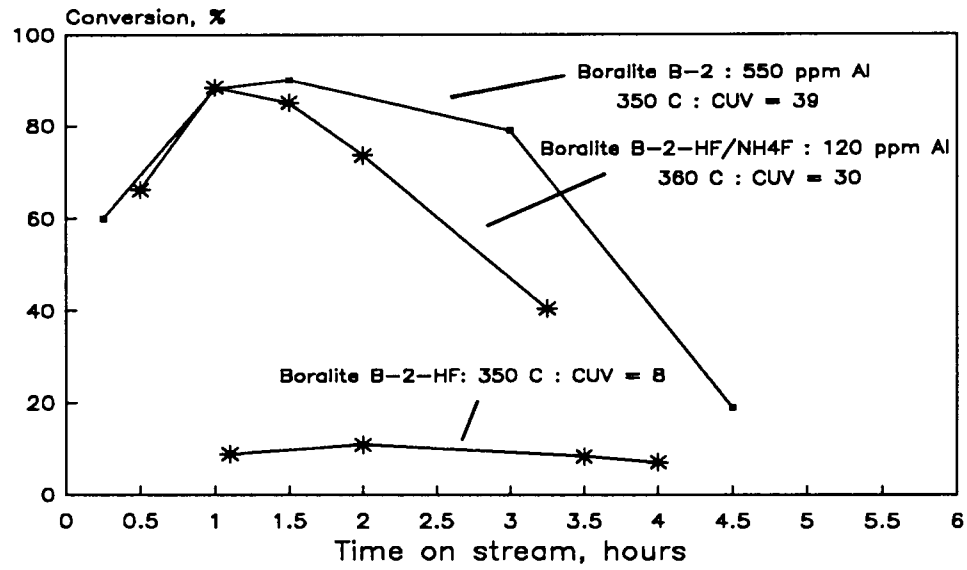

Figure 3.8 **The effect of fluorination on boralite activity**

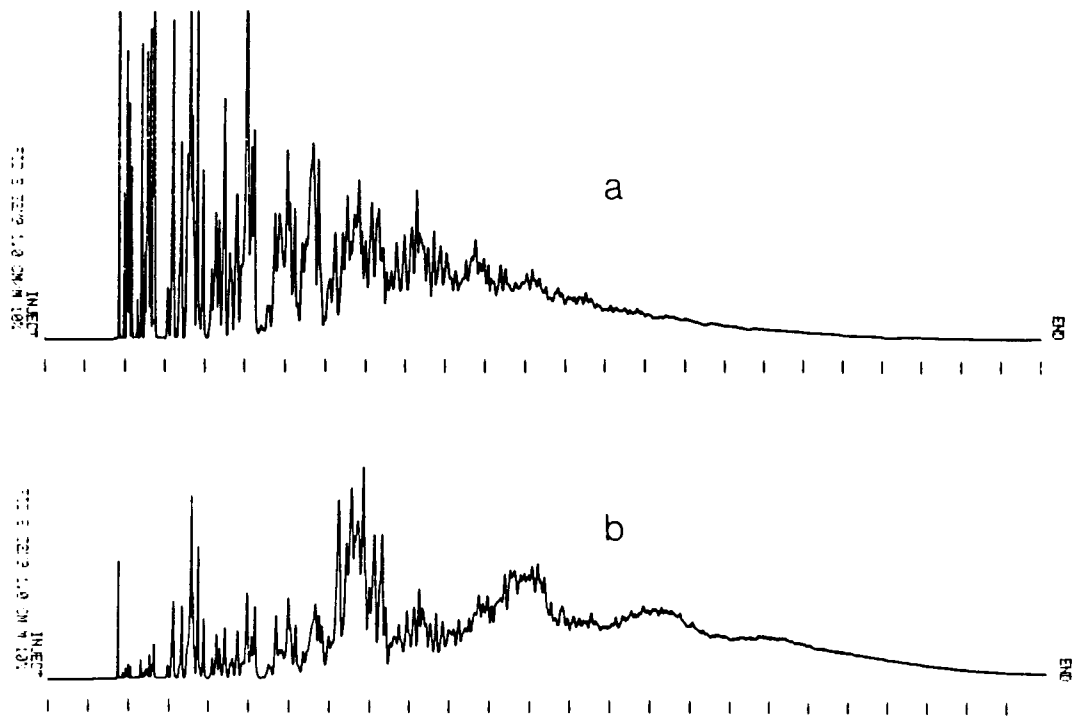

Figure 3.9 **Liquid product analysis of a) boralite B-2 (346 °C, 86% conversion), b) unmodified ZSM-5 (250 °C, 80% conversion)**

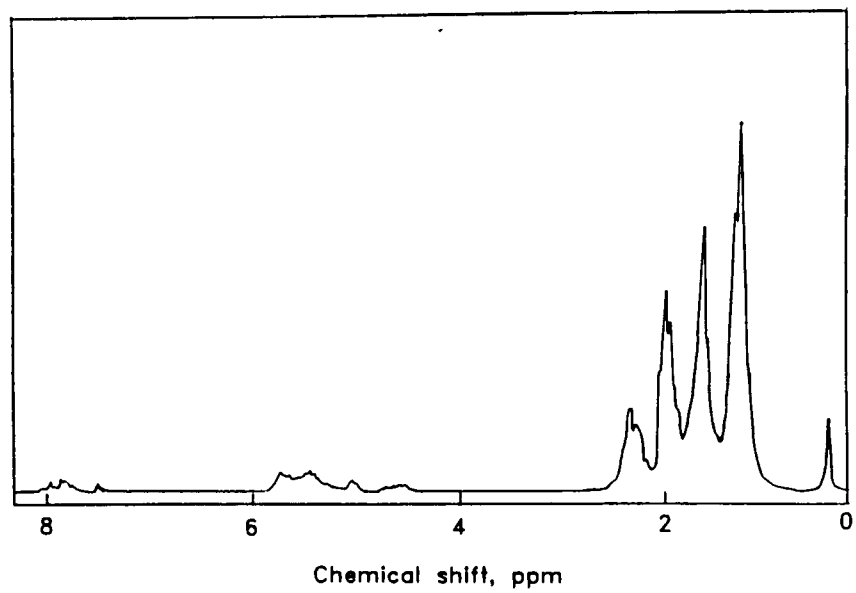

Figure 3.10 ^{1}H-n.m.r. of product of boralite (B-6) at 300 °C

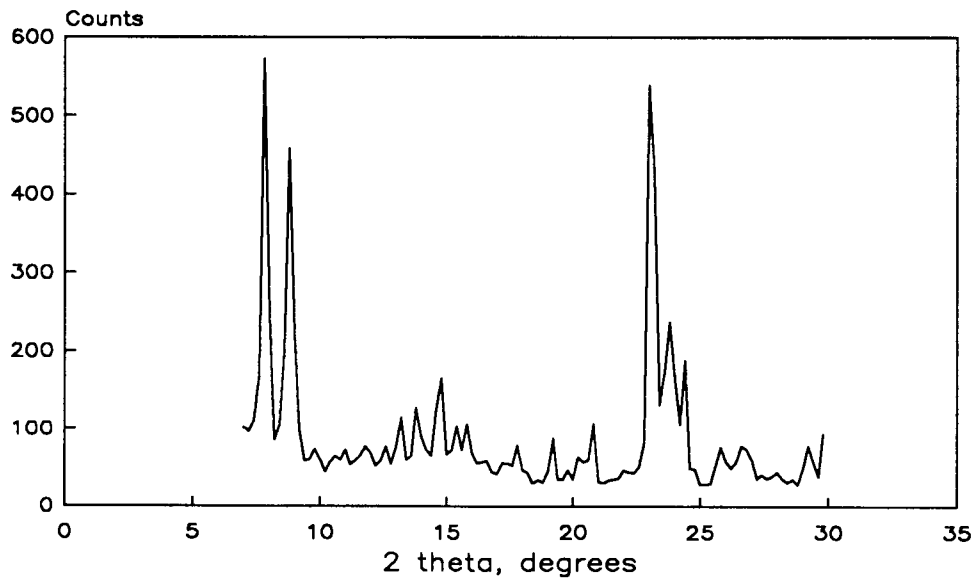

Figure 3.11 XRD spectrum of unmodified ZSM-5

3.1.2 Boron Impregnated ZSM-5

3.1.2.1 Catalyst nomenclature

The ZSM-5 catalysts modified by boric acid impregnation were labelled according to the following code:

ZB - m

where Z - indicates that the catalyst is a ZSM-5 (Si/Al = 41)
B indicates that the ZSM-5 was modified by boric acid impregnation
m - refers to the impregnation technique used and may be:

imp - incipient wetness impregnation
wash - incipient wetness impregnation followed by washing with distilled water
refl- impregnation by heating catalyst and a boric acid solution under reflux

For easy reference to catalyst coding refer to the fold out in Appendix 11.

3.1.2.2 Characterization

3.1.2.2.1 Relative crystallinity

XRD

A ZSM-5 catalyst of Si/Al = 41 was impregnated with boric acid both by refluxing catalyst with a solution of boric acid at 90 °C, and by using the incipient wetness technique (see Section 2.4.5.1). The catalyst used for these modifications was 95% crystalline relative to boralite B-3 (see Section 3.1.1.2.1). An XRD spectrum of the parent ZSM-5 is shown below in Figure 3.11. There was no indication that impregnation of the catalyst altered the crystallinity of the catalyst.

FTIR

The crystalline nature of ZSM-5 and its boron impregnated forms was confirmed by monitoring the optical density ratio. Values of R are given in Table 3.7.

Structural bands at 1230, 1100, 800, 550 and 450 cm^{-1} further confirmed the presence of the ZSM-5 structure (Flanigen and Khatami, 1971).

Table 3.7 Optical Density Ratios of Boron Impregnated ZSM-5

Catalyst	R (calcined)	R (as synthesized)
ZSM-5	0.66	0.72
ZB-refl	0.63	-
ZB-imp	0.69	-
ZB-wash	0.70	-

3.1.2.2.2 Crystallite size and morphology

Figure 3.12 shows a micrograph of the unmodified ZSM-5. The average crystallite size is between 2 and 3 microns. The crystallite size distribution determined by number averaged counting is shown in Figure 3.13. It should be noted that sizes of crystallites were taken as being an average of the longest and shortest axes.

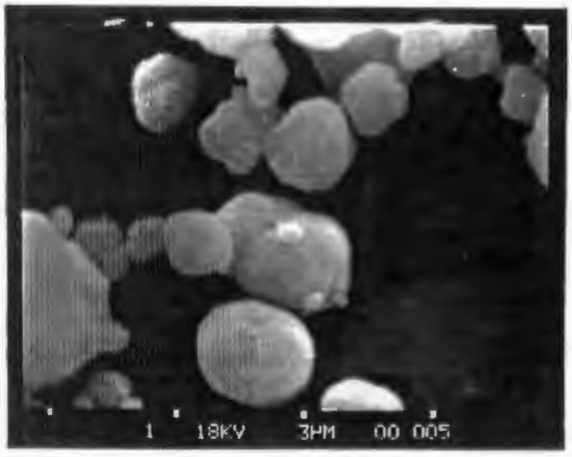

Figure 3.12 Electron micrograph of ZSM-5

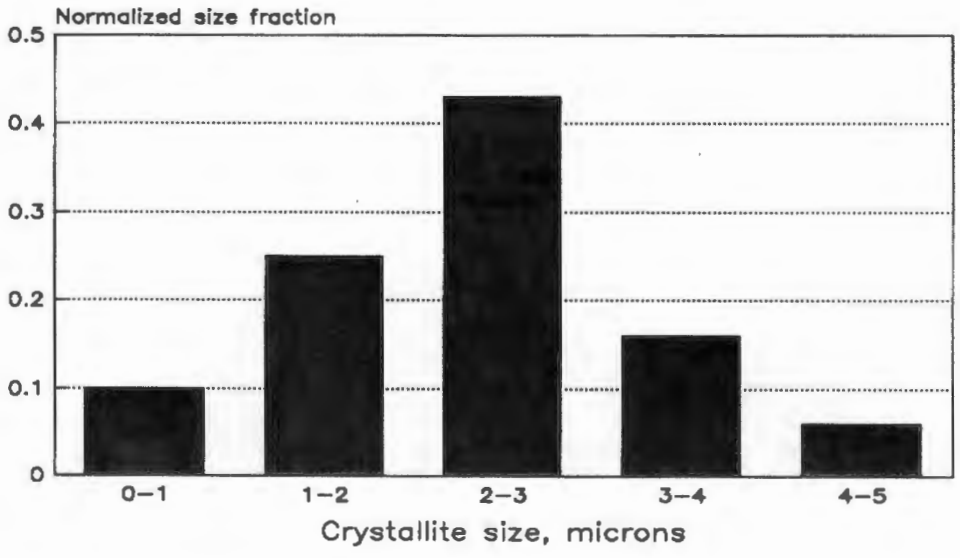

Figure 3.13 Crystallite size distribution of ZSM-5

3.1.2.2.3 Cyclohexane adsorption

Cyclohexane adsorption was carried out at 30 °C over ZSM-5 and its boron impregnated counterparts. The weight gain phenomenon observed during cooling was not included in Figure 3.14 which shows cyclohexane adsorption rates of the impregnated catalysts. Also included in the Figure is the adsorption behaviour of boralite B-1. While other researchers (Gabelica *et al.*, 1984b) have ascribed the weight gain during cooling to the physisorption of nitrogen and/or water the present study suggested that this phenomenon should rather be ascribed to the adsorption of cyclohexane impurities in the system on the catalyst. The cyclohexane adsorption values shown in Table 3.8 are inclusive of weight gain during cooling.

Table 3.8 Cyclohexane Adsorptions

Catalyst		Cyclohexane Adsorption (wt %)
Unmodified ZSM-5	(A)	11.5
ZB-imp	(B)	7.1
ZB-wash	(C)	9.8
ZB-refl	(D)	7.8
B-1	(E)	6.9

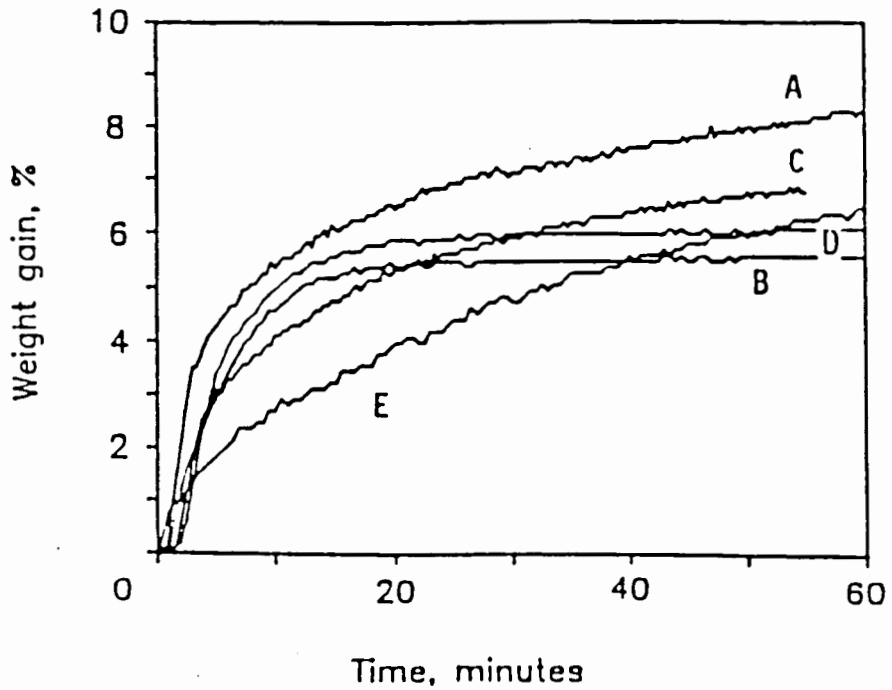

Figure 3.14 Cyclohexane adsorption; catalysts indicated by letters in brackets in Table 3.8

3.1.2.2.4 Boron and aluminium content

The aluminium content of the unmodified ZSM-5 was determined using EDX and confirmed by AA, while boron analysis was done using AA. Boron and Al contents of the boron impregnated samples are presented in Table 3.8. The unmodified ZSM-5 is labelled ZSM-5, while the impregnated forms of this catalyst are labelled according to the code described in Section 3.1.2.1. The sodium content of the unmodified ZSM-5 was 0.024 wt%.

Table 3.9 B and Al Contents of Boron Impregnated ZSM-5

Catalyst	Boron Content (wt%)	Si/Al
ZSM-5	-	41
ZB-refl	0.40	41
ZB-imp	1.5	41
ZB-wash	0.38	41

3.1.2.2.5 Boron and aluminium distributions

SIMS was used to analyze the Si, B and Al contents of ZB-wash. The Si/Al ratio (in arbitrary units) of the catalyst crystallites as a function of depth is shown in Figure 3.15. Although the sample appears to be more aluminium deficient at the external surface of the catalyst this may be an artefact of the SIMS technique in the outer layers of the catalyst. Similarly, it can be seen from Figure 3.16 which shows the SIMS Si/B ratio of the same catalyst that there appears to be a depletion of B at the external surface. Again this may be an artefact of the SIMS technique.

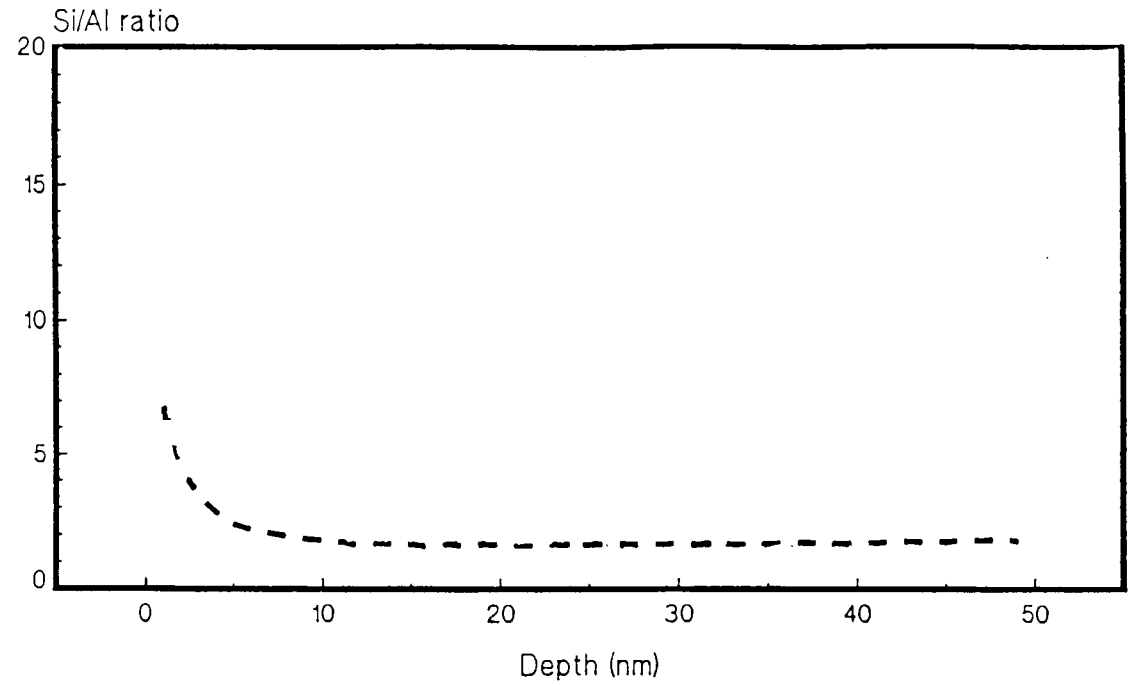

Figure 3.15 SIMS Si/Al as a function of depth

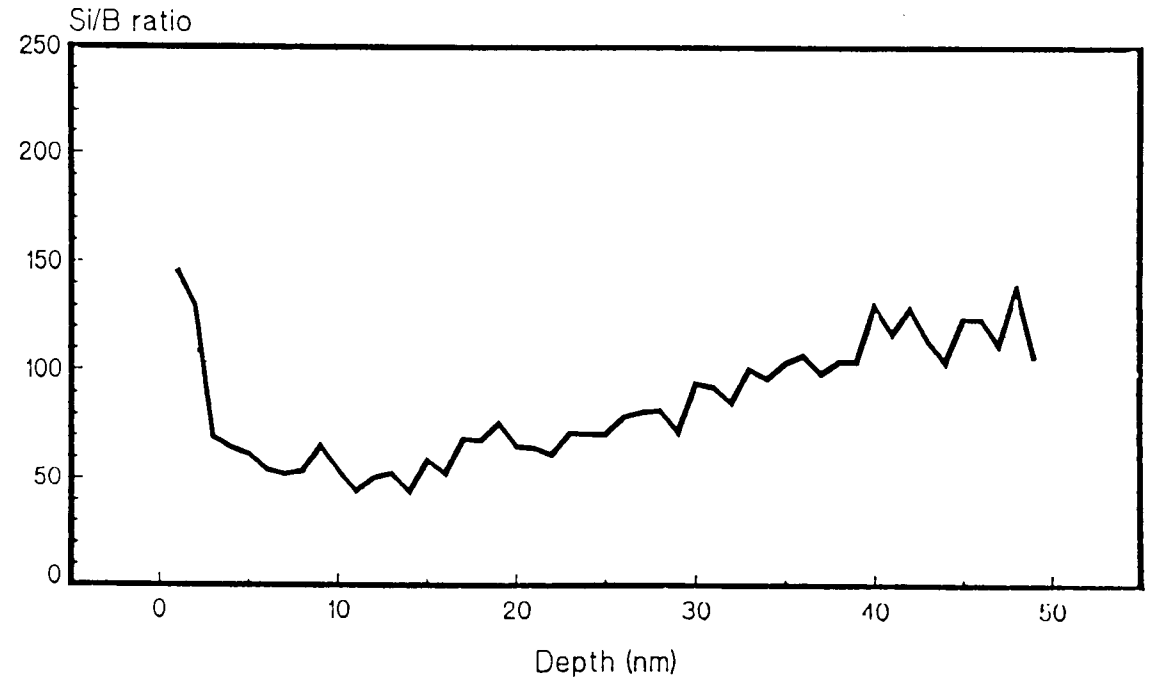

Figure 3.16 Si/B profiles as a function of depth

3.1.2.2.6 Surface area

BET surface areas of ZSM-5 and the incipient wetness impregnated ZSM-5 catalysts are shown in Table 3.10. Impregnation results in a decrease in surface area, which is slightly reversed upon washing.

Table 3.10 BET Surface Areas of Boron Impregnated ZSM-5

Catalyst	Surface Area (m^2/g)
Unmodified ZSM-5	480
ZB-imp	285
ZB-wash	295

3.1.2.2.7 Catalyst acidity

The acidity of the boron impregnated catalysts as measured by ammonia TPD are presented in Table 3.11. Included in the table are the temperatures corresponding to desorption peak maxima.

Table 3.11 Acidities of Boron Impregnated ZSM-5

Catalyst	Ammonia Desorption			
	Low T Peak		High T Peak	
	°C	mmol/g	°C	mmol/g
Unmodified ZSM-5	240	0.41	470	0.37
ZB-refl	240	0.35	470	0.32
ZB-imp	220	0.58	430	0.24
ZB-wash	240	0.33	470	0.35

Impregnation of ZSM-5 with boron reduced the number of strong sites as measured by NH_3 TPD, in agreement with work done by other researchers in the field (Auroux *et al.*, 1985; Chu *et al.*, 1985). This was particularly noticeable in the case of ZB-imp. The desorption peaks for this catalyst were also shifted to lower temperatures. After washing (ZB-wash) this effect was largely reversed with desorption peaks shifting back to higher temperatures with the number of strong sites also increasing to a value only a little lower than for unmodified ZSM-5. ZB-refl showed similar strong acidity to ZB-wash. The desorption profiles of ZB-imp, ZB-wash and unmodified ZSM-5 are shown in Figure 3.17. The increase in the number of weak sites at the expense of strong sites upon incipient wetness impregnation (ZB-imp) is readily apparent.

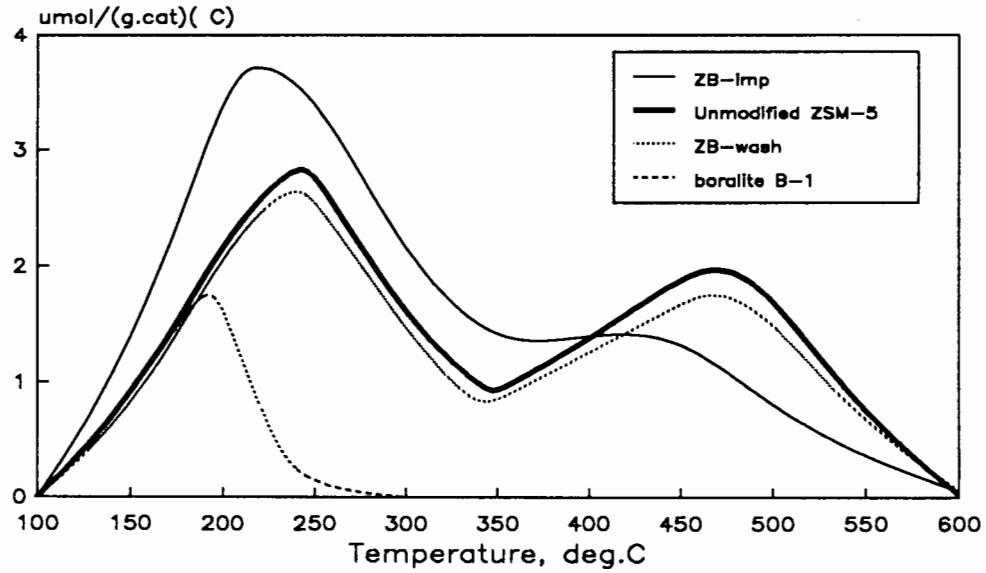

Figure 3.17 Desorption from boron impregnated catalysts

3.1.2.3 Xylene isomerization

The greatest increase in para-xylene selectivity was observed over ZB-imp. The selectivity to para-xylene as a function of o-xylene conversion level of this catalyst relative to the parent ZSM-5 is shown in Figure 3.18. ZB-wash and ZB-refl showed only slightly greater selectivity to para-xylene than the unmodified catalyst. The variation in p-xylene selectivity of ZB-imp with temperature is shown in Figure 3.19a. The selectivity change of the unmodified ZSM-5 with temperature is shown in Figure 3.19b.

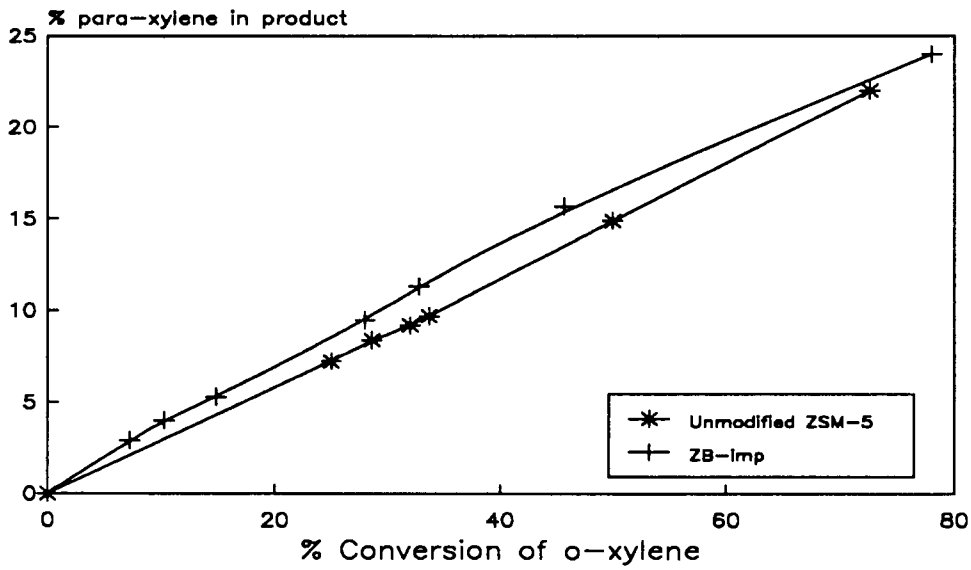

Figure 3.18 **Xylene isomerization of boron impregnated ZSM-5 (ZB-imp)**

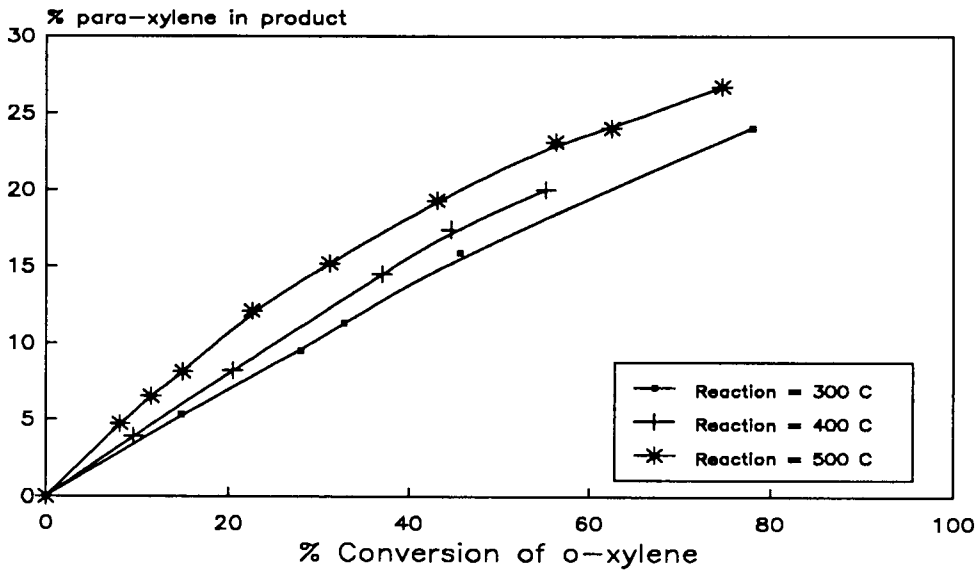

Figure 3.19 (a) **Effect of temperature on p-xylene selectivity of boron impregnated ZSM-5 (ZB-imp)**

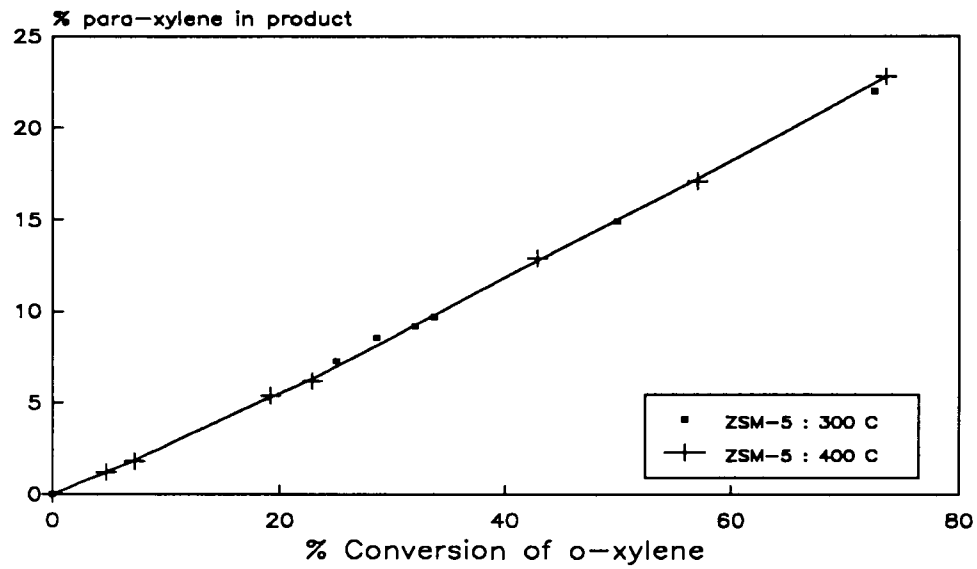

Figure 3.19 (b) Effect of temperature on p-xylene selectivity of ZSM-5

3.1.2.4 Propene oligomerization

3.1.2.4.1 Reproducibility

Two propene oligomerization runs were carried out at 250 °C and WHSV = 20-25. The CUVs for these two runs were 120 g/g and 126 g/g indicating reproducibility to within 5%.

3.1.2.4.2 Activity and lifetime

Figure 3.20 shows the conversion versus time on stream data for ZSM-5 and ZB-refl. The CUV of the unmodified ZSM-5 (600 g/g) was obtained by ramping the temperature at the onset of deactivation in the temperature range 200-290°C. The CUV of ZB-refl was substantially lower at 308 g/g cat.

The CUV of ZB-wash was 306 g/g (see Figure 3.21) and that of the impregnated catalyst (ZB-imp) was 23 g/g. Although the CUV of ZB-wash is similar to that of the heat refluxed catalyst (306 g/g and 308 g/g respectively) it should be noted that the impregnated and washed catalyst was monitored for 40 hours only. The conversion at the time of shut down

was 100%. The true CUV of this catalyst, therefore, is expected to be closer to that of unmodified ZSM-5. ZB-refl on the other hand was clearly deactivating at the time of shut down and therefore appears to have a much shorter lifetime than either ZB-wash or the unmodified ZSM-5.

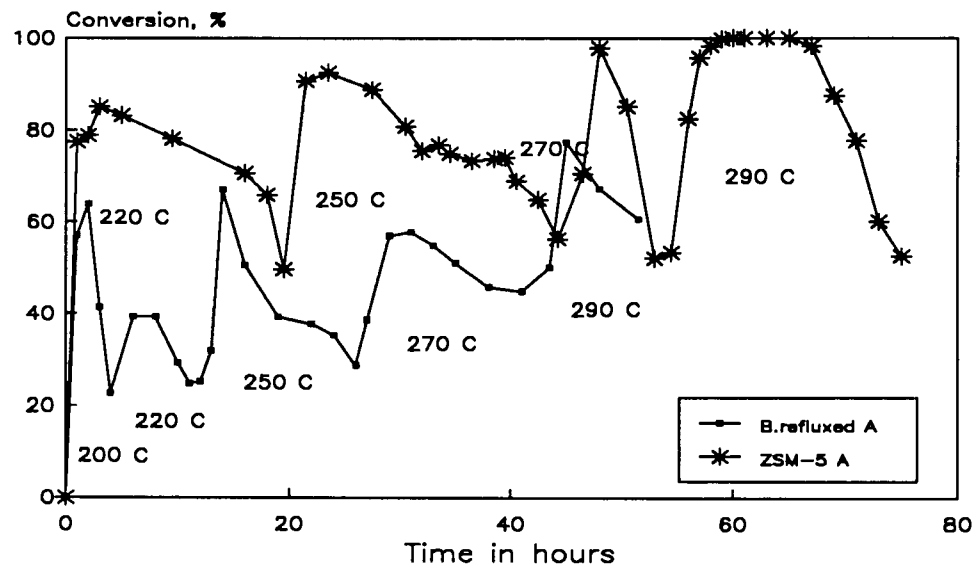

Figure 3.20 Propene oligomerization over ZSM-5 and ZB-refl

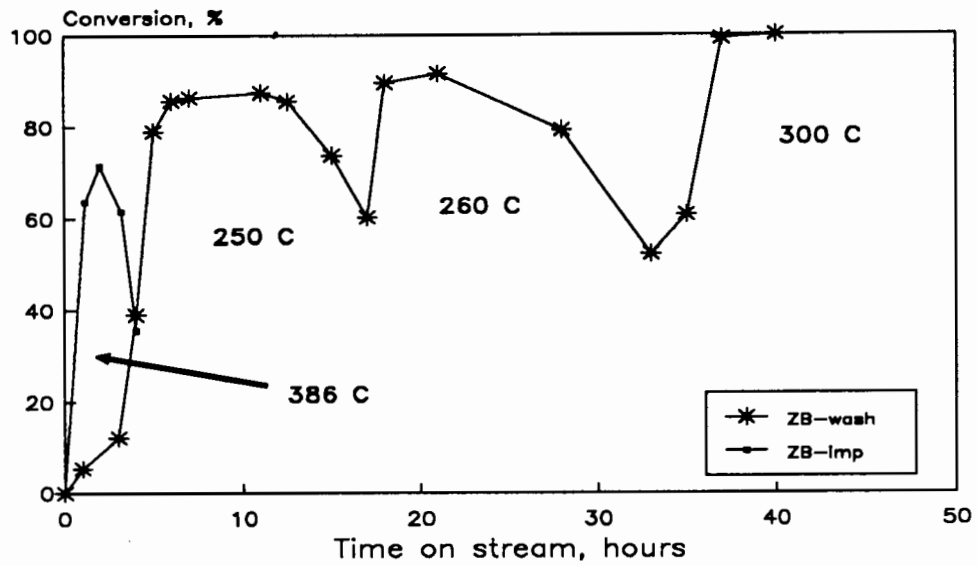

Figure 3.21 Propene oligomerization over ZB-imp and ZB-wash

3.1.2.4.3 Liquid product analysis

Table 3.12 shows the liquid product distribution for the impregnated catalysts. Carbon number distribution as well as cetane numbers are given.

Table 3.12 Carbon Number Distribution and Cetane Numbers for Boron Impregnated Catalysts

Catalyst	Temp °C	WHSV	Conv %	Dim. %	Tri. %	Tetr. %	Pent. %	Hex+ %	Cet. No.
ZSM-5	299	12	100	19	23	28	16	14	41.7
ZB-refl	291	14	77	23	24	26	14	13	38.6
ZB-imp	386	11	72	46	34	14	4	2	n.d.
ZB-wash	298	13	100	16	25	29	16	14	43.7

A point to note is the high percentage of dimer and trimer in the product of ZB-imp, a result no doubt of the high reaction temperature.

3.2 Phosphorus Modified ZSM-5

3.2.1 Catalyst Nomenclature

All catalysts modified with phosphorus were named according to the following code:

ZP - m

where Z indicates that the catalyst is a ZSM-5

P indicates the way in which the catalyst was modified with phosphorus and may have the values

- P^1 - indicates H_3PO_4 incorporation during synthesis
- P1 - signifies H_3PO_4 impregnation of ZSM-5
- P2 - signifies TMP impregnation of ZSM-5 according to the method laid out in Section 2.4.5.1.

m is a number identifying the catalyst batch

For easy reference to catalyst coding refer to the fold out in Appendix 11.

3.2.2 Characterization

3.2.2.1 Relative crystallinities

Relative crystallinities of the phosphorus modified catalysts are given in Table 3.13. Catalysts are labelled according to the code presented in Section 3.2.1. Catalysts ZP2-1 and ZP2-2, for example, were impregnated with trimethylphosphite, while catalysts ZP1-1 and ZP1-2 were impregnated with orthophosphoric acid (min. 85%) (see Section 2.4.5.1). Silicalite was modified by adding 2 g of silicalite to 1.72 g H_3PO_4 (min. 85%) which had been heated to 60 °C. The catalyst was added to the phosphoric acid while agitating and cooling to 0°C. The catalyst was loaded with 70% PO_4^{3-} by weight. The resulting catalyst was then dried at 80 °C for 16 hours.

Table 3.13 Relative Crystallinities of Phosphorus Modified Catalysts

Catalyst	% Crystallinity (relative to ZP[1]-3)
ZP[1]-1	96
ZP[1]-2	89
ZP[1]-3	100
ZP[1]-4	83
ZP2-1	92
ZP2-2	91
ZP1-1	88
ZP1-2	91
H_3PO_4 slurried Silicalite	82

In all cases presence of the ZSM-5 type structure for the unmodified ZSM-5 catalysts was further confirmed by the presence of infrared bands at 1200, 1100, 800, 550 and 450 cm^{-1}.

3.2.2.2 Crystallite size and morphology

Electron micrographs of the catalysts were used to determine number average crystallite sizes which are shown in Table 3.14. The crystallite sizes of ZP[1]-1 were very small (< 1 micron) with a very narrow size distribution. An electron micrograph of this catalyst is shown in Figure 3.22.

Table 3.14 Crystallite Sizes of Phosphorus Modified Catalysts

Catalyst	Average Crystallite Size (μm)
ZP1-1	< 1
ZP1-2	3.5
ZP1-3	4.0
ZP1-4	2.3
ZP2-1	2.0-3.0
ZP2-2	2.0
ZP1-1	2.0-3.0
ZP1-2	2.0-3.0
H_3PO_4 slurried Silicalite	2.0-3.0

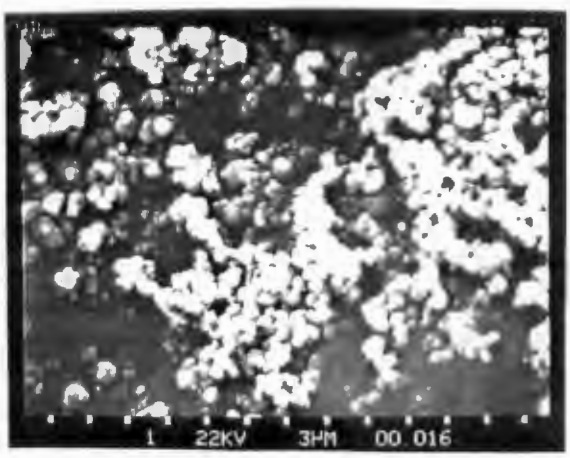

Figure 3.22 Micrograph of crystallites of ZP1-1

Table 3.15 Cyclohexane Adsorption of Phosphorus Modified Catalysts

Catalyst	Cyclohexane Adsorption (wt %)
ZP[1]-1	7.2
ZP2-1	7.0
ZP2-2	7.0
ZP1-1	8.0
ZP1-2	8.2
H_3PO_4 slurried Silicalite	2.7

Impregnation of ZSM-5 with TMP reduced the cyclohexane adsorption levels the most. Phosphoric acid impregnation also reduced adsorption levels relative to unmodified ZSM-5. Silicalite had the lowest adsorption value (2.7 wt%).

Table 3.16 Aluminium and Phosphorus Contents of Phosphorus Modified ZSM-5

Catalyst	Si/Al	P (wt %)
ZP[1]-1	42	0.4
ZP[1]-2	191	0.38
ZP[1]-3	261	0.18
ZP[1]-4	50	0.11
ZP2-1	40	1.2
ZP2-2	19	1.0
ZP1-1	40	0.4
ZP1-2	18	0.9
H_3PO_4 slurried Silicalite	380 ppm	70% PO_4^{3-} loaded

3.2.2.3 Cyclohexane adsorption

Cyclohexane adsorption capacities of the catalysts at 30 °C are given in Table 3.15.

3.2.2.4 Aluminium and phosphorus contents

The phosphorus and aluminium contents of the catalysts are shown in Table 3.16.

3.2.2.5 Aluminium and phosphorus coordination

^{31}P MAS n.m.r. was carried out on catalysts ZP1-1 to ZP1-4. The spectrum for ZP1-4 is shown below in Figure 3.23. The peak at ca. 0 ppm shift is characteristic of phosphates. There was no indication, for any of these catalysts, that there had been phosphorus incorporation in the framework. ^{27}Al MAS n.m.r., however, showed that all of the aluminium present in these catalysts was tetrahedrally coordinated framework Al with a peak at ca. 60 ppm shift.

3.2.2.6 Surface area

BET surface areas of the phosphorus impregnated catalysts are presented in Table 3.17. Also included for comparison is the surface area of unmodified ZSM-5. Catalysts ZP2-1, ZP2-2 and ZP1-2, all impregnated with approximately 1 wt% phosphorus, had reduced BET surface areas of about 300 m^2/g. Catalyst ZP1-1, impregnated with only 0.4 wt% P, had a higher surface area (421 m^2/g).

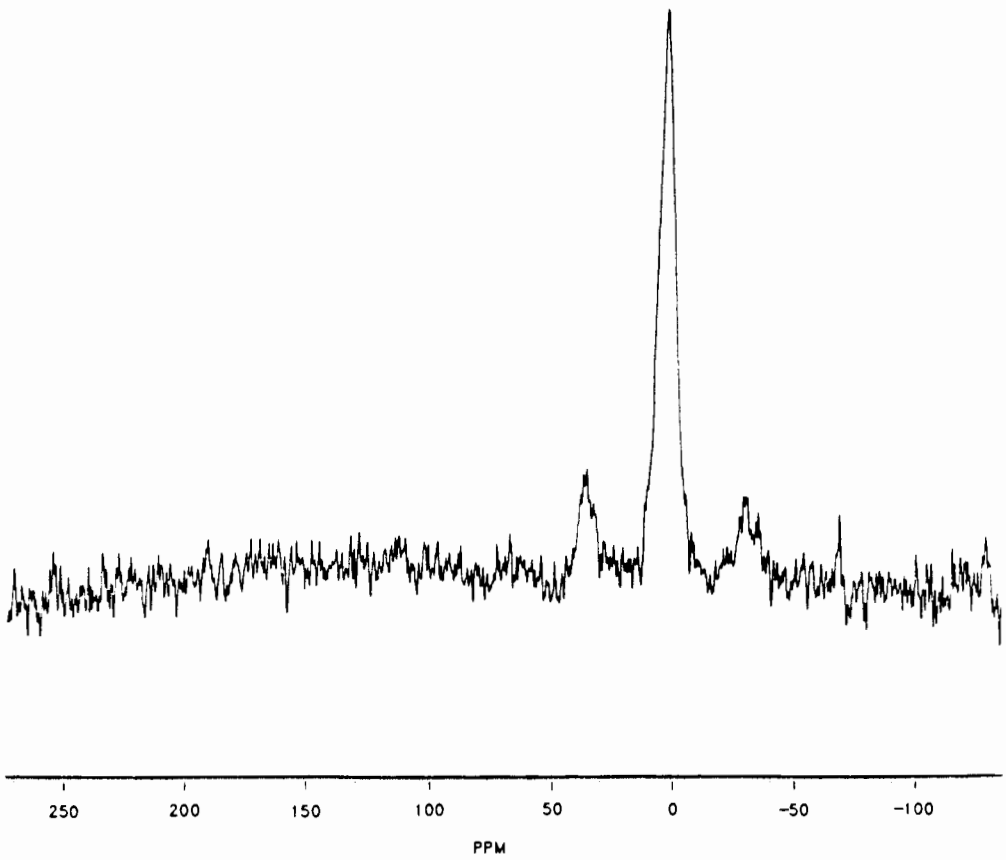

Figure 3.23 **^{31}P MAS n.m.r. spectrum of ZP1-4**

Table 3.17 Surface Areas of Phosphorus Impregnated Catalysts

Catalyst	% P (wt)	Surface Area (m^2/g)
Unmodified ZSM-5	-	480
ZP2-1	1.2	306
ZP2-2	1.0	304
ZP1-1	0.4	421
ZP2-2	0.9	308

3.2.2.7 Catalyst acidity

Acidities of the catalysts are presented in Table 3.18. Impregnation with phosphoric acid and TMP reduced the amount of strong acidity in agreement with work done by other researchers (Jentys *et al.*, 1989). Impregnation of ZSM-5 with TMP almost completely

removed the strong sites in the case of a catalyst with Si/Al = 40 (ZP2-1), resulting in a desorption profile with only one peak. It was not clear, however, whether impregnation with phosphoric acid converted strong sites to weak sites as proposed by Jentys *et al.* (1989). ZP2-2, with similar phosphorus content to ZP2-1, but lower Si/Al ratio, had much reduced strong acidity when compared to the acidity of the same catalyst prior to modification. Schwarz (1990) determined the acidity of the unmodified form of ZP2-2 to be 0.46 mmol /g. cat. The desorption profile of ZP2-1 is shown in Figure 3.24.

Table 3.18 Acidities of Phosphorus Modified Catalysts

Catalyst	Ammonia Desorption			
	Low T Peak		High T Peak	
	°C	mmol/g	°C	mmol/g
ZP[1]-1	220	0.28	450	0.30
ZP[1]-2	200	0.048	400	0.072
ZP[1]-3	210	0.06	400	0.078
ZP[1]-4	230	0.32	460	0.39
ZP2-1	200	0.30	-	-
ZP2-2	225	0.36	450	0.27
ZP1-1	220	0.35	430	0.33
ZP1-2	230	0.50	470	0.39

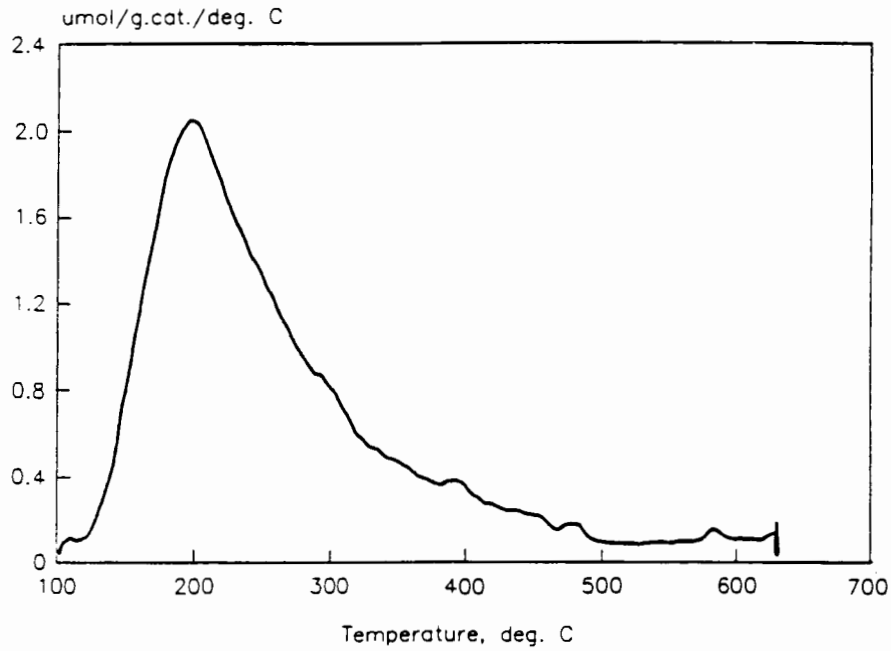

Figure 3.24 NH_3 Desorption profile of ZP2-1

3.2.3 Xylene Isomerization

The selectivities of phosphorus modified catalysts ZP[1]-1, ZP1-1 and ZP2-2 are shown in Figure 3.25 for a reaction temperature of 350 °C. Although not plotted in Figure 3.25, ZP2-1 had a para-xylene selectivity curve which was essentially the same as that of ZP[1]-1. The p-xylene selectivities of these catalysts were indistinguishable from the para-xylene selectivity of unmodified ZSM-5 at 350 °C. From Figure 3.25 it can be seen that ZP2-2 and ZP1-1 had almost identical selectivity to para-xylene.

In Figure 3.26 the para-xylene selectivity of ZP1-1 was compared to that of boron impregnated ZSM-5 (ZB-imp). The reaction temperature was 500 °C. Also included in Figure 3.26 is the performance of ZSM-5 synthesized with potassium hydroxide as the alkali-metal cation. The resulting catalyst, labelled K-ZSM-5, had an average crystallite size of ca. 10 μm and correspondingly had greater para-xylene selectivities, in keeping with work carried out by Chen *et al.* (1979). It should be stressed, at this stage, that although the differences in selectivity to para-xylene for most of the catalysts were comparatively small, they were repeatable.

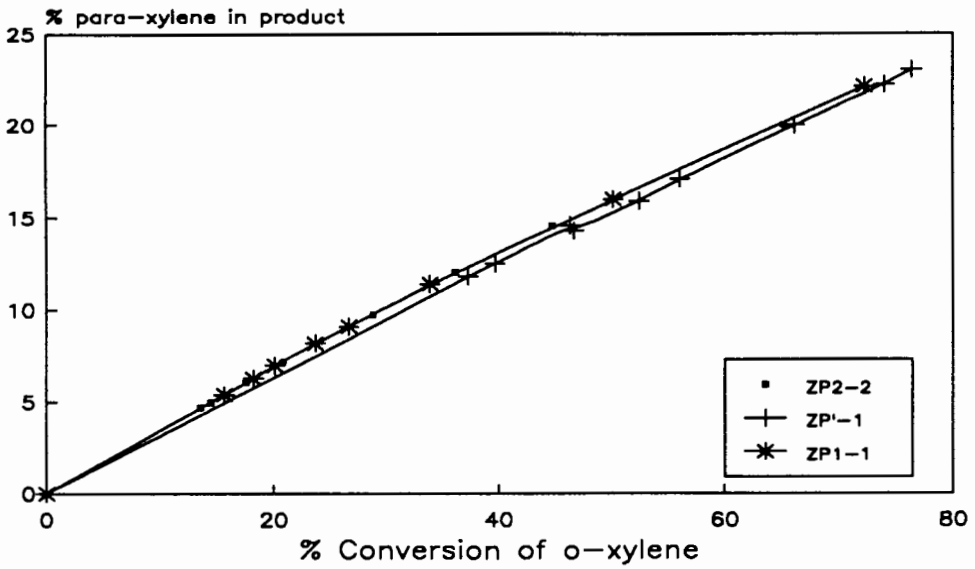

Figure 3.25 Para-xylene selectivity for phosphorus modified catalysts

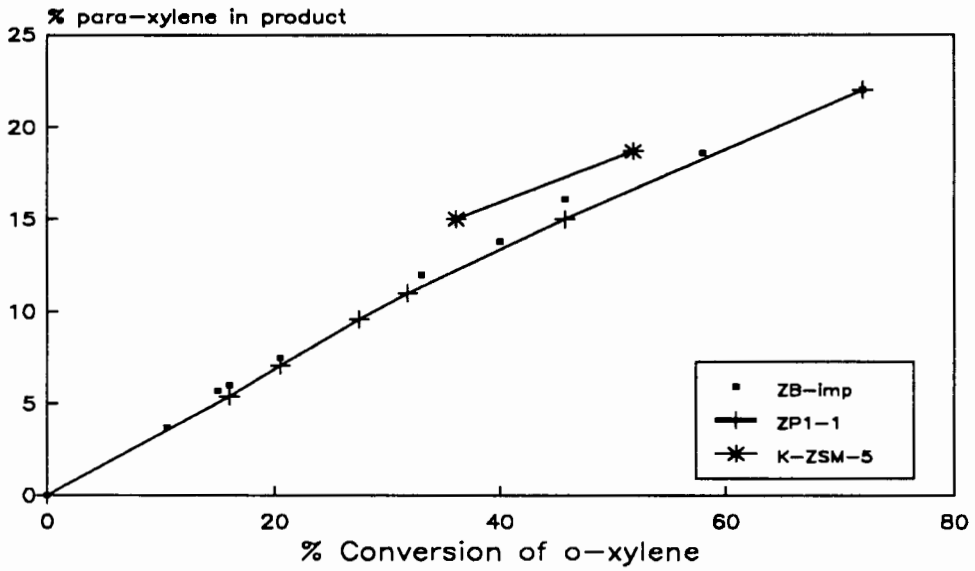

Figure 3.26 Para-xylene selectivity of phosphorus impregnated ZP1-1 (500 °C), ZB-imp (500 °C) and K-ZSM-5 (350 °C)

3.2.4 Propene Oligomerization

3.2.4.1 Activity and lifetime

The propene oligomerization activities of catalysts ZP[1]-1 to ZP[1]-4, synthesized with the incorporation of phosphorus in the synthesis gel, are shown in Figure 3.27. Reaction temperature was held between 250 °C and 260 °C. ZP[1]-3, with the lowest Al content (Si/Al = 261), had both the shortest lifetime and lowest maximum activity (64%) and yielded a CUV of only 11 g/g. ZP[1]-2 with a Si/Al ratio of 191 fared little better, having a CUV of 28 g/g.

ZP[1]-1 and ZP[1]-4 with Si/Al ratios of 42 and 50, respectively, performed considerably better. ZP[1]-1 (containing 0.4 wt% P) gave a CUV of 235 g/g at 250 °C. ZP[1]-4, with a slightly lower Al content but substantially lower P content (0.11 wt% P), had a CUV of 110 g/g. This figure is slightly misleading, however, since this catalyst was still running at over 80% conversion at time of shut down. This catalyst showed the greatest conversion level (96%).

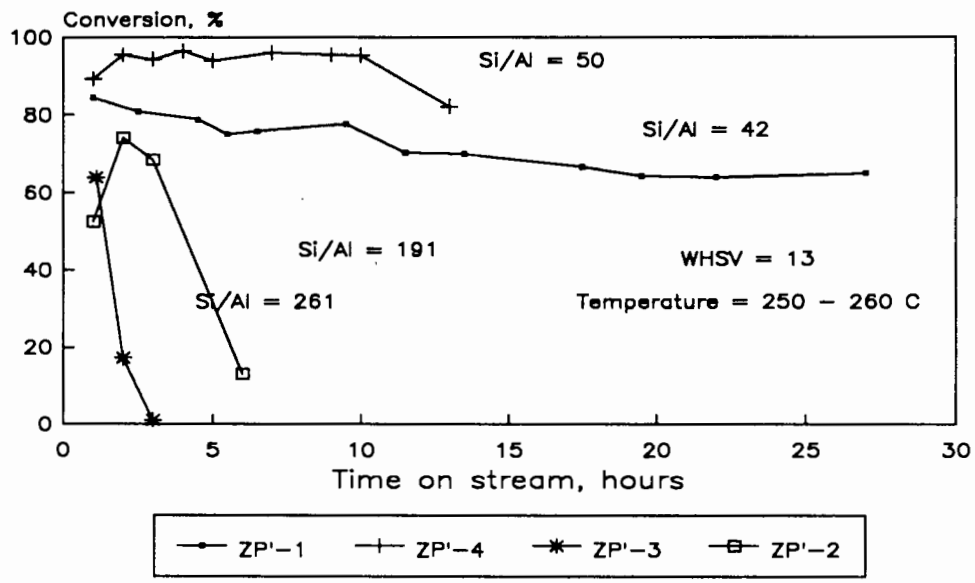

Figure 3.27 The effect of varying P and Al in the synthesis gel on oligomerization activity

The performance of catalysts impregnated with orthophosphoric acid and trimethylphosphite for propene oligomerization are shown in Figure 3.28. Catalysts ZP2-1 and ZP2-2, impregnated with TMP, had CUVs of only 7 and 8.6 respectively. It should be noted that, although these CUVs are similar, the reaction temperature for ZP2-2

(Si/Al = 40, 1.0 wt% P) was 320 °C. No liquid was produced by this catalyst below 300 °C. Temperature control was difficult for both of these catalysts with bed temperatures dropping sharply after only short times on stream (ca. 30 min). This behaviour is reflected to some extent in the very rapid drop in conversion level. The performances of ZP1-1 and ZP1-2, impregnated with phosphoric acid are also presented in Figure 3.28. Both these catalysts had longer oligomerization lifetimes than the TMP impregnated catalysts. Not surprisingly the CUVs were greater with ZP1-1 producing 38 g/g and catalyst ZP1-2 producing 28 g/g.

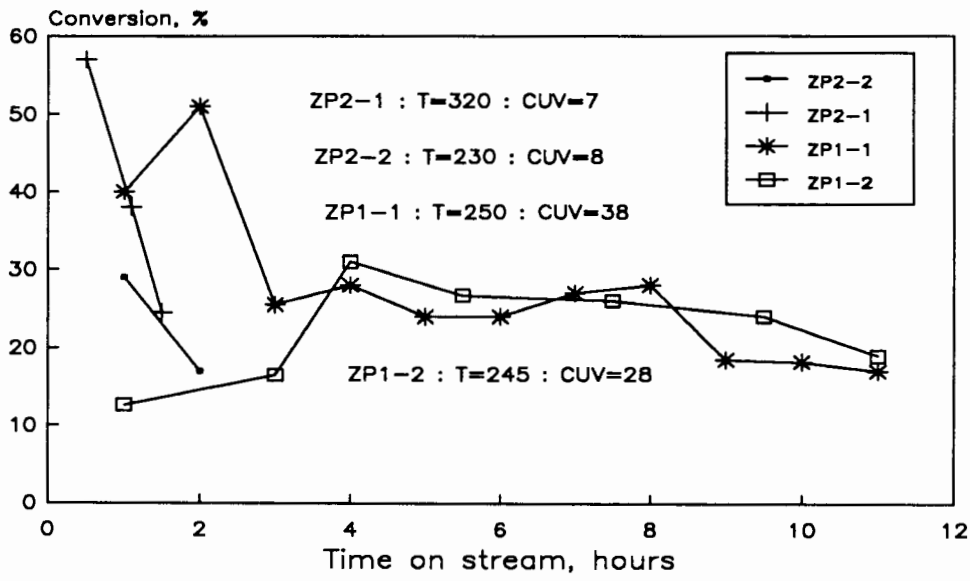

Figure 3.28 Oligomerization over phosphorus impregnated catalysts

The oligomerization time-on-stream conversion data for the H_3PO_4 slurried silicalite is shown in Figure 3.29. This catalyst was prepared by slowly adding phosphoric acid heated at 60 °C to silicalite while cooling and stirring the subsequent mixture to give a CATPOLY type catalyst. The catalyst was not calcined, but was reacted as is at 243 °C. The catalyst started producing liquid at 210 °C and produced 7 g/g. When this catalyst was calcined at 500 °C overnight in either air or N_2 it was inactive below 300 °C and gave a conversion vs. time-on-stream profile that was essentially the same as that of the unmodified silicalite. The performance of an industrial CATPOLY catalyst (phosphoric acid supported on Kieselguhr) is included for comparison purposes in Figure 3.29. The reaction was carried out at 210 °C and 50 atmospheres. The initial conversion level for this catalyst is very similar to that of the phosphorus modified silicalite.

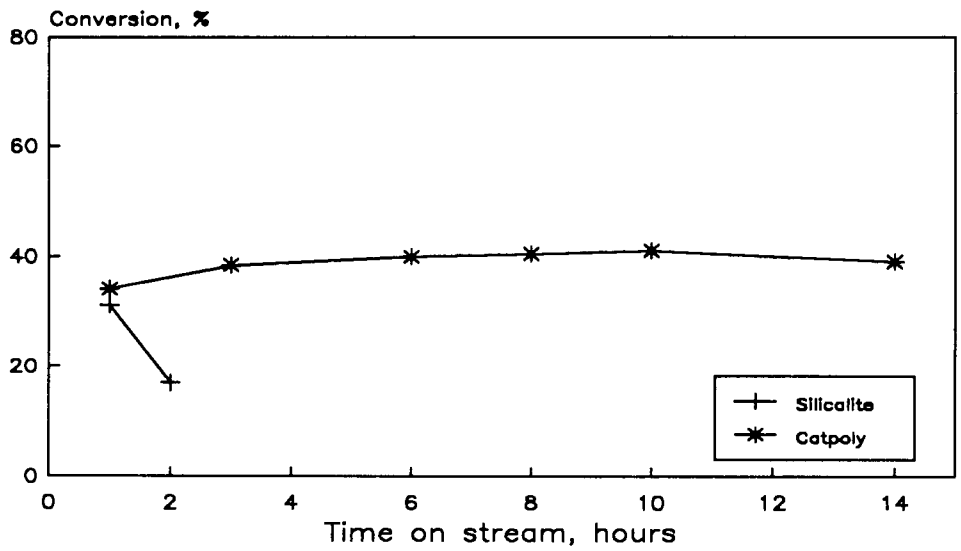

Figure 3.29 Oligomerization over CATPOLY type catalysts

3.2.4.2 Liquid product analysis

Liquid product distributions and cetane numbers of the phosphorus modified catalysts are presented in Table 3.19. The liquid product of ZP2-1, produced at 320 °C, was shown to contain traces of aromatics. The C_2, C_4 and C_5 fractions in the off-gas also increased. This was accompanied by an absence of distinct oligomer groupings in the G.C. trace of the liquid product.

Table 3.19 Liquid Product Distribution and Cetane Numbers for Phosphorus Modified Catalysts

Catalyst	Temp (°C)	WHSV	Conv. (%)	Dim.	Tri.	Tetr.	Pent.	Hex+	Cet. No
ZP[1]-1	250	14	84	25	28	23	17	12	39.5
ZP[1]-2	260	15	74	29	36	19	8	8	n.d.
ZP[1]-3	254	14	64	26	36	20	10	8	n.d.
ZP[1]-4	253	11	94	15	23	22	18	22	n.d.
ZP2-1	326	20	57	11	30	34	16	9	n.d.
ZP2-2	220	22	29	16	34	25	14	11	n.d.
ZP1-1	246	13	51	17	34	26	12	11	43.0
ZP2-2	245	11	31	13	37	26	14	10	38.6
H_3PO_4 slurried silicalite	207	11	12	12	57	22	5	4	41.0
Catpoly	210	9	40	11	59	26	3	1	n.d.

(n.d. = not determined)

3.3 Steam Dealuminated ZSM-5

3.3.1 Catalyst nomenclature

The steamed catalysts were labelled according to:

S-T-P-t-F

where S identifies the catalyst as a steam treated ZSM-5 (Si/Al = 40)
T is the steaming temperature in °C
P is the water partial pressure in the wet nitrogen stream in mm Hg
t is the steaming time in hours
F is the steaming flowrate in ml/min

According to this code a catalyst labelled "S-500-78-2-60" would be a ZSM-5 steamed at 500 °C for 2 hours at 78 mm Hg partial pressure of water at a flowrate of 60 ml/min. A reference guide to catalyst coding is supplied in Appendix 11.

3.3.2 Characterization

3.3.2.1 Relative crystallinity

XRD

A ZSM-5 catalyst of Si/Al = 40 was steamed at the following conditions in order to determine the effect of steaming on catalyst crystallinity as measured by XRD:

reactor temperature	=	500 °C
water concentration (partial pressure)	=	78 mm Hg
steaming time	=	2 hours

This was done at three different wet N_2 flowrates, namely, 30 ml/min, 60 ml/min and 140 ml/min. The catalysts were labelled according to the code set out in Section 3.3.1.

The crystallinities of the 3 steamed catalysts mentioned above, relative to the unmodified parent ZSM-5, are presented below in Table 3.20.

Table 3.20 Relative Crystallinities of some Steam Dealuminated ZSM-5 Relative to Unmodified ZSM-5

Catalyst	Crystallinity, % (Relative to ZSM-5)
Unmodified ZSM-5	100
S-500-78-2-30	91
S-500-78-2-60	91
S-500-78-2-140	91

It would appear, therefore, that the steam treatment lowers the crystallinity of the catalyst, but not by an appreciable amount. The reduction in crystallinity does not appear to be affected by the changing steaming flowrate. The XRD spectrum of S-500-78-2-60 is presented in Figure 3.30 together with that of the unmodified ZSM-5. It is clear that the lower crystallinity for the steamed catalyst is due to a reduction in the size of the two peaks

between 5 and 10 degrees 2-theta. The same phenomenon was observed for the spectra of the other steamed catalysts presented in Table 3.20.

FTIR

Optical density ratios, R, of a number of steamed catalysts were also determined to assess the influence of steam dealumination on crystallinity. Optical density ratios of various steamed catalysts as well as that of unmodified ZSM-5 are shown in Table 3.21.

The catalysts presented in Table 3.21 were all steamed at the same partial pressure of water (78 mm Hg) for two hours. There appears to be no clear trend, however, for changes in values of R with either flowrate, which was varied from 30 to 60 to 140 ml/min at a reactor temperature of 500 °C, or with reactor temperature. The reactor temperature was varied from 200 °C to 500 °C for flowrates of 30 ml/min. Although no clear trend is apparent for the effect of reactor temperature and flowrate on R, it is clear that R is slightly lower for the steamed catalysts than for unmodified ZSM-5. R ratios, however, are still sufficiently high to conclude that the catalysts are crystalline.

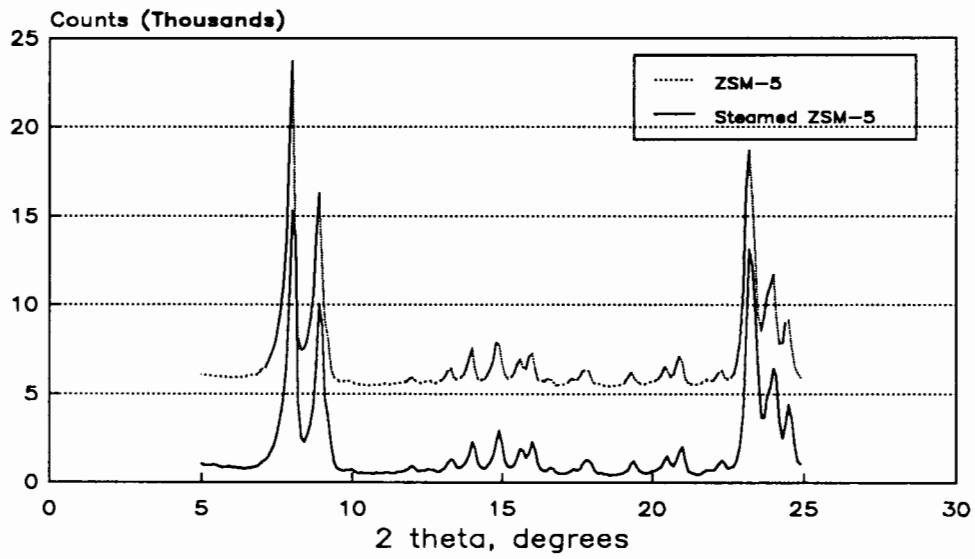

Figure 3.30 XRD spectra for ZSM-5 and S-500-78-2-60

Table 3.21 Optical Density Ratios of Steamed ZSM-5 Catalysts

Catalyst	Optical Density Ratio, R
S-500-78-2-60	0.60
S-500-78-2-140	0.55
S-500-78-2-30	0.58
S-400-78-2-30	0.61
S-300-78-2-30	0.63
S-200-78-2-30	0.62
S-400-78-2-60	0.53
S-300-78-2-60	0.56
ZSM-5	0.66

3.3.2.2 Crystallite size and morphology

The ZSM-5 catalyst used for the steaming study had an average crystallite size of between 2 and 3 microns (determined using SEM). The crystallite size distribution was essentially the same as that of the unmodified ZSM-5 used earlier in the boron impregnation study (see Figure 3.13).

3.3.2.3 Hexane adsorption

Hexane adsorption experiments at 70 °C were carried out on a number of steamed catalysts. Hexane adsorption levels for the steamed catalysts and unmodified ZSM-5 at 70 °C are presented in Table 3.22.

It can be seen from the data in Table 3.22 that the steamed catalysts have hexane adsorption values of between 9.0 and 9.5 wt%, only slightly lower than the adsorption level of unmodified ZSM-5 at the same temperature. The only exception was the catalyst S-200-78-2-30 which was steamed at a reactor temperature of 200 °C.

Table 3.22 Hexane Adsorption at 70 °C over Various Steam Dealuminated ZSM-5 Catalysts

Catalyst	Hexane Adsorption (wt%)
Unmodified ZSM-5	10.3
S-500-78-2-60	9.5
S-500-78-2-140	9.4
S-500-78-2-30	9.2
S-400-78-2-30	9.3
S-300-78-2-30	9.2
S-200-78-2-30	8.8
S-400-78-2-60	9.0

3.3.2.4 Aluminium content

Aluminium analysis was carried out on a ZSM-5 catalyst before and after steaming. The Si/Al ratio of the unmodified ZSM-5, as determined by atomic absorption, was 40. After steaming at a reactor temperature of 500 °C for 2 hours with a wet N_2 stream flowrate of 140 ml/min and a partial pressure of 78 mm Hg, the catalyst had a silica-alumina ratio of 43. The error in the method is estimated as being 5%, however. Consequently the difference in these values is within the limits of experimental error.

3.3.2.5 Aluminium coordination

^{27}Al MAS n.m.r. confirmed that steaming resulted in catalyst dealumination. Tetrahedral framework aluminium gave a peak at ca. 60 ppm., while extra-framework Al was represented at by a peak at ca. 0 ppm shift, in accordance with work done by other researchers (Hamdan *et al.*, 1989). The presence of a shoulder at ca. 30 ppm was also observed in some cases.

3.3.2.6 Catalyst acidity

Ammonia TPD

The ammonia TPD data for catalysts steamed as a function of steaming flowrate and reactor temperature is presented below in Table 3.23.

Table 3.23 Ammonia TPD Data for Steamed ZSM-5 Catalysts

Catalyst	Ammonia Desorption			
	Low Temp Peak		High Temp Peak	
	(°C)	(mmol/g)	(°C)	(mmol/g)
S-500-78-2-60	245	0.41	475	0.36
S-500-78-2-140	241	0.37	470	0.33
S-500-78-2-30	250	0.35	475	0.35
S-400-78-2-30	250	0.39	484	0.34
S-300-78-2-30	241	0.34	-	0.58
S-200-78-2-30	244	0.42	479	0.35
S-400-78-2-60	235	0.33	462	0.29
S-300-78-2-60	238	0.40	468	0.41
S-200-78-2-60	277	0.36	456	0.63

Pyridine adsorption/desorption infrared spectroscopy

Figure 3.31 shows the effect of vacuum calcination at 500 °C on the spectra of unmodified ZSM-5. Most noticeable is the decrease in the size of the broad band at ca. 3000-3500 cm^{-1}, ascribed previously to the removal of physisorbed water molecules (Topsøe *et al.,* 1981). This is accompanied by the appearance of hydroxyl group bands at ca. 3600 cm^{-1} and ca. 3720 cm^{-1}. The peak at ca. 3720 cm^{-1} was ascribed to Si-OH or siliceous impurities while the band at 3605 cm^{-1} was attributed to Si-OH-Al Bronsted acid sites (Topsøe *et al.,* 1981). The calcination procedure also resulted in the almost complete removal of the NH_4^+ bands at ca. 1450 cm^{-1} (Hidalgo *et al.,* 1984). The band at 1630-1640 cm^{-1} has been ascribed to overlap between the band assigned to the Si-O stretching mode and the H_2O bending mode of physisorbed water (Védrine *et al.,* 1979). From Figure 3.31 it can be seen that there is

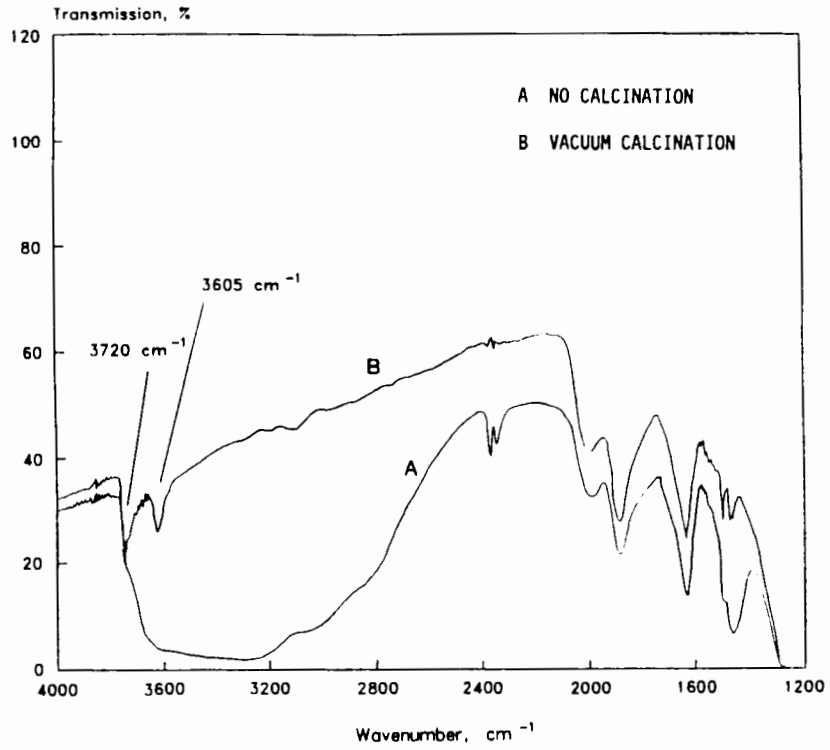

Figure 3.31 The effect of vacuum calcination at 500 °C on the IR spectrum of ZSM-5

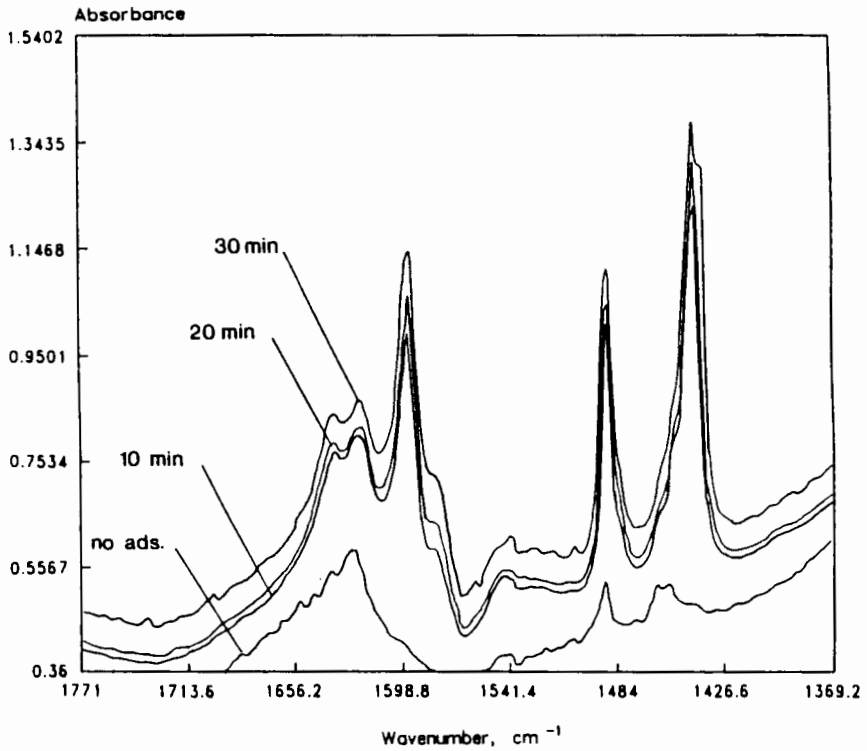

Figure 3.32 Pyridine adsorption with time at 30 °C on HZSM-5

very little change in the intensity of this band with calcination treatment. Védrine *et al.* (1979) also noted this phenomenon, concluding that the amount of physisorbed water on the catalyst was low.

Figure 3.32 shows the adsorption of pyridine at 30 °C on calcined ZSM-5 with time. Initial adsorption (up to 10 minutes) of pyridine is rapid. After 30 minutes adsorption time very little further change is noticed.

Most noticeable in Figure 3.32 is the peak at ca. 1445 cm^{-1} due to LPy and HPy with small shoulders at 1456 cm^{-1} and 1468 cm^{-1} due to LPy. The peak at 1491 cm^{-1} due to BPy and LPy is also quite pronounced while the peak at ca. 1545 cm^{-1} due to pyridinium (pyridine bonded to a Bronsted site) appears as a broad shoulder rather than a sharply defined peak. The sharp peak at 1602 cm^{-1} is due to hydrogen bonded pyridine. Also visible as a shoulder at ca. 1580 cm^{-1} is the absorption band due to physisorbed pyridine.

Evacuation at 2×10^{-6} mm Hg and 30 °C results in a substantial drop in the size of the peak at 1445 cm^{-1}. The shoulders at 1456 cm^{-1} and 1468 cm^{-1} becoming more pronounced (see Figure 3.33). Although the peak at 1545 cm^{-1} due to BPy also becomes more pronounced, it is apparent after 6, 12 and even 18 hours (see Figures 3.33 and 3.34) that not all of the physisorbed and hydrogen bonded pyridine has been removed at a desorption temperature of 30 °C. Increasing the desorption temperature from 30 °C to 130 °C, however, quickly results in the removal of Py and HPy (see Figure 3.34). Desorption at 130 °C for 2 hours, for example, completely removes the HPy peak at 1602 cm^{-1}. A substantial drop in the 1445 cm^{-1} peak, which can be ascribed to loss of HPy, also results from the higher desorption temperature.

If pyridine is adsorbed at 130 °C as opposed to 30 °C, however, it is clear from Figure 3.35 that, after 10 hours desorption at 130 °C and 2×10^{-6} mm Hg, not all HPy has been removed as evidenced by a shoulder at ca. 1602 cm^{-1}. Complete removal of the HPy occurs only at higher desorption temperatures (220°C and 360 °C). This is accompanied, however, by a decrease in the amount of BPy and LPy as measured by integrated absorbances of the peaks at 1545 cm^{-1} and 1456 cm^{-1}, respectively. For this reason it was decided that adsorption of pyridine at 30 °C would be followed by pyridine desorption at 130 °C and 2×10^{-6} mm Hg (overnight) to ensure complete removal of HPy and Py.

Infrared absorption band assignments are presented in Table 3.24. Absorption bands due to pyridine ring vibrations are also presented. Bands have been assigned to physisorbed (Py), hydrogen bonded (HPy), pyridinium ion (BPy), and coordinately bonded (LPy) pyridine species. Band assignments were based on the following synthesized standards:

Py - dilute solution of pyridine in chloroform (Parry, 1963, Bourne *et al.*, 1970)

HPy - pyridine water interactions (Siderov, 1960)

BPy - pyridine hydrogen chloride (Parry, 1963; Bourne *et al.*, 1970)

LPy - pyridine aluminium chloride (Bourne *et al.*, 1970) and pyridine borohydride (Parry, 1963)

Table 3.24 Infrared Absorption Band Assignments

Frequency, cm^{-1}	Vibration	Absorbing Species
3740	O-H stretch	silanol, siliceous impurity
3600	O-H stretch	structural hydroxyl
3435	O-H stretch	hyroxyaluminium species
3290-3300	N-H stretch	ammonium ion
3035	N-H stretch	ammonium ion
2820	N-H overtone	ammonium ion
1675	N-H band	ammonium ion
1635	O-H band	molecular water
1432	N-H band	ammonium ion
Pyridine ring vibrations		
1637	CC(N)	BPy
1618	CC(N)	BBy, LPy
1615	CC(N)	LPY, HPy
1602	CC(N)	HPy
1582	CC(N)	Py
1545	CC(N)	BPy
1491	CC(N)	BPy, LPy, HPy
1468	CC(N)	LPy
1456	CC(N)	LPy
1445	CC(N)	LPy, HPy
1437	CC(N)	HPy, Py

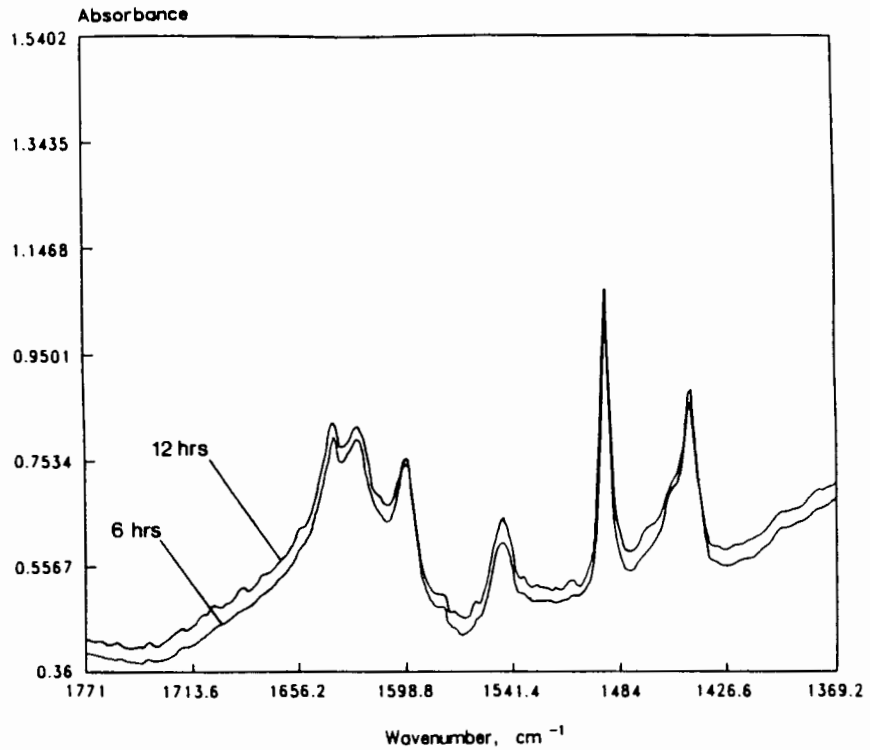

Figure 3.33 Desorption of pyridine with time at 30 °C and $2x10^{-6}$ mm Hg

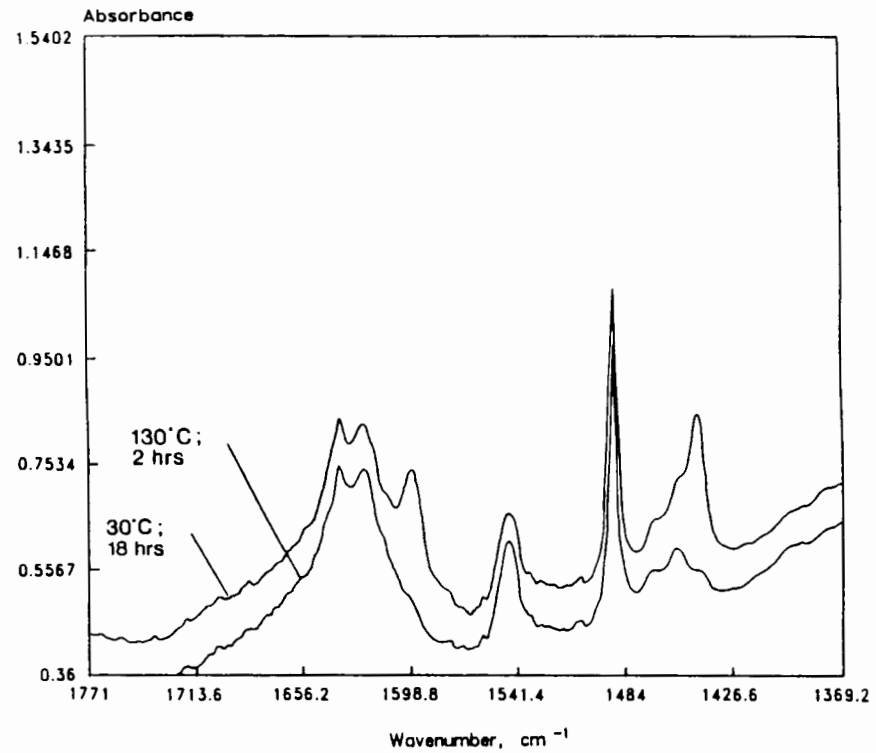

Figure 3.34 Pyridine desorption at 30 °C and 130 °C after adsorption at 30 °C

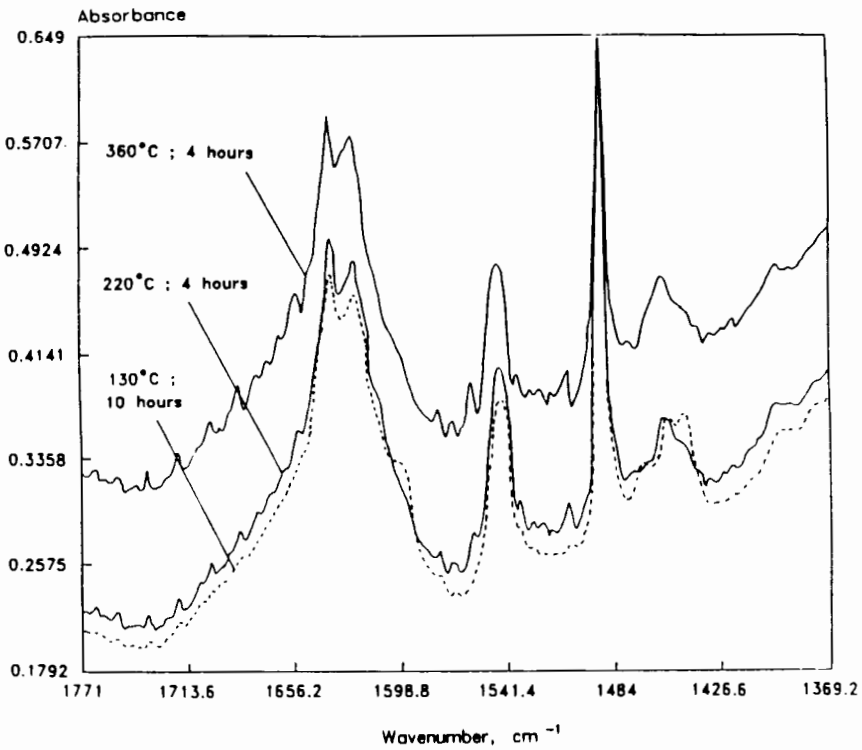

Figure 3.35 Desorption with temperature after 130 °C pyridine adsorption

Concentrations of Bronsted and Lewis acid sites were determined from integrated absorbances of peaks at 1545 cm^{-1} and 1456 cm^{-1} according to the method used by Hughes and White (1967). A detailed sample calculation is provided in Appendix 9. Bronsted and Lewis acid site concentrations, expressed as moles per gram of catalyst, are presented in Table 3.25.

Table 3.25 Bronsted and Lewis Acid Site Concentrations Determined from Pyridine Adsorption for Steamed ZSM-5

Catalyst	Bronsted Acidity moles /g. cat.	Lewis Acidity moles /g. cat	L/B*
Unmodified ZSM-5	2.431×10^{-4}	7.442×10^{-5}	0.306
S-500-78-2-60	2.586×10^{-4}	1.111×10^{-4}	0.43
S-500-78-2-140	2.821×10^{-4}	7.93×10^{-5}	0.281
S-500-78-2-30	2.091×10^{-4}	5.966×10^{-5}	0.285
S-400-78-2-30	3.03×10^{-4}	7.964×10^{-5}	0.263
S-300-78-2-30	2.94×10^{-4}	6.69×10^{-5}	0.228
S-200-78-2-30	2.659×10^{-4}	6.074×10^{-5}	0.228
S-400-78-2-60	2.478×10^{-4}	8.868×10^{-5}	0.358
S-300-78-2-60	3.354×10^{-4}	9.707×10^{-5}	0.289
S-200-78-2-60	3.181×10^{-4}	7.775×10^{-5}	0.244

* L/B = ratio of Lewis to Bronsted Acidity

The L/B ratios as a function of steaming temperature and at different flowrates (30 ml/min and 60 ml/min) are plotted in Figure 3.36. It is evident that the L/B ratios of the steamed catalysts increase with increasing steaming temperature. Increasing the wet N_2 (steaming) flowrate from 30 ml/min to 60 ml/min appears to shift the curve upwards i.e. at 60 ml/min at the same steaming temperature, water partial pressure and steaming time the ratio of L/B is greater than at 30 ml/min.

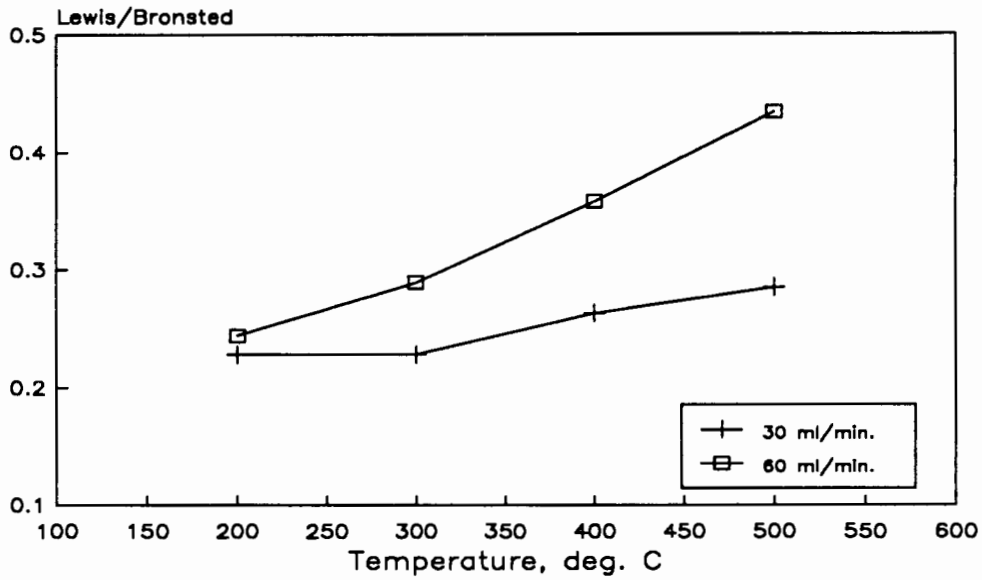

Figure 3.36 L/B (Lewis/Bronsted) acid site ratios as a function of steaming temperature

3.3.2.7 Surface areas

BET surface areas were determined for the same set of catalysts shown in Table 3.23. Surface areas for these catalysts are presented below in Table 3.26.

Table 3.26 BET Surface Areas of Steamed ZSM-5

Catalyst	Surface Area (m^2/g)
S-500-78-2-60	472.3
S-500-78-2-140	451.5
S-500-78-2-30	472.2
S-400-78-2-30	466.3
S-300-78-2-30	463.3
S-200-78-2-30	460.6
S-400-78-2-60	466.5
S-300-78-2-60	471.9
S-200-78-2-60	451.7

3.3.3 Hexene Oligomerization

Tabak (1985) examined the performance of various alkenes for the MOGD process. The good reactivities of propene and 1-butene ensure that these olefins are the preferred feed. When 1-hexene was used as feed the result was reduced activity and lifetime. The observed decrease in lifetime of ZSM-5 for oligomerization could be ascribed to the fact that for a large feed molecule fewer reaction steps are required to form a long oligomer. It is conceivable, therefore that the formation of molecules that are unable to desorb from acid sites is faster with 1-hexene than with propene. Since it is possible that steam dealumination can result in enhanced activity under certain conditions it was therefore decided that 1-hexene would be preferable as an oligomerization reactant molecule for catalyst screening.

3.3.3.1 Reproducibility

1-Hexene was oligomerized at 220 °C and 5 MPa. over a ZSM-5 catalyst of Si/Al = 40 and with an average crystallite size of 2-3 microns. The two oligomerization runs carried out over this catalyst are presented in Figure 3.37. It is clear that the performance of the catalyst was reproducible.

3.3.3.2 The effect of crystallite size and reaction temperature on activity

The effect of temperature and crystallite size on catalyst activity for 1-hexene oligomerization is shown in Figure 3.38. The catalysts were synthesized in autoclaves of the type shown earlier (see Figure 2.1). Where stirring was provided by means of a magnetic stirrer and stirrer bar, the average crystallite size of the catalyst was between 2 and 3 microns. To synthesize a catalyst with a smaller crystallite size a magnedrive with an impeller was connected to the autoclave. This method, as opposed to the one using magnetic stirrer bars, provides direct impeller motion. When the magnedrive was set to a speed of 300 rpm, the result was a catalyst with a narrow size distribution and crystallite sizes less than one micron.

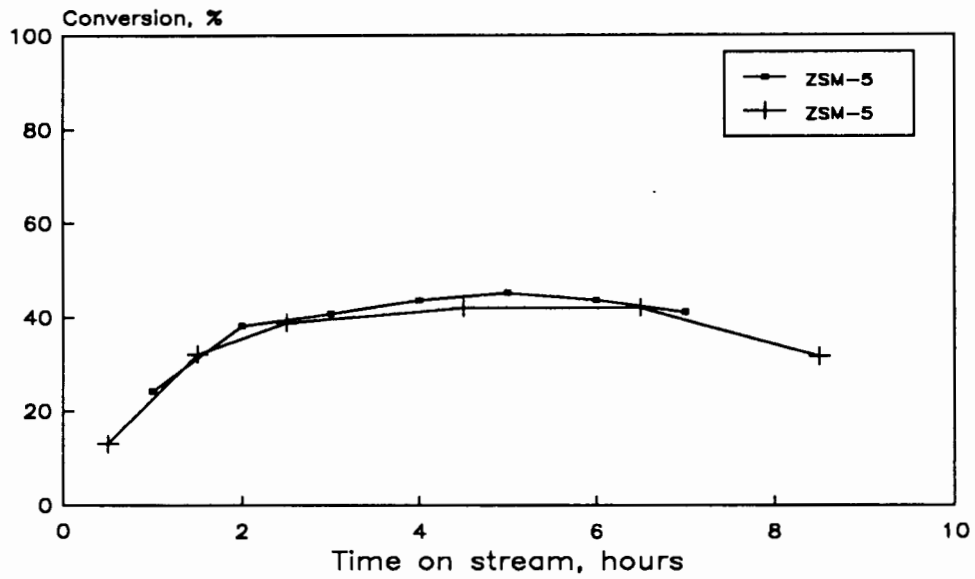

Figure 3.37 Reproducibility of hexene oligomerization

One can see that the oligomerization activity of the catalyst of crystallite size less than 1 micron is substantially higher than that of the magnetically stirred catalyst (size = 2-3 μm). The activity of both of these catalysts can also be seen to increase with increasing reaction temperature. Since it has been proposed that steaming increases the activity of ZSM-5 under certain conditions (Lago *et al.*, 1986; Brunner *et al.*, 1989) it was decided, for comparative purposes, to conduct the steaming study at conditions that would allow for both increases and reductions in activity. The steam dealumination study was therefore conducted at a hexene oligomerization reaction temperature of 220 °C using a ZSM-5 synthesized in a magnetically stirred autoclave (i.e. of crystallite size of 2-3 microns). The reaction pressure, as with propene oligomerization, was held at 5 MPa.

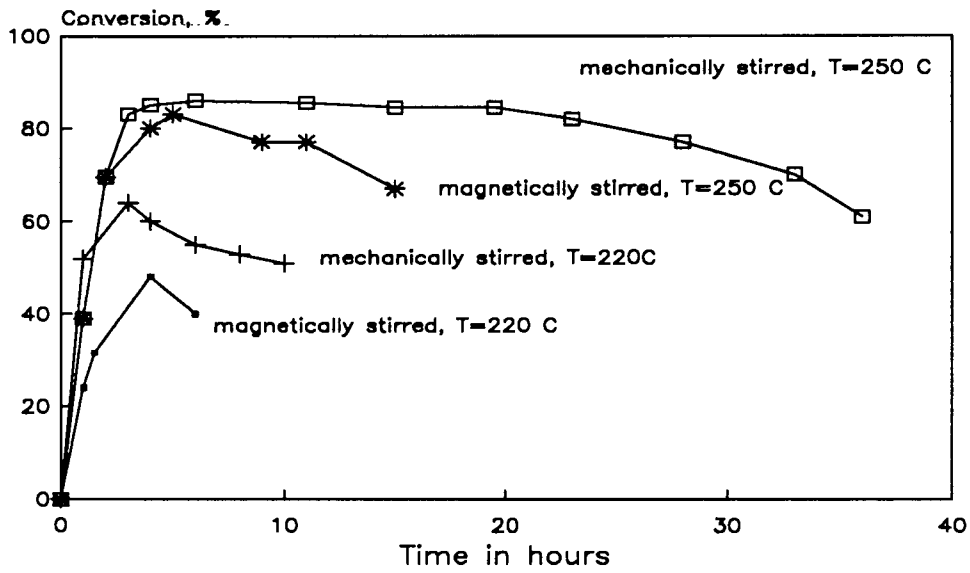

Figure 3.38 The effect of crystallite size and reaction temperature on hexene oligomerization activity

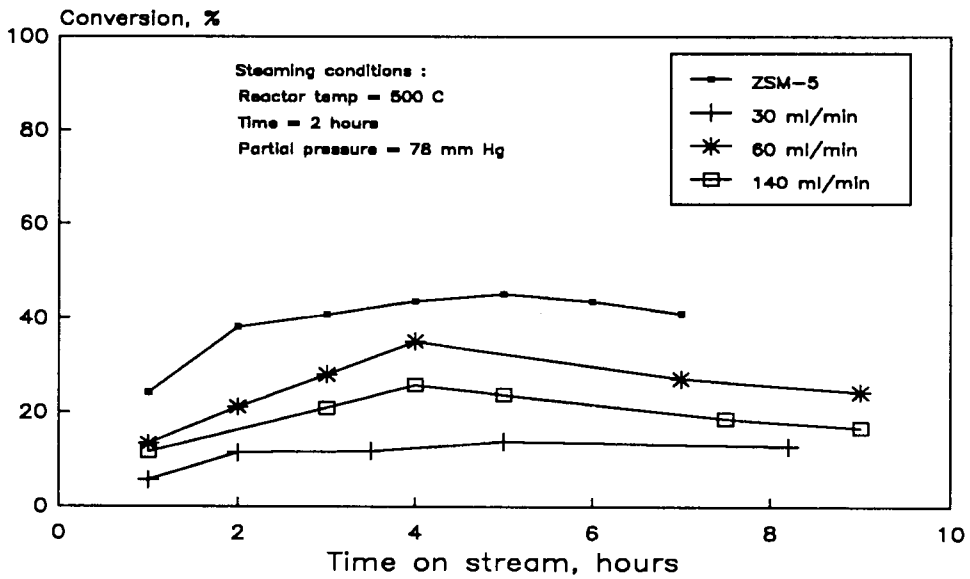

Figure 3.39 The effect of steaming flowrate on oligomerization activity

3.3.3.3 The effect of steaming flowrate on catalyst activity

Figure 3.39 shows the effect of steaming flowrate on the activity of ZSM-5 for hexene oligomerization. Three different flow rates were considered, namely, 30 ml/min, 60 ml/min and 140 ml/min. Compared to unmodified ZSM-5 it is evident that at the steaming conditions chosen (500 °C steaming temp., p.p. = 78 mm Hg and 2 hour steaming time) that the steaming process has resulted in catalysts with reduced activity compared to ZSM-5. There is a surprising trend, however, with the catalyst steamed at a flowrate of 60 ml/min showing significantly better activity than catalyst steamed at either 30 ml/min or 140 ml/min.

3.3.3.4 The effect of steaming temperature on catalyst activity

The effect of steaming temperature on catalyst activity was examined by varying the reactor temperature from 500 °C to 400 °C, 300 °C and 200 °C, while keeping the water vapour concentration and steaming time constant. This was done at two different flowrates, 30 ml/min and 60 ml/min.

The effect of steaming temperature at a flowrate of 30 ml/min is shown below in Figure 3.40. Again it is clear that, relative to unmodified ZSM-5 steaming has had a deleterious effect on the catalyst activity. All the catalysts steamed at these conditions show poorer activity than unmodified ZSM-5. There is, however, an optimum activity for the catalyst steamed at 300 °C which shows greater activity than the other steamed catalysts. The catalyst steamed at 500 °C shows the poorest activity while the activities of catalysts steamed at 400 °C and 200 °C are similar.

This behaviour of the catalysts with steaming temperature was mirrored when the steaming flowrate was increased to 60 ml/min (see Figure 3.41). Once again the water vapour concentration was held at 78 mm Hg while the steaming time was 2 hours. There is again an optimum in activity for the catalyst steamed at 300 °C. The activity decreases in the following order:

$$300\,^{\circ}C > 200\,^{\circ}C > 400\,^{\circ}C > 500\,^{\circ}C$$

Compared to the catalysts steamed at 30 ml/min, however, the activity of these catalysts is much higher. The catalysts steamed at 200 °C and 300 °C even show greater activities than unmodified ZSM-5 at the same WHSV. This behaviour confirms the trend shown in

Figure 3.39, namely that catalysts steamed at 60 ml/min show greater activities for hexene oligomerization than do those steamed at 30 ml/min.

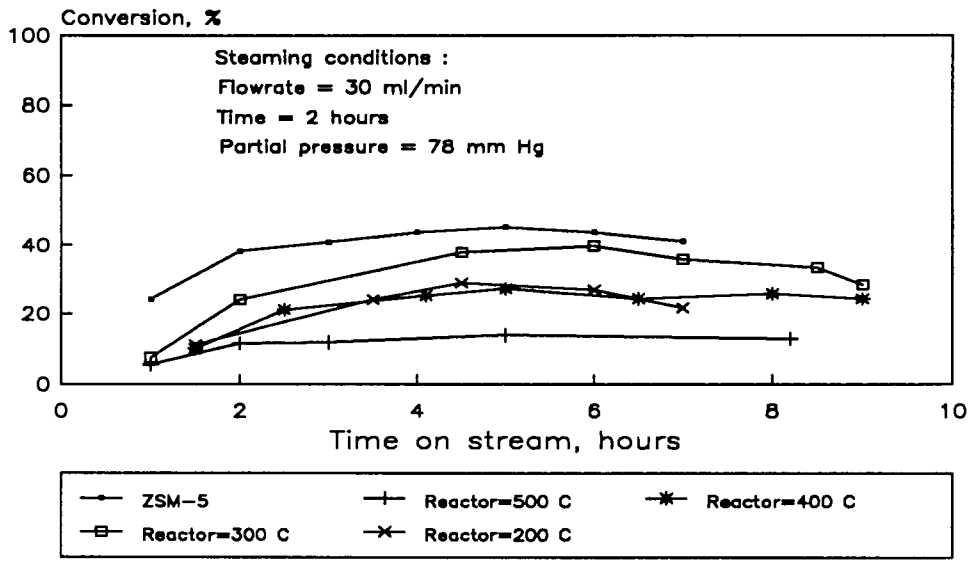

Figure 3.40 The effect of steaming temperature at a flowrate of 30 ml/min at 78 mm Hg for 2 hours

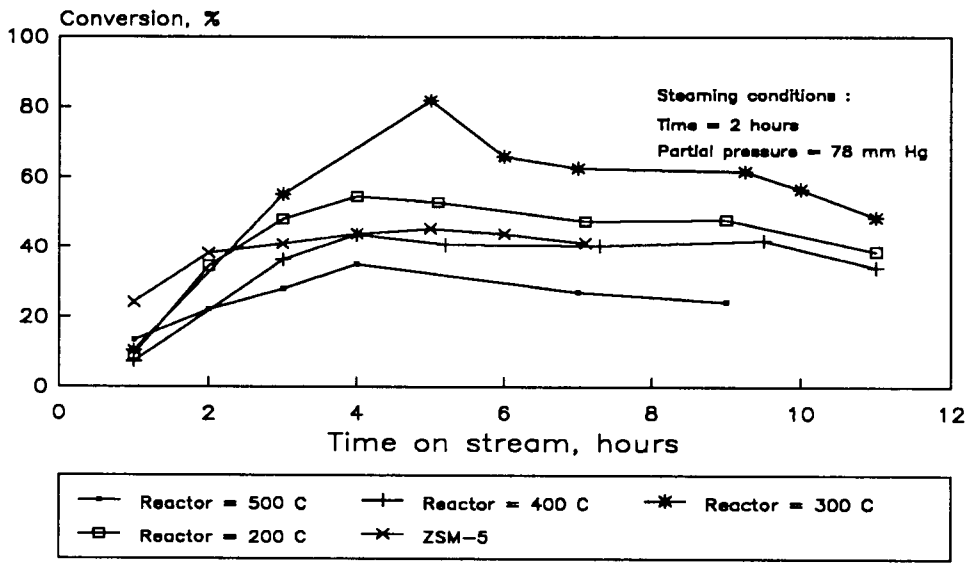

Figure 3.41 Oligomerization activity as a function of steaming temperature at 60 ml/min steaming flowrate

3.3.3.5 The effect of steaming time on catalyst activity

Figure 3.43 shows the conversion versus time on stream data for catalysts steamed at 300 °C and 78 mm Hg at 60 ml/min. Steaming times were varied from 1 hour to 2, 4 and 10 hours. The catalyst steamed for 2 hours showed the greatest activity while the catalyst steamed for 4 hours showed similar activity to that of unmodified ZSM-5.

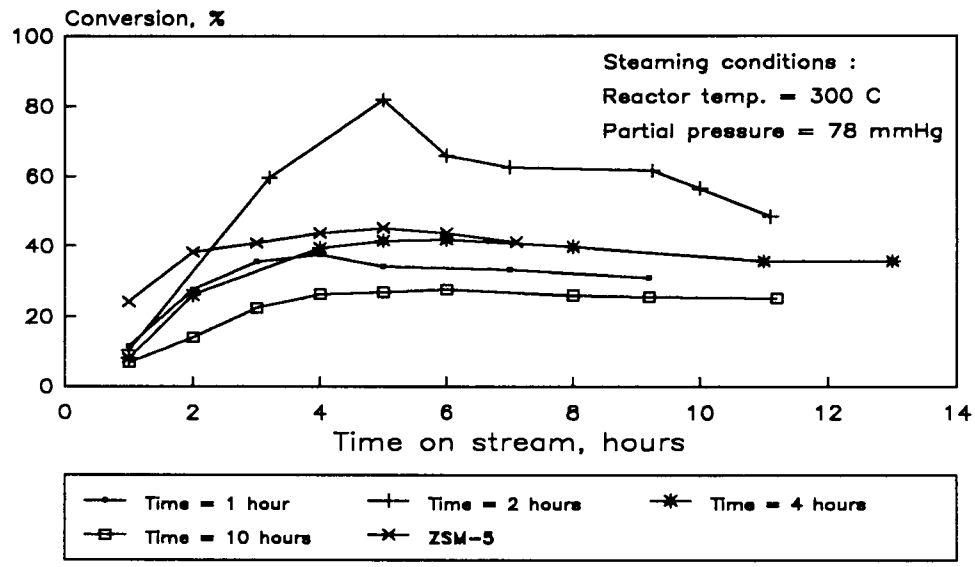

Figure 3.42 The effect of steaming time on catalyst activity

3.3.3.6 The effect of water concentration (partial pressure) on catalyst activity

The effect of changing water partial pressure is shown in Figure 3.44. Maximum activity was obtained at a partial pressure of 78 mm Hg as seen in previous figures. Catalysts steamed at higher partial pressures (230 mm Hg and 320 mm Hg) exhibited similar activities, slightly greater than that of unsteamed ZSM-5. The poorest performance was that of the catalyst steamed at a partial pressure of 21 mm Hg.

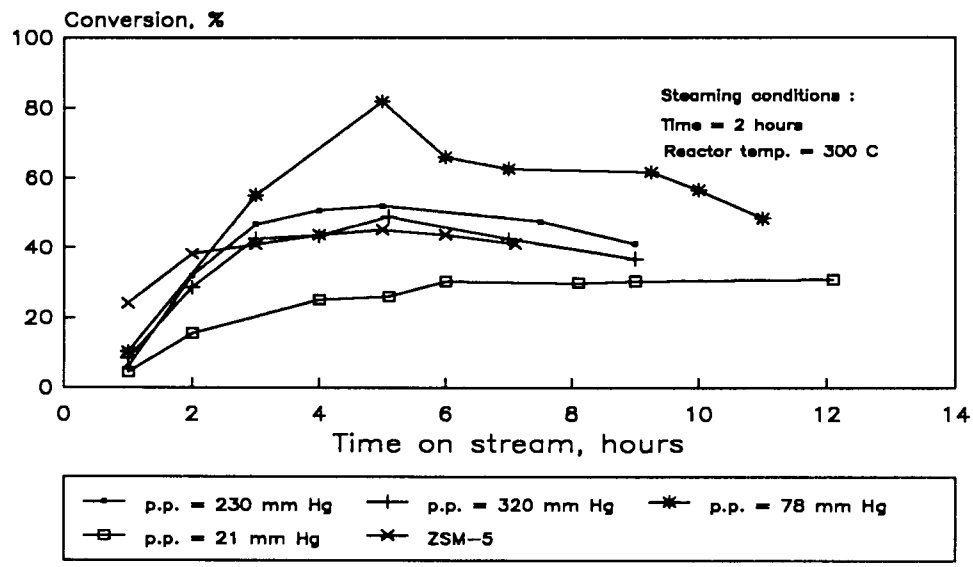

Figure 3.43 The effect of water partial pressure on catalyst activity

3.3.4 The effect of steaming on propene oligomerization activity and lifetime

The activity of ZSM-5 for propene oligomerization was examined after steaming at conditions which provided maximum activity enhancement for 1-hexene oligomerization (300 °C, 78 mm Hg, 2 hours, 60 ml/min). At a WHSV of ca. 25 and at 250 °C it can be seen that the activity of the ZSM-5 catalyst was enhanced by the steaming process (see Figure 3.45). The CUV's of the unsteamed and steamed catalysts were 120 g/g and 199 g/g respectively.

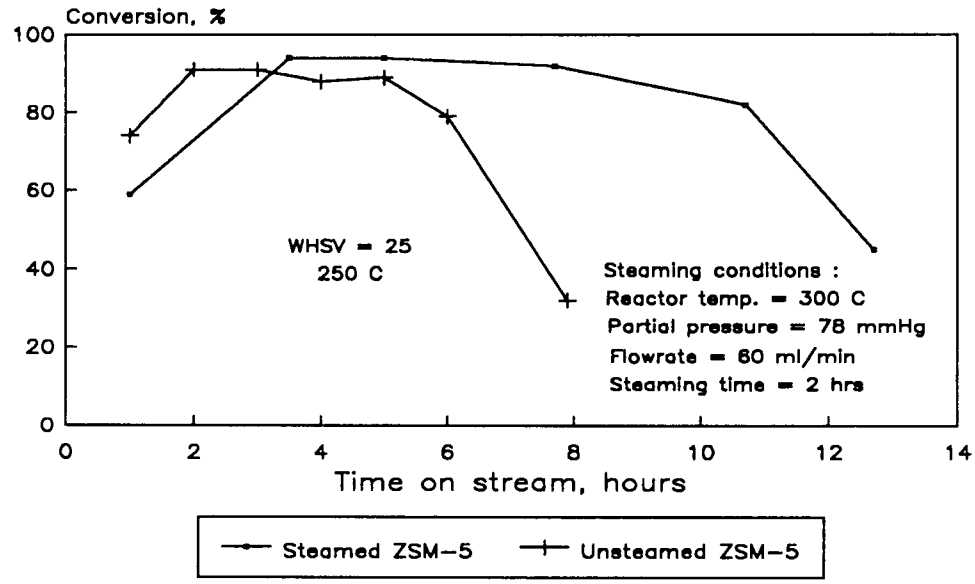

Figure 3.44 The effect of steaming on propene oligomerization activity

Chapter 4
Discussion

DISCUSSION

4.1 The Effect of Boron Incorporation in the Framework of ZSM-5

4.1.1 The Effect on Activity and Lifetime

The case for the activity of boralite catalysts was argued by Ione *et al.* (1984), who proposed that the acid strength of boralite type catalysts depends roughly on the value of $^{e}/_{r}$, the ratio of cation charge to cationic radius. If this is the case, boralite catalysts, it was suggested, will be more active than their aluminium counterparts. High pressure propene oligomerization work carried out by Occelli *et al.* (1985) seemed to confirm this hypothesis. These researchers reported that 20% sepiolite-bound boralite (SiO_2/B_2O_3 = 65; 860 ppm Al) was more active than sepiolite-bound ZSM-5 of SiO_2/Al_2O_3 = 77.5. The latter did not show significant activity until above 300 °C. At a reaction temperature of 315 °C the boralite catalyst had a conversion level of 96.5 wt% compared to only 64.4 wt% for the ZSM-5 catalyst.

Examination of the boralite catalysts investigated in this study shows clearly that the boralite catalysts performed poorly for propene oligomerization compared to unmodified ZSM-5. From comparisons of the low CUVs of the boralites shown in Figure 3.6 to that of unmodified ZSM-5 (CUV = 600 g/g; see Figure 3.20) it is clear that the incorporation of boron in place of aluminium in the zeolite framework has resulted in catalysts of substantially reduced oligomerization activity.

The boralite catalysts, unlike unmodified ZSM-5, were all essentially inactive below 300 °C, with activity levels following trace Al rather than boron content (see Figure 4.1). B-1, containing 760 ppm of Al, was the most active catalyst. B-2, containing 550 ppm and 1.2 wt% boron (compared to the 0.51 wt% B of boralite B-1) had a similar CUV. The slightly higher CUV of B-2 (39 g/g) compared to B-1 (37 g/g) can be ascribed to the higher reaction temperature. The matter is further complicated on account of varying crystallite size. Although B-2 contains less Al than B-1, B-2 made with Aerosil consisted of ca. 1 μm diameter spherical crystallites as opposed to the ca. 4 μm spherical crystallites of B-1. Boralite B-5 with only 25 ppm Al performed the poorest with a CUV of only 3 g/g at 340 °C. B-6, with 77 ppm Al, performed a little better giving 17 g/g and reaching a maximum conversion of almost 40% at 360 °C.

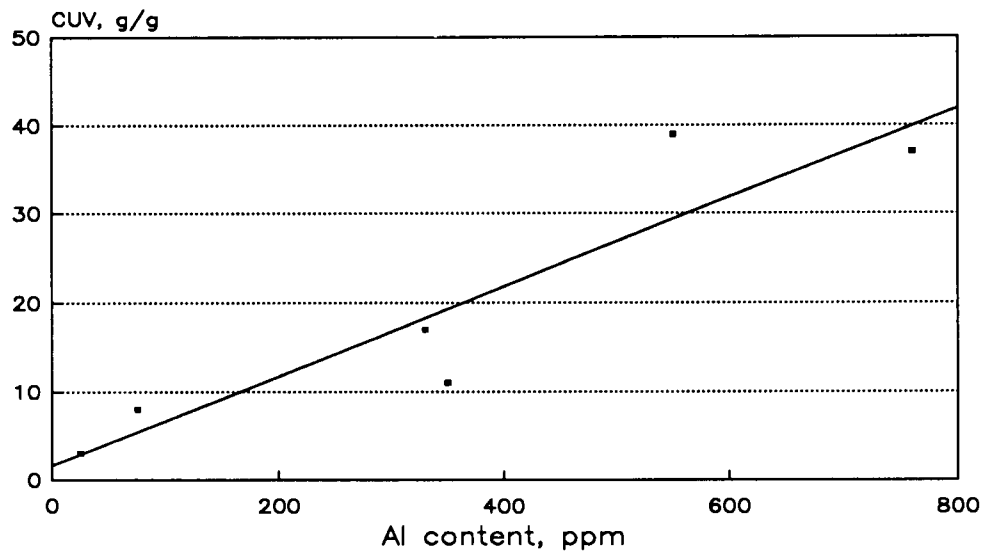

Figure 4.1 CUV as a function of Al content for boralite catalysts

An attempt was made to examine further the role played by framework boron and trace aluminium content by comparing the activity of a boralite catalyst to that of a silicalite catalyst of comparable aluminium content (see Figure 3.7). B-4 (330 ppm Al ; 0.59 wt% B) exhibited greater oligomerization activity than did silicalite (350 ppm of Al). Before attributing this activity difference to the presence of boron, however, one must recognize at this point the role played by crystallite size in determining oligomerization activity. Schwarz *et al.* (1990), for example, found that crystallite sizes played a major role in determining activity and lifetime of ZSM-5 for propene oligomerization, with small crystallites giving greater activities and longer times-on-stream. It is possible, therefore, that the performance of B-4 compared to silicalite is due, not to the presence of boron in the framework, but to the difference in crystallite sizes.

Despite differences in reaction temperature and crystallite size, however, there does appear to be a definite trend of CUV with trace Al content for the catalysts examined. A similar observation was made by Chen *et al.* (1985) for a number of acid catalyzed reactions. In each case it was found that catalyst activity could be ascribed mainly, if not entirely, to trace amounts (80-550 ppm) of framework Al. It is clear, therefore, that the role played by trace framework Al on catalyst activity should not be ignored. Indeed, the activity levels seen by Occelli *et al.* (1985) for sepiolite-bound boralite are consistent with those of the boralites

(of similar Al content) examined in this study. It should further be remarked that the conversion of 10.9 wt% at 260 °C observed by Ocelli *et al.* (1985) for unmodified ZSM-5 is surprisingly low when compared to the more than 90% conversion found in this work (see Figure 3.20) for a ZSM-5 of similar Al content.

From the TPD data presented in Table 3.5 it is clear that, unlike ZSM-5 which possesses both weak and strong acidity, the boralite catalysts examined in this study possessed only weak acidity. Since it has been shown that propene oligomerization is a reaction requiring strong acidity (Venuto and Landis, 1968) it is hardly surprising that the boralite catalysts perform poorly for propene oligomerization, compared to unmodified ZSM-5. The boralite catalysts possess acid sites with a desorption maximum at a temperature of ca. 180 °C compared to ca. 220 °C for the low temperature desorption peak of ZSM-5 (see Figure 3.17). This single ammonia desorption peak corresponds well with that observed by Coudurier and Védrine (1987) who reported a single desorption peak at ca. 190 °C for a boralite catalyst. In the present study only B-4 and silicalite (see Table 3.5) showed any sign of strong acidity, and this was only in trace amounts. This could possibly be ascribed to the presence of trace framework Al. It is not clear, however, why none of the other boralite catalysts, with greater amounts of Al and correspondingly greater catalytic activities, show no sign of any strong acidity.

Coudurier and Védrine (1987) suggested that lattice boron may be present in a trigonal or tetrahedral environment depending on the presence of ligand adsorbates, a view shared by other researchers (Kessler *et al.*, 1987; Datka and Piwowarska, 1989). Coudurier and Védrine (1987) further suggested that boron may induce weak acidity with almost negligible activity for reactions such as methanol conversion. This view was shared by Cornaro and Wojchiechowski (1989) who showed boralites to exhibit catalytic activity for double bond shift conversion, but not for the more demanding skeletal isomerization reaction. Ab initio molecular orbital calculations carried out by O'Malley and Dwyer (1987) on the acidic properties of boralites predicted the bridged boron hydroxyl group to be more silanol in character than the bridged Al form (as found in unmodified ZSM-5). This finding essentially agreed with earlier work carried out by Scholle *et al.* (1984). On the basis of the qualitative electrostatic valence model of Pauling, they concluded that the bond strength of the O-H bond in the Bronsted site of H-boralite was greater than that found in ZSM-5. This was in agreement with the results of their ammonia TPD work which showed ZSM-5 to have acid sites more acidic than those of H-boralite.

Topsøe *et al.* (1981) ascribed a weak ammonia desorption peak at ca. 227 °C over ZSM-5 to the desorption of ammonia from either terminal silanol groups on the external surface of

the zeolite or non-zeolitic impurities. The desorption peak found at higher temperatures was thought to be due to ammonia adsorbed on strong Bronsted and/or Lewis acid sites. For these assignments to hold one would expect, at the very least, the amount of ammonia desorbing at high temperatures to correspond approximately to the aluminium content for unmodified ZSM-5 calcined at 500 °C (i.e. with low amounts of Lewis acidity). This can be seen to be the case with unmodified ZSM-5 (Si/Al = 41) having a strong desorption peak of 0.37 mmol/g catalyst (see Table 3.11). This corresponds almost exactly to the framework aluminium content of the catalyst.

In an analogous argument one could reasonably expect that, if the low temperature NH_3 TPD peak exhibited by the boralite catalysts can be ascribed to the presence of a weak B(OH)Si site of the kind proposed by Scholle *et al.* (1984), the boron contents of these catalysts should correlate in some way with the magnitude of the low temperature TPD peak. This, however, does not appear to be the case. The boron contents of the boralite catalysts (see Table 3.4) do not correspond in any way to the magnitudes of the weak acid sites TPD peak. A possible explanation for this is that not all of the boron in these catalysts is present in the framework. Some may exist as extraframework B_2O_3 which, in turn, may partially occlude the zeolite pores.

Pore dimensions of zeolites given in the literature are based on crystallographic data and are nominal values only. Effective pore sizes can, in reality, be much larger than the calculated values since they are dependent on interactions of intermolecular and interatomic forces of the zeolite and diffusing molecules (Chen *et al.,* 1989a). Consequently, molecules about 1 Å larger than calculated pore diameters can readily diffuse into a zeolite (Haag and Chen, 1987). It should be possible therefore, for cyclohexane with a molecular diameter of ca. 6 Å (Breck, 1974) to diffuse readily into the pores of either unmodified ZSM-5 or boralite. If the boralite contains occluding B_2O_3 species as proposed above, however, it is likely that cyclohexane adsorption rates would be slower than for unmodified ZSM-5 corresponding to reductions in diffusivity as a result of channel constrictions. Indeed, this appears to be the case, with B-1 having a much slower cyclohexane adsorption rate than ZSM-5 (see Figure 3.14). It can be argued, therefore, that slower cyclohexane adsorption rates in conjunction with TPD data (showing no correlation of boron content with amount of acidity) provides evidence for the presence of extra-framework boron, possibly existing as B_2O_3.

It has been shown (Meyers *et al.,* 1985; Taramasso *et al.,* 1980; Coudurier and Védrine, 1987) that substitution of silicon by boron in pentasil type zeolites results in unit cell contraction, corresponding to shorter B-O bond lengths (1.39 Å) compared to that of Si-O

(1.61 Å). It was shown that variations in the unit cell size (corresponding to boron content) could be related to changes in the sum (ΣT) of the d-spacings of four peaks between $2\theta = 45°$ and $2\theta = 48°$. Although the (ΣT)s of the boralite catalysts investigated in this study were smaller than for unmodified ZSM-5 or silicalite, there was no clear trend corresponding to boron content (refer to the Table presented in Appendix 12. The apparent absence of such a trend does not invalidate the effect of boron content on unit cell size, however, but may rather provide further evidence for the presence of varying amounts of extra-framework boron in the boralite catalysts examined, as suggested by both TPD and cyclohexane adsorption results.

4.1.2 The Effect of Fluorination on Boralite Activity and Lifetime

Hölderich *et al.* (1984) treated boralite with HF, bound it with silica-alumina, and washed it with HCl to remove Al. The CUV of the resulting boralite for methanol conversion was eleven times greater than that observed in the absence of HF/HCl treatment. These researchers reported similar results with Al-free binder, maintaining that Al transfer to the boralite framework was not responsible for the changes in reactivity. While Hölderich *et al.* (1984) ascribed the increased time-on-stream and C_2-C_4 olefins for methanol conversion to increased cracking of coke precursors due to the presence of fluoride ions, Becker *et al.* (1985) showed that fluorine loading on ZSM-5 using NH_4F enhanced the activity of ZSM-5 for cumene cracking. Becker and Kowalak (1986; 1988) subsequently proposed that the acidity enhancement observed upon fluorination of ZSM-5 and mordenite arises from the inductive effect of F-atoms on the remaining OH groups or from the interaction of strong Bronsted acid sites and strong fluorine-bearing Lewis acid sites. In the light of the above findings it was decided to investigate the effect of mild fluorination treatments on boralite catalysts with a view to favourably influencing catalytic acidity and hence activity for propene oligomerization.

It is clear from Figure 3.8 that despite the fluorination treatments the CUVs for propene oligomerization of the boralite catalysts investigated were an order of magnitude lower than for ZSM-5. Moreover, none of the boralites examined showed significant activity below 300 °C. Treating B-2, for example, with mild HF (B-2-HF) resulted in a catalyst with drastically reduced catalytic activity. Treating this catalyst with NH_4F (B-2-HF-NH_4F) essentially restored the catalytic activity, however. B-2-HF-NH_4F contained only 120 ppm Al, but produced a CUV of 39 g/g. The enhanced activity of B-2-HF-NH_4F could have been due to fluoride ions interacting with the catalyst surface and generating enhanced active sites according to the model proposed by Becker and Kowalak (1988). Ammonia TPD, however, gave no indication of either the presence of more acid sites or of acid sites

of greater strength (see Table 3.5). Given that the reaction temperature for oligomerization was lower than that used by Hölderich *et al.* (1984) (ca. 350 °C vs. 500 °C) there was also no sign that the presence of fluoride ions had led to an increase in cracking of coke precursors resulting in either reduced deactivation rates or modified selectivity.

Treating B-3 with 100 ml of 5.4×10^{-4} molar NH_4F for 2 hours (mild NH_4F treatment), the result was a catalyst of almost negligible activity. The catalyst produced no liquid at 350 °C or lower. The low activity of this catalyst could no doubt be ascribed to the low Al content. The effect of the fluoride treatment in this case was probably detrimental, leaching trace Al out of the catalyst framework, rather than enhancing activity. Treating B-3 with a higher concentration of NH_4F solution (B-3-NH_4F) reduced the Al content from 200 to 100 ppm and resulted in a catalyst of only marginal activity (CUV = 6 g/g).

Becker and Kowalak (1988) showed that the range for activity enhancement with fluorine content is extremely narrow and that maximum activity enhancement occurred where the number of fluorine atoms corresponded with the number of Al atoms in the parent zeolite. It appears, therefore that activity enhancement by fluorination is extremely sensitive to fluorine content. From the boralites examined in this study it is evident that fluorine treatments may easily result in activity reduction rather than enhancement. It is possible that of the fluorinated boralites investigated, only B-2-HF-NH_4F possessed the correct amount of fluorine to activate the catalyst. Due to the complexity of the analytical techniques, the fluorine content of these catalysts was not determined. On the basis of previous work (Becker *et al.*, 1985; Becker and Kowalak, 1986, 1988) however, there is every reason to believe that the fluorination techniques used in this study have resulted in the presence of fluorine in these catalysts.

It would seem, from the performance of fluorinated boralites examined in this study, that even if activity enhancement due to the presence of fluorine modified "super-acids" can be achieved, the fluorination treatment is extremely sensitive to both the F as well as the Al content of the starting material and may lead instead to activity reduction. Moreover, where some activity enhancement was observed, it should be noted that the CUV of the catalyst (B-2-HF-NH_4F) was still an order of magnitude lower than that for unmodified ZSM-5. Ammonia TPD showed no sign that the strong acid sites which appear to be required for good propene oligomerization had been generated by any of the fluorination treatments. There was also no indication that the presence of fluorine had enhanced catalytic cracking of coke precursors to produce a catalyst of longer lifetime and altered selectivity as claimed by some researchers (Hölderich *et al.*, 1984) although it is possible that the reaction conditions were not extreme enough to promote cracking.

4.1.3 The Effect on Selectivity

Wendlandt *et al.* (1988) observed no correlation between boron content and activity, a finding supported by this study. It was noted, however, that the constraint index increased when the boron content exceeded 2 B per unit cell. These researchers concluded that shape selectivity could be altered by the incorporation of boron in the ZSM-5 framework, a postulate supported by Occelli *et al.* (1985), who observed more linear liquid products over boralite than over ZSM-5 for propene oligomerization.

No shape selectivity effects were observed in this study. No increases in para-xylene selectivity were observed, for example, over B-1 compared to ZSM-5 (see Figure 3.5). While the constraint index test used by Wendlandt *et al.* (1988) depends on the difference in sizes of the reaction intermediates of n-hexane (4.9 x 6 Å) and 3- methylpentane (6 x 7 Å) (Haag *et al.*, 1982), the ability of a catalyst to selectively isomerize o-xylene is dependent on catalyst pore size as well as the sizes of the xylene isomers which are of the order of 7-8 Å (Csicsery, 1971). One could reasonably expect therefore, that if changes in the c.i. have been observed upon boron incorporation in the ZSM-5 lattice, then changes in xylene selectivity should also be evident. The fact that no changes in xylene selectivity have been observed in this study appears to contradict the findings of Wendlandt *et al.* (1988). If much of the boron of the boralite catalysts examined in this study is extra-framework (as suggested earlier), however, it is possible that in this study insufficient boron has been incorporated in the catalyst framework to favourably alter catalyst selectivity to p-xylene.

While increased p-xylene selectivity has been used by many researchers as an indication of enhanced shape selectivity, it was felt that since cetane numbers as determined by the Gautier correlation are a measure of the CH_3/CH ratio of diesel fuels and hence can be used as an indication of branching, the cetane numbers of the liquid product of propene oligomerization could also be used as a measure of catalyst shape selectivity. It is evident, from the data presented in Table 3.6, however, that the boralite catalysts exhibit no significant changes in cetane number due to the presence of boron. Although B-6 had a cetane number of 43.6 compared to 41.7 for unmodified ZSM-5 it is not clear whether this is significant since the error in these values is thought to be between 5 and 10%.

Although no change in cetane number with boron and aluminium content is apparent from the data in Table 3.6, it is clear that the liquid product distribution is dependent on reaction temperature. ZSM-5 at 299 °C and boralite A at 331 °C give C_{18}^+ fractions of 14 and 8%, respectively. The other boralite catalysts, operating at much higher temperatures show even smaller C_{18}^+ fractions in their liquid products as well as increased dimer and trimer

fractions and greater amounts of methane in the off-gas. These phenomena, together with the absence of oligomer groups (see Figure 3.9), suggest an increase in cracking reactions resulting in a decrease in the diesel fraction (C_{11}-C_{18}) of the product. The dependence of carbon number distribution on temperature and the presence of aromatics in the liquid product formed above 300 °C is consistent with work carried out by Quann *et al.* (1988). These researchers observed that increasing temperature increased disproportionation and cracking reactions resulting in the formation of products with intermediate carbon numbers. Cyclization and hydrogen transfer were also observed at elevated temperatures resulting in the formation of cyclo-olefins and aromatics.

4.1.4 The Nature of the Active Site

From an analysis of NH_3 TPD data, in conjunction with propene reaction work, it would appear that boron incorporation leads to a reduction in the acidity of the catalyst. In agreement with work carried out by other researchers (Ratnasamy *et al.*, 1986b; Chu *et al.*, 1985; Sayed *et al.*, 1989) this reduction in acidity, especially strong acidity as measured by TPD and corresponding to strong Bronsted and/or Lewis acid sites (Topsøe *et al.*, 1981), can be seen to be directly responsible for a decrease in catalytic activity. A weak B(OH)Si site of the type shown below with the equilibrium lying far to the left as proposed by Scholle *et al.* (1984) would be consistent with this data:

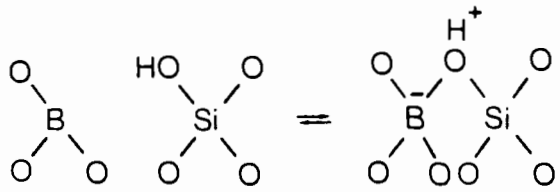

It has been suggested from IR studies (Coudurier and Védrine, 1987; Sayed *et al.*, 1989) that the acid strength of this Bronsted site lies somewhere between that of Al(OH) and Si(OH) and is reflected by a broad OH absorption band at ca. 3700 cm^{-1}. The position of the OH band corresponding to B(OH) indicates that the strength of the B(OH) hydroxyl group is closer to that of SiOH than AlOH, and consequently this site can be expected to have negligible activity for propene oligomerization. This has largely been reflected by the propene oligomerization activities of the catalysts examined in this work which showed activity due to the presence of Al rather than boron.

4.2 The Effect of Boron Impregnation

4.2.1 The Effect on Activity and Lifetime

Auroux *et al.* (1985) proposed that impregnation of ZSM-5 with boric acid followed by calcination can result in the condensation of boric acid with Bronsted acid sites according to the structure shown below.

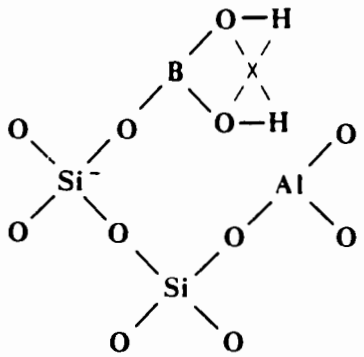

Replacing the strong Bronsted acid sites with those of the strongly hydrogen-bonded boric acid protons would result in reduced amount of strong zeolite acidity. Not only should the amount of weak acidity be increased, but one would also expect an increase in the total overall acidity since one Bronsted OH group is interacting with boric acid to give two B(OH) groups. Moreover, if boric acid impregnation poisons strong acid sites one could reasonably expect to see reduced activities for propene oligomerization.

It is evident from the ammonia TPD data presented in Table 4.1 that boric acid impregnation has resulted in reduced strong acidity. This is especially noticeable for ZB-imp which shows a significant reduction in strong acidity as indicated by the high temperature NH_3 TPD peak. This is accompanied by a substantial increase in the amount of weak acidity. Although there is no sign of increased overall acidity, it is possible that the reduction in strong acidity and the increase in the number of weak acid sites (0.58 mmol /g. cat.) could be due to a mechanism of the type shown above. It is possible that the reason overall number of acid sites has not increased as expected is due to only one of the B(OH) groups being able to react with ammonia, possibly as a result of geometric restrictions imposed by the introduction of boric acid.

Table 4.1 Characteristics of Boron Impregnated ZSM-5 Catalysts

Catalyst	Si/Al	%B (wt)	Ammonia Desorption Low T °C	Low T mmol/g	High T °C	High T mmol/g	Cyclohexane Adsorption (wt%)	Surface Area (m^2/g)
ZSM-5	41		240	0.41	470	0.37	11.5	480
ZB-imp	41	1.5	220	0.58	430	0.24	7.1	285
ZB-wash	41	0.38	240	0.33	470	0.35	9.8	295
ZB-refl	41	0.40	240	0.35	470	0.32	7.8	-

Gabelica *et al.* (1984b) stated that for hexane adsorption at room temperature, the amount of hydrocarbon adsorbed on ZSM-5 is indicative of catalyst pore volume and is sensitive to free volume modifications. n-Hexane adsorption volumes obtained at 25 °C by Olson *et al.* (1980) correspond precisely with the known micropore volume of the catalyst, namely 0.18 cm^3 /g. The SiO_2/Al_2O_3 molar ratio of the catalyst was 75. Since the molecular diameter of cyclohexane (6 Å; Breck, 1974) is also smaller than that of the effective pore diameter of ZSM-5, namely 7-8 Å (Wei, 1982), it should also be possible to monitor the pore volume of HZSM-5 by cyclohexane adsorption. Indeed, the value of 11.5 wt% cyclohexane adsorbed by unmodified ZSM-5 at 30 °C (see Table 4.1) corresponds to a volume of 0.15 cm^3 /g which agrees fairly well with the value obtained by Olson *et al.* (1980) using hexane. Moreover, it can be argued that, since the molecular diameter of cyclohexane is closer to that of a ZSM-5 pore than is hexane, cyclohexane adsorption should be even more sensitive to free volume modifications than hexane adsorption. For these reasons it was decided to monitor changes in catalyst pore volume as well as changes in geometric (steric) constraints by cyclohexane adsorption.

It is clear that boron impregnation has resulted not only in decreased strong acidity, but also in reduced cyclohexane adsorption levels. This is consistent with the proposal of Kaeding *et al.* (1981a) that boric acid impregnation can lead to the constriction of pore openings and/or pores. Indeed, ZB-imp containing 1.2 wt% boron showed the greatest reduction in both cyclohexane adsorption as well as surface area compared to ZB-wash and ZB-refl which only contained ca. 0.4 wt% boron, indicating a greater reduction in pore volume of ZB-imp. Although ZB-wash and ZB-refl had comparable boron loadings and acidity levels, ZB-refl adsorbed cyclohexane at a slower rate (see Figure 3.14) as well as adsorbing less (7.8 wt%) at equilibrium than the 9.8 wt% of ZB-wash. Since the

reproducibility of the technique is ca. 0.5% this difference in adsorption values is significant and together with the slower adsorption rate could indicate different locations of boron within the pores of these catalysts.

When one considers the lower acidities, surface areas and pore volumes of the boron impregnated catalysts, it is not surprising that they perform poorly for propene oligomerization compared to unmodified ZSM-5 (see Figures 3.20 and 3.21). The substantially poorer performance of ZB-refl compared to ZB-wash, despite similar amounts of strong acidity lends further support to the proposal that boron loading is not the only factor affecting the physical characteristics of the catalyst. The method of impregnation is also important resulting in the different location of boron in the catalyst pores. Impregnation with H_3BO_3 which has a molecular diameter of approximately 4.2 Å (calculated from known bond lengths and bond angles) reduces pore volume and surface area which is indicative of pore plugging and/or constriction of catalyst pores and reduced accessibility of acid sites to reactants. The dramatic decrease in activity of ZB-imp upon impregnation to a level comparable to boralite and silicalite catalyst is not consistent with the amount of strong acidity still present on this catalyst. Consequently, it is suggested that the reduction in catalytic activity upon boric acid impregnation is due to not only a reduction in strong acidity, but also to reduced diffusivity of reactant molecules.

4.2.2 The Effect on Selectivity

The molecular diameters of para-, ortho- and meta- xylene have been estimated using the Fischer-Hirschfelder-Taylor hard sphere model by Csicsery (1970, 1971) as being 7.0, 7.6 and 7.6 Å, respectively. As a result of its smaller dimensions, the diffusivity of the para-xylene isomer has been shown to be as much as 1000 times greater than for the other two isomers (Chen and Garwood, 1978). It seems obvious, therefore, to suggest that small modifications made to the ZSM-5 pore opening or pore diameter of ZSM-5 could have significant effects on catalyst selectivity as measured by selectivity to the para-isomer. Indeed Kaeding *et al.* (1981a) and Young *et al.* (1982) have observed increased para-xylene yields for toluene methylation and o-xylene isomerization and attributed enhanced para-xylene selectivity to a reduction in size of effective pore openings (diffusional effects) and/or poisoning on non-shape selective surface sites.

In agreement with work carried out by Kaeding *et al.* (1980, 1981a and 1981b) and by Young *et al.* (1982), the boron impregnated catalysts examined in this study showed greater selectivity to para-xylene for ortho-xylene isomerization. The greatest selectivity to para-

xylene was observed for ZB-imp which had the highest boron content, and lowest cyclohexane adsorption capacity, followed by ZB-wash and ZB-refl which showed only small increases in selectivity compared to unmodified ZSM-5.

Wei (1982) suggested that the product distribution for xylene isomerization is dependent on the following expression:

$$\phi = L\,(k_1 / D_o)^{0.5}$$

where L = the length of the pores
k_1 = the intrinsic rate constant
D_o = the species diffusivity

Increasing effective pore lengths, the rate constant or diffusional constraints (which reduce D_o) would therefore result in increased para-xylene selectivity according to this expression. Young *et al.* (1982) argued that increasing reaction temperature enhances the reaction rate more than diffusivity. Consequently there is a trade-off between diffusional effects and reaction rate. Where the reaction mechanism is controlled by reaction rate, for example, catalytic activity increases and para-xylene selectivity decreases with increasing temperature. This is ascribed to the increase in non-selective surface reactions with temperature as more reactions occur on the outer catalyst surface. When reactions are diffusion controlled, however, increased temperatures result in increased diffusivity of the para isomer compared to ortho- and meta-xylene.

The para-xylene selectivity of ZB-imp, unlike that of ZSM-5, does increase with increasing temperature (see Figures 3.19 (a) and (b)). According to the arguments outlined above one can conclude that boron impregnation has resulted in the presence of severe diffusional limitations leading to increased p-xylene selectivities which are further enhanced by increasing temperatures. The impregnated catalysts of lower boron content, namely, ZB-wash and ZB-refl no doubt also have diffusional limitations brought about by boric acid impregnation which constricts pores and pore openings, as reflected by reduced cyclohexane adsorption.

It would be reasonable to expect that, if catalyst selectivity to para-xylene increases upon boric acid impregnation in agreement with other work in the field, the resulting catalyst could also show increased propensity to produce linear oligomers for olefin oligomerization as measured by cetane number. Cetane numbers, which are directly related to the

CH_3/CH ratio and hence oligomer branching, show no sign, however of being influenced to any significant degree by boron impregnation. Although ZB-imp, which showed the greatest para-xylene selectivity, had the highest cetane number (43.7) it should be noted that the error inherent in the method could be responsible for the observed differences in cetane number.

In conclusion the o-xylene isomerization studies examined here had similar activities and selectivities to those observed by other workers (Young *et al.,* 1982) for boron impregnated ZSM-5. One of the motivations for using o-xylene in the present study was for comparative purposes with the work carried out by Young *et al.* (1982). On the basis of the agreement of the two xylene isomerization studies, therefore, it is valid to assume that one would see changes in the linearity of the products of oligomerization. Since this has not been the case it is reasonable to suggest that o-xylene isomerization may not be an ideal probe reaction. Some researchers have suggested that a more valid test for shape selectivity is the m-xylene isomerization reaction since this measures the rate difference between two parallel reactions. Ortho-xylene isomerization on the other hand uses consecutive reactions, namely o- to m- to p-xylene and consequently differences in p-/m- ratios are inherently small because all p-xylene comes from the primary product m-xylene and these differences may be difficult to measure accurately. Moreover, and more importantly, any differences may not correlate with shape selectivity effects observed for other reactions, but may instead be a reflection of the relative rates of the consecutive reactions ortho- to meta- to para-xylene.

Notwithstanding the discussion of the previous paragraph, in the light of work carried out by Haag *et al.,* (1982, 1987) the diffusivity of propene oligomers in ZSM-5 is estimated as being of the order of 10^{-8} cm ^{2}/s at 850 K. The diffusivity of xylene isomers is estimated to be ca. 10^{-15} cm ^{2}/s at 573 K (Ma and Savage, 1987). Despite the discrepancy in temperatures at which these diffusivities were measured, it is reasonable to conclude that propene oligomers diffuse through the pore systems of ZSM-5 far more easily than xylene isomers. On this basis then, modifications to the ZSM-5 channel which influence selectivity to xylene isomers through diffusional constraints will not influence the linearity of oligomer products in any way. It can be concluded therefore, that although boron impregnation favourably alters ZSM-5 selectivity for reactions such as ortho-xylene isomerization, propene oligomerization is essentially insensitive to the resulting changes in catalyst pore geometry.

4.3 The Effect of Phosphorus Modification on ZSM-5

4.3.1 The Influence of Phosphorus on Physical and Chemical Parameters

^{31}P MAS n.m.r. studies showed that attempts to incorporate phosphorus in the ZSM-5 framework by including H_3PO_4 in the synthesis gel were unsuccessful, merely producing ZSM-5 catalysts containing phosphates occluded in pores. Since high temperature (500 °C) air calcination of the impregnated catalysts results in the decomposition of H_3PO_4 and trimethylphosphite (TMP) to phosphates, the phosphorus impregnated catalysts and the catalysts modified by H_3PO_4 incorporation during synthesis will be treated together in the following discussion.

It is evident from the data presented in Table 4.2 that phosphorus impregnation of 0.4-1.0 wt% P resulted in catalysts with significantly reduced cyclohexane adsorption levels, indicating reduced pore volumes. One could conclude that the reduced pore volumes are due to pore plugging as was proposed by Sayed *et al.* (1986) for impregnation of ZSM-5 with boric acid. It should be noted, however, that changing SiO_2/Al_2O_3 ratios can also affect cyclohexane adsorption levels. Chen (1976), for example, showed for acid dealuminated mordenite that cyclohexane adsorption (at 25 °C) changes with changing SiO_2/Al_2O_3. Where the Al contents of catalysts are different, therefore, as is the case with some of the catalysts presented in Table 4.2, some reductions in cyclohexane adsorption level may be due not only to pore plugging as a result of impregnation, but also to the effect of changing Al content.

The reduced cyclohexane adsorption levels of the phosphorus impregnated catalysts were mirrored to a close approximation by reductions in BET surface areas. The exception is catalyst ZP1-1. Although this catalyst had a similar cyclohexane adsorption value to the other modified catalysts, the surface area was markedly higher (421 m^2 /g vs. ca. 300 m^2 /g), although still lower than the surface area of unmodified ZSM-5 (480 m^2 /g). The higher BET surface area for ZP1-1 is probably a reflection of the lower phosphorus content of this catalyst. BET measurements, which are dependent on the adsorption of the small N_2 molecule, are likely to be far less sensitive to changes in the diameters of pore openings than are cyclohexane adsorption levels which are dependent on the size of cyclohexane, which has a molecular diameter of 6 Å, very close to the effective pore size of ZSM-5. Small reductions in pore size due to partial occlusion of pore openings should consequently affect cyclohexane adsorption to a greater degree than BET surface area. Indeed, ZP1-1 containing 0.4 wt% P showed approximately the same reduction in cyclohexane adsorption capacity compared to unmodified ZSM-5, as ZP1-2 containing

0.9 wt% P, but had a higher surface area (421 m^2 /g vs 308 m^2 /g).

Table 4.2 Characteristics of Phosphorus Modified Catalysts

Catalyst	Si/Al	%P (wt)	Ammonia Low T °C	Ammonia Low T mmol/g	Desorption High T °C	Desorption High T mmol/g	Cyclohexane Adsorption (wt%)	Surface Area
ZP1-1	42	0.4	220	0.28	450	0.30	7.2	-
ZP1-2	191	0.38	200	0.048	400	0.072	-	-
ZP1-3	261	0.18	210	0.06	400	0.078	-	-
ZP1-4	50	0.11	230	0.32	460	0.39	-	-
ZP2-1	40	1.2	200	0.30	-	-	7.0	306
ZP2-2	19	1.0	225	0.36	450	0.27	7.0	304
ZP1-1	40	0.4	220	0.35	430	0.33	8.0	421
ZP1-2	18	0.9	230	0.30	470	0.39	8.2	308
H_3PO_4 slurried 350 ppm	-	-	-	-	-	-	2.7	-
Silicalite	-	-	-	-	-	-	-	-
ZSM-5	41	-	240	0.41	470	0.37	11.5	480

When examining the effect of phosphorus impregnation on catalyst acidity there are two parameters that need to be considered. The first is the aluminium content of the catalyst while the second is the amount of phosphorus. Catalysts ZP2-1 and ZP2-2 for example, were both impregnated with TMP and contained approximately the same amount of phosphorus. ZP2-2, however, had a much higher Al content and consequently had greater acidity as measured by ammonia TPD. ZP2-1 with a Si/Al ratio of 40 was impregnated with 1.2 wt% P which corresponded almost exactly, on a molar basis, with the Al content of the catalyst. This catalyst showed negligible amounts of strong acidity; indicated by the absence of the high temperature ammonia desorption peak (see Figure 3.24). Consequently one can conclude that impregnation of ZSM-5 with TMP resulted in extremely efficient poisoning of strong acid sites. ZP2-2 contained twice as much Al as

ZP2-1 and had approximately the same phosphorus content and accordingly, showed some strong acidity (0.27 mmol /g). This, however, is considerably less than the amount of strong acidity observed by Schwarz (1990), namely, 0.46 mmol /g for a catalyst of the same aluminium content.

Comparison of the TMP and H_3PO_4 impregnated catalysts showed that the H_3PO_4 impregnated catalysts exhibited greater acidity at comparable levels of phosphorus loading. ZP1-2, for example, with Si/Al = 18 and 0.9 wt% P had 0.39 mmol /g of strong acidity, much higher than that observed for ZP2-2 which had almost identical Al and P contents. ZP1-1, impregnated with 0.4 wt% P, had 0.33 mmol /g, not much less than the strong acidity of unmodified ZSM-5 of similar Al content.

It appears then, as if TMP interacts with and poisons the acid sites of ZSM-5 more efficiently than ortho-phosphoric acid. From a consideration of ^{31}P MAS n.m.r studies this is to be expected since TMP shows a chemical shift of -141 ppm relative to phosphoric acid (Tolman, 1970), indicating a greater electron donating ability. In the absence of steric effects, therefore, TMP should interact more readily with the acid sites of a zeolite than phosphoric acid. Examination of ammonia TPD data suggests that this is indeed the case.

The reduced cyclohexane adsorption levels, reduced surface areas and reduced amounts of strong acidity of the phosphorus impregnated catalysts examined in this study are consistent with work carried out by Chandawar *et al.* (1982). The reductions in strong acidity are also consistent with observations made by Jentys *et al.* (1988) and Vinek *et al.* (1989). There is, however, no evidence that phosphoric acid impregnation (ZP1-1 and ZP1-2) resulted in increases in the amount of weak acidity measured by NH_3 TPD as claimed by Vinek *et al.* (1989) and Lercher *et al.* (1985).

The acidities of the catalysts modified by phosphorus incorporation during synthesis were also affected by the presence of phosphorus. ZP^1-2, for example had a higher Al content than ZP^1-3, but exhibited a similar amount of strong acidity. The lower than expected strong acidity of ZP^1-2 can no doubt be ascribed to the higher P content (0.38 %). ZP^1-1, had almost identical P and Al content as ZP1-1 which was impregnated with phosphoric acid. Consequently the acidity levels of these catalysts were very similar, as were the cyclohexane adsorption levels. Comparison of ZP^1-1 and ZP1-1, therefore, shows that if phosphoric acid is incorporated during synthesis, and does not exist as tetrahedrally coordinated framework P, then the effect on catalyst parameters is the same as if the catalyst has been modified by impregnation with phosphoric acid. Comparison of TMP impregnated ZP2-2 and H_3PO_4 impregnated ZP1-2 suggests that in the case of TMP,

interaction with acid sites is more efficient, resulting in catalysts with lower strong acidity for equivalent P loadings.

In general, however, regardless of the method of phosphorus incorporation or modification, the phosphorus modified catalysts exhibited dramatically reduced catalyst pore volumes as measured by cyclohexane adsorption. Surface areas as well as strong acidity also showed significant decreases. Given the limitations of the study it would appear that increasing phosphorus content leads to even more severe reductions in catalyst pore volume, surface area and acidity. The findings of this study are consistent with those of other researchers (Chandawar *et al.*, 1982; Jentys *et al.*, 1989) who also observed reductions in pore volume and strong acidity upon phosphorus modification of ZSM-5.

4.3.2 The Influence of Phosphorus on Catalyst Performance

The effect of phosphorus modification on catalyst activity was monitored by examining performance for high pressure propene oligomerization (5 MPa, 250 °C, WHSV ~ 13). Catalyst selectivities, however, were examined for both propene oligomerization and o-xylene isomerization.

4.3.2.1 Activity and lifetime

Considering the H_3PO_4 and TMP impregnated catalysts, one can see that the activity data for these catalysts (see Figure 3.28) fits qualitatively with the high temperature TPD acidity data presented in Table 4.2. With the exception of ZP1-1, which contains only 0.4 wt% P and which consequently has a surface area of 421 m^2 /g, the catalysts show similar surface areas and cyclohexane adsorptions. Only the amounts of strong acidity are different and this is reflected in the different activities for high pressure propene oligomerization. ZP2-1, with little or no strong acidity (see Figure 3.24) shows no activity below 300 °C. At 320 °C this catalyst had a maximum conversion of 57%. Deactivation, however, was extremely rapid. ZP2-2 with a higher Al content and correspondingly greater acidity (0.27 mmol /g) performed much better, producing liquid at 230 °C. Catalysts impregnated with H_3PO_4, ZP1-1 and ZP1-2, having still greater acidity, performed even better. Activities for all of these catalysts, however, were substantially lower than for unmodified ZSM-5 (Si/Al = 41) which was earlier seen to have a conversion level of greater than 90% at 250 °C (see Figure 3.20).

The reduced activities of these catalysts are consistent with work carried out by other researchers who also observed a drop in activity with phosphorus impregnation. (Chandawar *et al.,* 1982; Vinek *et al.,* 1989; Nunan *et al.,* 1984). Suzuki *et al.,* (1988) did notice longer lifetimes for methanol conversion but this was accompanied by an increase in light olefin selectivity and reduced aromatization. These changes were ascribed to the presence of weaker acidity with reduced aromatization presumably accounting for the reduced coking tendency and longer lifetimes.

In comparison to the impregnated catalysts, the catalysts modified by H_3PO_4 incorporation during synthesis showed somewhat higher activities for propene oligomerization. This behaviour may be explained by the lower phosphorus content of these catalysts. ZP^1-4, for example, containing only 0.11 wt% P showed comparable activity to unmodified ZSM-5. Catalysts ZP^1-2 and ZP^1-3 exhibited low activities due in part to phosphorus poisoning, but also to the low Al content.

Although ZP^1-1 contains similar Al and P contents to ZP1-1 and has almost identical amounts of strong acidity, the catalyst does not behave as expected. The catalyst had much higher activity than ZP1-1 and showed only minimal deactivation after 25 hours on stream. The vastly superior performance of this catalyst is a result of the very small crystallite size (Schwarz, 1990). It was initially thought that the small crystallites of ZP^1-1 (less than 1 micron) could be ascribed to the presence of phosphorus, with phosphorus playing a structure breaking role similar to that played by aluminium during synthesis (Jacobs and Martens, 1988). There is, however, no clear evidence for this, with the other ZP^1 catalysts all having crystallite sizes greater than 2 microns.

In order to examine the activity of phosphates for propene oligomerization a H_3PO_4 slurried silicalite catalyst was made. The behaviour of this "CATPOLY" type ZSM-5 was also compared to the performance of industrial CATPOLY catalyst. Calcination of the slurried silicalite catalyst in either N_2 or air gave a catalyst with no activity below 300 °C. Activity above 300 °C was the same as that of the unmodified silicalite. Phosphate ions, of the type incorporated in the other phosphorus modified catalysts, can therefore be said to have no activity for propene oligomerization.

Without calcination the initial performance of the H_3PO_4 slurried silicalite was almost identical to that of H_3PO_4 supported on kieselguhr. The importance of the role played by water in determining activity and lifetime of the CATPOLY catalyst for propene oligomerization has been previously illustrated (McClean, 1988). While kieselguhr is hydrophillic and retains water, resulting in slow deactivation rates, silicalite is hydrophobic

and loses water with the result that the slurried silicalite quickly loses its ability to behave as a CATPOLY catalyst, and reverts to a silicalite catalyst containing low Al and having poor activity. This is reflected in the very rapid deactivation rate evident in Figure 3.29.

In general, then, phosphorus incorporation results in catalysts with reduced activity for propene oligomerization, which is in keeping with reductions in catalyst pore volume and strong acidity. Similar observations have been made by other researchers for reactions such as benzene ethylation (Chandawar *et al.,* 1982), toluene alkylation (Kaeding *et al.,* 1981a and 1981b; Vinek *et al.,* 1989) and xylene isomerization (Young *et al.,* 1982). In contrast to the findings of Védrine *et al.* (1982), which motivated some of this work, it is clear that trimethylphosphite interacts with, and efficiently poisons, strong acid sites of ZSM-5. The resulting catalysts show reduced activity for propene oligomerization. It is possible, however, that in the case of very small crystallites, the deleterious effect of phosphorus impregnation may not be readily apparent unless the catalyst is exposed to severe impregnation conditions.

4.3.2.2 Selectivity

For propene oligomerization there was no clear indication of increases in selectivity to linear products as measured by cetane number. Given the insensitivity of cetane number to changes in catalyst parameters (as discussed in Section 4.2.2) it is unlikely that changes made to the catalyst by phosphorus modification would result in desirable increases in cetane number.

In the case of xylene isomerization, which shows greater sensitivity to catalyst modifications, changes in selectivity were observed. At 500 °C the p-xylene selectivity of phosphorus modified ZP1-1, (see Figure 3.26) was very similar to that observed by Young *et al.,* (1982) for H_3PO_4 impregnated ZSM-5 at 550 °C. At 350 °C, the increases in selectivity relative to unmodified ZSM-5 are small (see Figure 3.25). The increases in selectivity can almost be considered negligible when compared to the cost on catalyst acidity and activity. This was found to be the case in this study whether the phosphorus source was H_3PO_4 or TMP. Nunan *et al.,* (1984) found that TMP impregnated ZSM-5 yielded higher para selectivities than quinoline poisoned ZSM-5. This was ascribed to the more effective reaction of TMP with external surface hydroxyls. Although the present study showed that TMP also poisoned acid sites more efficiently than phosphoric acid, in accordance with its greater electron donating ability, there was no indication which had been preferentially poisoned. The higher para-xylene selectivities of these catalysts, therefore, should be ascribed to

constriction of catalyst pores as indicated by reduced cyclohexane adsorption levels rather than to the selective poisoning of external surface acid sites. Some supporting evidence for this is provided by the fact that ZP1-1 showed very similar selectivity increases with temperature (see Figure 3.25 and 3.26) to the boron impregnated catalysts (ZB-imp) (discussed in Section 4.2.2). Accordingly the increases in p-xylene selectivity upon phosphorus modification should therefore, also be attributed to the influence of diffusion which is affected by changes in pore geometry.

Although ZP[1]-1 had 0.4 wt% P, very similar to the P content of ZP1-1, the catalyst showed almost identical selectivity to p-xylene as unmodified ZSM-5. This behaviour can be attributed to the small crystallite size, the effect of which can be significant as illustrated by the performance of K-ZSM-5 (see Figure 3.26) which had ca. 10 μm crystallites. The effect of crystallite size on catalyst selectivity has previously been observed by other researchers (Ratnasamy *et al.,* 1986; Chen, 1979).

4.3.3 Comments on the Behaviour of Phosphorus Modified ZSM-5

In general, irrespective of the method of phosphorus modification, the presence of phosphorus in ZSM-5 has resulted in catalysts with very similar characteristics, namely, reduced pore volumes, surface areas and strong acidity.

Although TMP was shown to interact more efficiently with acid sites than H_3PO_4, there was no evidence that this resulted in increased selectivity to p-xylene. There was also no evidence that changes in p-xylene selectivity for xylene isomerization are due to the selective poisoning of, external acid sites as claimed by some researchers (Nunan *et al.,* 1984). Instead, changes in selectivity can be ascribed to modified pore geometry, an observation made previously by Védrine *et al.* (1982). While these researchers suggested that TMP impregnation reduces acidity, but leaves the strongest sites unaffected, Gilson and Dérouane (1984) concluded from n-hexane and trimethylbenzene cracking experiments that TMP poisons primarily acid sites at pore mouths (i.e. near the outer surface) leading to a restriction of pore openings. It is evident, however, from the present study that modifications made with H_3PO_4, and especially TMP, result in ZSM-5 catalysts with radically reduced strong acidity. Indeed, with TMP impregnation, poisoning of all strong acid sites, as measured by NH_3 TPD, was achieved. This was in keeping with IR observations carried out by Nunan *et al.,* (1984). The resulting catalyst (ZP2-1), contrary to the claims of Védrine *et al.,* (1982) showed substantially reduced activity, for both xylene isomerization as well as propene oligomerization. In any event, it is clear that the changes

made to the ZSM-5 catalysts, particularly with respect to acidity, resulted in poor activity and that for oligomerization this loss in activity was not accompanied by altered selectivity.

It has been stated that phosphorus converts strong Bronsted acid sites into weak Bronsted acid sites without changing overall acid-base properties (Lercher and Rumpelmayr, 1986). Other researchers have suggested that the interaction of phosphorus with strong sites should not only convert strong Bronsted sites to weak ones, but also that the number of acid sites should increase according to the model shown below (Vinek *et al.*, 1989):

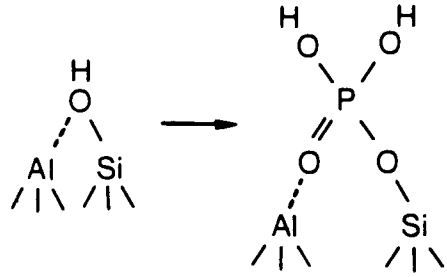

No evidence was found in the present study for either an increase in the number of weak sites or for an increase in total acidity. Jentys *et al.*, (1989) showed that H_3PO_4 treatment is accompanied by significant dealumination which leads to a reduction in the intensity of the 3610 cm^{-1} OH-band. It is possible that some dealumination occurs in this way and is partially responsible for the reduction in overall acidity observed in this study, but there is no clear evidence of this. It is possible that phosphorus in the form of phosphates formed during calcination may also play a role, either in influencing weak acid sites or by occluding pores leading to a reduction in catalyst pore volume.

4.4 Steam Dealumination of ZSM-5

4.4.1 The Influence of Steaming on Activity for Hexene Oligomerization

Steam dealumination can essentially be defined as dealumination that occurs due to the presence of water (vapour) at elevated temperatures (> 100 °C). The importance of steaming on the catalytic activity and selectivity of ZSM-5 for various reactions has been illustrated by a number of researchers. It has been shown for example, that co-feeding water with methanol over ZSM-5 for methanol conversion enhances the formation of olefins over iso-alkanes and aromatics (Caesar and Morrison, US Patent). Moreover, it has been stated by Owen *et al.* (1984) that the preferred catalyst for the MOGD process is an extrudate containing 65 wt% *"steamed"* ZSM-5 and 35 wt% alumina binder. Since Lago *et al.* (1986) showed that mild steaming (2 hours, 540 °C, 70-80 mm Hg) enhances the activity of ZSM-5 for n-hexane cracking much work has been carried out in an attempt to

elucidate the influence of steaming on catalytic activity.

While some of the research has merely looked at the effect of steaming partial pressure on activity in more detail than the study of Lago *et al.* (1986) (Reschetilowski *et al.*, 1989; Brunner *et al.*, 1989 and 1991) the effects of steaming time (Loeffler *et al.*, 1988 and 1990; Zholobenko *et al.*, 1990 and 1991; Kürschner *et al.*, 1990) and temperature (Topsøe *et al.*, 1988) have also been examined. The effect of flowrate as a steaming parameter, however, has not been reported. It is evident from this study, however, that steaming flowrate can significantly affect the subsequent activity of steamed ZSM-5 (see Figure 3.39). The effect of flowrate on catalyst activity is further emphasized by comparison of catalyst activity at two flowrates (30 ml/min and 60 ml/min) and different steaming temperatures (see Figures 3.40 and 3.41). The fact that flowrate influences steam dealumination is important since its effect has not been previously reported and makes direct comparisons of previous steaming work extremely difficult.

The fact that changing flowrate, equivalent to changes in the linear steaming velocity through the bed, affects catalyst behaviour when the other steaming parameters, particularly water concentration, are held constant implies that external mass transport (film) resistances exist at the steaming conditions used in the present study. Hidajat *et al.* (1987) stated that if such resistances exist then k_m, the external mass transfer coefficient, is given by:

$$k_m \equiv D/\delta$$

where D is the bulk molecular diffusivity of the key species and where δ is the thickness of the Nernst "diffusion layer" or film surrounding the catalyst particle. The diffusion layer thickness is reduced with increasing flowrate around the catalyst particle, thereby increasing k_m and hence the rate of reaction.

Another measure of the film thickness, δ, is the Reynolds number which is inversely proportional to δ, and proportional to particle diameter and linear velocity through the catalyst bed. Consequently for small values of the Reynolds number, δ is large and film diffusion plays an important role. Considering the low steaming flowrate (linear velocity) and the small catalyst particle size (ca. 2-3 μm) it is not surprising that the Reynolds numbers calculated in Appendix 10 are extremely small (ca. 1×10^{-4}). It is to be expected, therefore, that δ is large and that external mass transport resistances exist in the present study. Since it is probable that most laboratory studies are characterized, by reason of low flowrates and small particle diameters (Hidajat *et al.*, 1987), by small values of the

Reynolds number, care should be taken not to overlook flowrate as an important parameter in determining catalytic behaviour.

It is clear, therefore, that if steaming is achieved by means of a saturator, flowrate should not be overlooked as a steaming parameter since flowrate variations can significantly affect the dealumination rates and subsequent catalytic activity. It should be noted that for this study the reactor cross-sectional area was held constant and consequently, as mentioned above, flowrate changes reflect changes in the linear steaming velocity. Extrapolating to other reactor systems would therefore require that reactor cross-sectional area be taken into account in order to make meaningful comparisons to the results obtained here.

The effect of steaming temperature on the activity of ZSM-5 for 1-hexene oligomerization is shown in Figures 3.40 and 3.41. It is clear that a maximum in catalytic activity is achieved at a steaming temperature of 300 °C as compared to either lower (200 °C) or higher (400 °C, 500 °C) temperatures. The effect of steaming temperature has previously been noted for hexane cracking activity. For conditions of 101 kPa steam partial pressure and 5 hours steaming time, maximum activity for hexane cracking was observed by Topsøe *et al.* (1988) at 350 °C. From pyridine IR studies they concluded that the Bronsted sites of the sample steamed at 350 °C were stronger than those steamed at higher or lower temperatures. The temperature at which maximum activity was observed by these researchers, viz. 350 °C, agrees well with the optimum temperature of 300 °C observed in this study for olefin oligomerization.

The performance of ZSM-5 for 1-hexene oligomerization as a function of steaming time is shown in Figure 3.42. Maximum activity (enhanced relative to unmodified ZSM-5) is observed after steaming for 2 hours. This is very similar to the steaming time observed by other researchers which yielded a maximum in activity for hexane cracking at similar partial pressures of water. Brunner *et al.* (1989), for example, observed maximum activity after 2.5 hours at 50 mm Hg water vapour pressure, while Lago *et al.* (1986) observed maximum activity after 2.5 hours treatment with water vapour at ca. 80 mm Hg. In both of these studies the steaming temperature was 540 °C.

The effect of steaming time on ZSM-5 has been examined by Loeffler *et al.* (1988 and 1990) and by Zholobenko *et al.* (1990 and 1991). Short steaming times (<3 hours) led to an increase in the intensity of the 3665 cm^{-1} OH band which was ascribed to extraframework Al species (Loeffler *et al.*, 1988). Although these OH groups have been shown to possess acidity (Loeffler *et al.*, 1988) activity enhancement was instead ascribed to the presence of Lewis sites formed during steam dealumination (Zholobenko *et al.*, 1990 and 1991). These

researchers then proposed that an optimal ratio of the concentration of Bronsted sites to these Lewis sites exists. Depending on the steaming conditions chosen, therefore, maximum activity is achieved by carefully optimizing the steaming time. The influence of steaming time, as observed in this study, is not inconsistent with this proposal with only 2 hours steaming time resulting in maximum catalytic activity for hexene oligomerization.

The effect of water partial pressure on catalytic activity for hexene oligomerization is shown in Figure 3.43. Maximum activity was observed at 78 mm Hg of water vapour. Although the steaming temperature is 300 °C as opposed to the 540 °C used by Brunner *et al.* (1989) and Lago *et al.* (1986), the water concentration at which maximum activity occurred in the present study was close to those noted by these researchers for short steaming times. Once again it is apparent that at either too mild (21 mm Hg) or more severe conditions (> 100 mm Hg) activity is lower than at intermediate conditions (78 mm Hg).

The effect of steaming at increasing water partial pressure is shown below in Figure 4.2. Above a partial pressure of 150 mm Hg, there is very little effect of changing concentration on catalyst activity. Indeed, the difference in activities observed earlier between catalysts steamed at 230 mm Hg and 320 mm Hg (see Figure 3.43) no longer appear significant. It appears that at ca. 150 mm Hg a point is reached at which further increases in water partial pressure have no further effect. In other words, above 150 mm Hg of water dealumination has reached equilibrium. Brunner *et al.* (1989) using ^{27}Al MAS n.m.r. showed that above a water concentration of ca. 100 mm Hg no further dealumination occurred. The results of the present study, therefore, are in keeping with the findings of Brunner *et al.* (1989) which suggested that above ca. 100 mm Hg water there is saturation of the dealumination reaction.

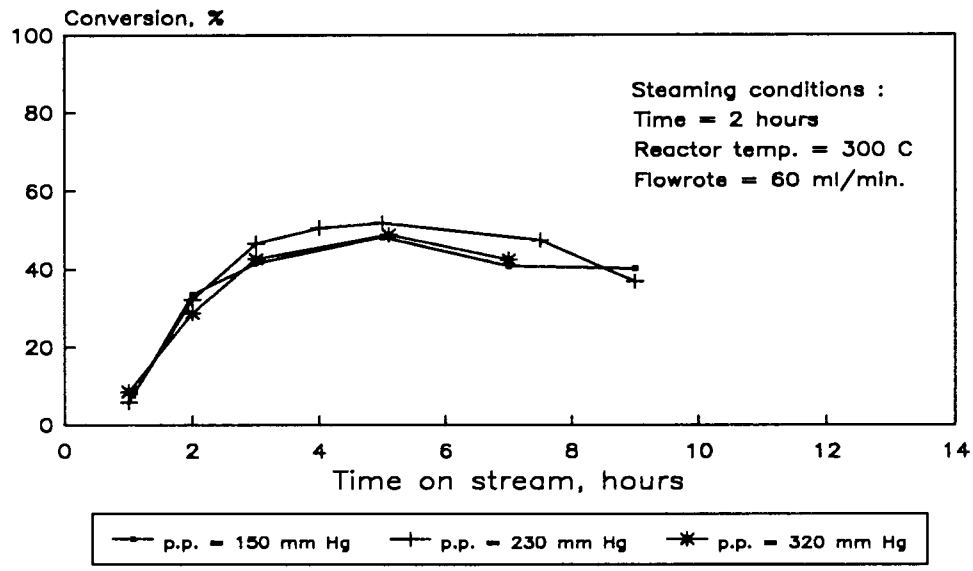

Figure 4.2 **The effect of steaming partial pressures of greater than 150 mm Hg on hexene oligomerization activity**

4.4.1.1 The influence of steaming on hexene oligomerization activity of a silicalite coated catalyst

The influence of steaming on a silicalite coated catalyst was examined briefly. The catalyst was synthesized in the following manner. After 6 hours crystallization time a ZSM-5 catalyst of charged Si/Al = 40 was removed from the synthesis autoclave. The gel was then filtered to yield the crystalline catalyst which was washed and replaced in the autoclave in a synthesis mixture devoid of Al. After a further 2.75 days at synthesis temperature, the catalyst was removed and activated according to the procedures outlined in Section 2.4. The catalyst was then steamed at 500 °C, 78 mm Hg for 2 hours at 30 ml/min and 60 ml/min. The activities of these steamed catalysts as well as of the unmodified catalyst for hexene oligomerization are shown below in Figure 4.3

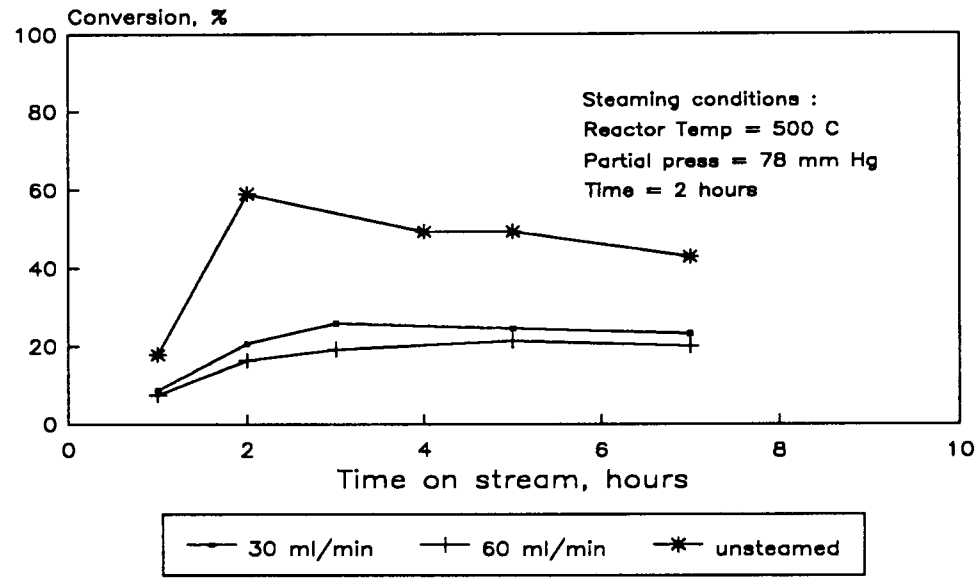

Figure 4.3 The effect of steaming on silicalite coated catalyst

Although the silicalite coated catalyst has comparable activity to unmodified ZSM-5 prior to steaming it is evident from comparison of Figure 4.3 and Figure 3.39 that the effect of steaming on the silicalite coated catalyst is quite different to that of normally synthesized ZSM-5. The effect of flowrate, on activity for example, is not nearly as pronounced as for normally synthesized and steamed ZSM-5. Although this could be ascribed to the existence or non-existence of a water film of the type alluded to by Hill and Seddon (1985), it is more likely to be due to a difference in the hydrophobic properties of the catalysts. The highly hydrophobic nature of the external surface of the coated catalyst may result in coulombic interaction effects which are highly significant and in comparison to which mass transfer limitations (i.e. film resistances) are negligible, with the result that steaming flowrate no longer plays an important role.

4.4.2 The Effect of Steaming on Propene Oligomerization Activity and Lifetime

The performance of unmodified ZSM-5 for propene oligomerization at 5 MPa and 250 °C was compared to that of S-300-78-2-60 which showed maximum activity for hexene oligomerization. The conversion versus time-on-stream behaviour of these catalysts is shown in Figure 3.44. As was the case for hexene oligomerization, S-300-78-2-60 clearly

performs better than unmodified ZSM-5 for propene oligomerization. The CUV increased from 120 g/g to 199 g/g upon steaming. A catalyst steamed at conditions that ensure maximum (enhanced) catalytic activity, therefore, will result in increased performance for not only 1-hexene but also propene oligomerization. Such a steamed catalyst is likely to also show improved performance for industrial processes such as MOGD.

4.4.3 The Nature of Steamed Catalysts

The crystallinities of some of the steamed catalysts are shown in Table 3.20. Although crystallinities are slightly lower than for unmodified ZSM-5 this is due to the presence of water interacting with the ZSM-5 framework as reflected by the reduction in intensity of the peaks at 6 and 8 degrees 2 theta. The slightly lower crystallinities observed upon steaming, therefore, are not a sign of lattice destruction, but are an artefact of the steaming process. IR spectra showed that water present on the catalysts after steaming could only be removed by prolonged evacuation at 2×10^{-6} mm Hg and the appropriate steaming temperature. The resistance of the ZSM-5 structure to steaming is further illustrated by optical density ratios of ca. 0.6. This is in keeping with work carried out by other researchers who also demonstrated the stability of the ZSM-5 framework to steaming (Tallon and Buckley, 1987; Wang *et al.*, 1979). Certainly the small changes in crystallinity that may occur as a result of steaming can not be responsible for changes (reductions) in activity that have been observed in this study.

In an attempt to examine the influence of steaming on catalyst acidity ammonia TPD was carried out on a number of steamed catalysts. The ammonia TPD data, however, sheds little light on the reason for enhanced activity. If stronger Bronsted acid sites are responsible for enhanced activity as suggested by the findings of Topsøe *et al.* (1988) one would expect to see shifts in the high temperature ammonia desorption peaks with changing steaming conditions, all other things being equal. From the data presented in Table 3.23 one can see that this has clearly not been the case. Shifts in peak position are small, have no trend and do not correlate with activity data.

While ammonia TPD failed to clarify the role played by acidity on catalyst activity one would expect pyridine desorption IR studies to at least confirm or negate the proposal of Zholobenko *et al.* (1990), namely that an optimal ratio of the concentration of Bronsted to Lewis sites is required for enhanced activity. Lewis/Bronsted acid site ratios, determined from pyridine desorption IR, as a function of steaming temperature are presented in Figure 3.36 for two different steam flowrates.

It can be seen from Figure 3.36 that increasing the steaming temperature in the range 200 °C to 500 °C results in increased Lewis/Bronsted acid site ratios. Moreover, increasing the steam flowrate from 30 ml/min to 60 ml/min results in an increase in the ratio reflected by an upward shift of the Lewis/Bronsted vs. steaming temperature curve. This increase in Lewis acidity relative to Bronsted acidity with steam flowrate may be responsible for the differences in activity that were observed earlier (see Figure 3.39, 3.40 and 3.41). It does not, however, explain the activity maximum that is observed at 300 °C steaming temperature at both flowrates. Clearly the Lewis/Bronsted ratios at 300 °C are different at 30 ml/min and 60 ml/min. Corma (1989), in a study of dealuminated HY zeolite, suggested that if the nature of the extra-framework Al sites thought to be responsible for enhanced activity is important, then so too must be their location and distribution. It has been reported that during steaming, part of the Al leaving the zeolite framework migrates to the surface producing Al surface rich zeolite Y (Dwyer *et al.*, 1981; Meyers *et al.*, 1986). One can therefore expect to see Al gradients in zeolite crystals, which may profoundly influence catalyst activity. Any measurements of acidity using pyridine desorption IR would not be able to measure Al gradients of this nature or their influences. Moreover, if a particular type of Lewis site is responsible for activity enhancement this would also not be detected by Lewis/Bronsted acid site concentration ratios as given in Figure 3.36.

Hexane adsorptions (at 70 °C, Table 3.22) and BET surface areas (Table 3.24) were also measured to determine the effect of steaming on ZSM-5. Both N_2 and hexane adsorption levels are slightly lower for steamed catalysts than for unmodified ZSM-5. As was the case with crystallinity, the differences between steamed and unmodified ZSM-5 are small and show no trend with changing steaming conditions. The relative insensitivity of nitrogen and n-hexane adsorption experiments to the presence of extra-framework Al was also observed by Vasquez *et al.* (1989) who concluded that pore blockage due to the presence of extra-framework Al as a result of steam dealumination was not apparent from N_2 and n-hexane adsorption experiments.

In general, then, it can be concluded that steaming at conditions used in this study does not significantly affect the physical characteristics of ZSM-5 as reflected by small changes in crystallinity, surface area and catalyst pore volume. While it is felt that altered acidity is responsible for changes in catalytic activity upon steaming, these changes appear to be too subtle to be easily detected by either ammonia TPD or pyridine desorption IR studies.

Indeed, attempts to clarify the exact nature of the aluminium species responsible for enhanced activity will be difficult due to the amphoteric nature of the hydroxy species of Al^{3+} and the propensity of oxygen to bridge different Al^{3+} ions. The situation can be

further complicated by both dimerization as well as polymerization of the hydroxyaluminium species (Grunwald and Fong, 1969; Cotton and Wilkinson, 1980).

Lago *et al.* (1986) proposed that activity enhancement results from the partial hydrolysis of a pair of framework Al atoms, so that one aluminium atom in a trigonal coordination acts as a strong electron withdrawing centre on the remaining tetrahedral Al, creating a stronger Bronsted acid site. Subsequent hydrolysis of the partially hydrolyzed site at more severe steaming conditions would then destroy this enhanced site leading to a reduction in catalytic activity. This model suitably explains how changes in partial pressure, steaming time and even temperature (related to the activation energy of the hydrolysis reactions) can affect catalytic activity. Brunner *et al.* (1989), however, pointed out that no evidence for the partially hydrolysed (trigonal) framework Al proposed by Lago *et al.* (1986) has been found in the ^{27}Al MAS n.m.r. spectra of hydrated catalysts. Moreover, ^{29}Si MAS n.m.r. spectra showed that the concentration of paired Al sites is much less than required by the partial hydrolysis model. Brunner *et al.* (1989) proposed that the interaction of hexane with a Bronsted site and an extraframework Al species is responsible for enhanced activity for hexane cracking.

More recent work by Zholobenko (1990 and 1991) has provided evidence for the existence of extraframework Lewis sites. They concluded that these sites are responsible for enhanced activity by increasing the rate of the initial step for hexane cracking. Neither the proposal of Brunner *et al.* (1989) nor that of Zholobenko *et al.* (1990 and 1991) can be convincingly supported by any of the characterization work carried out in this study although pyridine desorption IR work did suggest that Lewis/Bronsted site ratios change with changing steaming flowrate mirroring the behaviour of activity data. It is argued on this basis, therefore, that a specific Lewis site is being created during steaming which can have significant influence on catalyst activity.

4.4.4 The Influence of Steaming on Catalyst Selectivity

The C_{18}^{+} fraction of hexene oligomerization for a number of steamed catalysts are plotted against maximum conversion level in Figure 4.4 below.

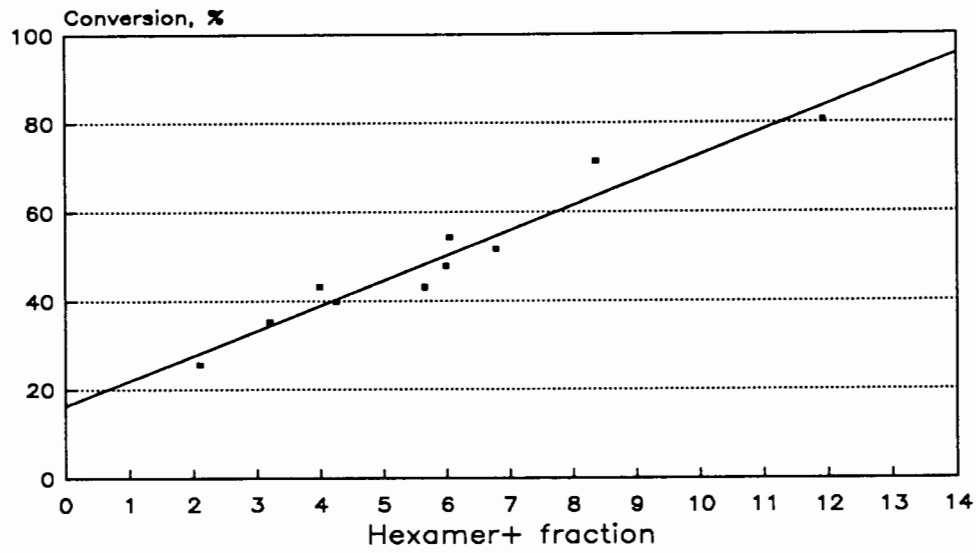

Figure 4.4 Conversion vs. C_{18}^+ for a number of steamed catalysts

It can be seen from Figure 4.4 that the maximum conversion levels achieved by the steamed catalysts correspond well with the C_{18}^+ fraction in the liquid product of hexene oligomerization. This dependence of liquid product distribution on conversion level is in no way affected by the changing steam dealumination conditions. Some researchers (Kürschner *et al.,* 1990) have shown that extra-framework Al resulting from steam dealumination can enhance the selectivity to p-xylene for toluene disproportionation and m-xylene isomerization. In the light of boron and phosphorus modifications carried out earlier in this study, it is unlikely, however, that this would in any way affect the linearity of oligomerized products. Once again carbon number distribution of oligomer products appears to be unaffected by catalyst parameters with the products of both 1-hexene and propene oligomerization being dependent on temperature, WHSV and conversion level.

4.4.5 A Comparison of the Effect of Steaming on the Activity of ZSM-5 for Oligomerization and Hexane Cracking

Results reported by Lago *et al.* (1986) showed that activity enhancement could be achieved for hexane cracking by steaming at 540 °C for 2.5 hours at low partial pressures of water. Activity enhancement for hexane cracking has also been observed by other researchers when steaming at 540 °C (Brunner *et al.,* 1989; Zholobenko *et al.,* 1990 and 1991). In

general, the effects of steaming on olefin oligomerization activity observed in this study have been very similar to the effects on hexane cracking activity reported by other researchers. It is probable that the same site is responsible for the enhanced activity observed for both reactions. Since the present study showed that steaming at ca. 300 °C is preferable to 500 °C steaming for hexene oligomerization it is possible that the activity observed by other researchers for hexane cracking after steaming at 540 °C may not be optimum. Some support for this has already been provided by Topsøe *et al.* (1988) who showed that for steaming conditions of 1 atmosphere water p.p., 5 hours and various temperatures a maximum activity for hexane cracking was observed at ca. 350°C. This corresponds closely to the optimum steaming temperature of 300 °C observed in the present study.

Although previous steaming studies have not reported the effect of flowrate the importance of flowrate as a steaming parameter is clearly evident from the present study. While the present study examined the effect of steaming flowrate on the activity of ZSM-5 for hexene oligomerization, it is reasonable to conclude that if this can be ascribed to the existence of external mass transport resistances during dealumination then flowrate is also likely to affect catalytic performance for other reactions such as hexane cracking. This being the case, care should be taken not to overlook the effect of flowrate on dealumination rates, particular at the low flowrates often used in laboratory studies.

Chapter 5
Conclusions

CONCLUSIONS

A number of boralite catalysts were synthesized by substituting B_2O_3 for $Al(OH)_3$ in the synthesis gel. Both Aerosil and Ludox were used as silica sources, with Aerosil producing catalysts with lower trace aluminium contents. Boron incorporation resulted in catalysts having only one ammonia TPD peak at ca. 190 °C corresponding to ammonia adsorbed on weak B(OH)Si sites.

The poor correlation between the low temperature NH_3 TPD peak and the boron content as well as the reduced adsorption levels suggested that not all the boron was incorporated into the zeolite framework, but existed as B_2O_3 species occluded in catalyst pores. As a result of the weak acidity and the reduced adsorption levels, the activity of these catalysts was extremely low. Activity for propene oligomerization, in almost all cases, could only be achieved at reaction temperatures above 300 °C and corresponded to Al rather than boron content. Treating a boralite catalyst with a mild HF solution resulted in a catalyst with drastically reduced activity, presumably as a result of reduced Al content. Subsequent treatment of this HF modified catalyst with NH_4F essentially restored the catalytic activity for propene oligomerization. Mild NH_4F treatment also marginally increased catalytic activity. It was found, however, that although mild fluorination treatment could enhance catalyst activities for propene oligomerization, these activities were an order of magnitude lower than for unmodified ZSM-5.

As a consequence of the high reaction temperatures required to produce liquid product from propene oligomerization, viz. 300 °C, boralite catalysts produced liquid products with reduced C_{12}^+ fractions and increased amounts of dimer. This was ascribed to the effect of increased secondary products arising from catalytic cracking. The aromatics contents also increased. Xylene isomerization experiments showed no changes in p-xylene selectivity with boron incorporation. Linearity of liquid product from propene oligomerization as measured by cetane numbers was also unchanged.

Impregnation of ZSM-5 with boric acid resulted in reduced amounts of strong acidity as well as reduced surface area and cyclohexane adsorption. Although catalytic activity was reduced, selectivity to p-xylene for o-xylene isomerization increased. The catalyst showed marked selectivity increases with increases in reaction temperature suggesting the presence of significant diffusional constraints. As a result of the reduced strong acidity as well as reduced pore volume, the activity of this catalyst for propene oligomerization was low. Moreover, no increases in the linearity of the liquid products of oligomerization were

observed. This was attributed to the relative insensitivity of oligomerization products to changes in ZSM-5 pore diameters. Washing this catalyst removed occluded boron, increasing the amount of strong acidity, surface area and cyclohexane adsorption. Activity relative to unmodified ZSM-5, however, was reduced while no improvements in the amount of linear oligomers in the product was observed. Impregnation of ZSM-5 with boric acid using heat refluxing resulted in a catalyst with lower activity than the impregnated and washed catalyst. It was proposed that both boron content as well as impregnation method were important with different impregnation methods resulting in the incorporation of boron in different locations in the ZSM-5 pores.

Phosphoric acid and TMP impregnation also resulted in reduced amounts of strong acidity, surface area and cyclohexane adsorption levels. The catalysts showed reduced activities for propene oligomerization which was ascribed to a combination of weak acidity and pore blockage. Although increases in p-xylene selectivity were observed these were not significant when compared to the loss in catalytic activity. Despite the reduced pore volumes these catalysts did not show increased linearity of oligomerization products. This is not surprizing given the insensitivity of oligomers to changes in catalyst diameter, as measured by the cetane number. The carbon number distribution of the oligomerization products was again dependent on the reaction temperature rather than on the method or degree of phosphorus loading.

Incorporation of phosphorus in the synthesis gel produced catalysts whose activities and acidities were comparable to phosphoric acid and trimethylphosphite impregnated catalysts. No evidence was found for phosphorus incorporation in the framework with phosphorus instead being present as occluding phosphates. No changes were observed in selectivity for either xylene isomerization or propene oligomerization.

A ZSM-5 catalyst of Si/Al = 40 was steamed at various temperatures, water partial pressures, flowrates and times. All of these parameters were found to have an important effect on catalytic activity. By carefully optimizing these parameters catalytic activity for both hexene and propene oligomerization could be achieved. The optimum conditions for activity enhancement were: steaming temperature = 300 °C, water p.p. = 78 mm Hg, steaming time = 2 hours and steaming flowrate = 60 ml/min (corresponding to a linear steaming velocity of 24 ml/min/cm^2 of empty reactor cross-sectional area).

The effect of flowrate on steaming has been ignored in previous dealumination studies. It was found that steaming flowrate affects the rate of dealumination possibly as a result of external mass transfer (film) resistances that exist during steam dealumination. If the effect

of steaming flowrate is ignored, it is difficult to make quantitative comparisons of previous dealumination studies with the present work. In previous studies the effect of flowrate has not been reported and this has been found to be an important parameter. Saturation of the dealumination reaction was observed above ca. 150 mm Hg. Above this water concentration no further effect of partial pressure on subsequent catalytic activity was observed.

The effect of steaming on the activity of a silicalite coated catalyst was also investigated. While the unsteamed version of this catalyst had comparable activity to that of unmodified ZSM-5. It was proposed that the highly hydrophobic nature of the external surface of the silicalite coated catalyst results in coulombic interaction effects. In comparison film resistances are insignificant and consequently steaming flowrate no longer plays an important role.

Characterization studies showed that at the steaming conditions used in this study, the physical characteristics of the ZSM-5 catalyst are hardly affected. This was reflected by only very small changes in crystallinity, surface area and hexane adsorption capacity. Although altered acidity is thought to be responsible for enhanced activity, attempts to clarify the exact nature of the site responsible for enhanced activity by ammonia TPD and pyridine desorption IR were unsuccessful. On the basis of Lewis/Bronsted acid site ratios determined from IR studies, however, it was suggested that a specific Lewis site may be created during steaming which can significantly affect catalytic activity. This may well be the extra-framework Al hydroxy complex proposed by other workers in hexane cracking studies.

Appendices

APPENDIX 1

Na, B, Al concentrations from AA

Catalyst : ZSM-5 (Si/Al = 41, 3 day synthesis)

Before exchange :

mass catalyst dissolved	= 0.1824 g. cat.
volume of flask	= 50 ml
Na conc. (from AA)	= 34.3 μg/ml
	(= 34.3 ppm)

so : wt% Na = 34.3×10^{-6} g/ml x 50 ml / 0.1824 g. cat. x 100
= 0.940 wt% Na

After exchange:

mass catalyst dissolved	= 0.2122 g. cat.
volume of flask	= 250 ml
Na conc. (from AA)	= 0.2 μg/ml

so : wt% Na = 0.2×10^{-6} g/ml x 250 ml / 0.2122 g. cat. x 100
= 0.024 wt% Na

and % exchange = (0.94 - 0.024)/0.94 x 100
= 97% exchanged

Boron concentration from AA

catalyst: Boralite/NH_4F

mass of catalyst dissolved	= 0.5244 g. cat.
volume of flask	= 50 ml

Boron conc. determined by AA = 145 μg/ml

so : wt% boron = 145 x 10^{-6} g/ml x 50 ml/0.5244 g. cat. x 100
= 1.38 wt% B

Al concentration from AA

catalyst: Boralite/NH_4F

mass of catalyst dissolved = 1.4635 g. cat. x 100
volume of flask = 50 ml
Al conc. determined from AA = 3 μg

so: wt% Al = 3 x 10^{-6} g/ml x 50 ml/1.4635 g. cat. x 100
= 0.0102 wt% Al
= (102 ppm)

APPENDIX 2

Calibration of the steaming saturators

This calibration was carried out to check that the apparatus was working correctly. Ideally the calibration curve for the apparatus (a plot of saturator (2nd stage) temperature vs. H_2O content in the N_2 stream) should match known vapour pressure data for N_2 saturated with water at different temperatures. Calibration was performed by connecting the apparatus to a dry-ice/acetone trap and a wetgas flowmeter. In this way the amount of water in the N_2 stream (set at 60 ml/min) could be trapped and weighed while the corresponding amount of N_2 (dry) could be measured for different saturator temperatures. A sample calculation is given below.

Saturator temperature (2nd stage)	= 52 °C
Initial WGFM reading	= 725.4
Final WGFM reading	= 728.6
Mass of trap before i.e. empty	= 143.64
Mass of trap containing condensed H_2O	= 143.98
Temperature of WGFM	= 20 °C
Correction factor, Cf, for WGFM	= 0.975 (see Appendix 4)

so mass of water = 0.34 g
≡ 0.0189 moles H_2O

now using PV	= ZnRT for the dry N_2 stream
where Z	= 1.00 for N_2 at 1 atm and 20 °C
V	= Cf x (WGFM2 - WGFM1) litres
P	= 1 atm
T	= (273 + 20)K
R	= 0.082 atm-l.K^{-1}

then moles dry N_2 = n = PV/(ZRT)
= (1 x 0.975 x (728.6-725.4))/(1 x 0.082 x 293)
= 0.1298 moles dry N_2

and now partial pressure H_2O (mm Hg)

$$= \text{moles } H_2O/(\text{moles } H_2O + \text{moles } N_2) \times 760$$
$$= 0.0189/(0.0189 + 0.1298) \times 760 \text{ mm Hg}$$
$$= 97 \text{ mm Hg}$$

Water concentrations as a function of a number of different saturator temperatures were calculated in the same manner:

Saturator Temperature °C		Mass H_2O g	WGFM-WGFM1 l	p.p. H_2O mm Hg
41		0.42	7.6	53
52		0.34	3.2	97
52	(repeat)	0.34	3.2	97
61		1.79	10.8	140
70		1.86	6.35	217
79		2.48	4.15	341

APPENDIX 3

Calculation of average molecular mass of gas

The average molecular mass of the exit gas propene oligomerization is calculated from the analysis of the gas as determined by the GOWMAC GC. An analysis for a sample taken from a ZSM-5 catalyst (Si/Al = 41, synthesis time = 3 days) running at ~ 270 °C and 95% conversion is shown below.

Basis : 100 g

Component	Mass g	Molar Mass g/gmol	Moles (= mass/molar mass)
methane	0.012	16.04	0.0007
ethane	1.389	30.07	0.0462
propane	77.10	44.1	1.7483
propene	13.58	42.08	0.3227
iso-butane	2.536	58.12	0.0436
n-butane	1.405	58.12	0.0242
n-butene	0.376	56.1	0.0067
iso-butene	0.688	56.1	0.0123
trans-2-butene	0.945	56.1	0.0168
cis-2-butene	0.617	72.15	0.0086
pentanes	1.352	72.15	0.0187
			Σ = 2.2488

So the average molecular mass = mass/Σ moles
= 100/2.2488
= 44.47 g/mol

Table

Name	Mass	RT	Area	BC	RF
methane	0.012	3.62	223	01	1.058
ethane	1.389	4.46	25955	01	1.024
propane	77.1	6.39	1475275	08	1.
propene	13.58	7.58	267611	05	0.971
iso-butene	2.536	10.09	54569	01	0.889
n-butane	1.405	11.49	26155	01	1.028
n-butene	0.376	14.79	6807	01	1.056
iso-butene	0.688	16.74	13151	02	1.002
T-2-butene	0.945	17.91	18193	02	0.994
C-2-butene	0.617	19.3	11462	02	1.029
C-5	1.093	21.38	20912	03	1.
N-pentane	0.259	24.36	4964	01	1.
Totals	100.		1925277		

APPENDIX 4

Calibration of the wet gas flowmeter

It is necessary to calibrate the flowmeters since they are often slightly inaccurate. The flowmeters are calibrated by allowing a known mass of the feed mix to flow through the flowmeter, the readings on the flowmeter can then be taken. Using the ideal gas law with a compressibility factor (Z) then enables the known mass to be converted to a known volume. This volume can then be compared to that given by the flowmeter. If this process is repeated a number of times, a straight line correlation relating the true volume. V_t, to the flowmeter volume, V_{fl} can be made. Calculations are shown below.

For a propene/propane/ethane feed with a composition as follows:

ethane	= 0.201
propene	= 86.696
propane	= 13.103

then from the procedure in Appendix 3:

molecular mass	= 43.81 g/gmol
and Z	= 0.984
at 1 atmosphere : R	= 0.082 atm. l/k/mol
and T (WGFM)	= 28 °C
and so rearranging PV	= ZnRT
gives V	= ZnRT/P
	= $(0.984 \times 0.082 \times 301/1)^{xn}$
	= 24.287 x mass/molecular mass
	= 24.287 x mass/43.81
	= (0.5544 x mass) litres

Then:

Feed Cylinder mass, g	D (Mass) g	V_t l	WGFM l	V_{fl} l
6594.3			3293.9	
6543.5	50.8	28.2	3323.9	30
6491.4	52.1	28.9	3354.6	30.7
6437.7	53.7	29.8	3386.2	31.6

Now correlating V_t and V_{fl} by drawing a straight line through the origin gives:

$V_t = M \times V_{fl}$

or $V_t = C_f \times V_{fl}$, where C_f the correction factor is the slope of the line plotted

and so: $V_t = 0.942 \times V_{fl}$

with a regression coefficient of 0.999997

APPENDIX 5

Calculation of Compressibility Factors

Compressibility factors were calculated using the method outlined by Himmelblau (1982) i.e. calculating compressibility factors from generalized compressibility charts, although the algorithm presented by Smith and van Ness (1983) can also be used. A sample calculation will be shown for the feed mixture composition presented below.

Component	MW	Mass %	Mole %	T_c (K)	P_c (atm)	T_r	P_r	Z
ethane	30.07	0.201	0.28	305.4	48.2	0.976	5.8×10^{-5}	1.0
propane	44.09	13.103	12.57	369.9	42.0	0.806	3×10^{-3}	0.99
propene	42.08	86.696	87.1	365.1	45.4	0.816	1.92×10^{-2}	0.98

The method outlined by Himmelblau requires that the critical temperatures and pressures of the components in the gas stream be known. Values for T_c and P_c were obtained from Table D1 in Himmelblau (1982). The reduced temperatures and pressures can then be calculated from the expressions:

$$T_r = T/T_c$$

$$P_r = p_A/P_c \text{ - (assuming Dalton's law of partial pressures)}$$

where T is the temperature of the exit gas stream (298 K and p_A is the partial pressure of component A and is given by P x y_A where y_A is the mole fraction of component A and P is the exit gas pressure, i.e. 1 atm.

Knowing T_r and P_r, the compressibility factor, Z, for each component can be calculated from generalized compressibility charts.

The mean compressibility factor can now be calculated from

$Z_m = \Sigma Z_i Y_i$ where Z_i and Y_i are the compressibility and mole fractions for each component

so then Z_m for the above mixture is:

$$Z_m = 0.0028 \times 1 + 0.1257 \times 0.99 \times 0.871 \times 0.98$$
$$= 0.981$$

APPENDIX 6

Propene oligomerization data work-up

The following is a sample calculation of conversion of a ZSM-5 catalyst of Si/Al = 41 after 21.5 hours on stream at a temperature of 270 °C.

Data collected:

Run Time	= 21.5 hours	
WGFM1	= 13513.8	(taken at t = 20.5 hours)
WGFM2	= 13515.9	
Temperature of WGFM	= 19 °C	
Pump setting	= 5.0	
Mass of catalyst	= 1.9727 g	
Pressure	= 5 MPa (= 50 atm)	
Reactor setpoint	= 205 °C	
Reactor bed temperatures	= (Top) = 270 °C	
	= (bottom) = 255 °C	
mass of liquid collected in this hour	= 18.827 g	
From Appendix 3: Average molecular mass of gas	= 44.47 g /gmol	
From procedure in Appendix 5	= Z = 0.98	
and the calibration factor for the wetgas flowmeter at this stage was C_f	= 0.975	
so V	= 0.975 x (13515.9 - 13513.8)/1.0	
	= 2.048	
now mass of gas	= 12.187 x 2.048 x 44.47/(0.98 x (292))	
	= 3.88	

and the % dissolved gases in this liquid was 0.935%

so : $\underline{L_t = 18.651\ g}$

and A = 18.651/1.9727
= 9.45

and WHSV = (18.8271/1 + 3.88)/1.9727
= 11.51

and so conversion based on total feed,

Co = 9.45/11.51 x 100
= 82.10

and on the basis of 86.7% propene as feed (see Appendix 5)

Conversion = 82.10/0.867
= 95% conversion

APPENDIX 7

Ortho-xylene isomerization

A G.C. trace obtained over modified ZSM-5 (Si/Al = 42, phosphorus included in the synthesis mixture) is shown below:

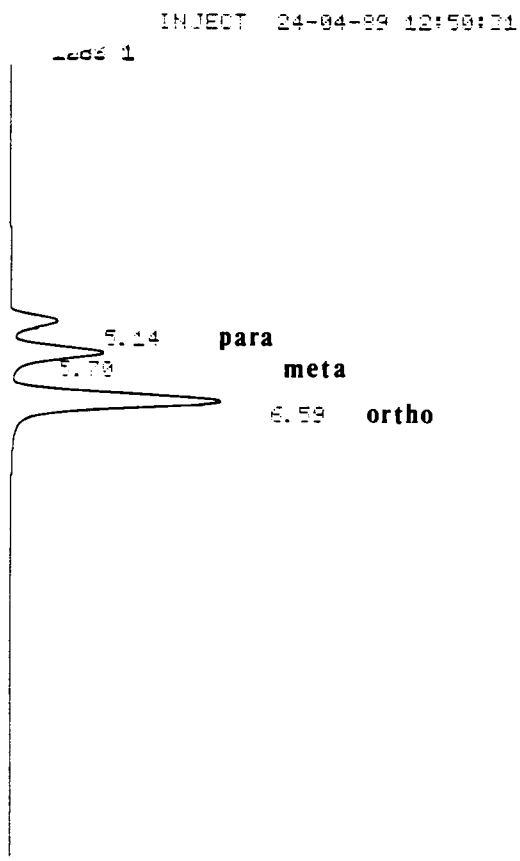

24-04-99 12:50:21 CH= "B" PG= 1.

FILE 1. METHOD 0. RUN 87 INDEX 87

ANALYST: W PW=10

PEAK#	AREA%	RT	AREA BC
1	11.765	5.14	174027 00
2	25.528	6.7	377613 00
3	62.709	6.59	927592 01
TTL	100.		1479232

Xylene isomerization over ZP[1]-1

The following data were collected:

Reactor Bed Temperature	=	349 °C
Ambient Temperature	=	19 °C
Cooling Water Temperature	=	19 °C
Flowrate	=	382 ml/min ≡ 22.92 l/hr
Mass of catalyst	=	0.599

Now, from the expression used by Stuckey and Saylor (1940):

P_o $= 10^{(-2908.07/292 - 5 \log 292 + 22.95279)}$

$= 4.642$ mm Hg $\equiv 6.107 \times 10^{-3}$ atm

and N_o $= P_o\ V/(R\ Ta)$

$= 6.107 \times 10^{-3} \times 22.92/(0.082 \times 292)$

$= 5.846 \times 10^{-3}$ moles/hr

and from the expression shown in Section 2.5.2.2

M_o $= 106.17 \times N_o$

$= 0.621$ g o-xylene/hr

and WHSV $= 0.62/0.599$

$= 1.036$

At this feedrate the conversion of o-xylene is calculated from the G.C. trace.

% conversion $= 100 - 62.708$

$= 37.29$

$\sim 37.3\%$

and % p-xylene in product ~ 11.8%

Plotting % o-xylene conversion versus % p-xylene in product at different WHSV results in a curve of the type shown below. Since selectivity to para-xylene can be expressed as the amount of para-xylene to the amount of o-xylene converted the shape of the curve shown below is an indication of the selectivity of the catalyst to para-xylene. The further the curve shifts upwards as shown by the direction of the arrow, the greater the selectivity of the catalyst.

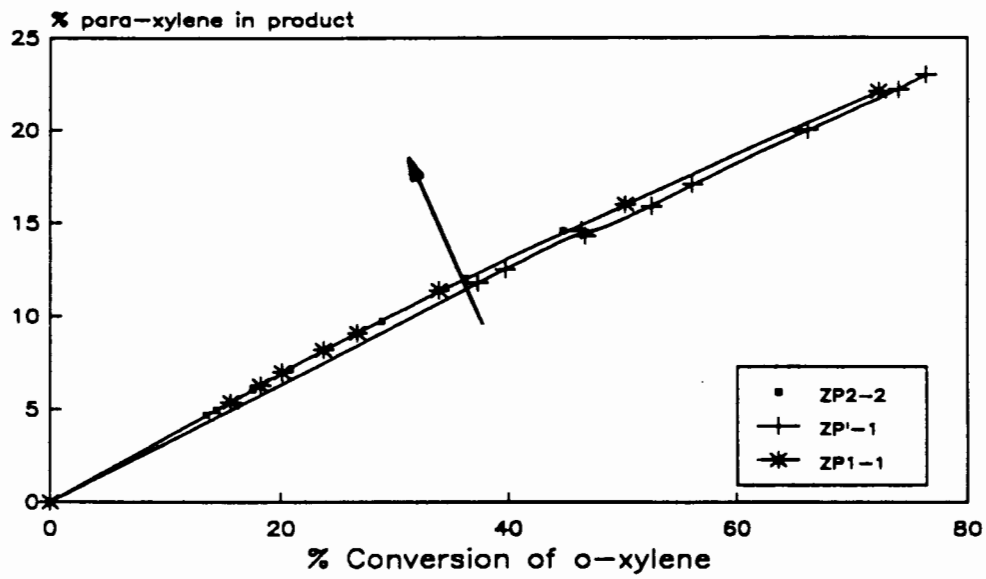

Shape selectivity as determined by xylene isomerization

APPENDIX 8

Cetane number distribution

A sample calculation for the determination of a cetane number for an unmodified ZSM-5 catalyst of Si/Al = 41 reacting at temperatures between 220 °C and 290 °C. Areas are obtained by integrating the areas under the curve for the relevant scan ranges.

H group	Scan Range (ppm)	Integrated area, A.U.	Normalized area, %
H_3	0.5 - 1.06	84.5	49.27
H_2	1.06 - 1.8	83.5	48.69
H	1.8 - 4.0	3.5	2.04
H_a	6.5 - 7.05	0	-
H_d	7.05 - 9.0	0	-
		Σ = 171.5	Σ = 100

A.U. = arbitrary units

and then using the Gautier correlation (Gautier, 1988)

$$\text{C.N.} = -0.0571\,H_3 + 0.935\,H_2 - 0.454\,H - 0.718\,Ha + 0.102\,Hd$$
$$= -0.0571 \times 49.27 + 0.935 \times 48.69 - 0.454 \times 2.04$$
$$= 41.8$$

APPENDIX 9

Determination of Bronsted and Lewis acid site concentrations

From the integrated form of the Beer-Lambert law:

$$B = (cl)\ E_\nu^{(a)}\, d\nu \qquad (1)$$

where B is the integrated absorbance, cm^{-1}
(cl) is the concentration of adsorbate expressed
as micromoles per square centimetre of wafer cross-section

$E_\nu^{(a)}$ is the apparent molar extinction coefficient at wavenumber v
and $E_\nu^{(a)}\, d\nu$ = 0.4343 x apparent integrated absorption intensity

and from Hughes and White (1967)

for the Bronsted band at 1540 cm^{-1} (pyridine ads)
for zeolite Y $(NH_4)^+$:
the apparent integrated absorption intensity = 3.03 cm/μ mole

for the Lewis band at 1450 cm^{-1} (pyridine ads.)
for Al - 600:
the apparent integrated absorption intensity = 3.26 cm/μ mole

so for BPy:

$$E_\nu^{(a)}\, d\nu = 0.4343 \times 3.03 = 1.32$$

and rearranging equation (1) and converting the units and knowing the wafer surface area to be 1.327 cm^2

then concentration (BPy) = B/wafer mass x 1.005 x 10^{-3}
where concentration is in moles /g. catalyst
and wafer mass is in mg
and B is the integrated area shown in the figure below

Similarly for LPy:

$$E_V^{(a)}\, dv = 0.4343 \times 3.26 = 1.42$$

again knowing the wafer surface area = 1.327 cm^2 and rearranging equation (1) and converting the units gives

concentration (LPy) = B/wafer mass x 9.35 x 9.35 x 10^{-4}

and for the example in the figure (S-300-78-2-30)

B (BPy) = 3.159
B (LPy) = 0.773
and wafer mass = 10.8 mg

and so BPy = 2.94 x 10^{-4} moles /g. cat
LPy = 6.69 x 10^{-5} moles /g. cat

APPENDIX 10

Calculation of Reynold's number for a look at bulk diffusion

If reactor conditions are

reactor temperature	= 500 °C
flowrate	= 30 ml/min wet N_2 stream
partial pressure	= 78 mm Hg
	≡ 0.1 atm

At this low partial pressure one can assume that the properties of wet N_2 are approximately the same as those of air

$$Re = \frac{\rho d_p u}{\mu}$$, $\rho u = G$ = superficial mass flow, $kg/m^2/5$

where Re - the Reynolds number
d_p - the particle diameter ≡ 2.5 μm
u - the linear velocity through the bed
ρ - the fluid density , kg/m^3
μ - the fluid viscosity, Pa.S

From the ideal gas law and V = 30 ml/min
≡ $30 \times 1/1000 \times 1/60$
= 5×10^{-4} l/s

and PV = nRT , R = gas constant = 0.082

so n = PV/RT; P = 1 atm., T = Temp at which V is measured, i.e. 298 K

therefore n = $1 \times 5 \times 10^{-4}/0.082/298$
= 2.05×10^{-5} moles wet N_2 /minute

since partial pressure (H_2O) = 0.1

the average M.W. of this stream is

MWav. = $0.9 \times MW_2 + 0.1$ MN water
= $0.9 \times 28 + 0.1 \times 18$
= 27 g/mol

so mass flow of wet N_2 stream = $27 \times 2.05 \times 10^{-5}$
= 5.554×10^{-4} g/s
= 5.554×10^{-2} kg/s

Cross sectional area of reactor = $\pi \times 0.009^2$
= 2.54×10^{-4} m^2

so superficial mass velocity = mass flow/cross-sectional area
= $5.554 \times 10^{-7} / 2.54 \times 10^{-4}$
= 2.19×10^{-3} $kg.m^{-2}\ s^{-1}$

d_p = catalyst particle diameter = 2.5×10^{-6} m

Assuming properties of wet nitrogen stream are similar to air then: μ air (480 °C) ≡ μ wet stream (500 °C)

μ air (480 °C) = 3.72×10^{-5} Pa.s

and Re = d_pG/μ = $2 \times 10^{-6} \times 2.19 \times 10^{-3} / 3.7 \times 10^{-5}$

= $\underline{1.18 \times 10^{-4}}$ at 30 ml/min, 500 °C, 78 mm Hg p.p.

If the flow rate is doubled to <u>60 ml/min</u>

then : Re = $\underline{2.36 \times 10^{-4}}$

APPENDIX 11

CATALYST CODING

APPENDIX 11

CATALYST CODING

Boralite Catalysts

Catalysts coded as B - m (-O)

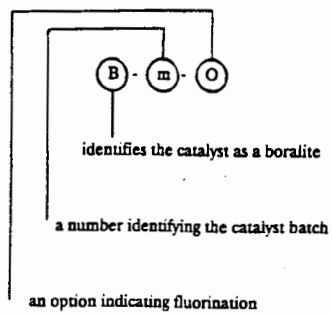

where O = HF
= $HF\text{-}NH_4F$
NH_4F according to fluorination

Boron Impregnated Catalysts

Catalysts coded as Z B - m

where z - indicates the catalyst is a ZSM-5 of Si/Al ~ 40, μ = 2-3 microns
B - indicates Boron impregnation
m - indicates impregnation method
= "imp" : incipient wetness impregnation
= wash : incipient wetness impregnation followed by washing
= relf : impregnation with an H_3BO_3 solution heated under reflux

Phosphorus Modified Catalysts

Catalysts coded as ZP-M

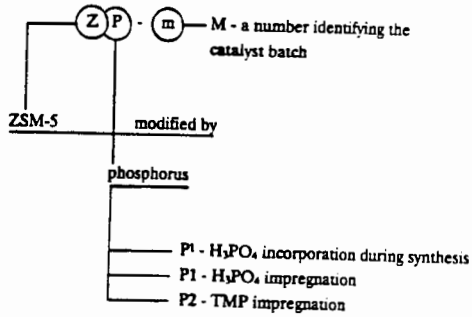

Steam Dealuminated Catalysts

Catalysts coded as S - T - p - t - f

S - T - p - t - f

indicates a steamed ZSM-5 of Si/Al ~ 40
and av. crystallite size of ~ 2-3 μ

T - steaming temperature, °C
P - water partial pressure, mm Hg
t - steaming time, hrs
F - steaming flowrate, ml/min

APPENDIX 12

X-ray diffraction data

Table ΣT values for some boralite and silicalite catalysts compared to ZSM-5

Catalyst	ΣT
ZSM-5	7.8706
silicalite	7.8757
B-1	7.8616
B-2-HF-NH_4F	7.8673
B-3-NH_4F	7.8629

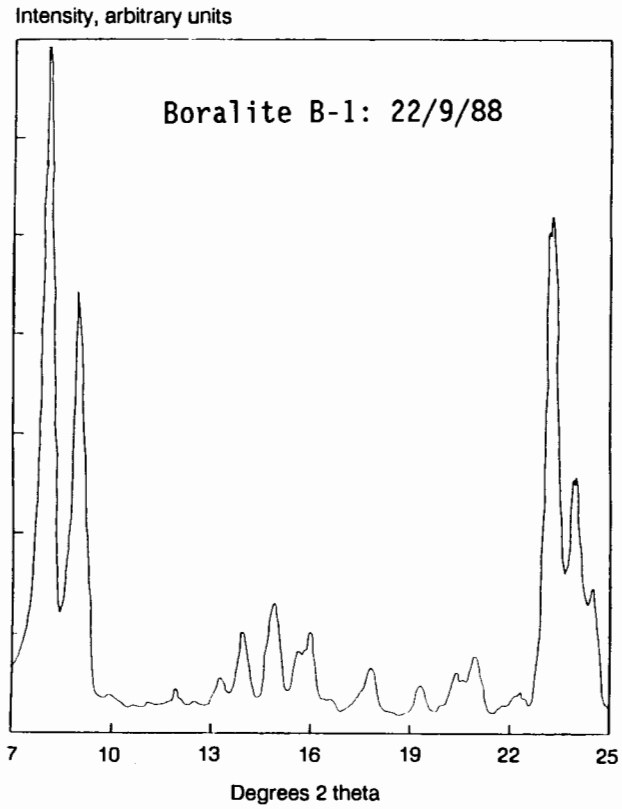

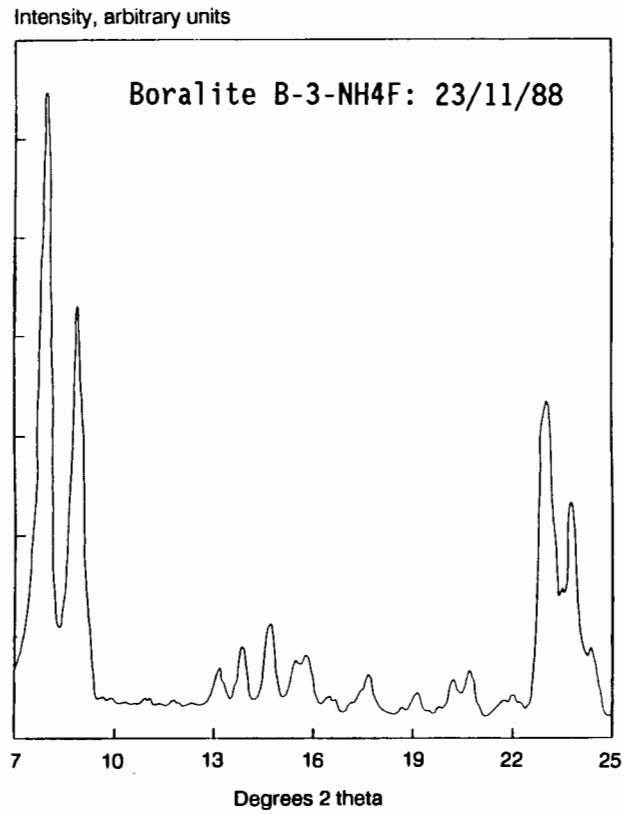
Intensity, arbitrary units
Boralite B-3-NH4F: 23/11/88
7
10
13
16
19
22
25
Degrees 2 theta

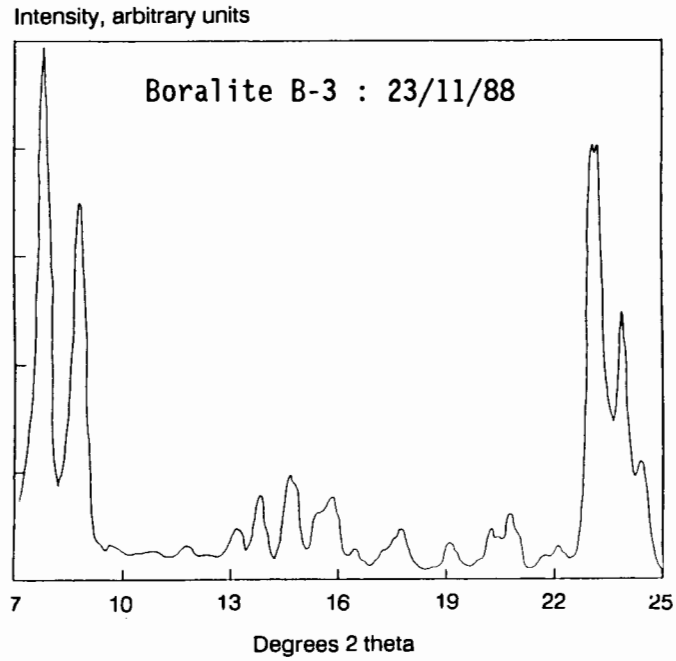
Intensity, arbitrary units
Boralite B-3 : 23/11/88
7
10
13
16
19
22
25
Degrees 2 theta

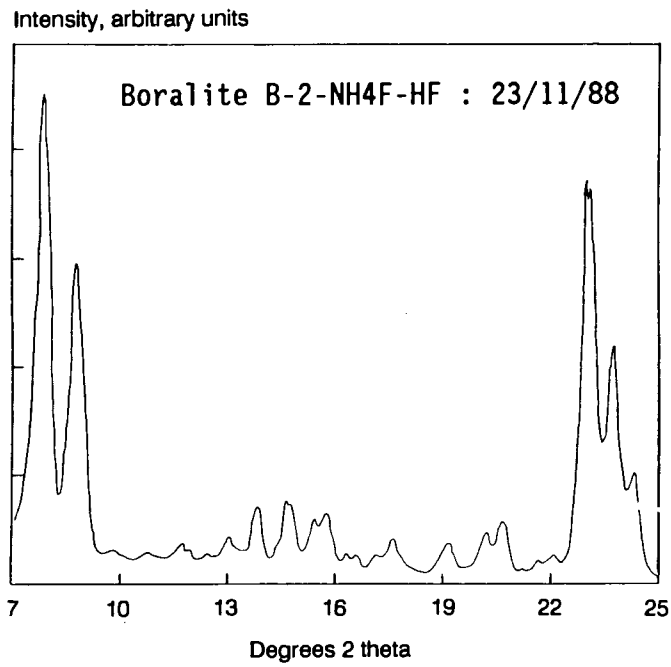
Intensity, arbitrary units
Boralite B-2-NH4F-HF : 23/11/88
7
10
13
16
19
22
25
Degrees 2 theta

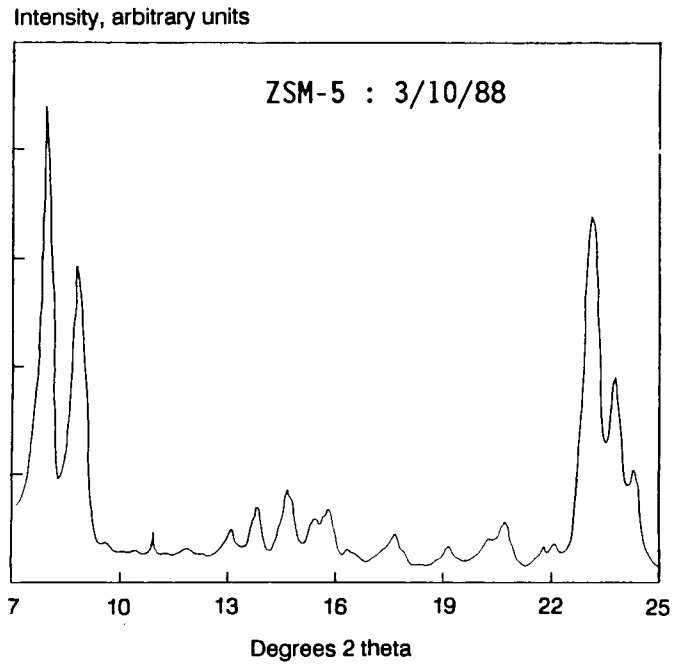
Intensity, arbitrary units
ZSM-5 : 3/10/88
7
10
13
16
19
22
25
Degrees 2 theta

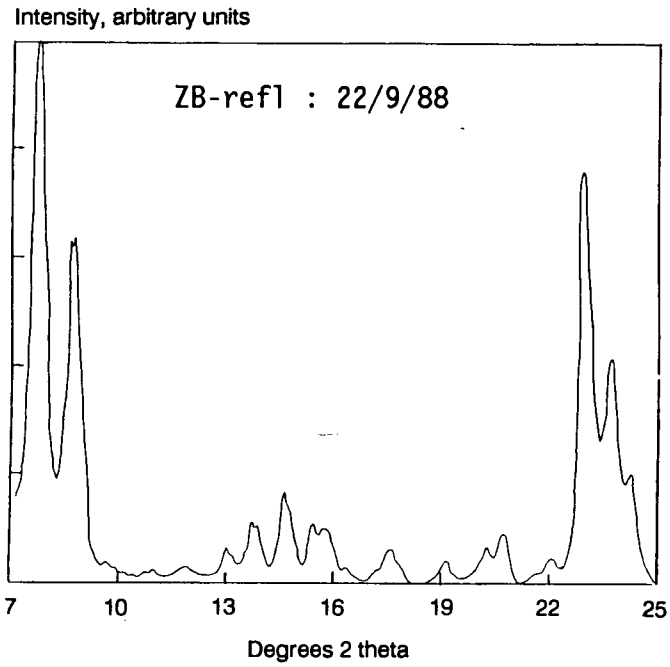
Intensity, arbitrary units
ZB-refl : 22/9/88
7
10
13
16
19
22
25
Degrees 2 theta

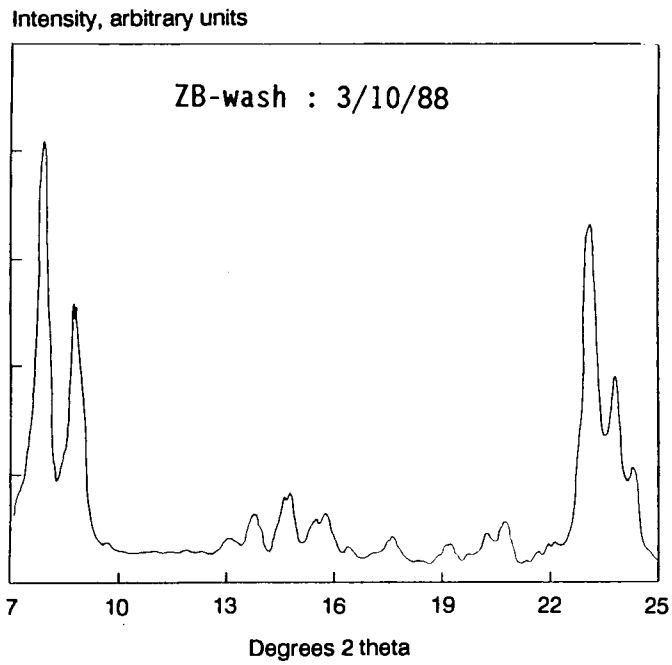
Intensity, arbitrary units
ZB-wash : 3/10/88
7
10
13
16
19
22
25
Degrees 2 theta

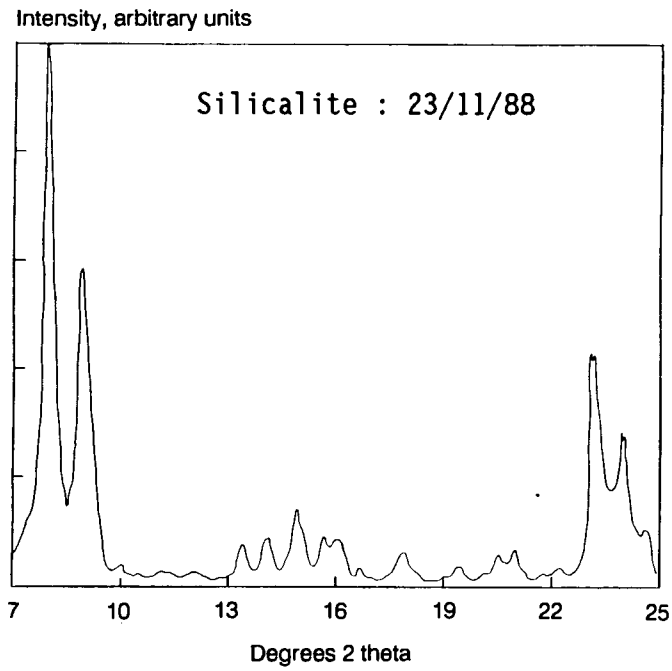
Intensity, arbitrary units
Silicalite : 23/11/88
7
10
13
16
19
22
25
Degrees 2 theta

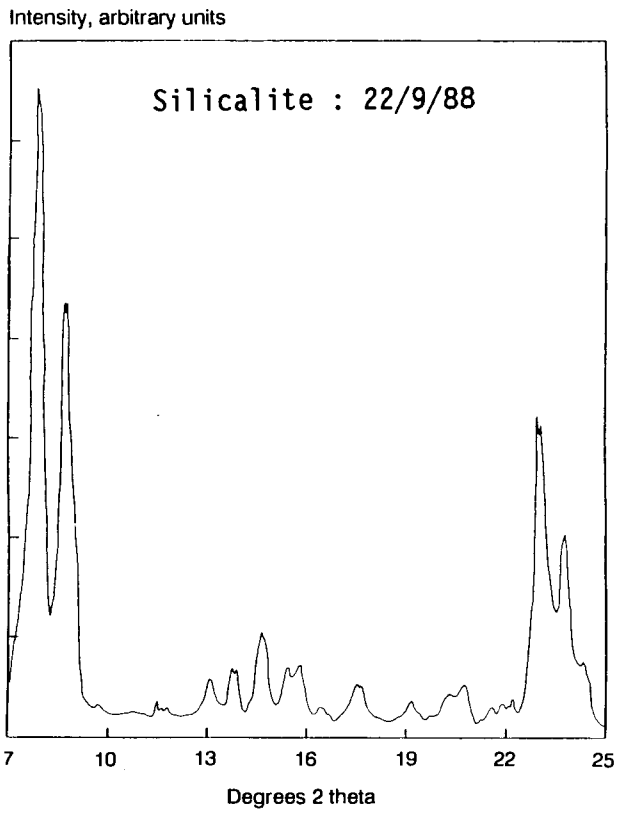
Intensity, arbitrary units
Silicalite : 22/9/88
7
10
13
16
19
22
25
Degrees 2 theta

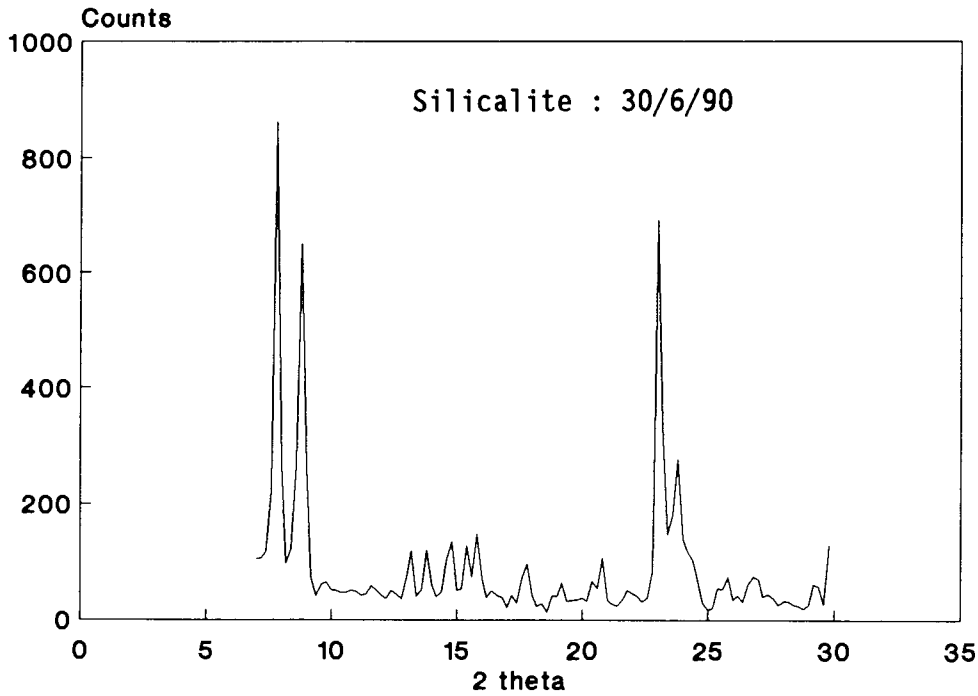
Counts
1000
800
600
400
200
0
Silicalite : 30/6/90
0
5
10
15
20
25
30
35
2 theta

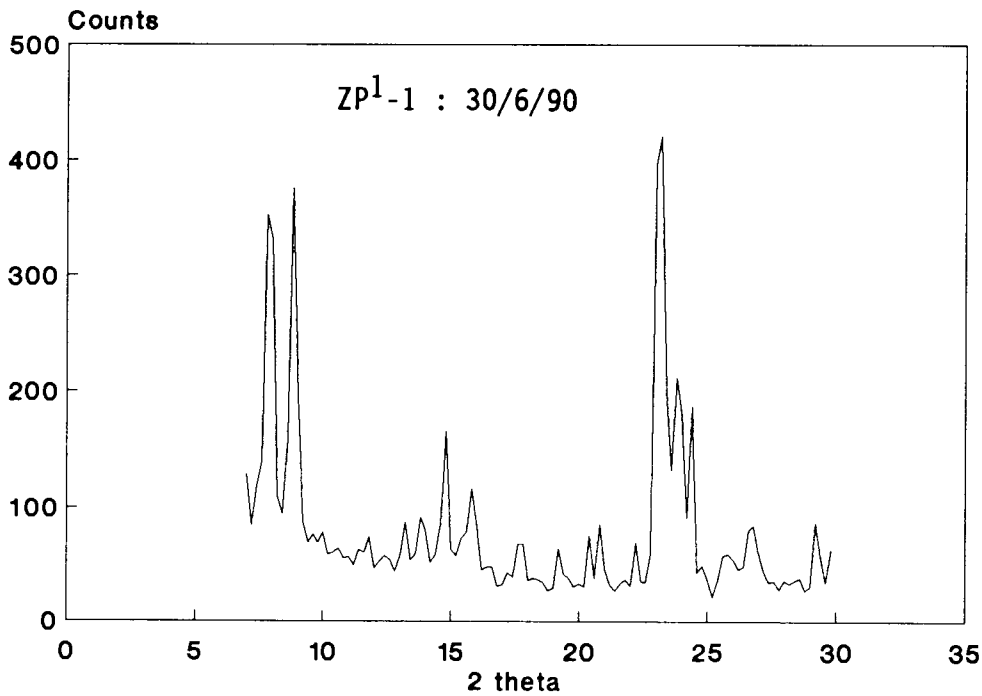
Counts
500
400
300
200
100
0
ZP1-1 : 30/6/90
0
5
10
15
20
25
30
35
2 theta

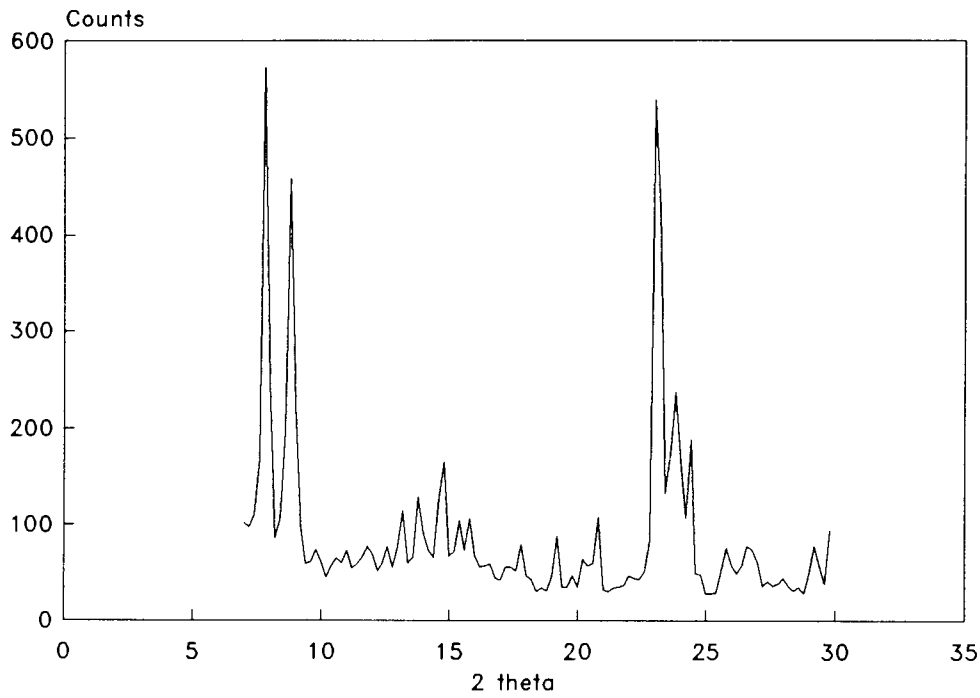
Counts
600
500
400
300
200
100
0
0
5
10
15
20
25
30
35
2 theta

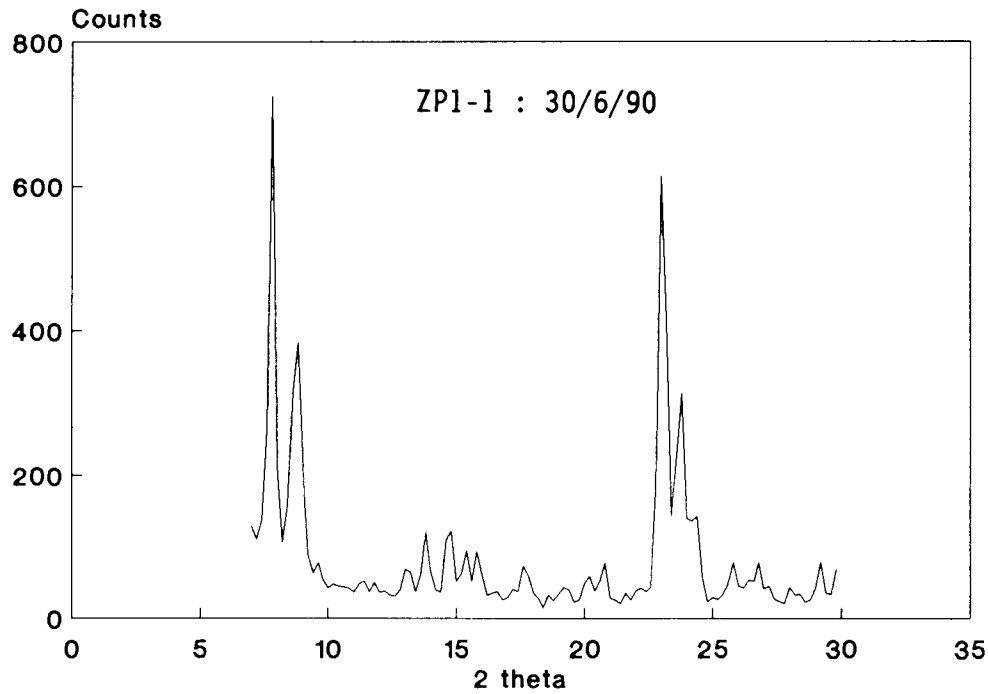
Counts
800
600
400
200
0
ZP1-1 : 30/6/90
0
5
10
15
20
25
30
35
2 theta

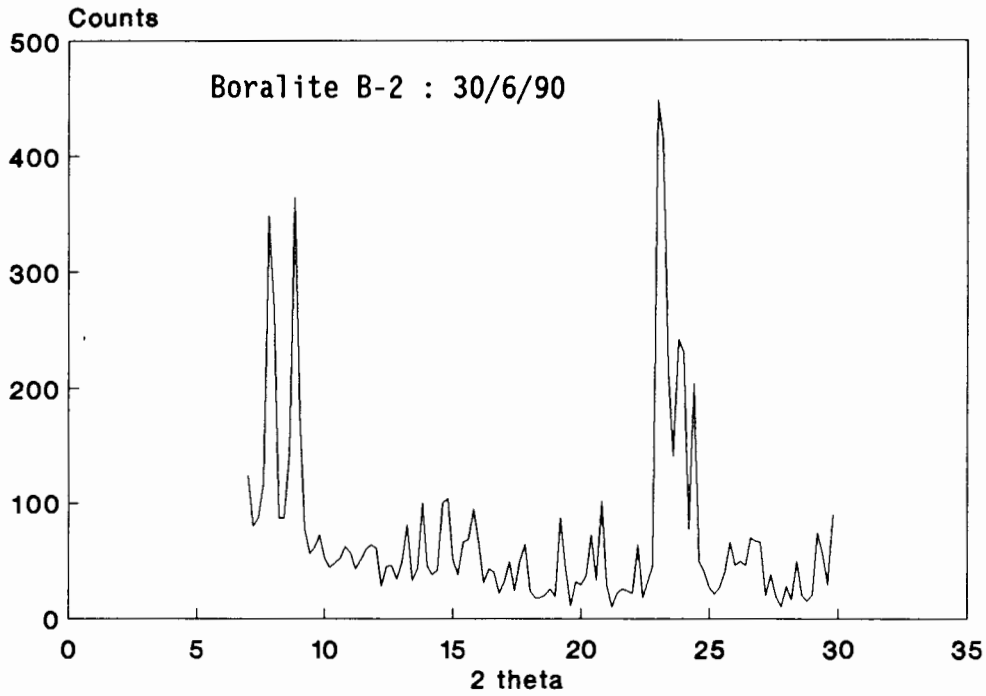
Counts
Boralite B-2 : 30/6/90
500
400
300
200
100
0
0
5
10
15
20
25
30
35
2 theta

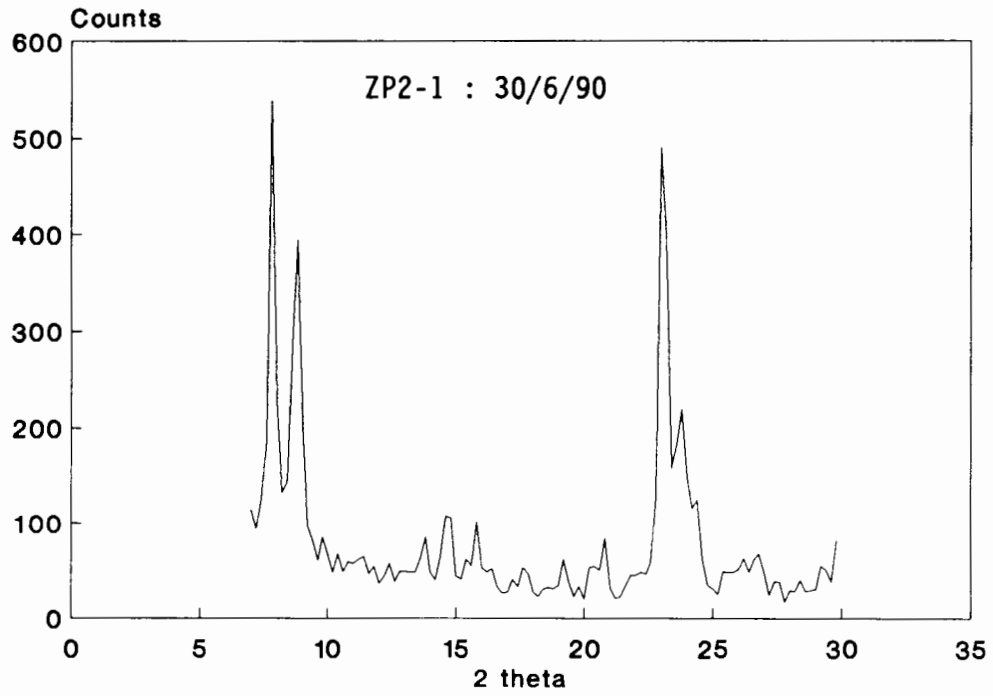
Counts
ZP2-1 : 30/6/90
600
500
400
300
200
100
0
0
5
10
15
20
25
30
35
2 theta

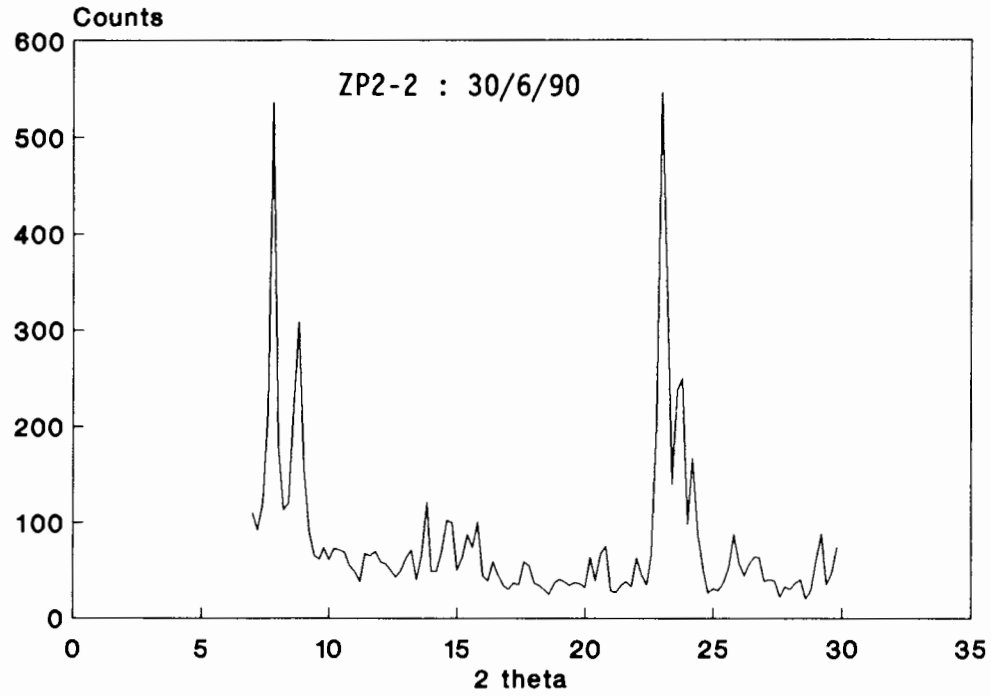
Counts
ZP2-2 : 30/6/90
600
500
400
300
200
100
0
0
5
10
15
20
25
30
35
2 theta

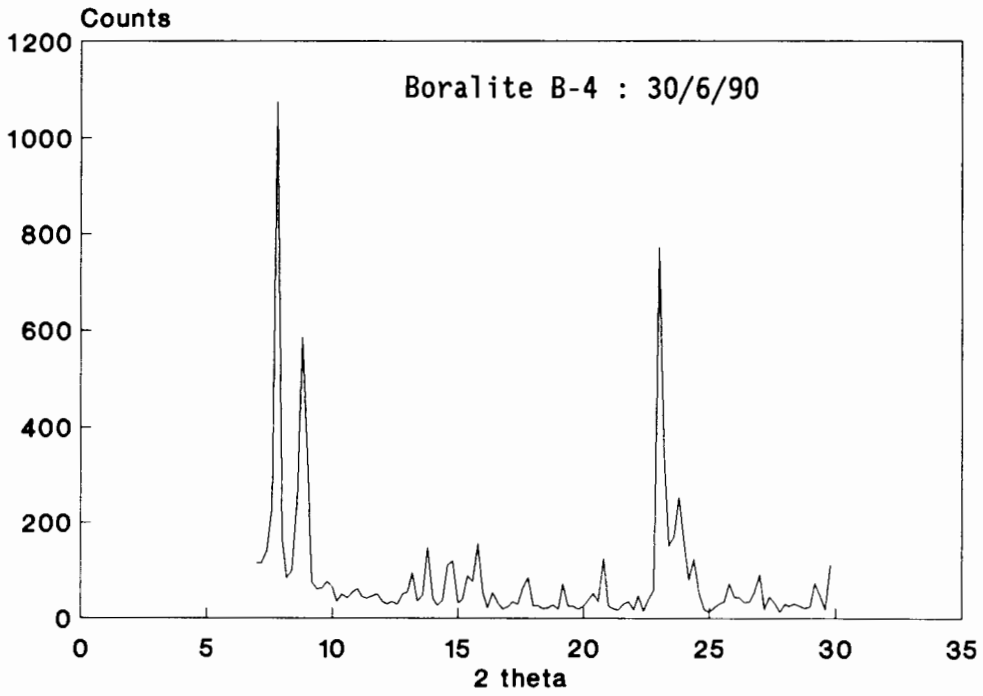
Counts
Boralite B-4 : 30/6/90
1200
1000
800
600
400
200
0
0
5
10
15
20
25
30
35
2 theta

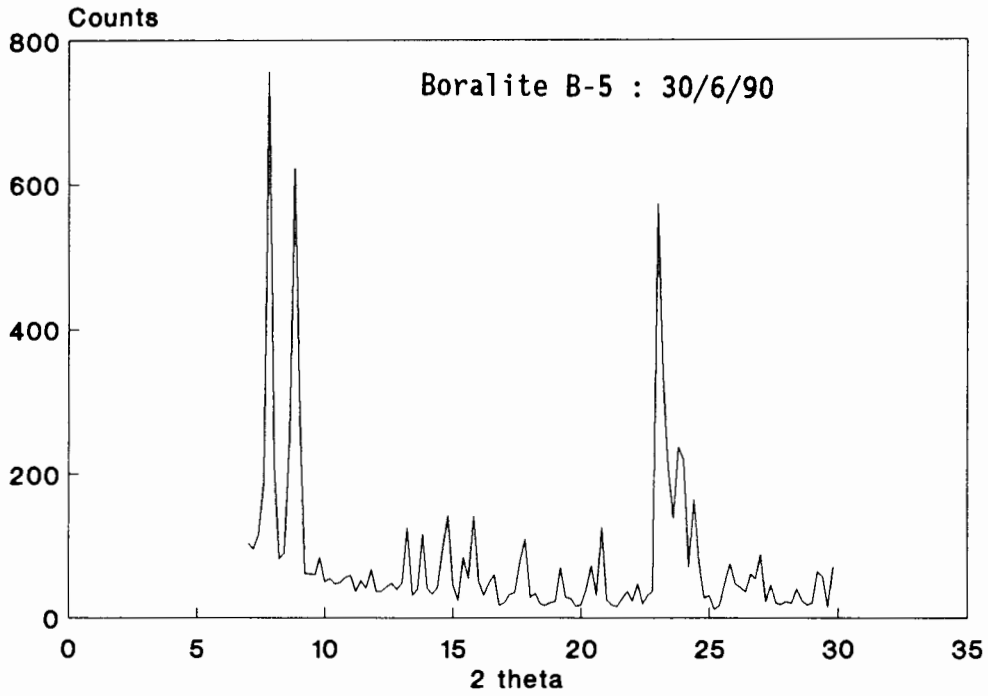
Counts
800
600
400
200
0
Boralite B-5 : 30/6/90
0
5
10
15
20
25
30
35
2 theta

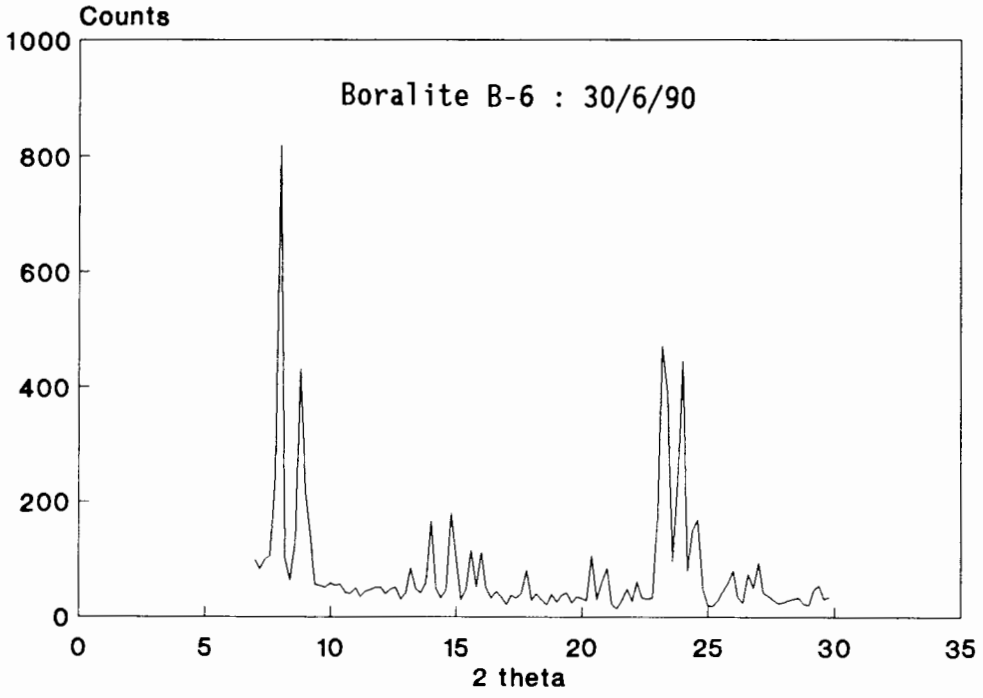
Counts
1000
800
600
400
200
0
Boralite B-6 : 30/6/90
0
5
10
15
20
25
30
35
2 theta

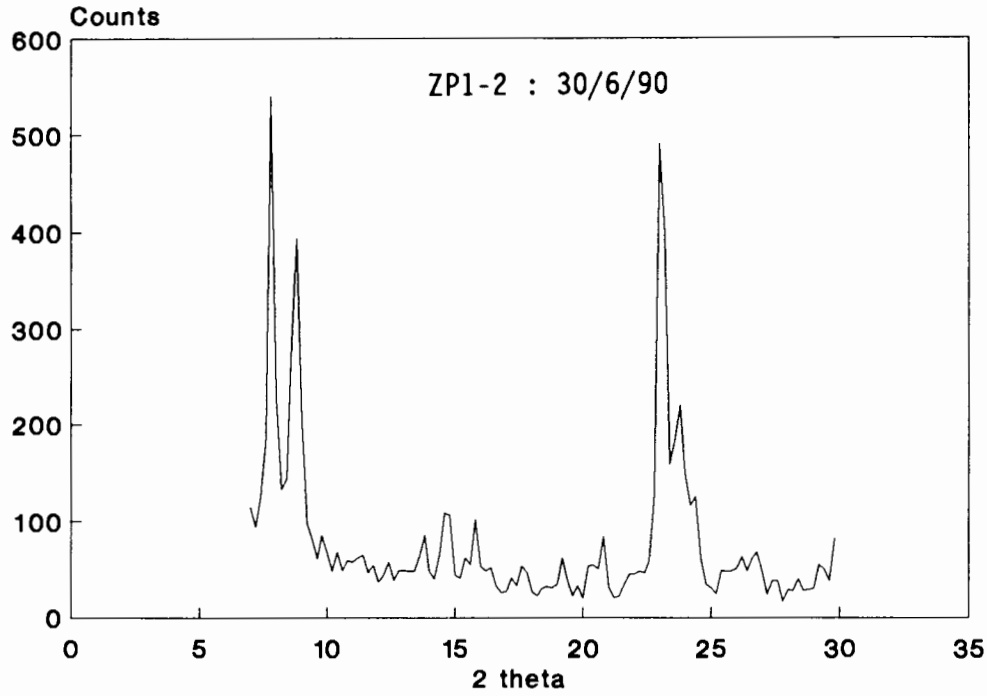
Counts
ZP1-2 : 30/6/90
600
500
400
300
200
100
0
0
5
10
15
20
25
30
35
2 theta

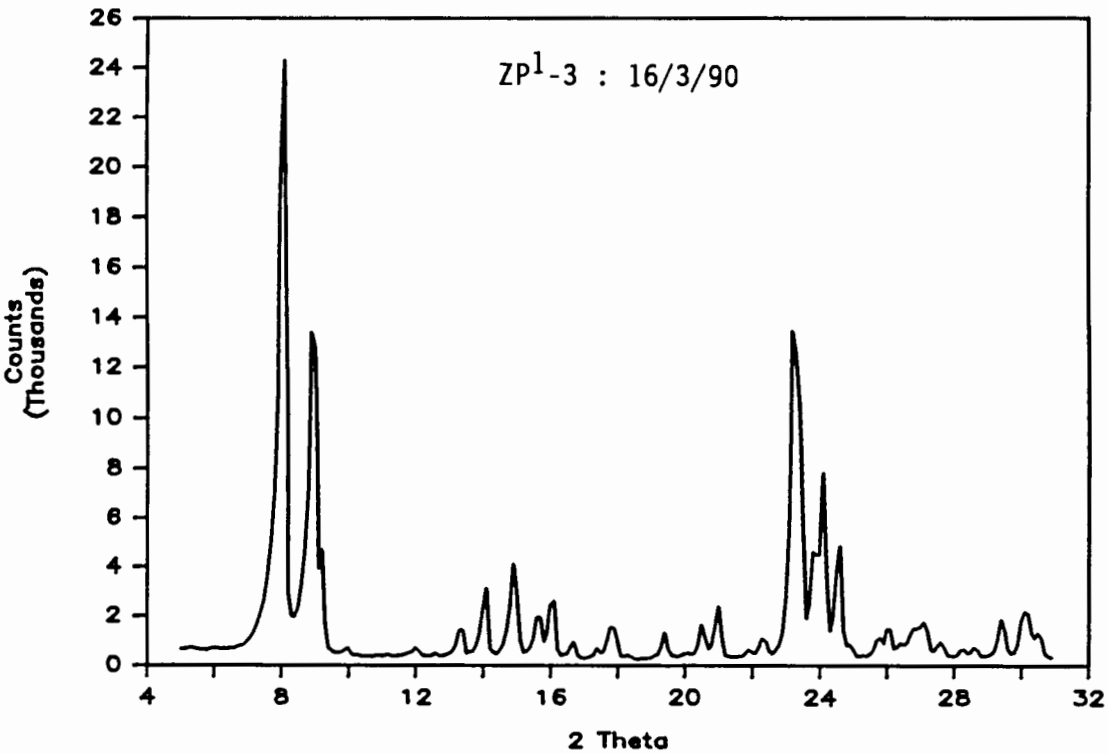
ZP1-3 : 16/3/90
Counts (Thousands)
26
24
22
20
18
16
14
12
10
8
6
4
2
0
4
8
12
16
20
24
28
32
2 Theta

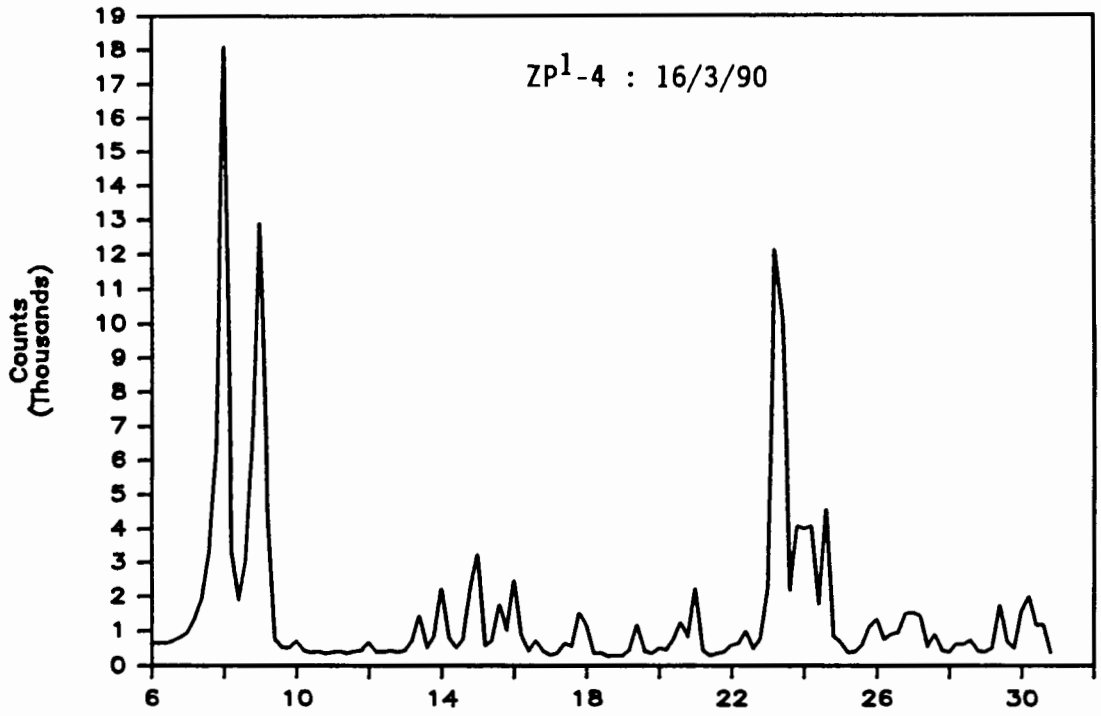
ZP1-4 : 16/3/90
Counts (Thousands)
0
1
2
3
4
5
6
7
8
9
10
11
12
13
14
15
16
17
18
19
6
10
14
18
22
26
30

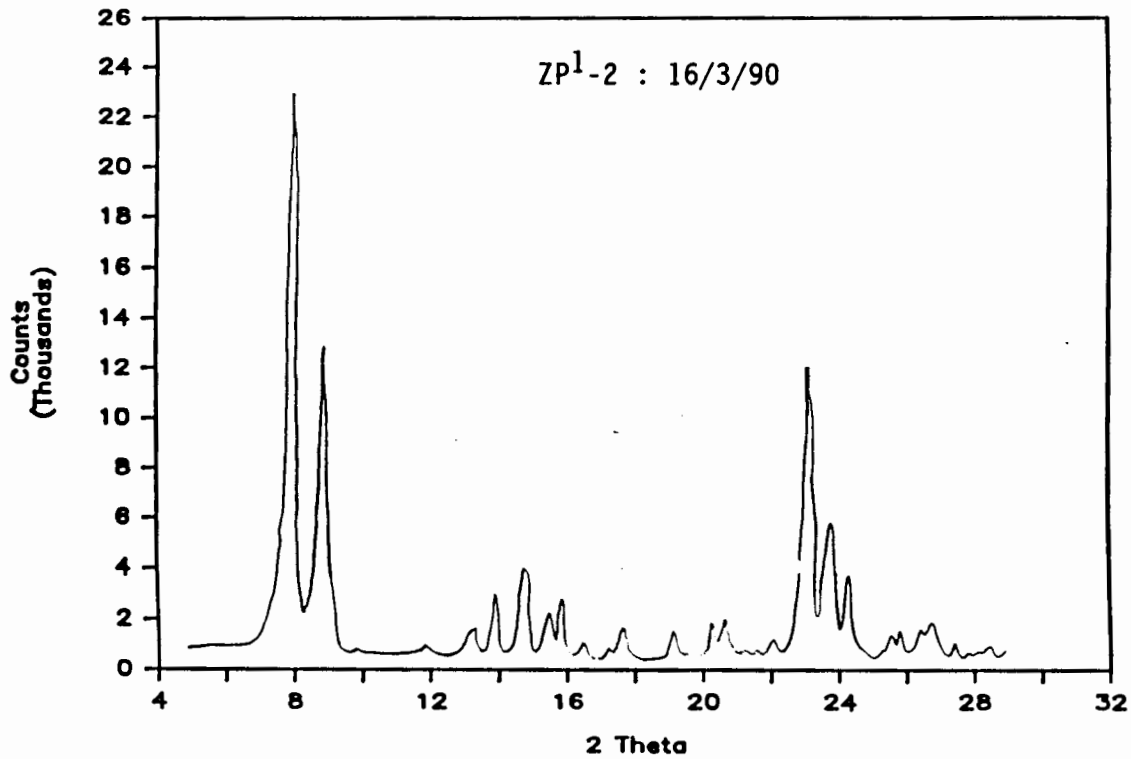
ZP1-2 : 16/3/90
Counts (Thousands)
26
24
22
20
18
16
14
12
10
8
6
4
2
0
4
8
12
16
20
24
28
32
2 Theta

References

REFERENCES

R.A. Alberty, Chem. Eng. Sci., *42*, (10), 2325, 1987a.
R.A. Alberty, J. Phys. Chem., *87*, (6), 3660, 1987b.
B. Andersen, C.T. O'Connor, M. Kojima, Stud. in Surf. Sci. & Catal., *49B*, 1193, Elsevier, Amsterdam, 1989.
A. Araya, B.M. Lowe, Zeolites, *6*, 111, 1986.
R.J. Arguer, G.R. Landolt, US Patent, 3702, 886, 1972.
A. Auroux, H. Dexpert, C. Leclerq, J.C. Védrine, App. Catal, *6*, 95, 1983.
A. Auroux, M.B. Sayed, J.C. Védrine, Thermochimica Acta, *93*, 557, 1985.
R.M. Barrer, Hydrothermal Chemistry of Zeolites, p.2, Academic Press, 1982.
R.S. Bauer, H. Ching, P.W. Glockner, W. Kei, H. van Zwet, U.S. Patent, *3* 635 937, 1972.
K.A. Becker, K. Fabianska, S. Kowalak, Acta Phys. Chem, *31*, 63, 1985.
K.A. Becker, S. Kowalak, J. Chem. Soc., Faraday Trans 1, *82*, 2151, 1986.
K.A. Becker, S. Kowalak, Int. Symposium on Zeolites as Catalysts, Sorbents and Detergent Builders, Würzberg, p 164, 1988.
K.A. Becker, S. Kowalak, Int. Symposium on Zeolites as Catalysts, Sorbents and Detergent Builders, Stud. in Surf. Sci & Catal., 164, Würzenburg, 1988.
G. Bellussi, G. Perego, A. Carati, U. Cornaro, V. Fattore, Stud. Surf. Sci & Catal, *37*, 37, 1988.
S.R. Bethea, J.H. Karchmer, Ind. Eng. Chem., 48 (3), 370, 1956.
D.M. Bibby, L.P. Alderidge, N.B. Milestone, J. Catal., *72*, 373, 1981.
D.M. Bibby, N.B. Milestone. J.E. Patterson, L.P. Aldridge, J. Catal., *97*, 493, 1986.
P. Bodart, J.B. Nagy, Z. Gabelica, E.G. Dérouane, App. Catal., *24*, 315, 1986.
K.H. Bourne, F.R. Cannings, R.C. Pitkethly, J. Phys. Chem., *74* (10), 2197, 1970.
G. Boxhoorn, O. Südmeier, P.H.G. van Kasteren, J. Chem Soc. Commun., 1416, 1983.
D.W. Breck, "Zeolite Molecular Sieves", 1st ed., Wiley, N.Y, 1974.
A. Brink, J.S. de K. Swart, "The Fischer-Tropsch Synthesis as applied at Secunda with special reference to Product Work-up and Product Quality", Int. Coal Conversion Conference, CSIR, South Africa, 1982.
E. Brunner, H. Ernst, D. Freude, M. Hunger, C.B. Krause, D. Prager, W. Reschetilowski, W. Schwieger, K-H. Bergk, Zeolites, *9*, 282, 1989.
P.D. Caesar, R.A. Morrison, U.S. Patent, 4 083 889.
G-Y. Cai, G-Q. Chen, Q-X Wang, Q. Xin, Q-Z. Wang, Z-Z. Wang, X-Y. Li, J. Liang, Zeolites, B. Draj, S. Hocevar (Eds.), p. 319, Elsevier, Amsterdam, 1985.
R.B. Calvert, L.D. Rollmann, Zeolites: Sci & Tech., F.R. Ribeiro, M. Nijhoff (Eds.), Den Haag, 1983.

K.H. Chandawar, S.B. Kulkarni, P. Ratnasamy, App. Catal, *4*, 287, 1982.
C.D. Chang, C.T-W Chu, R.F. Socha, J. Catal., *86*, 289, 1984.
C.D. Chang, S.D. Hellring, J.N. Miale, K.D. Schmitt, J. Chem. Soc. Faraday, Trans 1, *81*, 2215, 1985.
K.J. Chao, J.C. Tasi, M.S. Chen, I. Wang, J. Chem. Soc. Faraday, Trans 1, *77*, 547, 1981.
N.Y. Chen, S.J. Lucki, E.B. Mower, J. Catal., *13*, 329, 1969.
N.Y. Chen, J. Phys. Chem, *80* (1), 60, 1976.
N.Y. Chen, W.E. Garwood, J. Catal., *52*, 453, 1978.
N.Y. Chen, W.E. Garwood, F.G. Dwyer, "Shape Selective Catalysis in Industrial Applications", p.10, Marcel Dekker Inc., N.Y., 1989.
N.Y. Chen, W.W. Kaeding, F.G. Dwyer, J. Amer. Chem. Soc., *101* (22), 6783, 1979.
N.Y. Chen, W.E. Garwood, Catal. Rev. - Sci. Eng., *28* (2 & 3), 185, 1986.
N.Y. Chen, P.B. Weisz, Chem. Eng. Progr. Symp. Serv., *73*, 86, 1967.
C.T-W. Chu, G.H. Kuehl, R.M. Lago, C.D. Chang, J. Catal., *93*, 451, 1985.
C.T-W Chu, E.W. Valyocsik, US Patent, 4665250, 1987.
A. Corma, "Proceedings of the 8th International Zeolite Conference", in Stud. in Surf. Sci. & Catal., *49* A, 49, Elsevier, Amsterdam, 1989.
U. Cornaro, B.W. Wojchiechowski, J. Catal., *120*, 1982, 1989.
F.A. Cotton, G. Wilkinson, "Advanced Inorganic Chemistry, A Comprehensive Text," (4th Ed.), p. 333, J. Wiley & Sons, 1980.
G. Coudurier, J.C. Védrine, Pure & Appl. Chem., *58*, 1389, 1986.
G. Coudurier, A. Auroux, J.C. Védrine, R.D. Farlee, L. Abrams, R.D. Shannon, *108*, 1, 1987.
G. Coudurier, J.C. Védrine, Proc., 7th Int. Zeolite Conference, Tokyo, 643, 1987.
G. Coudurier, C. Naccache, J.C. Védrine, J. Chem. Soc., Chem. Comm., 1414, 1982.
S.M. Csicsery, J. Catal., *19*, 394, 1970.
S.M. Csicsery, J. Catal., *23*, 124, 1971.
S.M. Csicsery, Zeolites, *4*, 205, 1984.
S.M. Csicsery, J. Org. Chem., *34*, 3338, 1969.
J. Datka, Z. Piwowarska, J. Chem. Soc., Faraday Trans 1, *85*, (1), 47, 1989.
P. Dejaifve, J.C. Védrine, V. Bolis, E.G. Dérouane, J. Catal., *86*, 289, 1984.
E.G. Dérouane, J.B. Nagy, J-P. Gilson, J.H.C. van Hooff, J.P. van den Burg, J. Wolzhuizen, J. Catal, *59*, 248, 1979.
E.G. Dérouane, J. Catal., *77*, 177, 1981.
E.G. Dérouane, Z. Gabelica, J. Catal., *65*, 486, 1980.
E.G. Dérouane, J. Catal., *100*, 541, 1986.
E.G. Dérouane, J-B. Nagy, Z. Gabelica, V. Blom, Zeolites, *2*, 299, 1981.
E.G. Dérouane, P. Dejaifve, Z. Gabelica, Faraday Discuss. Chem. Soc., *72*, 331, 1982.

R.M. Dessau, K.D. Schmitt, G.T. Kerr, G.L. Woolery, L.B. Alemany, J. Catal., *104*, 484, 1987.

M.E. Dry, Cat: Sci & Tech., *1*, 159, J.R. Anderson, M. Boudart (Eds.), Springer Verlag, N.Y., 1981.

M.E. Dry, "High Yield, High Quality Diesel from Fischer-Tropsch Processing", Int. Coal Conversion Conference, CSIR, South Africa, 1982a.

M.E. Dry, Chemtech, 744, 1982b.

M.E. Dry, Catalysis Today, *6*, (3), 183, 1990.

F.G. Dwyer, Stud. in Surf. Sci. & Catal., *67*, 185, 1991.

J. Dwyer, F.R. Fitch, F. Machado, G. Quin, S.M. Smyth, J.C. Vickerman, J. Chem. Soc. Chem. Comm., 422, 1981.

J. Dwyer, F.R. Fitch, F. Machado, G. Qin, S.M. Smyth, J.C. Vickerman, J.C.S. Chem. Comm., 422, 1981.

A. Dyer, An Introduction to Molecular Sieves, p.1., J. Wiley & Sons, 1988.

P.E. Eberly, Jr., J. Phys. Chem., *71*, 1717, 1967.

G. Engelhardt, H.-G. Jerschkewitz, U. Lohse, P. Sarv, A. Samoson, E. Lippmaa, Zeolites, *7*, 289, 1987.

A.G. Evans, M. Polanyi, J. Chem. Soc, 252, 1947.

S.G. Fegan, B.M. Lowe, J. Chem. Soc., Faraday Trans 1, *82*, 785, 1986.

E.M. Flanigen, M. Khatami, Adv. Chem. Ser., *101*, 201, 1971.

E.M. Flanigen, in "Zeolite Chemistry and Catalysis," J.A. Rabo (ed.), ACS monograph 171, Chpt 3., *80*, 1979.

J.C.Q. Fletcher, M. Kojima, C.T. O'Connor., App. Catal., *28*, 181, 1986.

R. Fraenkel, M. Cherniavsky, M. Levy, Proc. 8th Int. Congr. Catal., *4*, 454, 1984.

V.J. Frilette, W.O. Haag, R.M. Lago, J. Catal., *67*, 218, 1981.

Z. Gabelica, E.G. Dérouane, N. Blom, American Chem. Soc. 1984a.

Z. Gabelica, B. Nagy, E. G. Dérouane, J-P Gilson, Clay Minerals, *19*, 803, 1984b.

L.G. Galya, M.L. Ocelli, J.T. Hsu, D.C. Young, J. Mol. Catal., *32*, 396, 1985.

S. Gautier, Diplome - Ingenieur Thesis, Conservatoire National des Arts et Métiers, Paris, 1988.

M. Gharmani, L.B. Sand, Zeolites, *3*, 155, 1983.

R.L. Gorring, J. Catal., *31*, 13, 1973.

R.W. Grose, E.M. Flanigen, US Patent, 4061 742, 1977.

E. Grunwald, F.W. Fong, J. Phys. Chem, *73*, 650, 1969.

J.L. Guth, H. Kessler, R. Wey, Stud. in Surf. Sci & Catal., *28*, 121, 1986.

W.O. Haag, Chem. Eng. Progr. Symp. Ser., 63 (73), 140, 1967.

W.O. Haag, N.Y. Chen, Catalyst Design with Zeolites, in Catalyst Design, Progress and Perspectives, p. 163, Wiley, N.Y., 1987b.

W.O. Haag, N.Y. Chen, Catalyst Design with Zeolites, in Catalyst Design, Progress and Perspectives, p. 168, Wiley, N.y., 1987.
W.O. Haag, R.M. Lago, P.B. Weisz, J. Chem. Soc., Faraday Disc., *72*, 317, 1982
W.O. Haag, R.M. Lago, P.B. Weisz, Nature, *309*, 589, 1984.
H. Hamdan, J. Klinowski, J. Chem. Soc., Chem. Commun., 240, 1989.
S.M. Harms, M. Kojima, C.T. O'Connor, Fuel Proc. Tech, *31*, 231, 1989.
R.K. Harris, C.T.G. Knight, J. Am. Chem. Soc., Faraday Trans., *79*, 1525, 1983.
K. Hidajat, F.J. Aracil, J.J. Carberry, C.N. Kenney, J. Catal., *105*, 245, 1987.
C.V. Hidalgo, H. Hoh, T. Hattori, M. Niwa, Y. Murakami, J. Catal., *85*, 362, 1984.
S.G. Hill, D. Seddon, Zeolites, *5*, 173, 1985.
D.M. Himmelblau, "Basic Principles and Calculations in Chemical Engineering", 4th Ed. pp. 228-238, Prentice-Hall Inc., N.J., 1982.
J.P. Hogan, R.L. Banks, W.C. Lanning, A. Clark, Ind. Eng. Chem., *47* (4), 752, 1955.
W. Hölderich, H. Eichorn, R. Lehnert, L. Marosi, W. Mross, R. Reinke, W. Ruppel, H. Schlimper, Proc. 6th Int. Zeolite Conf., Reno, USA, July 1983, Butterworths, p. 545, 1984.
L.Y. Hou, L.B. Sand, R.W. Thompson, "New Developments in Zeolite Sci and Tech.", Y. Murakami, A. Iijima, J.W. Ward (Eds.), Elsevier, Amsterdam, 1986.
M.G. Howden, CSIR Report, C Eng 413, Pretoria, 1982.
T.R. Hughes, H.M. White, J. Phys Chem., *71*, (7), 2192, 1967.
M. Hunger, J. Kärger, H. Pfeifer, J. Caro, B. Zibrowius, M. Bulow, R. Mostowicz, J. Chem Soc.,J. Chem. Soc., Faraday Trans 1, *83* (11), 3459, 1987.
T. Inui, F. Okazumi, J. Catal., *90*, 366, 1984.
T. Inui, H. Matsuda, H. Okaniwa, A. Miyamoto, App. Catal., *58*, 155, 1990.
K.G. Ione, L.A. Vostrikova, A.V. Petrova, V.M. Mastikhiu, Proc. 8th Int. Congress on Catalysis, Berlin, *4*, 519, 1984.
V.N. Ipatieff, Ind. Eng. Chem., 1067, 1935.
L.E. Iton, R.B. Beal, D.T. Hodul, J. Molec. Catal., *21*, 151, 1983.
G.A. Jablonski, L.B. Sand, J.A. Gard, Zeolites, *6*, 396, 1986.
P.A. Jacobs, H.K. Beyer, J. Phys. Chem., *83* (9), 1174, 1979.
P.A. Jacobs, R. von Ballmoos, J. Phys. Chem., *86*, 3050, 1982.
P.A. Jacobs, J.A. Martens, Pure & Appl. Chem., *58*, (10), 1329, 1986.
P.A. Jacobs, J.A. Martens, Stud. Surf. Sci. & Catal., *33*, 134, 1987.
B. Jager, Fischer-Tropsch Synthesis, Spring School in Coal Conversion, RAU, South Africa, 1978.
A. Jentys, G. Rumpelmayr, J.A. Lercher, App. Catal., *53*, 299, 1989.
L. Jinxiang, W. Qingxia, Y. Lixin, Thermochimica Acta, *135*, 385, 1988.
W.W. Kaeding, S.A. Butter, J. Catal., *61*, 155, 1980.

W.W. Kaeding, C. Chu, L.B. Young, B Weinstein, S.A. Butter, J. Catal., *67*, 159, 1981a.
W.W. Kaeding, C. Chu, L.B. Young, S.A. Butter, *69*, 392, 1981b.
L.S. Kassel, J. American Chem. Soc., *58*, 670, 1936.
H. Kessler, J.M. Chezeau, J.L. Guth, H. Strub, G. Coudurier, Zeolites, *7*, 360, 1987.
C.T.G. Knight, Zeolites, *10*, 143, 1990.
G.T. Kokotailo, P. Chu, S.L. Lawton, W.M. Meier, Nature, *275*, 170, 1978a.
G.T. Kokotailo, S.L. Lawton, D.H. Olson, W.M. Meier, Nature, *277*, 437, 1978b.
B. Kraushaar, J.W. de Haan, J.H.C. Van Hooff, J. Catal., *109*, 470, 1988.
G.H. Kühl, ACS Symposium Series, *40*, 96, 1977.
U. Kürschner, H-G. Jerschkewitz, J. Völter, App. Catal., *57*, 167, 1990.
U. Kürschner, B. Parlitz, E. Schreier, G. Ohlmann, J. Volter, App. Catal., *30*, 159, 1987.
R.M. Lago, W.O. Haag, R.J. Mikovsky, R.H. Olson, S.D. Hellring, K.D. Schmitt, G.T. Kerr, "Proc. 7th Int. Zeolite Conf., Y. Murakami, A. Iigima, J.T. Ward (Eds.), p 677, Elsevier, Amsterdam, 1986.
J.A. Lercher, G. Rumpelmayr, *25*, 215, 1986.
J.A. Lercher, G. Rumpelmayr, H. Nöller, Acta Phys Chem, *31*, 71, 1985.
E. Loeffler, Ch. Peuker, H.G. Jerschkewitz, Cat. Today, *3*, 415, 1988.
E. Loeffler, U. Lohse, Ch. Penker, G. Oehlmann, L.M. Kustov, V.L Zholobenko, V.B. Kazansky, Zeolites, *10*, 266, 1990.
U. Lohse, E. Loeffler, M. Hunger, J. Stöckner, V. Patzelova, Zeolites, *7*, 11, 1987.
J.H. Lunsford, J. Phys. Chem., *72*, (12), 4163, 1968.
Y.L. Ma, L.A. Savage, AIChE J, *33*, 1233, 1987.
C.J. Maiden, Stud. Surf. Sci. Catal., *36*, 1, 1988.
J.A. Martens, P.A. Jacobs, Zeolites, *6*, 334, 1986.
J.E. Maxwell, J. of Inclusion Phenomena, *4*, 1, 1986.
D. McClean, PhD Thesis, University of Cape Town, 1987.
J.F. McMahon, C. Bednars, E. Solomon, "Adv. Pet. Chem. Refin. 1", J.J. Mcketta, jr. (Ed), Chapt. 5, Interscience Publishers, 1963.
W.M. Meier, in "Molecular Sieves", p.10, Society for Chemical Industry, London, 1968.
W.M. Meier, D.H. Olson, Advan. Chem. Ser., *101*, 155, 1971.
W.M. Meier, D.H. Olson, "Atlas of Zeolite Structure Types", Structure Commission of IZA, Polycrystal Book Service, Pittsburgh, 1978.
S.L. Meisel, J.P. McCullough, C.H. Lechthaler, P.B. Weisz, Chemtech, *86*, 1976.
B.L. Meyers, S.R. Ely, N.A. Kutz, J.A. Kaduk, E van den Bosche, J. Catal., *91*, 352, 1985.
B.L. Meyers, T.H. Fleisch, C.L. Marshall, App. Surf. Science, *26*, 503, 1986.
R. Mostowicz, L.B. Sand, Zeolites, *3*, 219, 1983.
U. Mueller, K.K. Unger, Zeolites, *8*, 154, 1988.
J.B. Nagy, Z. Gabelica, E.G. Dérouane, Zeolites, *3*, 43, 1983.

S. Namba, A. Inaka, T. Yashima, Zeolites, *6*, 107, 1986.
V.S. Nayak, V.R. Choudhary, J. Catal., *81*, 26, 1983.
V.S. Nayak, V.R. Choudhary, App. Catal., *10*, 137, 1984.
J. Nunan, J. Cronin, J. Cunningham, J. Catal., *87*, 77, 1984.
M.L. Ocelli, J.T. Hsu, L.G. Galya, M. Mol. Catal., *32*, 377, 1985.
C.T. O'Connor, M. Kojima, W.K. Schumann, App. Catal., *16*, 193, 1985.
C.T. O'Connor, L.L. Jacobs, M. Kojima, Appl. Catal., *40*, 277, 1988.
C.T. O'Connor, M. Kojima, Catalysis Today, *6* (3), 329, 1990.
D.H. Olson, W.O. Haag, R.M. Lago, J. Catal., *61*, 390, 1980.
D.H. Olson, G.T. Kokotailo, S.L. Lawton, W.M. Meier, J. Phys Chem., *85*, 2238, 1981.
P.J. O'Malley, J. Dwyer, J. Chem. Soc., Chem. Comm., *72*, 1987.
Y. Ono, H. Nakatani, H. Kitagawa, E. Suzuki, "Successful Design of Catalysts", T. Inui (Ed.), Elsevier, Amsterdam, 1988.
H. Owen, S.K. Marsh, B.S. Wright, U.S. Patent, 4 456 779, 1984.
E.P. Parry, J. Catal., *2*, 371, 1963.
J. Pohlisch, R. Sangl, A. Mersmann, Process Technology Proceedings, *6*, p. 125. Proc. of the 10th Symp. on Industrial Crystallization, Czechoslovakia, Sept. 1987, J. Nyvlt, S. Zacek (Eds.), Elsevier, 1989.
J. Patarin, M. Soulard, H. Kessler, J.L. Guth, J. Baron, Zeolites, *9*, 397, 1989.
C.G. Pope, J. Catal., *72*, 174, 1981.
R.J. Quann, L.A. Green, S.A. Tabak, F.J. Krambeck, Ind. Eng. Chem. Res., *27*, 565, 1988.
R.J. Quann, L.A. Green, S.A. Tabak, F.J. Krambeck, Ind. Eng. Chem. Res., *27*, 567, 1988.
P. Ratnasamy, G.P. Babu, A.J. Chandwakar, S.B. Kulkarni, Zeolites, *6*, 98, 1986.
P. Ratnasamy, S.G. Hegde, A.J. Chandawar, J. Catal., *102*, 467, 1986.
W. Reschetilowski, W-D. Einecke, M. Jusek, R. Schölner, App. Catal., *56*, 15, 1989.
L.D. Rollmann, E.W. Valyocsik, European Patent, 21674 and 21675, 1981.
L.D. Rollmann, "Zeolites : Sci & Tech.", F.R.Ribeiro, M Nijhoff (Ed.), Den Haag, 1983.
V.N. Romannikov, V.M. Mastikhin, S. Hocevar, B. Draj (Eds.), Zeolites, *3*, 211, 1983.
Roozeboom, H.E. Robson, S.S. Chan, Zeolites, *3*, 321, 1983.
A. Samoson, E. Lippmaa, G. Engelhardt, U. Lohse, H-G. Jerschkewitz, Chem. Phys. Lett., *134* (6), 589, 1987.
L.B. Sand, Pure & Appl. Chem., *52*, 2105, 1980.
T. Sano, K. Suzuki, H. Shoji, S. Ikai, K. Okabe, T. Murakami, S. Shin, H. Hagiwara, H. Takay, Chem. Lett., 1421, 1987.
A. Sans, E. Schmidl, J. Catal., *94*, 187, 1985.
M.B. Sayed, A. Auroux, J.C. Védrine, App. Catal. *23*, 49, 1986.
M.B. Sayed, J.C. Védrine, J. Catal., *101*, 43, 1986.
M.B. Sayed, J. Chem. Soc., Faraday Trans 1, *83*, 1751, 1987.

M.B. Sayed, A. Auroux, J.C. Védrine, J. Catal., *116*, 1, 1989.
J. Sanz, V. Fornes, A. Corma, J. Chem. Soc. Far. Trans. 1, *84* (9), 3113, 1988.
K.F.M.G.J. Scholle, A.P.M. Kentgens, W.S. Veeman, P. Frenken, G.P.M. van der Velden, J. Phys. Chem., *88*, 5, 1984.
S. Schwarz, PhD. Thesis, University of Cape Town, 1990.
S. Schwarz, M. Kojima, C.T. O'Connor, App. Catal., *68*, 81, 1991.
A.N. Siderov, Optika i Spektroskopiya, *8*, 51, 1960.
J.V. Smith, Zeolite Chem. and Catal., ACS Monograph 171, J.A. Rabo (Ed.), 1979.
J.M. Smith, H.C. van Ness, "Introduction to Chemical Engineering Thermodynamics", (3rd Ed.), pp. 270-273, 569, McGraw-Hill, 1983.
J.M. Stuckey, J.H. Saylor, J. Amer. Chem. Soc., *62*, 2922, 1940.
K. Suzuki, Y. Koyozumi, K. Matsuzaki, S Ikai, S. Shin, App. Catal., *39*, 315, 1988.
R. Szostak, V. Nair, V.L. Thomas, J. Chem. Soc., Faraday Trans 1, *83*, 487, 1987.
R. Szostak, T.L. Thomas, J. Catal, *100*, 555, 1986.
S.A. Tabak, U.S. Patent, 4254295, 1981.
S.A. Tabak, U.S. Patent, 4547612, 1985.
S.A. Tabak, F.J. Krambeck, W.E. Garwood, I.I. ChE J., *32* (9), 1526, 1986.
S.A. Tabak, S Yurchak, Cat. Sci. & Tech. p307, J.R. Andersen, M. Boudart (Eds.), Springer Verlag, N.Y., 1990.
J.L. Tallon, R.G. Buckley, J. Phys Chem., *91*, (6), 1469, 1987.
M. Taramasso, G. Perego, B. Notari, Proc. 5th Int. Zeolite Conf., Naples, Italy, Sept. 1980, p40, Heyden & Sons, London, 1980.
J.M. Thomas, A-S Liu, J. Phys. Chem., *90*, 4843, 1986.
A. Tissler, P. Polanek, U. Girrbach, U. Müller, K.K. Unger, Stud. in Surf. Sci. & Catal., *46*, 399, 1989.
C.A. Tolmann, J. Amer. Chem. Soc., *92* (10), 2956, 1970.
N-Y Topsøe, K. Pedersen, E.G. Dérouane, J. Catal., *70*, 41, 1981.
N-Y Topsøe, F. Joensen, E. G. Dérouane, J. Catal., *110*, 404, 1986.
J.B. Uytterhoeven, L.G. Christener, W.K. Hall, J. Phys. Chem. *69*, 2117, 1965.
F.J. van der Gaag, J.C. Jansen, H. van Bekkum, App. Catal., *17*, 261, 1985.
E.F. Vansant, G. Schulz-Ely (Eds.), Belgium, 1987.
M.H. Vasquez, F.R. Ribeiro, N. Gnep, M. Guisnet, React. Vcinet. Catal. Lett., *38* (2), 301, 1989.
J.C. Védrine, A. Auroux, V. Bolis, P. Dejaifve, C. Naccache, P. Wierzchowski,
E.G. Dérouane, J.B. Nagy, J-P Gilson, J.H.C. van Hooff, J.P. van den Burg, J. Wolzhuizen, J. Catal., *59*, 248, 1979.
J.C. Védrine, A. Auroux, P. Dejaifve, V. Ducarme, H. Hoser, S. Zhou, J. Catal., *73*, 147, 1982.

P.B. Venuto, P.S. Landis, Adv. in Catal., *18*, 315, 1968.
H. Vinek, G. Rumpelmayr, J.A. Lercher, J. Catal., 115, 291, 1989.
R von Ballmoos, "Collection of Simulated ZRD Powder Patterns for zeolites", 75, Butterworth Scientific Limited, 1984.
I. Wang, T-J. Chen, K-J. Chao, T-C. Tsai, J. Catal, *60*, 140, 1979.
D.E. Walsh, L.D. Rollmann, J. Catal., *49*, 369, 1977.
D.E. Walsh, L.D. Rollmann, J. Catal., *56*, 195, 1979.
J.W. Ward, J. Catal., *9*, 225, 1967.
J.W. Ward, R.C. Hansford, J. Catal., *13*, 364, 1969.
J. Wei, J. Catal., *76*, 433, 1982.
J. Weitkamp, S. Ernst, H. Dauns, E. Gallei, Chem.-Ing.-Tech., *58* (8), 623, 1986.
J. Weitkamp, N.Y. Chen, S. Ernst, "Successful Design of Catalysts", p. 343, T. Inui (Ed.), Elsevier, Amsterdam, 1988.
P.B. Weisz, Chemtech, *3*, 498, 1973.
P.B. Weisz, W.O. Haag, P.G. Rodewald, Science, *206*, 57, 1979.
K-P. Wendlandt, W.P. Reschetilowski, B. Unger, B.V. Romanovskij, E.V. Suchkova, D. Freude, Stud. in Surf. Sci & Catal., *37*, p207, Proc. Int. Symp., P.J. Grobet, W.J. Mortier, E.L. Wu, S.L. Lawton, D.H. Olson, A.C. Rohrmann, jr., G.T. Kokotailo, J. Phys Chem., *83*, 2777, 1979.
Ya. S. Yakhaev, S.N. Khadziev, T.M. Gaitbekov, S.E. Spiridinov, React. Kinet. Catal. Lett., *30* (2), 263, 1986.
T. Yashima, Y. Sakaguchi, S. Namba. Stud. Surf. Sci & Catal., *7* p.739 "New Horizons in Catalysis", Proc. 7th ICC, Tokyo, 1980, T. Seijama, K. Tanabe (Eds.), Elsevier, Amsterdam, 1981.
L.B. Young, S.A. Butter, W.W. Kaeding, J. Catal., *76*, 418, 1982.
V.L. Zholobenko, L.M. Kustov, V.B. Kazansky, E. Loeffler, U. Lohse, Ch. Peuker, G. Oehlmann, Zeolites, *10*, 304, 1990.
V.L. Zholobenko, L.M. Kustov, V.B. Kazansky, E. Loeffler, U. Lohse, G. Oehlmann, Zeolites, *11*, 132, 1991.